ICRP ref: 4933-1637-2073

Annals of the ICRP

ICRP PUBLICATION 1XX

Dose coefficients for intakes of radionuclides by members of the public: Part 3

Editor-in-Chief
C.H. CLEMENT

Associate Editor
Q. FAN

Authors on behalf of ICRP
F. Paquet, M.R. Bailey, V. Berkovskyy, E. Blanchardon,
D. Gregoratto, R.W. Leggett, G. Ratia, C. Samuels, T. Smith

PUBLISHED FOR

The International Commission on Radiological Protection
by

SAGE

Please cite this issue as 'ICRP, 202Y. Dose coefficients for intakes of radionuclides by members of the public: Part 3. ICRP *Publication* 1XX, Ann. ICRP XX (0).'

CONTENTS

145

ICRP Publication XXX

DOSE COEFFICIENTS FOR INTAKES OF RADIONUCLIDES BY MEMBERS OF THE PUBLIC: PART 3

ICRP PUBLICATION 1XX

Approved by the Commission in MMMMM 202X

Abstract–This report is the third in a series of documents giving age-dependent dose coefficients for members of the public for environmental intakes of radionuclides by inhalation and ingestion. This series replaces the *Publication 56* series (ICRP, 1989, 1993, 1995b,c, 1996a, 2001, 2004) of documents. The revised dose coefficients have been calculated using the *Publication 100* (ICRP, 2006) human alimentary tract model (HATM) and *Publication 130* (ICRP, 2016) revision of the human respiratory tract model (HRTM). Revisions have also been made to many of the models that describe the systemic biokinetics of radionuclides absorbed to blood, making them more physiologically realistic representations of uptake and retention in organs and tissues and of excretion. Changes have been implemented that were introduced in *Publication 103* (ICRP, 2007) to: the radiation weighting factors used in the calculation of equivalent doses to tissues; the tissue weighting factors used in the calculation of effective dose; and the separate calculation of equivalent doses to males and females with sex-averaging in the calculation of effective dose. Reference voxel anatomical computational phantoms (i.e. models of the human body based on medical imaging data), have replaced the composite mathematical models used for previous calculations of organ doses. Dose calculations were also improved by using *Publication 107* (ICRP, 2008) updated radionuclide decay data and implementing the *Publication 116* (ICRP, 2010) treatment of radiation transport, using the *Publication 110* (ICRP, 2006) adult reference computational phantoms of the human body and the *Publication 143* (ICRP, 2020) paediatric reference computational phantoms.

Keywords: Environmental exposure; Internal dose assessment; Biokinetic and dosimetric models

MAIN POINTS

- **This report is the third in a series of documents giving age-dependent dose coefficients for members of the public for environmental intakes of radionuclides by inhalation and ingestion. This series replaces the *Publication 56* series (ICRP, 1989, 1993, 1995b,c, 1996a, 2001, 2004) of documents.**

- **The data provided are age-dependent dose coefficients for members of the public for environmental intakes of radionuclides by inhalation and ingestion. As in the *Publication 56* series (ICRP, 1989, 1993, 1995b,c, 1996a, 2001, 2004), dose coefficients are presented in this series of reports for intakes by 3-mo-old infants, 1-, 5-, 10-, and 15-y-old children, and adults.**

- **The data provided in the printed reports are restricted to tables of committed effective dose per intake (Sv Bq^{-1}) for inhalation and ingestion. Data are provided for all absorption types and for the most common isotope(s) of each element. The electronic annex that accompanies this series of reports contains a comprehensive set of committed effective and equivalent dose coefficients per intake.**

- **This current report provides the above data for the following elements: beryllium (Be), fluorine (F), sodium (Na), magnesium (Mg), aluminium (Al), silicon (Si), chlorine (Cl), potassium (K), scandium (Sc), titanium (Ti), vanadium (V), chromium (Cr), manganese (Mn), copper (Cu), gallium (Ga), germanium (Ge), arsenic (As), bromine (Br), rubidium (Rb), rhodium (Rh), palladium (Pd), cadmium (Cd), indium (In), tin (Sn), hafnium (Hf), tantalum (Ta), tungsten (W), rhenium (Re), osmium (Os), platinum (Pt), gold (Au), mercury (Hg), thallium (Tl), astatine (At) and francium (Fr).**

1. INTRODUCTION

(1) The present report is Part 3 of a report series aimed at providing revised dose coefficients for members of the public, for intakes of radionuclides by inhalation and ingestion. This report series replaces *Publications 56*, *67*, *69*, *71*, *72*, *88* and *95* (ICRP, 1989, 1993b, 1995b,c, 1996a, 2001, 2004). The revised dose coefficients provided in this new series have been calculated using the Human Alimentary Tract Model (HATM) (ICRP, 2006) and a revision of the Human Respiratory Tract Model (HRTM) (ICRP, 2015), which takes account of more recent data. Revisions have also been made to many models for the systemic biokinetics of radionuclides, making them more physiologically realistic representations of uptake and retention in organs and tissues and of excretion.

(2) Dose coefficients have been calculated for radioisotopes of the elements which are expected to be released into the environment as a result of human activities, such as uranium mining and milling, conversion, enrichment and fabrication, power station operations, fuel reprocessing, waste storage and disposal, and considered to be of significance for public radiation protection purposes. In addition, naturally occurring radionuclides are present in the environment, and their concentrations may be modified by human activities. Consequently, the range of radionuclides to be addressed includes those of natural origin, fission products, actinides, and activation products.

1.1. Methodology used in this publication series

(3) The general methodology for producing the biokinetic and dosimetric models is described in Part 1 of this report series (ICRP, 2024). For each element, detailed reviews of the literature were carried out to identify experimental studies and human contamination cases that provide information to quantify absorption to blood from the respiratory and alimentary tracts, and the biokinetics following systemic uptake. These reviews, and the analyses of the data obtained from them, are summarised in each element section.

(4) The chemical forms considered in this report series are those found in workplaces and already described in the Occupational Intakes of Radionuclides (OIR) series (ICRP, 2015, 2016, 2017, 2019, 2022). Since most of the radionuclides released in the environment may be gradually internalised in the food chain, an additional organic chemical form is taken into consideration for ingestion by humans.

(5) To provide dose coefficients for members of the public, it is necessary to consider the effect of age on the biokinetics of radionuclides and on anatomical and physiological parameters. The biokinetic parameter values used for the adults in this series of report are taken from the OIR series (ICRP 2015, 2016, 2017, 2019, 2022). Age-specific biokinetic parameter values are given in this series of reports for intakes by 3-mo-old infants, 1-, 5-, 10-, and 15-y-old children, in addition to the adults. Contamination of embryo and foetus from intakes of radionuclides by mothers and from ingestion of radionuclides in milk will be treated in further reports.

(6) Dose coefficients are presented in this series of reports for intakes by 3-mo-old infants and 1-, 5-, 10-, and 15-y-old children, in addition to adults. In most cases the adult is taken to be age 20 y and higher. This means that computational phantoms for adults and biokinetic parameter values for adults including transfer coefficients, deposition fractions for inhaled activity, and f_A values for activity entering the alimentary tract are applied to age 20 y and higher. The only exception is for transfer coefficients for biokinetic models describing the systemic behaviour of absorbed "bone-seeking" radionuclides such as the alkaline earth elements and actinide elements (See Part 2 of this Series, ICRP 20XX); for these models the

transfer coefficients for the adult apply to age 25 y and higher, the rationale being that the skeleton is not fully mature until about age 25 y. In the calculations of the activity in source regions of the body following intakes at preadult ages, continuous changes with age in the transfer coefficients and other age-specific biokinetic parameter values governing the distribution and retention of the radionuclide are obtained by interpolation according to age.

(7) For application to other ages and for protracted intakes, it is considered here, as in the *Publication 56* series (e.g., ICRP, 1989) that tissue doses can be estimated by applying the age-specific dose coefficients to the age ranges given below:

- 3 mo: from 0 to 12 mo of age
- 1 y: from 1 y to 2 y
- 5 y: more than 2 y to 7 y
- 10 y: more than 7 y to 12 y
- 15 y: more than 12 y to 17 y
- adult: more than 17 y.

(8) in the *Publication 56* series, a single Reference Person is used to represent each age-group. Generally, biokinetic parameter values for males have been adopted because of the availability of biokinetic data. Where there are known differences between sexes in the biokinetics of an element, this is noted in the relevant section of the biokinetic data in OIR: Parts 2–5 (ICRP, 2016a, 2017, 2019, 2022) or in this volume. Energy absorption is considered in models representing the Reference Male and Reference Female at each age.

1.2. Data presented in this report series

(9) Each element section of this report series includes reviews of data on, ingestion and systemic biokinetics and the structure and parameter values of the reference systemic biokinetic model. For inhalation, reviews of data in OIR Parts 2 – 5 are adopted and are simply summarised in this series of reports. More specifically, the data used in this third report in the series come mainly from *Publication 151* (OIR Part 5; ICRP, 2022)

(10) The data provided are age-dependent dose coefficients for members of the public for environmental intakes of radionuclides by inhalation and ingestion. As in the *Publication 56* series, dose coefficients are presented in this series of reports for intakes by 3-mo-old infants, 1-, 5-, 10-, and 15-y-old children, and adults.

(11) The data provided in the printed reports are restricted to tables of committed effective dose per intake (Sv Bq^{-1}) for inhalation and ingestion. Data are provided for all absorption types and for the most common isotope(s) of each element. In cases for which sufficient information is available [principally for actinide elements, see Part 2 (ICRP, 20XX)], lung absorption is specified for certain chemical forms, and dose coefficients are calculated accordingly. The sizes of particles inhaled by the Reference Individuals are assumed to be log-normally distributed with an activity median aerodynamic diameter (AMAD) of 1 μm and geometric standard deviation σ_g of approximately 2.5 (ICRP, 2024). They are assumed to have a density of 3.00 g cm^{-3}, and a shape factor of 1.5. An exception is made for the short-lived progeny of radon, described in the previous report of this series (ICRP, 2024).

(12) The electronic annex that accompanies this series of reports contains a comprehensive set of committed effective and equivalent dose coefficients. Data are presented for almost all radionuclides included in *Publication 107* (ICRP, 2008) that have half-lives equal to or greater than 10 min, and for other selected radionuclides. Data are provided for a range of physico-chemical forms and for aerosols with median sizes ranging from an activity median

thermodynamic diameter (AMTD) of 0.001 μm to an AMAD of 20 μm. Data for intake by ingestion (for specified values of f_A) are also provided.

(13) This current report provides the above data for all the elements included in OIR Part 5, except Ni, Se and Ag, which have already been reported in Part 1 of this series: beryllium (Be), fluorine (F), sodium (Na), magnesium (Mg), aluminium (Al), silicon (Si), chlorine (Cl), potassium (K), scandium (Sc), titanium (Ti), vanadium (V), chromium (Cr), manganese (Mn), copper (Cu), gallium (Ga), germanium (Ge), arsenic (As), bromine (Br), rubidium (Rb), rhodium (Rh), palladium (Pd), cadmium (Cd), indium (In), tin (Sn), hafnium (Hf), tantalum (Ta), tungsten (W), rhenium (Re), osmium (Os), platinum (Pt), gold (Au), mercury (Hg), thallium (Tl), astatine (At), and francium (Fr).

2. BERYLLIUM (Z = 4)

2.1. Routes of Intake

2.1.1. Inhalation

(14) For beryllium, default parameter values were adopted on absorption to blood from the respiratory tract (ICRP, 2015). Absorption parameter values and types, and associated f_A values for particulate forms of beryllium are given in Table 2.1 [taken from Section 2 of *Publication 151* (ICRP, 2022)].

Table 2.1. Absorption parameter values for inhaled and ingested beryllium.

	Absorption parameter values*		
Inhaled particulate materials	f_r	s_r (d^{-1})	s_s (d^{-1})
Default parameter values†			
Absorption type			
F	1	30	–
M‡	0.2	3	0.005
S	0.01	3	1×10^{-4}

Ingested materials§	Age-dependent absorption from the alimentary tract, f_A					
Assigned forms	3 months	1 year	5 years	10 years	15 years	adult
All compounds	8×10^{-3}	5×10^{-3}	5×10^{-3}	5×10^{-3}	5×10^{-3}	5×10^{-3}

*It is assumed that the bound state can be neglected for beryllium (i.e. $f_b = 0$). The values of s_r for Type F, M and S forms of beryllium (30, 3 and 3 d^{-1} respectively) are the general default values.

†For inhaled material deposited in the respiratory tract and subsequently cleared by particle transport to the alimentary tract, the default f_A values for inhaled materials are applied: i.e. the product of f_r for the absorption type and the f_A value for ingested soluble forms of beryllium applicable to the age-group of interest (e.g., 0.005 for adults).

‡Default Type M is recommended for use in the absence of specific information on which the exposure material can be assigned to an absorption type (e.g. if the form is unknown, or if the form is known but there is no information available on the absorption of that form from the respiratory tract).

§Activity transferred from systemic compartments into segments of the alimentary tract is assumed to be subject to reabsorption to blood. The default absorption fraction f_A for the secreted activity is the highest value for ingestion of the radionuclide applicable to the age-group of interest (e.g. 0.005 for adults).

2.1.2. Ingestion

2.1.2.1. Adults

(15) On the basis of the available data, a fractional absorption of 0.005 was adopted for all beryllium compounds in *Publications 30*, *72* and *151* (ICRP, 1981, 1995c, 2022; for details see Section 2 of *Publication 151*). The same value of $f_A = 0.005$ is used in this publication for all forms of beryllium ingested by adult members of the public.

2.1.2.2. Children

(16) Moskalev et al. (1988) reported that beryllium absorption from the fluoride in the gastro-intestinal tracts of 1-, 2- and 4-week-old rats was 1.5 times greater than in adults. A

value of f_A = 0.008 is therefore adopted here for 3-month-old infants. The adult value of f_A = 0.005 is used for 1-y-old and older children.

2.1.3. Systemic distribution, retention and excretion of beryllium

2.1.3.1. Biokinetic data

(17) Zhu et al. (2010) determined concentrations of beryllium in 17 tissues obtained from autopsies of up to 68 Chinese men from four areas of China. The subjects were considered healthy until the time of sudden accidental death, unrelated to ionizing radiations. The beryllium concentration was also measured in blood of living subjects from the same areas. Based on median beryllium concentrations in tissues together with reference tissue masses, about 36% of systemic beryllium (defined here as total-body beryllium minus beryllium in the lungs) was contained in bone, 30% in skeletal muscle, 17% in fat, 8% in blood, 3% in skin, 1.5% in liver, and 0.05% in kidneys. As a central estimate, the mass of beryllium in the total-body was ~20 µg, including ~1 µg in the lungs.

(18) Studies on rodents indicate that the systemic distribution of beryllium depends on the dosage, chemical form, and route of entry (Vacher and Stoner, 1968). The fractions of systemic beryllium retained in bone and excreted in urine tended to increase with decreasing mass of administered beryllium. Beryllium accumulated to a large extent in the liver when administered intravenously as sulfate or chloride but not when administered intravenously as citrate (Van Cleave and Kaylor, 1953). Following intratracheal administration, the skeleton was the main repository for all forms of administered beryllium (Cleave and Kaylor, 1955). Following oral intake of beryllium sulphate by rats, the skeleton contained >75% of the systemic content (Reeves, 1965).

(19) Scott et al. (1950) examined the effect of added carrier (beryllium sulphate) on the distribution and excretion of intravenously administered ^{7}Be in rabbits and rats. In all cases, the preponderance of excretion of ^{7}Be over the 7-d observation period was in urine and occurred during the first 24 h. The cumulative urinary to faecal excretion ratio over 7 d was 2.1 and 6.8 in rats injected with ^{7}Be with and without carrier, respectively, and 11 and 14 in rabbits injected with ^{7}Be with and without carrier, respectively. Activity was removed from blood more rapidly in the animals injected with ^{7}Be without carrier than in animals injected with ^{7}Be with carrier. At 7 d, the animals injected with ^{7}Be without carrier showed higher uptake by the skeleton and greater loss in urine than animals injected with ^{7}Be with carrier. The most pronounced effect of the added carrier was increased accumulation of activity in the liver.

(20) Vacher and Stoner (1968) studied the disappearance of beryllium from blood in rats following its injection as carrier-free ^{7}Be or $BeSO_4$ labelled with ^{7}Be. Carrier-free ^{7}Be cleared rapidly from blood, with only a few percent retained after 2 h. Beryllium cleared much more slowly from blood when injected as $BeSO_4$ because only a small portion of the injected material remained in diffusible form. The residence time in blood increased with the mass of injected $BeSO_4$.

(21) Furchner et al. (1973) compared the biokinetics of ^{7}Be ($T_{1/2}$ = 53.2 d) in mice, rats, monkeys, and dogs after oral or parenteral administration, over observation periods up to 380 d. Cumulative urinary plus faecal excretion of ^{7}Be measured over the first week (6 days for dogs and monkeys) was about 51% of the administered amount for mice, 45% for rats, 55% for dogs, and 29% for monkeys. Urinary to faecal excretion ratios were 2.9 for mice, 9.7 for rats, 1.7 for monkeys, and 10.2 for dogs. For each of the four animal types, total-body retention following intravenous injection could be described as a sum of three exponential terms. The long-term component of retention represented about 40% of the injected amount for dogs, 46% for mice, 50% for rats, and 59% for monkeys. Assuming a physical half-life of 52 d for ^{7}Be,

the investigators derived biological half-times of 1210 d for mice, 890 d for rats, 1270 d for dogs, and 1770 d for monkeys. The more recently estimated radiological half-life of 53.22 d for ^{7}Be (ICRP, 2008) would yield higher estimated biological half-times, up to ~3900 d for monkeys, due to the small difference between the effective long-term half-time in the animals and the physical half-life of ^{7}Be. The systemic distribution of ^{7}Be was determined for rats at 0.25-71 d post intraperitoneal injection. Bone was the dominant repository at all measurement times, containing about 64% of the retained activity at 1 d, 81% at 10 d, and 93% at 71 d. The liver contained about 8% of retained ^{7}Be at 1 d, 3% at 10 d, and 0.7% at 71 d. The kidneys contained about 6% at 1 d, 1% at 10 d, and 0.6% at 71 d.

(22) Finch et al. (1990) investigated the behaviour of inhaled ^{7}Be in dogs after inhalation of ^{7}BeO particles calcined at either 500° or 1000° C. Faecal excretion was the dominant mode of excretion at early times after exposure, but urinary excretion dominated at later times. The distribution of activity in the body was determined at 8, 32, 64, and 180 d post exposure. Lung retention at 180 d was much higher for BeO calcined at 1000° (62% of ILB) than for BeO calcined at 500° (14% of ILB). Most of the activity cleared from the lungs but not excreted was contained in the lymph nodes, skeleton, liver, and blood. On average, the skeleton contained about 8 times as much activity as the liver.

2.1.3.2. Biokinetic model for systemic beryllium

(23) The biokinetic model for systemic beryllium applied in *Publication 151* (ICRP, 2022) to workers is applied in this report to all age groups. The model structure is shown in Fig. 2.1. Transfer coefficients are listed in Table 2.2.

(24) The transfer coefficients describing the short- and intermediate-term kinetics of beryllium were selected to yield reasonable reproductions of the distribution, retention, and excretion of beryllium observed over the first ~1 y in laboratory animals administered low masses of soluble forms of Be. The transfer coefficients describing the long-term behaviour were selected to approximate the long-term distribution of beryllium indicated by autopsy data for adult humans. The return of beryllium from compartments with extended retention to a second blood compartment with relatively slow loss was a convenient way to model both the rapid blood clearance at early times after administration of beryllium to animals and the relatively large portion of total-body beryllium in blood (an estimated 8%) in environmentally exposed persons.

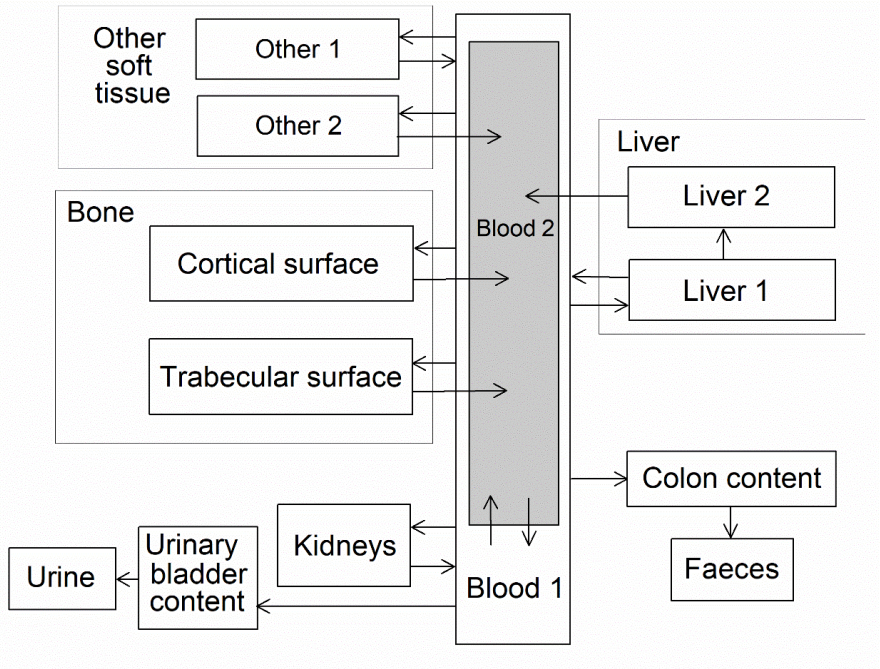

Fig. 2.1. Structure of the biokinetic model for systemic beryllium.

Table 2.2. Age-specific transfer coefficients for beryllium.

		Transfer coefficients (d^{-1})					
Pathway		100 d	1 y	5 y	10 y	15 y	Adult
Blood 1	UB content	2.00E+01	2.00E+01	2.00E+01	2.00E+01	2.00E+01	2.00E+01
Blood 1	RC content	5.00E+00	5.00E+00	5.00E+00	5.00E+00	5.00E+00	5.00E+00
Blood 1	Trab surface	1.50E+01	1.50E+01	1.50E+01	1.50E+01	1.50E+01	1.50E+01
Blood 1	Cort surface	1.50E+01	1.50E+01	1.50E+01	1.50E+01	1.50E+01	1.50E+01
Blood 1	Liver 1	5.00E+00	5.00E+00	5.00E+00	5.00E+00	5.00E+00	5.00E+00
Blood 1	Kidneys	3.00E+00	3.00E+00	3.00E+00	3.00E+00	3.00E+00	3.00E+00
Blood 1	Other 1	3.00E+01	3.00E+01	3.00E+01	3.00E+01	3.00E+01	3.00E+01
Blood 1	Other 2	5.00E+00	5.00E+00	5.00E+00	5.00E+00	5.00E+00	5.00E+00
Blood 1	Blood 2	2.00E+00	2.00E+00	2.00E+00	2.00E+00	2.00E+00	2.00E+00
Blood 2	Blood 1	1.40E-02	1.40E-02	1.40E-02	1.40E-02	1.40E-02	1.40E-02
Trab surface	Blood 2	2.50E-03	2.50E-03	2.50E-03	2.50E-03	2.50E-03	2.50E-03
Cort surface	Blood 2	2.50E-03	2.50E-03	2.50E-03	2.50E-03	2.50E-03	2.50E-03
Liver 1	Blood 1	2.00E-01	2.00E-01	2.00E-01	2.00E-01	2.00E-01	2.00E-01
Liver 1	Liver 2	5.00E-02	5.00E-02	5.00E-02	5.00E-02	5.00E-02	5.00E-02
Liver 2	Blood 2	1.90E-03	1.90E-03	1.90E-03	1.90E-03	1.90E-03	1.90E-03
Kidneys	Blood 1	1.50E-01	1.50E-01	1.50E-01	1.50E-01	1.50E-01	1.50E-01
Other 1	Blood 1	7.00E-02	7.00E-02	7.00E-02	7.00E-02	7.00E-02	7.00E-02
Other 2	Blood 2	2.50E-04	2.50E-04	2.50E-04	2.50E-04	2.50E-04	2.50E-04

UB, urinary bladder; RC, right colon; Cort, cortical; Trab, trabecular.

2.2. Dosimetric data for beryllium

Table 2.3. Committed effective dose coefficients (Sv Bq^{-1}) for the inhalation or ingestion of ^{7}Be compounds.

	Effective dose coefficients (Sv Bq^{-1})					
	3m	1y	5y	10y	15y	Adult
Inhaled particulate materials (1 µm AMAD aerosols)						
Type F	2.2E-10	1.8E-10	9.8E-11	6.4E-11	4.8E-11	4.9E-11
Type M, default	2.4E-10	2.0E-10	1.2E-10	8.1E-11	6.0E-11	7.0E-11
Type S	3.1E-10	2.6E-10	1.5E-10	1.1E-10	7.8E-11	9.2E-11
Ingested materials						
All compounds	8.2E-11	7.4E-11	4.2E-11	3.0E-11	2.1E-11	2.1E-11

AMAD, activity median aerodynamic diameter.

Table 2.4. Committed effective dose coefficients (Sv Bq^{-1}) for the inhalation or ingestion of ^{10}Be compounds.

	Effective dose coefficients (Sv Bq^{-1})					
	3m	1y	5y	10y	15y	Adult
Inhaled particulate materials (1 µm AMAD aerosols)						
Type F	8.1E-08	7.0E-08	3.4E-08	2.2E-08	1.8E-08	1.5E-08
Type M, default	4.5E-08	4.2E-08	2.3E-08	1.5E-08	1.3E-08	1.1E-08
Type S	1.5E-07	1.5E-07	1.2E-07	9.4E-08	9.4E-08	9.6E-08
Ingested materials						
All compounds	3.6E-09	2.0E-09	1.1E-09	7.2E-10	5.6E-10	4.4E-10

AMAD, activity median aerodynamic diameter.

3. FLUORINE (Z = 9)

3.1. Routes of Intake

3.1.1. Inhalation

(25) For fluorine, default parameter values were adopted for the absorption to blood from the respiratory tract (ICRP, 2015). Absorption parameter values and types, and associated f_A values for gas and vapour forms of fluorine are given in Table 3.1 and for particulate forms in Table 3.2 [both taken from Section 3 of *Publication 151* (ICRP, 2022)]. By analogy with the halogen iodine, considered in detail in *Publication 137* (OIR Part 3) (ICRP, 2017), default Type F is recommended for particulate forms in the absence of specific information on which the exposure material can be assigned to an absorption type.

(26) For fluorine, and the other halogens, intakes could be in both particulate and gas and vapour forms, and it is therefore assumed that inhaled fluorine is 50% particulate and 50% gas/vapour in the absence of information (ICRP, 2002b).

Table 3.1. Deposition and absorption for gas and vapour compounds of fluorine.

	Percentage deposited (%)*						Absorption†	
Chemical form/origin	Total	ET_1	ET_2	BB	bb	AI	Type	Absorption from the alimentary tract, f_A‡,¶
Unspecified	100	0	20	10	20	50	F	1.0

ET_1, anterior nasal passage; ET_2, posterior nasal passage, pharynx and larynx; BB, bronchial; bb, bronchiolar; AI, alveolar-interstitial.

*Percentage deposited refers to how much of the material in the inhaled air remains in the body after exhalation. Almost all inhaled gas molecules contact airway surfaces, but usually return to the air unless they dissolve in, or react with, the surface lining. The default distribution between regions is assumed: 20% ET_2, 10% BB, 20% bb, and 50% AI.

†It is assumed that the bound state can be neglected for fluorine (i.e. $f_b = 0$).

‡For inhaled material deposited in the respiratory tract and subsequently cleared by particle transport to the alimentary tract, the default f_A values for inhaled materials are applied [i.e. the product of f_r for the absorption type (or specific value where given) and the f_A value for ingested soluble forms of fluorine (1.0)].

¶The value of $f_A = 1.0$ is applicable to all age-groups.

3.1.2. Ingestion

(27) Absorption of fluoride present in food or as added fluoride in drinking water is rapid and almost complete. This seems also to be true for most inorganic compounds of fluorine in solution (see Section 3 of *Publication 151*). In *Publications 30*, *72* and *151* (ICRP, 1980, 1995c, 2022), the fractional absorption was taken to be 1 for all compounds of fluorine. In the present publication, the same value $f_A = 1$ is used for all chemical forms of fluorine and for all ages.

Table 3.2. Absorption parameter values for inhaled and ingested fluorine.

	Absorption parameter values*		
Inhaled particulate materials	f_r	s_r (d^{-1})	s_s (d^{-1})
Default parameter values†			
Absorption type			
F‡	1	30	–
M	0.2	3	0.005
S	0.01	3	1×10^{-4}

Ingested materials§

	Age-dependent absorption from the alimentary tract, f_A					
Assigned forms	3 months	1 year	5 years	10 years	15 years	adult
All forms	1	1	1	1	1	1

*It is assumed that the bound state can be neglected for fluorine (i.e. $f_b = 0$). The values of s_r for Type F, M and S forms of fluorine (30, 3 and 3 d^{-1} respectively) are the general default values.

†For inhaled material deposited in the respiratory tract and subsequently cleared by particle transport to the alimentary tract, the default f_A values for inhaled materials are applied: i.e. the product of f_r for the absorption type and the f_A value for ingested soluble forms of fluorine applicable to the age-group of interest (1).

‡Default Type F is recommended for use in the absence of specific information on which the exposure material can be assigned to an absorption type (e.g. if the form is unknown, or if the form is known but there is no information available on the absorption of that form from the respiratory tract).

§Activity transferred from systemic compartments into segments of the alimentary tract is assumed to be subject to reabsorption to blood. The default absorption fraction f_A for the secreted activity is the highest value for ingestion of the radionuclide applicable to the age-group of interest ($f_A = 1$).

3.1.3. Systemic distribution, retention and excretion of fluorine

3.1.3.1. Biokinetic data

(28) Fluorine-18 is widely used in skeletal imaging. Its systemic behaviour has been studied in human subjects and laboratory animals, usually as the fluoride ion (Suttie and Phillips, 1959; Costeas et al., 1970; Wootton, 1974; Hall et al., 1977; Charkes et al., 1978; Hawkins et al., 1992; Whitford, 1994; Schiepers et al., 1997).

(29) Fluoride entering blood deposits primarily in bone. Uptake by bone is rapid and thought to occur mainly by adsorption onto hydroxyapatite crystals, followed by exchange with hydroxyl groups in the hydroxyapatite. Uptake by bone is correlated with calcium influx and hence varies with age, with higher deposition in immature than mature bone. The highest concentrations of fluoride in bone occur at sites of bone growth or remodelling (Neuman and Neuman, 1958; Whitford, 1994; Schiepers et al., 1997).

(30) Charkes et al. (1978) developed a biokinetic model for systemic fluoride (Fig. 3.1) based on collected results of published studies of the kinetics of ^{18}F in human subjects. Two compartments were used to describe the behaviour of fluoride in bone: a buffer compartment between blood and mineral bone, assumed to represent an extracellular fluid space of bone, and a compartment representing mineral bone. A portion of fluoride entering the buffer pool was assumed to return rapidly to blood. The remainder was assumed to enter a mineral bone compartment that returns fluoride to the buffer pool.

3.1.3.2. Biokinetics of systemic fluorine

(31) The biokinetic model for fluorine applied to workers in *Publication 151* (ICRP, 2022) is a modified version of the model of Charkes et al. (1978) for shown in Fig. 3.1. The model of *Publication 151* incorporates flow rates derived by Charkes and coworkers but applies these

rates within a modified model framework. Specifically, the compartment called Bone ECF in Fig. 3.1 was divided into compartments called Trabecular Surface 1 (T1) and Cortical Surface 1 (C1), and the compartment called Bone was divided into compartments called Trabecular Surface 2 (T2) and Cortical Surface 2 (C2). The compartment called "Tubular urine" in Fig. 3.1 was replaced by a compartment named "Kidneys". The ratio of flow rates from Blood to T1 and C1 was assumed to be the same as the trabecular to cortical deposition ratio applied in the model for calcium in *Publication 134* (ICRP, 2016). The sum of flow rates from Blood to T1 and C1 was required to be the same as the flow rate from Blood to Bone ECF in Fig. 3.1.

(32) The fluorine model applied to workers in *Publication 151* is applied in this report to adult members of the public. For application to pre-adult ages, the rates of transfer from Blood to T1 and C1 are assumed to be proportional to rates of transfer of calcium from blood to trabecular and cortical bone surfaces, respectively, indicated in the age-specific model for calcium applied in Part 1 of the present series of reports.

(33) The structure of the fluorine model applied in the present report is shown in Fig. 3.2. Transfer coefficients are listed in Table 3.2.

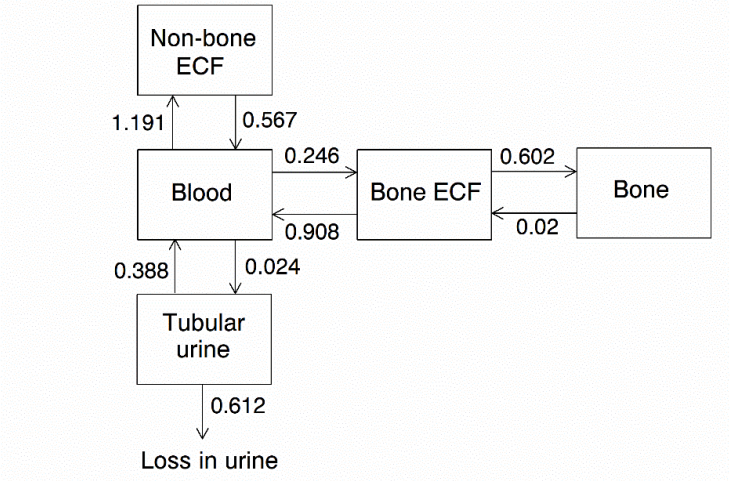

Fig. 3.1. Biokinetic model of Charkes et al. (1978) for systemic fluoride. Numbers next to arrows are transfer coefficients (min^{-1}). ECF, extracellular fluids.

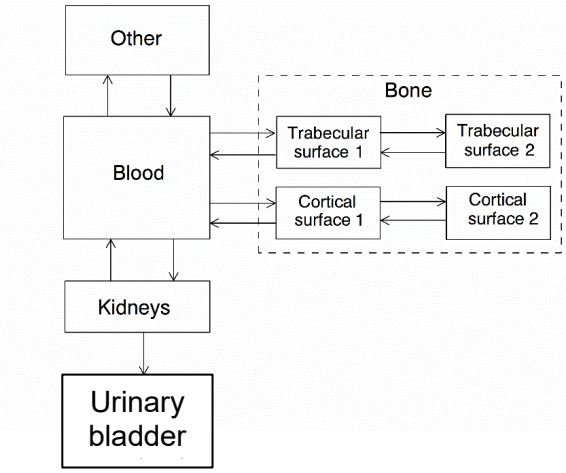

Fig. 3.2. Structure of the biokinetic model for systemic fluoride used in this report. Transfer coefficients are listed in Table 3.2.

517 Table 3.2. Age-specific transfer coefficients for fluorine.

		Transfer coefficients (d^{-1})					
Pathway		100 d	1 y	5 y	10 y	15 y	Adult
Blood	Trab surface 1	2.13E+02	1.28E+02	1.26E+02	2.01E+02	2.93E+02	1.97E+02
Blood	Cort surface 1	8.52E+02	5.11E+02	4.42E+02	5.94E+02	7.57E+02	1.58E+02
Blood	Other	1.02E+03	1.44E+03	1.51E+03	1.29E+03	1.04E+03	1.72E+03
Blood	Kidneys	2.06E+01	2.90E+01	3.04E+01	2.59E+01	2.09E+01	3.46E+01
Trab surface 1	Blood	1.31E+03	1.31E+03	1.31E+03	1.31E+03	1.31E+03	1.31E+03
Cort surface 1	Blood	1.31E+03	1.31E+03	1.31E+03	1.31E+03	1.31E+03	1.31E+03
Trab surface 1	Trab surface 2	8.67E+02	8.67E+02	8.67E+02	8.67E+02	8.67E+02	8.67E+02
Cort surface 1	Cort surface 2	8.67E+02	8.67E+02	8.67E+02	8.67E+02	8.67E+02	8.67E+02
Trab surface 2	Trab surface 1	2.88E+01	2.88E+01	2.88E+01	2.88E+01	2.88E+01	2.88E+01
Cort surface 2	Cort surface 1	2.88E+01	2.88E+01	2.88E+01	2.88E+01	2.88E+01	2.88E+01
Other	Blood	8.17E+02	8.17E+02	8.17E+02	8.17E+02	8.17E+02	8.17E+02
Kidneys	Blood	5.59E+02	5.59E+02	5.59E+02	5.59E+02	5.59E+02	5.59E+02
Kidneys	UB content	8.81E+02	8.81E+02	8.81E+02	8.81E+02	8.81E+02	8.81E+02

518 UB, urinary bladder; Cort, cortical; Trab, trabecular.

519 3.2. Dosimetric data for fluorine

520 Table 3.3. Committed effective dose coefficients (Sv Bq^{-1}) for the inhalation or ingestion of
521 ^{18}F compounds.

	Effective dose coefficients (Sv Bq^{-1})					
Inhaled gases or vapours	3m	1y	5y	10y	15y	Adult
Unspecified	3.4E-10	2.6E-10	1.6E-10	1.1E-10	8.2E-11	7.8E-11
Inhaled particulate materials (1 µm AMAD aerosols)						
Type F, default	1.4E-10	1.0E-10	4.7E-11	3.4E-11	2.3E-11	2.0E-11
Type M	2.0E-10	1.5E-10	7.6E-11	5.6E-11	4.3E-11	3.6E-11
Type S	2.0E-10	1.5E-10	7.7E-11	5.7E-11	4.4E-11	3.7E-11
Ingested materials						
All compounds	2.6E-10	2.0E-10	1.3E-10	8.9E-11	6.1E-11	4.8E-11

522 AMAD, activity median aerodynamic diameter.

4. SODIUM (Z = 11)

4.1. Routes of Intake

4.1.1. Inhalation

(34) For sodium, default parameter values were adopted on absorption to blood from the respiratory tract (ICRP, 2015). Absorption parameter values and types, and associated f_A values for particulate forms of sodium are given in Table 4.1 [taken from Section 4 of *Publication 151* (ICRP, 2022)].

Table 4.1. Absorption parameter values for inhaled and ingested sodium.

	Absorption parameter values*		
Inhaled particulate materials	f_r	s_r (d^{-1})	s_s (d^{-1})
Default parameter values†			
Absorption type			
F	1	30	–
M‡	0.2	3	0.005
S	0.01	3	1×10^{-4}

Ingested materials§	Age-dependent absorption from the alimentary tract, f_A					
Assigned forms	3 months	1 year	5 years	10 years	15 years	adult
All compounds	1	1	1	1	1	1

*It is assumed that the bound state can be neglected for sodium (i.e. $f_b = 0$). The values of s_r for Type F, M and S forms of sodium (30, 3 and 3 d^{-1} respectively) are the general default values.

†For inhaled material deposited in the respiratory tract and subsequently cleared by particle transport to the alimentary tract, the default f_A values for inhaled materials are applied: i.e. the product of f_r for the absorption type and the f_A value for ingested soluble forms of sodium applicable to the age-group of interest (1).

‡Default Type M is recommended for use in the absence of specific information on which the exposure material can be assigned to an absorption type (e.g. if the form is unknown, or if the form is known but there is no information available on the absorption of that form from the respiratory tract.

§Activity transferred from systemic compartments into segments of the alimentary tract is assumed to be subject to reabsorption to blood. The default absorption fraction f_A for the secreted activity is the highest value for ingestion of the radionuclide applicable to the age-group of interest ($f_A = 1$).

4.1.2. Ingestion

(35) Virtually all sodium is absorbed from the gastrointestinal tract of man [see *Publication 151* (ICRP, 2022)]. The fractional absorption was therefore taken to be 1 in *Publications 30, 72* and *151* (ICRP, 1980, 1995c, 2022). The same value of $f_A = 1$ is adopted here for sodium intake from diet at all ages.

4.1.3. Systemic distribution, retention and excretion of sodium

4.1.3.1. Biokinetic data

(36) The human body's sodium is freely exchangeable with the extracellular fluids except for a portion of sodium in bone representing roughly 10% of total-body sodium in an adult (Mole, 1984). The turnover rate of the body's exchangeable sodium is inversely related to the

level of sodium in diet. The concentration of sodium in the adult body typically is about 1 g Na per kg (Mole, 1984)

(37) Richmond (1980) studied the biokinetics of ^{22}Na over time periods up to ~9 months after its oral administration to mice, rats, and human subjects; intraperitoneal (IP) administration to mice and rats; and intravenous (IV) administration to monkeys and dogs. Average biological retention of Na (%) in three human subjects was described as a sum of three exponential terms:

$$R(t) = 48.8e^{-0.0815t} + 51.0e^{-0.0513t} + 0.267e^{-0.0015t} \quad (4.1)$$

where t is in days.

(38) Total-body retention in dogs and monkeys resembled that in human subjects. Activity was removed from the body at a moderately higher rate in rats and a much higher rate in mice than in human subjects. Distribution studies on rats indicated that muscle, bone, skin, gastrointestinal tract, and blood plasma contained the preponderance of the retained activity 1-20 d after intraperitoneal administration. Blood plasma contained ~10% and bone contained 17-31% of total-body activity during this period.

(39) Richmond et al. (1962) examined the effect of age on long-term retention of intravenously injected ^{22}Na in rats. Animals of age 30 d (immature rats) and 86 d (adult rats) at injection were used. Animals were divided into groups with normal or low levels of sodium in diet. Total-body retention was measured for 173 days. Biological retention of activity in all groups was expressed as a sum of three exponential terms. In animals with normal levels of sodium in diet, biological retention of the tracer was higher in the adults than in the younger animals for ~35 d post injection but lower thereafter. The coefficient (size) of the long-term component of retention was about 50% greater for the younger animals than for the adults. Similar long-term effects of age were seen in animals with low sodium intake; i.e., the size of the long-term component was about 50% greater in the younger animals than in the older animals. In all groups, the long-term biological half-time was about 9 months.

(40) Vennart (1963) reported a long-term component of sodium retention in the human body of about 1100 d, representing about 0.3% of the administered amount. At 6-11 mo after oral administration of ^{22}Na to 12 patients, median total-body retention represented ~0.35% of the administered amount (Smilay et al., 1961). In other human studies, Veall et al. (1955) estimated ^{22}Na retention of 1% after 75 d, and Miller et al. (1957) estimated ^{22}Na retention of 0.1% at 1 y.

(41) Bergstrom (1955) studied the sodium loss from bone in rats due to various procedures resulting in acute acidosis or sodium depletion. Only about 29% of bone sodium could be mobilized.

(42) Forbes and McCoord (1969) studied the behaviour of sodium in bone for periods up to 650 d post intraperitoneal injection of ^{22}Na into rats. Most of the activity taken up by bone was removed with a half-time of a few days, but about 5% of the deposited activity exhibited slow removal with an estimated half-time of ~700 d. The investigators concluded that the tenaciously retained activity had become an integral part of the bone crystal structure.

4.2.3.2. Biokinetic model for systemic sodium

(43) A biokinetic model proposed by Samuels and Leggett (2021) for systemic sodium in adults was adopted in *Publication 151* (ICRP, 2022) for application to workers. That model is applied in this report to adult members of the public. The model structure (Fig. 4.1) divides systemic sodium into blood, an exchangeable sodium pool consisting of sodium in all soft tissues, an exchangeable pool in bone represented by cortical and trabecular bone surfaces, and

a relatively non-exchangeable pool in bone represented by cortical and trabecular bone volume. Transfer coefficients for adults were set for consistency of model predictions with the following observations or assumptions: observed long-term total-body retention of radio-sodium in healthy human subjects; central rates of sodium excretion via urine, sweat, and faeces based on literature review; equilibrium between blood and soft tissues by 1 h after IV injection of a sodium tracer; equilibrium between blood and bone surfaces by 1.5 h after IV injection of a sodium tracer; a steady-state distribution of sodium of about 13% in blood, 40% in bone, and the remainder in soft tissues; reasonably accurate reproduction of total-body sodium in adults using model input of typical daily intake of sodium by an adult.

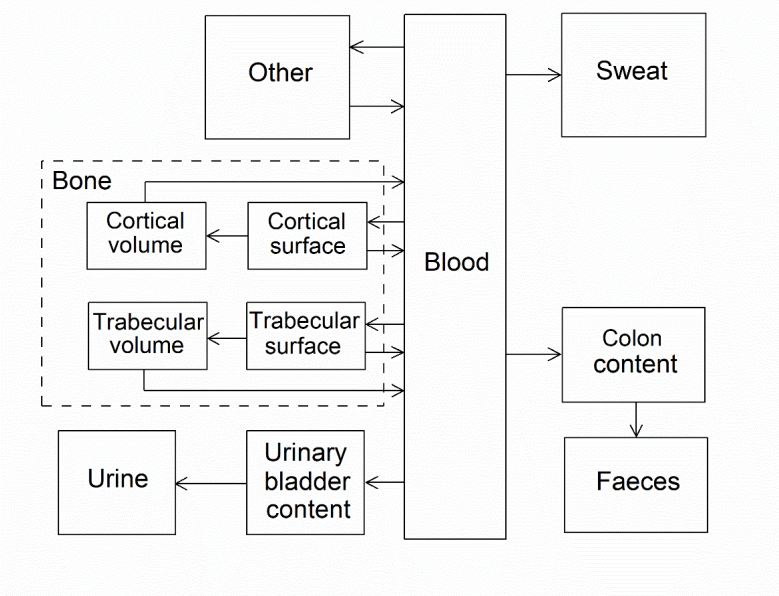

Fig. 4.1. Structure of the biokinetic model for systemic sodium.

(44) Extension of the model for sodium applied in *Publication 151* to preadult ages was based on the following general assumptions, or guiding principles, regarding sodium kinetics at any given age: daily excretion of sodium is equal to daily intake (homeostatic equilibrium); the total-body concentration of sodium is about 1 g kg^{-1} at all ages; the distribution of sodium among blood and exchangeable pools of the body is nearly the same at all ages; the rate of transfer of sodium into the virtually nonexchangeable portion of bone is greater for immature bone than for mature bone; and removal of sodium from a nonexchangeable compartment of bone is a sum of the bone turnover rate, T, and a slow, age-invariant rate of transfer, R, from bone to blood due to other causes. The following specific assumptions were used to develop transfer coefficients for preadult ages consistent with these guiding principles. Total-body masses at the ages addressed in the model (100 d, 1 y, 5 y, 10 y, 15 y, and adult) were taken from *Publication 89* (ICRP, 2002). Dietary intake of sodium was based on results of extensive surveys of age-specific dietary sodium in the US since the 1990s (National Health and Nutrition Examination Survey, or NHANES) (Alaimo et al., 1994; Tian et al., 2013; Wallace et al., 2019), and a review by Powles et al. (2013) of reported worldwide data for adults from 142 surveys of urinary sodium and 103 surveys of dietary sodium between 1980 and 2010 in 66 countries. The central values determined by Powles et al. for male and female adults are reasonably consistent with those determined for the US in NHANES studies. The following estimated sodium intakes in males of different ages were used to estimate sodium excretion rates: 0.6, 2.0, 2.7, 3.1, 4.0, and 4.1 g d^{-1} for ages 100 d, 1 y, 5 y, 10 y, 15 y, and adult, respectively. For pre-adult age P, the transfer coefficient from blood to each excretion pathway was scaled from the rate for adults using the scaling factor $F=(I_P/M_P/)/(I_A/M_A)$, where M_P and I_P are total-body

mass and daily sodium intake, respectively, at the pre-adult age; and M_A and I_A are corresponding values for an adult male. The derived scaling factors are 1.8, 3.6, 2.5, 1.7, and 1.3 for ages 100 d, 1 y, 5 y, 10y, and 15 y, respectively. The transfer coefficients between blood and exchangeable soft tissue or bone pools were not changed from the values applied to adults in *Publication 151* (ICRP, 2022). The rate of transfer from bone surface compartments (representing the sodium-exchangeable portion of bone) to bone volume compartments (representing the nonexchangeable portion of bone) was set at 1.5 times the value for adults for ages 5-15 y and 2.0 times the value for adults for ages 100 d and 1 y. In the model for adults used in *Publication 151*, the transfer rate from a bone volume compartment to blood was set at 0.002 d^{-1}, based on a curve fit to long-term ^{22}Na retention data for healthy adult males. This rate is greater than the bone turnover rates in adult bones and for a given bone type presumably represents the sum of the bone turnover rate T and return of sodium to blood at a rate R due to other causes. For development of transfer rates from nonexchangeable bone to blood in preadults, the value R was assumed to be invariant with age as its nature is unknown, but reference age-specific turnover rates T for cortical and trabecular bone (ICRP, 2002) were applied. The result is that the assigned transfer coefficients from nonexchangeable bone pools to blood increase with decreasing age.

(45) The age-specific transfer coefficients for systemic sodium are listed in Table 4.2.

Table 4.2. Age-specific transfer coefficients for sodium

		Transfer coefficients (d^{-1})					
Pathway		100 d	1 y	5 y	10 y	15 y	Adult
Blood	UB-cont	7.95E-01	1.59E+00	1.10E+00	7.51E-01	5.74E-01	4.42E-01
Blood	RC-cont	8.46E-03	1.69E-02	1.18E-02	7.99E-03	6.11E-03	4.70E-03
Blood	Excreta*	4.23E-02	8.46E-02	5.88E-02	4.00E-02	3.06E-02	2.35E-02
Blood	Other	9.50E+01	9.50E+01	9.50E+01	9.50E+01	9.50E+01	9.50E+01
Blood	Trab surface	1.00E+00	1.00E+00	1.00E+00	1.00E+00	1.00E+00	1.00E+00
Blood	Cort surface	4.00E+00	4.00E+00	4.00E+00	4.00E+00	4.00E+00	4.00E+00
Other	Blood	2.50E+01	2.50E+01	2.50E+01	2.50E+01	2.50E+01	2.50E+01
Trab surface	Blood	2.00E+00	2.00E+00	2.00E+00	2.00E+00	2.00E+00	2.00E+00
Trab surface	Trab volume	1.10E-03	1.10E-03	8.25E-04	8.25E-04	8.25E-04	5.50E-04
Cort surface	Blood	2.00E+00	2.00E+00	2.00E+00	2.00E+00	2.00E+00	2.00E+00
Cort surface	Cort volume	1.10E-03	1.10E-03	8.25E-04	8.25E-04	8.25E-04	5.50E-04
Trab volume	Blood	9.73E-03	4.39E-03	3.32E-03	2.83E-03	2.47E-03	2.00E-03
Cort volume	Blood	1.01E-02	4.80E-03	3.45E-03	2.82E-03	2.44E-03	2.00E-03

UB, urinary bladder; RC, right colon; Cort, cortical; Trab, trabecular.
*Sweat.

4.2. Dosimetric data for sodium

Table 4.3. Committed effective dose coefficients (Sv Bq^{-1}) for the inhalation or ingestion of ^{22}Na compounds.

	Effective dose coefficients (Sv Bq^{-1})					
	3m	1y	5y	10y	15y	Adult
Inhaled particulate materials (1 μm AMAD aerosols)						
Type F	6.5E-09	2.5E-09	1.7E-09	1.5E-09	1.3E-09	1.5E-09
Type M, default	3.1E-08	2.7E-08	1.6E-08	1.1E-08	8.4E-09	9.3E-09
Type S	1.1E-07	1.0E-07	6.7E-08	4.6E-08	4.0E-08	4.4E-08
Ingested materials						
All compounds	1.2E-08	4.6E-09	3.6E-09	3.3E-09	3.0E-09	3.5E-09

AMAD, activity median aerodynamic diameter.

Table 4.4. Committed effective dose coefficients (Sv Bq^{-1}) for the inhalation or ingestion of ^{24}Na compounds.

	Effective dose coefficients (Sv Bq^{-1})					
	3m	1y	5y	10y	15y	Adult
Inhaled particulate materials (1 μm AMAD aerosols)						
Type F	1.6E-09	1.0E-09	4.8E-10	3.4E-10	2.1E-10	1.8E-10
Type M, default	2.2E-09	1.6E-09	8.1E-10	5.8E-10	3.9E-10	3.7E-10
Type S	2.3E-09	1.7E-09	8.7E-10	6.3E-10	4.2E-10	4.0E-10
Ingested materials						
All compounds	2.9E-09	1.9E-09	1.2E-09	8.0E-10	5.6E-10	4.8E-10

AMAD, activity median aerodynamic diameter.

5. MAGNESIUM (Z = 12)

5.1. Routes of Intake

5.1.1. Inhalation

(46) For magnesium, default parameter values were adopted on absorption to blood from the respiratory tract (ICRP, 2015). Absorption parameter values and types, and associated f_A values for particulate forms of magnesium are given in Table 5.1 [taken from Section 5 of *Publication 151* (ICRP, 2022)].

Table 5.1. Absorption parameter values for inhaled and ingested magnesium.

	Absorption parameter values*		
Inhaled particulate materials	f_r	s_r (d^{-1})	s_s (d^{-1})
Default parameter values†			
Absorption type			
F	1	30	–
M‡	0.2	3	0.005
S	0.01	3	1×10^{-4}

Ingested materials§

	Age-dependent absorption from the alimentary tract, f_A					
Assigned forms	3 months	1 year	5 years	10 years	15 years	adult
Magnesium oxide	0.4	0.2	0.2	0.2	0.2	0.2
All other forms	1	0.5	0.5	0.5	0.5	0.5

*It is assumed that the bound state can be neglected for magnesium (i.e. $f_b = 0$). The values of s_r for Type F, M and S forms of magnesium (30, 3 and 3 d^{-1} respectively) are the general default values.

†For inhaled material deposited in the respiratory tract and subsequently cleared by particle transport to the alimentary tract, the default f_A values for inhaled materials are applied: i.e. the product of f_r for the absorption type and the f_A value for ingested soluble forms of magnesium applicable to the age-group of interest (e.g. 0.5 for adults).

‡Default Type M is recommended for use in the absence of specific information on which the exposure material can be assigned to an absorption type (e.g. if the form is unknown, or if the form is known but there is no information available on the absorption of that form from the respiratory tract).

§Activity transferred from systemic compartments into segments of the alimentary tract is assumed to be subject to reabsorption to blood. The default absorption fraction f_A for the secreted activity is the highest value for ingestion of the radionuclide applicable to the age-group of interest (e.g. 0.5 for adults).

5.1.2. Ingestion

5.1.2.1. Adults

(47) Estimates of the fractional intestinal absorption of magnesium were reported from 10 to 70%. This absorption seems to be lower for the oxide than for soluble forms and to be influenced by the total amount of magnesium in diet. For details, see Section 5 of *Publication 151* (ICRP, 2022).

(48) In *Publications 30* and *72* (ICRP, 1981, 1995c), f_1 was taken to be 0.5 for all compounds of magnesium. In *Publication 151* (ICRP, 2022), a lower $f_A = 0.2$ was applied to magnesium oxide. In this publication, the same $f_A = 0.2$ is used for intakes of magnesium oxide by adults, while $f_A = 0.5$ is applied to all other chemicals forms, including magnesium in diet.

5.1.2.2. Children

(49) The United States Institute of Medicine (IOM, 1997) noted that there are no data indicating that serum magnesium concentration is increased during pregnancy. The bioavailability of magnesium was observed to be negatively correlated with age in adult men (Verhas et al., 2002) and rats (Coudray et al., 2006); however, magnesium balance does not seem to be affected by age in adults (Hunt and Johnson, 2006).

(50) Consistently with the approach of *Publication 56* (ICRP, 1990), an $f_A = 0.4$ is adopted here for intakes of magnesium oxide by 3 month old infants and the value of $f_A = 0.2$ is applied to intakes of magnesium oxide by older children. For all other forms an $f_A = 1$ is used for intakes by 3-month-old infants and the value of $f_A = 0.5$ is applied to older children.

5.1.3. Systemic distribution, retention and excretion of magnesium

5.1.3.1. Biokinetic data

(51) The adult human body typically contains ~24 g of the essential element magnesium. The normal concentration in plasma is 0.75-1.0 mmol Mg L^{-1}. The concentration in red blood cells (RBC) is about three times that in plasma. Bone contains about 60% of the total-body content. Part of bone magnesium exchanges extremely slowly with plasma magnesium. Magnesium residing on bone surfaces is readily released to blood when plasma concentrations decline but remains bound to bone surface at adequate plasma concentrations (Elin, 1987; Vormann, 2003).

(52) In healthy adult human subjects injected intravenously with ^{28}Mg, mean urinary and faecal excretion accounted for about 17% and 2.6%, respectively, of the administered amount (corrected for radioactive decay) after 6 d (Aviola and Berman, 1966). Exchangeable magnesium presumably consisting mainly of extracellular fluid was estimated to represent about 15% of total-body magnesium. A larger pool of the tracer exchanged with stable magnesium with a biological half-life of ~42 d.

(53) In healthy adult human subjects ~20% of intravenously administered ^{28}Mg ($Tb_{1/2}$ = 20.9 h) was removed in urine over 24 h (Aikawa et al., 1960). Faecal excretion was negligible. Exchangeable magnesium was estimated to represent less than 16% of total-body magnesium. Activity exchanged slowly with stable magnesium in bone, muscle, and RBC.

(54) Watson et al. (1979) studied magnesium kinetics in the whole body, plasma, and RBC in five healthy adult male humans following intravenous administration of ^{28}Mg. Exchangeable magnesium was estimated to represent less than one-fourth of total-body magnesium after 5 d. Total-body retention over the relatively short observation period was described as a sum of two exponential terms, with ~4.5% removed with a biological half-time of a few hours and the remainder with a half-time of ~30 d.

(55) Sabatier et al. (2003) developed a compartmental model of magnesium metabolism based on results of a stable isotope study involving oral administration of ^{26}Mg and intravenous administration of ^{25}Mg to six healthy adult men in the age range 26-41 y. Isotopic concentrations were determined in blood, urine, and faeces collected over 12 d. The use of stable isotopes enabled longer observation of exchange of magnesium tracers with the body's magnesium stores and identification of a larger exchangeable pool than estimated in an earlier study by Aviola and Berman (1966) involving the relatively short-lived radionuclide ^{28}Mg. The exchangeable pool was interpreted as representing 25% of total-body magnesium and consisting of two extra-plasma pools that exchange magnesium with plasma and contain 80% and 20% of exchangeable magnesium. The model also described exchange of systemic magnesium with the gastrointestinal (GI) tract resulting from secretion of magnesium into the GI content and reabsorption to blood. Excretion of magnesium was depicted as transfer from

plasma to urine and faecal loss of unabsorbed magnesium. The model did not address non-exchangeable magnesium.

(56) At 1 d after intravenous administration of ^{28}Mg to dogs, the heart showed the highest activity, followed by kidney, liver, and pancreas, among eight examined soft tissues (Brandt et al., 1958). The activity concentration in bone varied greatly from one bone to another and generally was lower than that in heart, kidneys, liver, and pancreas.

(57) Lazzara et al. (1963) performed a detailed examination of the time-dependent behaviour of ^{28}Mg in dogs over the first 68 h after intravenous administration. There were considerable differences in the rate of exchange of ^{28}Mg with stable magnesium in different tissues. The activity concentration in the kidneys rose rapidly, peaked at about 4 h, and then gradually declined. The left ventricle, liver, and pancreas initially showed similar ^{28}Mg uptake curves, but peak concentrations occurred at different times for the three organs. There was a continual rise in activity in the cerebellum throughout the observation period. Bone and teeth showed highly variable activity concentrations from one location to another, and neither reached a peak average concentration over the 68-h observation period. The biological half-time for the total body was about 11 d.

5.1.3.2. Biokinetic model for systemic magnesium

(58) The biokinetic model for systemic magnesium applied to workers in *Publication 151* (2022) is applied in this report to intakes at any age. The model is an extension of the model of Sabatier et al. (2003) summarized above. The median transfer coefficients derived by Sabatier and coworkers were used as a starting point. Their extra-plasma compartment with relatively slow return to blood was assumed to represent exchangeable magnesium in bone. Compartments representing longer retention in bone were added. A soft-tissue compartment was added to represent slowly exchangeable magnesium and to approximate the total-body stable magnesium content of adult humans. Model predictions are reasonably consistent with the bone and soft tissue magnesium contents in adult humans (about 55-60% in bone), central urinary and faecal excretion rates reported for magnesium reported in the literature, and buildup of the magnesium ratio RBC:Plasma as observed by Watson et al (1979) in normal male subjects.

(59) The structure of the biokinetic model for systemic magnesium used in this report is shown in Fig. 5.1. Transfer coefficients are listed in Table 5.2.

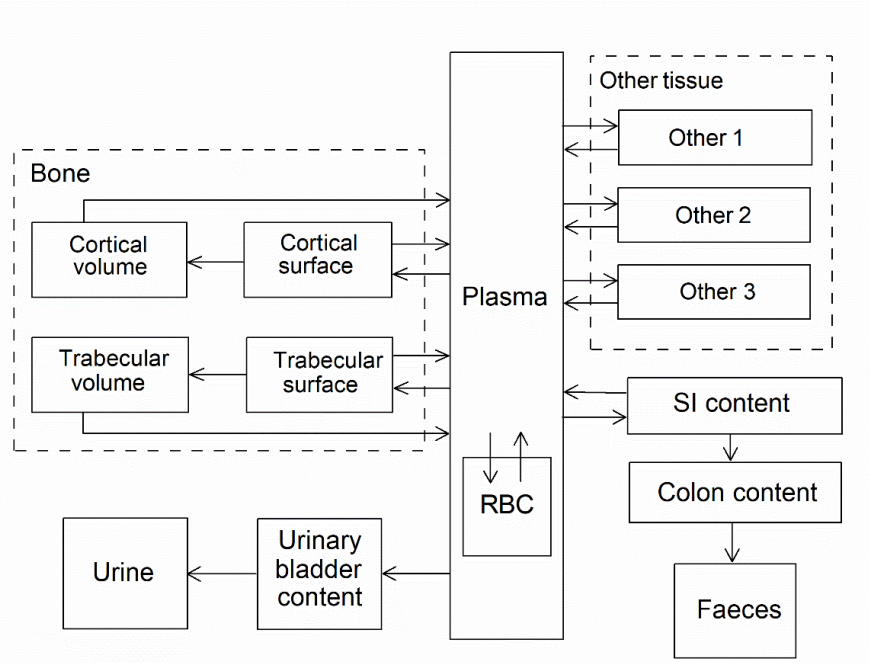

Fig. 5.1. Structure of the biokinetic model for systemic magnesium. RBC, red blood cells; SI, small intestine.

Table 5.2. Age-specific transfer coefficients for magnesium.

		Transfer coefficients (d^{-1})					
Pathway		100 d	1 y	5 y	10 y	15 y	Adult
Plasma	RBC	5.00E-02	5.00E-02	5.00E-02	5.00E-02	5.00E-02	5.00E-02
Plasma	UB content	1.00E+00	1.00E+00	1.00E+00	1.00E+00	1.00E+00	1.00E+00
Plasma	SI content	2.00E-01	2.00E-01	2.00E-01	2.00E-01	2.00E-01	2.00E-01
Plasma	Trab surface	4.00E+00	4.00E+00	4.00E+00	4.00E+00	4.00E+00	4.00E+00
Plasma	Cort surface	4.00E+00	4.00E+00	4.00E+00	4.00E+00	4.00E+00	4.00E+00
Plasma	Other 1	7.00E+01	7.00E+01	7.00E+01	7.00E+01	7.00E+01	7.00E+01
Plasma	Other 2	1.98E+01	1.98E+01	1.98E+01	1.98E+01	1.98E+01	1.98E+01
Plasma	Other 3	1.00E+00	1.00E+00	1.00E+00	1.00E+00	1.00E+00	1.00E+00
RBC	Plasma	3.00E-02	3.00E-02	3.00E-02	3.00E-02	3.00E-02	3.00E-02
Trab surface	Plasma	1.80E-01	1.80E-01	1.80E-01	1.80E-01	1.80E-01	1.80E-01
Trab surface	Trab volume	2.00E-02	2.00E-02	2.00E-02	2.00E-02	2.00E-02	2.00E-02
Cort surface	Plasma	1.80E-01	1.80E-01	1.80E-01	1.80E-01	1.80E-01	1.80E-01
Cort surface	Cort volume	2.00E-02	2.00E-02	2.00E-02	2.00E-02	2.00E-02	2.00E-02
Other 1	Plasma	6.00E+01	6.00E+01	6.00E+01	6.00E+01	6.00E+01	6.00E+01
Other 2	Plasma	3.00E+00	3.00E+00	3.00E+00	3.00E+00	3.00E+00	3.00E+00
Other 3	Plasma	2.30E-02	2.30E-02	2.30E-02	2.30E-02	2.30E-02	2.30E-02
Trab volume	Plasma	2.30E-02	2.30E-02	2.30E-02	2.30E-02	2.30E-02	2.30E-02
Cort volume	Plasma	2.30E-02	2.30E-02	2.30E-02	2.30E-02	2.30E-02	2.30E-02

RBC, red blood cells; SI, small intestine; Trab, trabecular; Cort, cortical.

5.1.3.3. Treatment of radioactive progeny

(60) The treatment of radioactive progeny produced in systemic compartments after intake of a radioisotope of magnesium is described in Section 5.2.3.3. of *Publication 151* (ICRP, 2020).

5.2. Dosimetric data for magnesium

Table 5.3. Committed effective dose coefficients (Sv Bq^{-1}) for the inhalation or ingestion of ^{28}Mg compounds.

	Effective dose coefficients (Sv Bq^{-1})					
	3m	1y	5y	10y	15y	Adult
Inhaled particulate materials (1 μm AMAD aerosols)						
Type F	3.8E-09	2.6E-09	1.1E-09	7.2E-10	4.7E-10	3.5E-10
Type M, default	4.8E-09	3.5E-09	1.8E-09	1.2E-09	8.5E-10	7.7E-10
Type S	4.9E-09	3.7E-09	1.9E-09	1.3E-09	9.1E-10	8.4E-10
Ingested materials						
Magnesium oxide	6.1E-09	4.6E-09	2.7E-09	1.8E-09	1.3E-09	1.1E-09
All other forms, unspecified forms	7.0E-09	4.8E-09	2.7E-09	1.8E-09	1.2E-09	1.0E-09

AMAD, activity median aerodynamic diameter.

6. ALUMINIUM (Z = 13)

6.1. Routes of Intake

6.1.1. Inhalation

(61) There is extensive information available on the behaviour of aluminium after deposition in the respiratory tract from animal experiments (mainly in rats), in-vitro dissolution studies, and some accidental human intakes. For details see Section 6 of *Publication 151* (ICRP, 2022). Absorption parameter values and Types, and associated f_A values for particulate forms of aluminium are given in **Fel! Hittar inte referenskälla.**6.1 [taken from Section 6 of *Publication 151* (ICRP, 2022)].

Table 6.1. Absorption parameter values for inhaled and ingested aluminium.

		Absorption parameter values*		
Inhaled particulate materials		f_r	s_r (d^{-1})	s_s (d^{-1})
Default parameter values†,‡				
Absorption Type	Assigned forms			
F	-	1	30	-
M	aluminium metal	0.2	3	0.005
S§	aluminium oxide, fluoride, bauxite ore, chlorhydrate, sulphate, all unspecified forms	0.01	3	0.0001

Ingested materials¶

	Age-dependent absorption from the alimentary tract, f_A					
Assigned forms	3 months	1 year	5 years	10 years	15 years	adult
Soluble forms and aluminium in diet	0.03	0.003	0.003	0.003	0.003	0.003
Insoluble forms	0.001	0.0001	0.0001	0.0001	0.0001	0.0001

*It is assumed that the bound state can be neglected for aluminium (i.e. f_b = 0.0). The values of s_r for Type F, M and S forms of aluminium (30, 3 and 3 d^{-1} respectively) are the general default values.

†Materials (e.g. oxide) are generally listed here where there is sufficient information to assign to a default absorption type, but not to give specific parameter values [see Section 6.2.1 of *Publication 151* (ICRP, 2022)].

‡For inhaled material deposited in the respiratory tract and subsequent cleared by particle transport to the alimentary tract, the default f_A values for inhaled materials are applied: i.e. the product of f_r for the absorption type and the f_A value for ingested soluble forms of aluminium applicable to the age-group of interest (e.g. 0.003 for adults).

§Default Type S is recommended for use in the absence of specific information (i.e. if the form is unknown, or if the form is known but there is no information available on the absorption of that form from the respiratory tract).

¶Activity transferred from systemic compartments into segments of the alimentary tract is assumed to be subject to reabsorption to blood. The default absorption fraction f_A for the secreted activity is the highest value for ingestion of the radionuclide applicable to the age-group of interest (e.g. 0.003 for adults).

6.1.2. Ingestion

6.1.2.1. Adults

(62) A fractional absorption value of 0.01 was recommended in *Publications 30* and *72* (ICRP, 1981, 1995c) for all compounds of aluminium. Based on more recent data, a f_A value of 0.003 was adopted for soluble forms at the workplace in *Publication 151* while a value of 1 × 10^{-4} was adopted for insoluble forms (ICRP, 2022).

(63) Aluminium absorption from the diet was estimated to be 0.1 to 0.3% based on normal urinary aluminium excretion of 20 to 50 μg d^{-1} and a daily aluminium intake of 20 mg (Ganrot, 1986). From updated estimates of typical daily intake and daily urinary excretion, Priest (1993) and Nieboer et al. (1995) evaluated fractional absorption in the order of 0.1%. Based on a daily intake of 10 mg and aluminium body burdens of 5 and 60 mg, Priest (2004) estimated fractional absorptions of 0.14 and 1.6%. Greger and Baier (1983) conducted a 40-day balance study on 8 adult males: measurement of urinary and faecal excretion indicated gastro-intestinal absorption of 0.78% of aluminium intake over 20 days. This was reduced to 0.09% when excess aluminium lactate was added to the diet for 20 days. The urinary aluminium excretion after consumption of two litres of tea by one subject suggested fractional absorption of 0.3% (Powell et al., 1993). Stauber et al. (1999) investigated the relative absorption of aluminium naturally present in food and drinking water: 0.3 to 0.4% of aluminium was absorbed from both water and food by 29 healthy volunteers. Stauber et al. corrected the estimate of absorption for non-measured aluminium excretion and body retention, thus likely providing a more realistic estimate than other studies.

(64) The simultaneous ingestion of citric acid or orange juice increased the gastrointestinal absorption of aluminium by a factor of up to 50 (Weberg and Berstad, 1986). Day et al. (1991) measured the plasma concentration of aluminium 26 days after ingestion of the citrate and estimated a fractional absorption of at least 1%. By measuring plasma levels of aluminium in 5 volunteers after ingestion of aluminium in citrate-rich orange juice, Edwardson et al. (1993) estimated a gastrointestinal absorption of about 0.015% of ingested aluminium. This was reduced by a factor of about 7 in the presence of dissolved silicon. Priest et al. (1996) assessed 50-time higher aluminium absorption from the citrate than from the hydroxide. The co-administration of citrate increased aluminium absorption from aluminium hydroxide by a factor of about 13. Moore et al. (1997) reported an increased absorption of 0.14% ^{26}Al and ^{27}Al ingested in the presence of citrate by 15 patients with Down's syndrome as compared to 0.02 – 0.03% in 15 control subjects.

(65) An f_A value of 0.003 is adopted in this publication for soluble forms and for aluminium in diet ingested by adult members of the public. The value of 1×10^{-4} is used for insoluble forms.

6.1.2.2. Children

(66) Yokel and McNamara (1985) did not find any age-related differences in the systemic clearance or half-time of aluminium lactate in rabbits following intravenous, oral, or subcutaneous exposure. Oral exposure to aluminium nitrate resulted in higher brain aluminium levels in young rats as compared to older rats, but there was no difference in toxicity between young and adult rats (Gomez et al. 1997a). In other tissues examined, the aluminium levels in the young rats tended to be lower than in the adult or older animals (Gomez et al. 1997b).

(67) Consistently with the approach of *Publication 56* (ICRP, 1990), an $f_A = 0{,}03$ is adopted here for ingestion of soluble forms and of aluminium in diet by 3 month old infants ; an $f_A = 0{,}001$ is used for ingestion of insoluble forms by 3 month old infant. For children of older ages, the same values as for adults ($f_A = 0{,}003$ for soluble forms and for aluminium in diet, $f_A = 1 \times 10^{-4}$ for insoluble forms) are used.

6.1.3. Systemic distribution, retention and excretion of aluminium

6.1.3.1. Biokinetic data

(68) Following absorption into blood, most of the circulating aluminium binds to the iron-transport protein transferrin, but an estimated 15-20% forms small-molecule complexes that

may be readily excreted (Devoto and Yokel, 1994). Over 90% of endogenous excretion of aluminium is in urine. Post-mortem measurements of aluminium in tissues of adult males indicate a total-body content of ~0.2 g, with bone accounting for about 30% as a central estimate (Zhu et al., 2010). These values are reasonably consistent with conclusions of Skalsky et al. (1983), who estimated a total body content of ~0.3 g with about 40% in bone based on a review of the literature.

(69) Priest et al. (1995) studied the biokinetics of ^{26}Al ($T_{1/2}$ = 7.2 × 10^5 y) administered intravenously as citrate to a healthy adult male. Less than 1% of the administered amount remained in blood after 2 d. Cumulative urinary and faecal excretion accounted for 83% and 1.8%, respectively, of the injected amount after 13 d. Total-body retention declined to ~4% by 1178 d. The investigators estimated a long-term biological half-time of 7 y.

(70) Talbot et al. (1995) investigated the kinetics of ^{26}Al in six healthy adult males over 5-6 d after intravenous administration as citrate. The concentration in blood was in the range 3.3-13% of injected ^{26}Al L^{-1} blood at 1 h and 0.093-0.73% L^{-1} at 1 d. Mean cumulative urinary ^{26}Al represented 59% (46-74%) of injected activity at 1 d and 72% (62-83%) at 5 d. Faecal excretion accounted for about 1% of injected ^{26}Al over the first 5 d. Mean total-body retention at 5 d represented 27% (16-36%) of administered activity.

(71) Important systemic repositories of aluminium identified in animal studies include bone, liver, and kidneys (Berlyne et al., 1972; Zafar et al., 1997; Wu et al., 2012). The brain shows a low rate of uptake of aluminium but a relatively long retention time (Yokel, 2002).

6.1.3.2. Biokinetic model for systemic aluminium

(72) The biokinetic model for aluminium applied in *Publication 151* (ICRP, 2022) to workers is applied here to adult members of the public. The transfer coefficients were set primarily for consistency of model predictions with two data sets: blood clearance, urinary and faecal excretion rates, and total-body retention of intravenously administered ^{26}Al in human subjects (Priest et al., 1995; Talbot et al., 1995), and the distribution of aluminium in adult males as indicated by autopsy data (Skalsky et al., 1983; Zhu et al., 2010). Transfer coefficients for the adult are assigned to pre-adult ages except that the ICRP's generic age-specific transfer coefficients are applied to activity transferring from bone surface to bone volume or blood and from bone volume to blood.

(73) The structure of the biokinetic model for systemic aluminium applied in this report is shown in Fig. 6.1. Transfer coefficients are listed in Table 6.2.

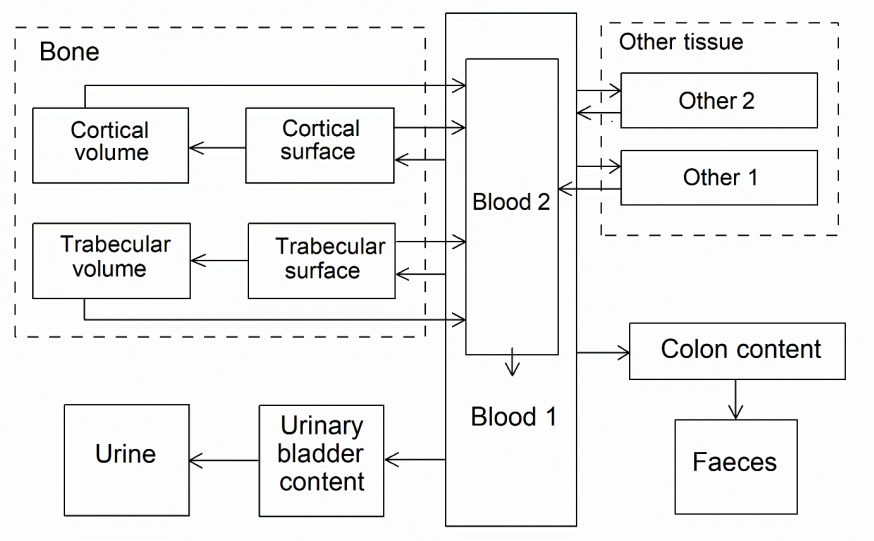

Fig. 6.1. Structure of the biokinetic model for systemic aluminium.

901 Table 6.2. Age-specific transfer coefficients for aluminium

		Transfer coefficients (d^{-1})					
Pathway		100 d	1 y	5 y	10 y	15 y	Adult
Blood 1	UB content	9.98E+00	9.98E+00	9.98E+00	9.98E+00	9.98E+00	9.98E+00
Blood 1	RC content	1.66E-01	1.66E-01	1.66E-01	1.66E-01	1.66E-01	1.66E-01
Blood 1	Trab surface	8.32E-02	8.32E-02	8.32E-02	8.32E-02	8.32E-02	8.32E-02
Blood 1	Cort surface	8.32E-02	8.32E-02	8.32E-02	8.32E-02	8.32E-02	8.32E-02
Blood 1	Other 1	5.74E+00	5.74E+00	5.74E+00	5.74E+00	5.74E+00	5.74E+00
Blood 1	Other 2	5.82E-01	5.82E-01	5.82E-01	5.82E-01	5.82E-01	5.82E-01
Blood 2	Blood 1	3.50E-02	3.50E-02	3.50E-02	3.50E-02	3.50E-02	3.50E-02
Other 1	Blood 1	5.00E-01	5.00E-01	5.00E-01	5.00E-01	5.00E-01	5.00E-01
Other 2	Blood 2	5.00E-04	5.00E-04	5.00E-04	5.00E-04	5.00E-04	5.00E-04
Trab surface	Blood 2	8.22E-03	2.88E-03	1.81E-03	1.32E-03	9.59E-04	4.93E-04
Trab surface	Trab volume	8.22E-03	2.88E-03	1.81E-03	1.32E-03	9.59E-04	2.47E-04
Trab volume	Blood 2	8.22E-03	2.88E-03	1.81E-03	1.32E-03	9.59E-04	4.93E-04
Cort surface	Blood 2	8.22E-03	2.88E-03	1.53E-03	9.04E-04	5.21E-04	8.21E-05
Cort surface	Cort volume	8.22E-03	2.88E-03	1.53E-03	9.04E-04	5.21E-04	4.11E-05
Cort volume	Blood 2	8.22E-03	2.88E-03	1.53E-03	9.04E-04	5.21E-04	8.21E-05

902 UB, urinary bladder; RC, right colon; Cort, cortical; Trab, trabecular.

903 6.2. Dosimetric data for aluminium

904 Table 6.3. Committed effective dose coefficients (Sv Bq^{-1}) for the inhalation or ingestion of
905 ^{26}Al compounds

	Effective dose coefficients (Sv Bq^{-1})					
	3 m	1 y	5 y	10 y	15 y	Adult
Inhaled particulate materials (1 µm AMAD aerosols)						
Type F	2.3E-08	2.1E-08	1.3E-08	9.9E-09	9.3E-09	1.1E-08
Type M, aluminium metal	5.9E-08	5.4E-08	3.3E-08	2.3E-08	1.9E-08	2.1E-08
Type S (default), aluminium oxide, fluoride, bauxite ore, chlorhydrate, sulphate, all unspecified forms	5.4E-07	5.6E-07	4.6E-07	3.9E-07	4.0E-07	4.2E-07
Ingested materials						
Soluble forms and aluminium in diet	7.7E-09	4.6E-09	2.8E-09	2.0E-09	1.4E-09	1.3E-09
Insoluble forms, all unspecified forms	5.0E-09	4.4E-09	2.6E-09	1.9E-09	1.3E-09	1.2E-09

906 AMAD, activity median aerodynamic diameter.

7. SILICON (Z=14)

7.1. Routes of Intake

7.1.1. Inhalation

(74) For silicon, default parameter values were adopted on absorption to blood from the respiratory tract (ICRP, 2015). Absorption parameter values and types, and associated f_A values for particulate forms of silicon are given in Table 7.1 [taken from Section 7 of *Publication 151* (ICRP, 2022)].

Table 7.1. Absorption parameter values for inhaled and ingested silicon.

		Absorption parameter values*		
Inhaled particulate materials		f_r	s_r (d^{-1})	s_s (d^{-1})
Default parameter values†,‡				
Absorption Type	Assigned forms			
F	-	1	30	-
M		0.2	3	0.005
S§		0.01	3	0.0001

Ingested materials¶

	Age-dependent absorption from the alimentary tract, f_A					
Assigned forms	3 months	1 year	5 years	10 years	15 years	adult
Silicon dioxide and silicates, silicon in food	0.02	0.01	0.01	0.01	0.01	0.01
Orthosilicic acid, silicon in drinking water	1	0.5	0.5	0.5	0.5	0.5

*It is assumed that the bound state can be neglected for silicon (i.e. $f_b = 0$). The values of s_r for Type F, M and S forms of silicon (30, 3 and 3 d^{-1} respectively) are the general default values.

†For inhaled material deposited in the respiratory tract and subsequently cleared by particle transport to the alimentary tract, the default f_A values for inhaled materials are applied: i.e. the product of f_r for the absorption type and the f_A value for ingested soluble forms of silicon applicable to the age-group of interest (e.g. 0.5 for adults).

‡Default Type M is recommended for use in the absence of specific information on which the exposure material can be assigned to an absorption type (e.g. if the form is unknown, or if the form is known but there is no information available on the absorption of that form from the respiratory tract).

§Activity transferred from systemic compartments into segments of the alimentary tract is assumed to be subject to reabsorption to blood. The default absorption fraction f_A for the secreted activity is the highest value for ingestion of the radionuclide applicable to the age-group of interest (e.g. 0.5 for adults).

7.1.2. Ingestion

7.1.2.1. Adults

(75) Silicon occurs naturally in food as silicon dioxide and silicates. Orthosilicic acid, formed by hydration of the oxide, is the major silicon species present in drinking water and other liquids. All forms of silica are considered to be poorly soluble particles which absorption is not well documented, except orthosilicic acid that is readily absorbed from the gastro-intestinal tract in humans. For details, see *Publication 151* (ICRP, 2022).

(76) In *Publications 30* and *72* (ICRP, 1981, 1995c), f_1 was taken to be 0.01 for all compounds of silicon. In *Publication 151* (ICRP, 2022) a value of $f_A = 0.01$ was used for silicon dioxide and silicates, and a larger $f_A = 0.5$ was adopted for orthosilicic acid. In this publication,

the same values of f_A = 0.01 and f_A = 0.5, respectively, are adopted for ingestion of silicon in food and in drinking water, respectively, by adult members of the public.

7.1.2.2. Children

(77) Consistently with the approach of *Publication56* (ICRP, 1990), an f_A = 0.02 is adopted here for ingestion of silicon dioxide and silicates and of silicon in diet by 3 month old infants ; an f_A = 1 is used for ingestion of orthosilicic acid and of silicon in drinking water by 3 month old infant. For children of older ages, the same values as for adults (f_A = 0.01 for silicon dioxide and silicates and for silicon in diet, f_A = 0.5 for orthosilicic acid and for silicon in drinking water) are used.

7.1.3. Systemic distribution, retention and excretion of silicon

7.1.3.1. Biokinetic data

(78) Popplewell et al. (1998) measured urinary excretion of ^{32}Si ($T_{1/2}$ =132 y) following ingestion by a healthy adult male human. About 34% of ingested activity was excreted over 0-12 h, 1% over 12-24 h, and 0.5% over 24- 48 h.

(79) Sauer et al. (1959) measured the concentration of ^{31}Si in tissue of guinea pigs over the first 8 h after oral administration of $^{31}SiO_2$. The highest concentration was found in kidney at all measurement times, but the liver contained roughly twice as much and the skeletal muscle 20-50 times as much total activity as the kidneys.

(80) Adler et al. (1986) studied the behaviour of ^{31}Si in rats after injection of $^{31}Si(OH)_4$. Activity in blood was nearly equally distributed between plasma and erythrocytes. The highest tissue concentration at 1-2 h was found in kidney. At 3 h nearly equal concentrations were seen in kidney and liver. Initially, ~85% of total-body activity was found in skin, muscle, and bone. An increasing concentration ratio of bone to plasma was observed over the first few hours.

(81) Berlyne et al. (1986) studied the distribution of ^{31}Si in rats 30 min after its injection as ^{31}S-labeled silicic acid. The highest concentration was found in kidney, followed by skin and testis (each 0.35, normalized to 1.0 for kidney), bone (0.30), and liver (0.25). The skeletal muscle, skin, bone, liver, and kidneys contained about 15%, 11%, 3.4%, 1.6%, and 1.5%, respectively, of the administered amount.

(82) Silicon and germanium are chemical analogues and show similar biokinetics. Mehard and Volcani (1975) compared the kinetics of ^{31}Si ($T_{1/2}$ = 157 min) and ^{68}Ge (271 d) in rats after intravenous (IV) or intraperitoneal (IP) injection of $^{31}Si(OH)_4$ and $^{68}Ge(OH)_4$. The peak concentration of ^{31}Si in kidney was about 3 times that in liver following IV injection and about 5 times that in liver following IP injection. An apparent difference in kinetics of ^{68}Ge and ^{31}Si was more rapid depletion of ^{68}Ge. The concentration of ^{31}Si in the liver was moderately higher than that of ^{68}Ge over the first two hours after intravenous injection.

7.1.3.2. Biokinetic model for systemic silicon

(83) The biokinetic model for systemic silicon applied to workers in *Publication 151* (ICRP, 2022) is applied in this report to adult members of the public. The basis for the model is described in that report. The same model is applied to preadults except that increased rates of loss from bone compartments are assigned to preadults, as the rate of removal from bone is based on the bone turnover rate. The bone turnover rates applied in the model are reference values given in *Publication 89* (ICRP, 2002).

(84) The structure of the biokinetic model for systemic silicon used in this report is shown in Fig. 7.1. Transfer coefficients are listed in Table 7.2.

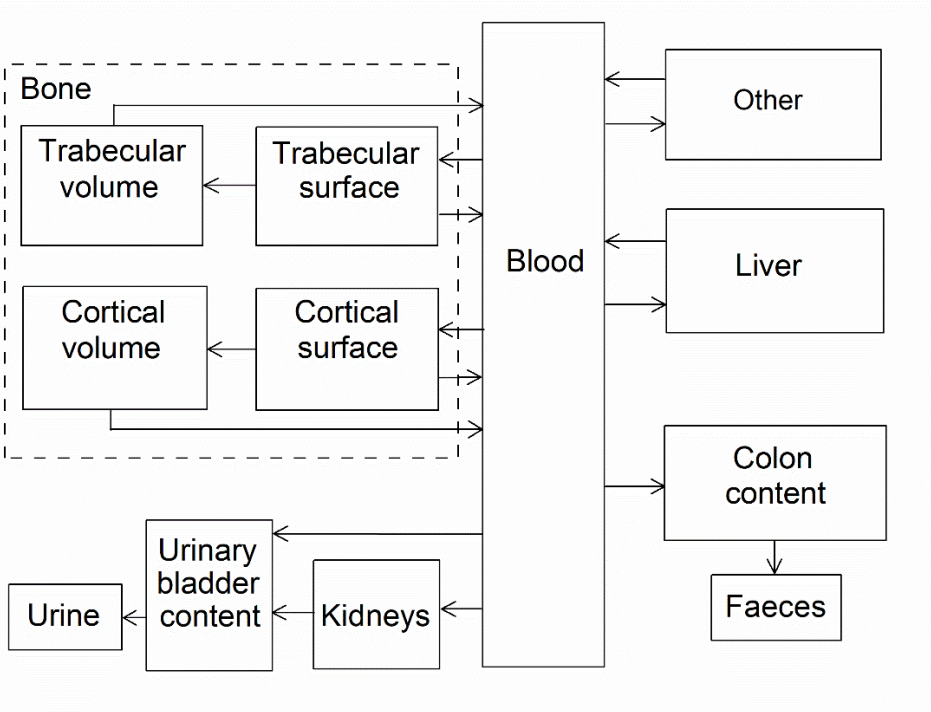

Fig. 7.1. Structure of the biokinetic model for systemic silicon.

Table 7.2. Age-specific transfer coefficients for silicon.

		Transfer coefficients (d^{-1})					
Pathway		100 d	1 y	5 y	10 y	15 y	Adult
Blood	Other	1.20E+00	1.20E+00	1.20E+00	1.20E+00	1.20E+00	1.20E+00
Blood	Kidneys	2.71E-01	2.71E-01	2.71E-01	2.71E-01	2.71E-01	2.71E-01
Blood	Liver	5.41E-01	5.41E-01	5.41E-01	5.41E-01	5.41E-01	5.41E-01
Blood	UB content	7.70E+00	7.70E+00	7.70E+00	7.70E+00	7.70E+00	7.70E+00
Blood	RC content	1.35E-02	1.35E-02	1.35E-02	1.35E-02	1.35E-02	1.35E-02
Blood	Trab surface	1.35E-01	1.35E-01	1.35E-01	1.35E-01	1.35E-01	1.35E-01
Blood	Cort surface	1.35E-01	1.35E-01	1.35E-01	1.35E-01	1.35E-01	1.35E-01
Other	Blood	3.00E-01	3.00E-01	3.00E-01	3.00E-01	3.00E-01	3.00E-01
Kidneys	UB content	1.20E+00	1.20E+00	1.20E+00	1.20E+00	1.20E+00	1.20E+00
Liver	Blood	9.00E-01	9.00E-01	9.00E-01	9.00E-01	9.00E-01	9.00E-01
Trab surface	Blood	3.00E-01	3.00E-01	3.00E-01	3.00E-01	3.00E-01	3.00E-01
Cort surface	Blood	3.00E-01	3.00E-01	3.00E-01	3.00E-01	3.00E-01	3.00E-01
Trab surface	Trab volume	1.50E-03	1.50E-03	1.50E-03	1.50E-03	1.50E-03	1.50E-03
Cort surface	Cort volume	1.50E-03	1.50E-03	1.50E-03	1.50E-03	1.50E-03	1.50E-03
Trab volume	Blood	8.22E-03	2.88E-03	1.81E-03	1.32E-03	9.59E-04	4.93E-04
Cort volume	Blood	8.22E-03	2.88E-03	1.53E-03	9.04E-04	5.21E-04	8.21E-05

UB, urinary bladder; RC, right colon; Cort, cortical; Trab, trabecular.

7.1.3.3. Treatment of radioactive progeny

(85) The treatment of radioactive progeny produced in systemic compartments after intake of a radioisotope of silicon is described in Section 7.2.3.3. of *Publication 151* (ICRP, 2022).

7.2. Dosimetric data for silicon

Table 7.3. Committed effective dose coefficients (Sv Bq^{-1}) for the inhalation or ingestion of ^{32}Si compounds.

	Effective dose coefficients (Sv Bq^{-1})					
	3m	1y	5y	10y	15y	Adult
Inhaled particulate materials (1 µm AMAD aerosols)						
Type F	8.3E-10	4.4E-10	1.9E-10	1.2E-10	9.3E-11	7.5E-11
Type M, default	4.6E-08	4.2E-08	2.5E-08	1.7E-08	1.3E-08	1.3E-08
Type S	4.8E-07	5.0E-07	4.0E-07	3.3E-07	3.4E-07	3.5E-07
Ingested materials						
Silicon dioxide and silicates, silicon in food	3.5E-10	2.1E-10	1.1E-10	6.9E-11	5.0E-11	3.8E-11
Orthosilicic acid, silicon in drinking water	1.3E-09	5.2E-10	2.6E-10	1.6E-10	1.4E-10	1.1E-10

AMAD, activity median aerodynamic diameter.

8. CHLORINE (Z=17)

8.1. Routes of Intake

8.1.1. Inhalation

(86) For chlorine, default parameter values were adopted for the absorption to blood from the respiratory tract (ICRP, 2015). Absorption parameter values and types, and associated f_A values for gas and vapour forms of chlorine are given in Table 8.1 and for particulate forms in Table 8.2 [both taken from Section 8 of *Publication 151* (ICRP, 2022)]. By analogy with the halogen iodine, considered in detail in *Publication 137* (ICRP, 2017), default Type F is recommended for particulate forms in the absence of specific information on which the exposure material can be assigned to an absorption type.

(87) For chlorine, and the other halogens, intakes could be in both particulate and gas and vapour forms, and it is therefore assumed that inhaled chlorine is 50% particulate and 50% gas/vapour in the absence of information (ICRP, 2002b).

Table 8.1. Deposition and absorption for gas and vapour compounds of chlorine.

	Percentage deposited (%)*						Absorption†	
Chemical form/origin	Total	ET_1	ET_2	BB	bb	AI	Type	Absorption from the alimentary tract, f_A‡,¶
Unspecified	100	0	20	10	20	50	F	1.0

ET_1, anterior nasal passage; ET_2, posterior nasal passage, pharynx and larynx; BB, bronchial; bb, bronchiolar; AI, alveolar-interstitial.

*Percentage deposited refers to how much of the material in the inhaled air remains in the body after exhalation. Almost all inhaled gas molecules contact airway surfaces but usually return to the air unless they dissolve in, or react with, the surface lining. The default distribution between regions is assumed: 20% ET_2, 10% BB, 20% bb, and 50% AI.

†It is assumed that the bound state can be neglected for chlorine (i.e. $f_b = 0$).

‡For inhaled material deposited in the respiratory tract and subsequently cleared by particle transport to the alimentary tract, the default f_A values for inhaled materials are applied [i.e. the product of f_r for the absorption type (or specific value where given) and the f_A value for ingested soluble forms of chlorine (1.0)].

¶The value of $f_A = 1.0$ is applicable to all age-groups.

Table 8.2. Absorption parameter values for inhaled and ingested chlorine.

	Absorption parameter values*		
Inhaled particulate materials	f_r	s_r (d^{-1})	s_s (d^{-1})
Default parameter values†			
Absorption type			
F‡	1	30	–
M	0.2	3	0.005
S	0.01	3	1×10^{-4}

Ingested materials§

	Age-dependent absorption from the alimentary tract, f_A					
Assigned forms	3 months	1 year	5 years	10 years	15 years	adult
All compounds	1	1	1	1	1	1

*It is assumed that the bound state can be neglected for chlorine (i.e. $f_b = 0$). The values of s_r for Type F, M and S forms of chlorine (30, 3 and 3 d^{-1} respectively) are the general default values.

[†]For inhaled material deposited in the respiratory tract and subsequently cleared by particle transport to the alimentary tract, the default f_A values for inhaled materials are applied: i.e. the product of f_r for the absorption type and the f_A value for ingested soluble forms of chlorine (1).

[‡]Default Type F is recommended for use in the absence of specific information on which the exposure material can be assigned to an absorption type (e.g. if the form is unknown, or if the form is known but there is no information available on the absorption of that form from the respiratory tract).

[§]Activity transferred from systemic compartments into segments of the alimentary tract is assumed to be subject to reabsorption to blood. The default absorption fraction f_A for the secreted activity is the highest value for any form of the radionuclide ($f_A = 1$).

8.1.2. Ingestion

(88) Ingested chlorine is largely absorbed from the gut. For details, see *Publication 151* (ICRP, 2022). In *Publications 30*, *72* (ICRP, 1980, 1995c) and *Publication 151*, the fractional absorption was taken to be 1 for all compounds of chlorine. In this publication, an $f_A = 1$ is also used for all chemical forms of chlorine ingested at all ages.

8.1.3. Systemic distribution, retention and excretion of chlorine

8.1.3.1. Biokinetic data

(89) The dominant form of chlorine in the human body is inorganic chloride. Ingested chloride is rapidly and nearly completely absorbed to blood and largely cleared from blood within a few minutes (Ray et al., 1952). It is distributed mainly in extracellular fluids. The biological half-time for the total body is typically on the order of 8-15 d (Ray et al., 1952) but may be reduced by elevated intake of chloride or increased by a salt-deficient diet.

(90) The systemic kinetics of chloride closely resembles that of bromide (Reid et al., 1956; Pavelka, 2004). Absorbed bromide clears rapidly from blood and replaces part of the extracellular chloride, with the molar sum of chloride and bromide remaining constant at about 110 mmol/L (Pavelka, 2004). The biological half-time of bromide in the human body typically is on the order of 12 d (Söremark, 1960).

8.1.3.2. Biokinetic model for systemic chlorine

(91) The biokinetic model for systemic chlorine in workers (ICRP, 2002) is applied in this report to all age groups. The systemic behaviour of chlorine is assumed to be the same as that of bromine. The relevant physiological forms of chlorine and bromine are assumed to be chloride and bromide, respectively. The common biokinetic model for chloride and bromide is based on the assumptions of rapid removal from blood ($T_{1/2}$ = 5 min), a uniform distribution in tissues, removal of 50% of absorbed chloride or bromide from the body in 12 d, and a urinary to faecal excretion ratio of 100:1. These conditions are approximated, using a first-order recycling model, with the transfer coefficients listed in Table 8.3.

Table 8.3. Age-specific transfer coefficients for chlorine.

		Transfer coefficients (d^{-1})					
Pathway		100 d	1 y	5 y	10 y	15 y	Adult
Blood	Other	2.00E+02	2.00E+02	2.00E+02	2.00E+02	2.00E+02	2.00E+02
Blood	UB content	8.30E-01	8.30E-01	8.30E-01	8.30E-01	8.30E-01	8.30E-01
Blood	RC content	8.30E-03	8.30E-03	8.30E-03	8.30E-03	8.30E-03	8.30E-03
Other	Blood	1.50E+01	1.50E+01	1.50E+01	1.50E+01	1.50E+01	1.50E+01

UB, urinary bladder; RC, right colon.

8.1.3.3. Treatment of radioactive progeny

(92) The treatment of radioactive progeny produced in systemic compartments after intake of a radioisotope of chlorine is described in Section 8.2.3.3. of *Publication 151* (ICRP, 2022).

8.2. Dosimetric data for chlorine

Table 8.4. Committed effective dose coefficients (Sv Bq^{-1}) for the inhalation or ingestion of ^{36}Cl compounds.

	Effective dose coefficients (Sv Bq^{-1})					
Inhaled gases or vapours	3m	1y	5y	10y	15y	Adult
Unspecified	9.3E-09	6.3E-09	3.3E-09	1.9E-09	1.2E-09	1.0E-09
Inhaled particulate materials (1 μm AMAD aerosols)						
Type F, default	4.9E-09	3.3E-09	1.5E-09	8.9E-10	4.9E-10	4.3E-10
Type M	2.0E-08	1.8E-08	1.0E-08	6.6E-09	5.1E-09	4.9E-09
Type S	1.6E-07	1.7E-07	1.3E-07	1.0E-07	1.0E-07	1.1E-07
Ingested materials						
All compounds	9.1E-09	6.2E-09	3.2E-09	1.9E-09	1.2E-09	9.9E-10

AMAD, activity median aerodynamic diameter.

9. POTASSIUM (Z = 19)

9.1. Routes of Intake

9.1.1. Inhalation

(93) For potassium, default parameter values were adopted on absorption to blood from the respiratory tract (ICRP, 2015). Absorption parameter values and types, and associated f_A values for particulate forms of potassium are given in Table 9.1 [taken from Section 9 of *Publication 151* (ICRP, 2022)].

Table 9.1. Absorption parameter values for inhaled and ingested potassium.

	Absorption parameter values*		
Inhaled particulate materials	f_r	s_r (d^{-1})	s_s (d^{-1})
Default parameter values†			
Absorption type			
F	1	30	–
M‡	0.2	3	0.005
S	0.01	3	1×10^{-4}

Ingested materials§

	Age-dependent absorption from the alimentary tract, f_A					
Assigned forms	3 months	1 year	5 years	10 years	15 years	adult
All compounds	1	1	1	1	1	1

*It is assumed that the bound state can be neglected for potassium (i.e. $f_b = 0$). The values of s_r for Type F, M, and S forms of potassium (30, 3, and 3 d^{-1} respectively) are the general default values.

†For inhaled material deposited in the respiratory tract and subsequently cleared by particle transport to the alimentary tract, the default f_A values for inhaled materials are applied: i.e. the product of f_r for the absorption type and the f_A value for ingested soluble forms of potassium (1).

‡Default Type M is recommended for use in the absence of specific information on which the exposure material can be assigned to an absorption type (e.g. if the form is unknown, or if the form is known but there is no information available on the absorption of that form from the respiratory tract).

§Activity transferred from systemic compartments into segments of the alimentary tract is assumed to be subject to reabsorption to blood. The default absorption fraction f_A for the secreted activity is the highest value for any form of the radionuclide ($f_A = 1$).

9.1.2. Ingestion

(94) Absorption of potassium from the gastrointestinal tract being nearly complete, it has been taken to be 100% in *Publications 30*, *72* and *151* (ICRP, 1980, 1995c, 2022). In this publication, $f_A = 1$ is also used for all forms of potassium ingested at all ages.

9.1.3. Systemic distribution, retention and excretion of potassium

9.1.3.1. Biokinetic data

(95) The alkali metal potassium is an essential element with multiple functions in the human body including regulation of fluid balance and control of electrical activity of the heart, skeletal muscle, and nerves. The concentration of K in the human body is about 2 g kg^{-1} body mass but varies with a variety of factors, particularly the mass of muscle as a fraction of body mass. Measurements of K concentrations in postmortem tissues and in plasma and red blood

cells of living subjects indicate the following approximate distribution of K in an adult male human: skeletal muscle, 65% of the total-body content, skeleton 9%, red blood cells 8%, liver 3%, brain 3%, kidneys 0.6%, blood plasma 0.4%, and remainder 11% (based on a review by Leggett and Williams, 1986, and a detailed autopsy study by Zhu et al., 2010). About 85% of losses from the body are in urine, with the remainder removed mainly in faeces and sweat.

(96) About 98% of the body's K resides in cells, and 2% is distributed in extracellular fluids (ECF). The ECF concentration is maintained in a range of about 137-215 mg L^{-1}. The kidneys are primarily responsible for homeostatic control of the body's K content through adjustment of urinary losses to accommodate variation in K intake. Adjustments in renal K excretion occur over several hours, and changes in extracellular K are buffered during that time by movement of K between skeletal muscle and blood plasma (Langham-New and Lambert, 2012; Palmer, 2015; Hinderling, 2016; Udensi and Tchounwou, 2017).

(97) Intravenously injected radio-potassium is rapidly removed from blood plasma and distributed almost entirely to tissues, but a small percentage enters excretion pathways (Corsa et al., 1950; Black et al., 1955; Burch et al., 1955). About 2% remains in plasma at 20 min and 1% or less remains at 2 h (Corsa et al., 1950; Black et al., 1955). The rate of transfer of K from plasma to a tissue depends on the percentage of cardiac output received by the tissue and the tissue's K extraction fraction, i.e., the fraction of K extracted by the tissue from plasma during a single passage from the tissue's arterial input to its venous output. For example, a K extraction fraction of ~0.9 has been estimated for kidneys, heart tissue, and lung tissue; ~0.8 for intestines, ~0.6 for liver, and ~0.01-0.02 for brain (review by Leggett and Williams, 1986). The kidneys, which have a high K extraction fraction and receive roughly a fifth of cardiac output, accumulate as much as 20% of an intravenously injected K tracer within a few minutes (Emery et al, 1955; Black et al., 1955). Tissues with a low blood perfusion rate such as fat or resting skeletal muscle, or a low extraction fraction such as brain, accumulate the tracer relatively slowly. Tissues such as kidneys with a high rate of uptake but a relatively low content of K return much of the accumulated tracer to blood over a short period (Black, 1955). After several hours, skeletal muscle typically contains most of the retained amount. The red blood cells gradually accumulate several percent of the injected amount over 2-3 d (Corsa et al., 1950).

(98) Various aspects of the biokinetics of K have been studied in human subjects and laboratory animals (Love and Burch, 1953; Ginsburg and Wilde, 1954; Black et al., 1955; Ginsburg, 1962; Johnson et al., 1969; Jasani and Edmonds, 1971; Downey and Bashour, 1975; Sterns et al., 1979; ICRP, 1980; Leggett and Williams, 1986; Hinderling, 2016). A detailed, physiologically based biokinetic model for systemic K in adult humans was proposed by Leggett and Williams (1986). The model was built around a blood flow model depicting the distribution of cardiac output to 12 tissue compartments. Additional compartments were added to address transfer of K between plasma and red blood cells and between systemic pools and gastrointestinal content. Removal from the body was assumed to be primarily in urine with relatively small losses in faeces and sweat. Movement of K was depicted as a system of first-order processes. The transfer rate from plasma into a tissue T was estimated as the product of the plasma flow rate to that tissue and a tissue-specific extraction fraction, E_T. The transfer rate from tissue T to plasma was estimated from the inflow rate and the relative contents of K in plasma and tissue T at equilibrium based mainly on autopsy data for K and typical concentrations of K in plasma and red blood cells. Transfer rates between plasma and red blood cells and between systemic compartments and gastrointestinal contents were based on empirical data. Model predictions of the blood clearance, uptake and loss by systemic tissues, total-body retention, and path-specific excretion rates of K were consistent with observations for human subjects. The model predicts that the biological half-time of an intravenously injected tracer in an adult is ~31 d, derived as the time for the total-body content to decrease from 50% to 25% of the injected amount.

(99) The biokinetic model for systemic K applied in *Publication 30*, Part 2 (ICRP, 1980), depicted total-body K in an adult human as a well-mixed pool from which K is removed with a biological half-time of 30 d. This half-time was based on daily intake of 3.3 g K and total-body content of 140 g K for a reference adult (ICRP, 1975). Similar derivations of biological half-times of K in pre-adults based on reported age-specific dietary K (e.g., Alaimo et al., 1994; Hunt and Meachum, 2001; Hoy et al., 2012) and estimated total-body K (e.g. Flynn et al., 1972; Novak, 1973; Lloyd et al., 1973; Lebedev and Yakovlev, 1993) are variable but suggest monotonically increasing biological half-times from infancy to age 15 y. Central estimates are roughly 10 d for the first year of life, 15 d for age 5 y, 20 d for age 10 y, and 30 d for age 15 y.

(100) The alkali metal rubidium (Rb) is a close chemical and physiological analogue of K. The section on Rb in this report cites studies indicating that the rate of biological removal of radio-rubidium from the body in the early hours or days after injection is about two-thirds that of radio-potassium. This is consistent with relative biological half-times of K (30 d) and Rb (44 d) estimated for adults in *Publication 30*, Part 2 (ICRP, 1980). The following long-term biological half-times for Rb in pre-adults were based on data on retention of radio-rubidium in healthy children and adults and the similarity in the kinetics of Rb and the frequently studied physiological analogue caesium (Cs) early in life: 17 d for age 100 d, 19 d for age 1 y, 25 d for age 5 y, 31 d for age 10 y, and 41 d for age 15 y. Assuming the rate of loss of Rb from the body is two-thirds that of K, the estimated long-term biological half-times of K are about 11, 13, 17, 21, and 27 d for ages 100 d, 1 y, 5 y, 10 y, and 15 y, respectively. These half-times are reasonably consistent with values based on age-specific intake and total-body content of K.

9.1.3.2. Biokinetic model for systemic potassium

(101) The biokinetic model for systemic K in workers used in *Publication 151* (ICRP, 2022) is a simplification of the model of Leggett and Williams (1986) with a structure (Fig. 9.1) more consistent with the structures of other systemic models applied in this report series. That is, the model depicts a central blood compartment (plasma) in exchange with a set of peripheral tissue compartments representing relatively important systemic repositories of K. In *Publication 151* the transfer coefficients were set for consistency with the original model (Leggett and Williams, 1986) regarding retention in the total body as well as in individual tissues that were depicted explicitly in both the original and simplified versions of the model.

(102) The biokinetic model for systemic K applied to workers in *Publication 151* is applied in this report to adult members of the public. The model is extended to pre-adult ages by adjustment of transfer coefficients to reflect pertinent anatomical or physiological changes during growth and to approximate the following estimated long-term biological half-times in the total body based on the assumed relation of K and Rb retention: 11 d for infants, 13 d for age 1 y, 17 d for age 5 y, 21 d for age 10 y, and 27 d for age 15 y.

(103) The following adjustments of the model for adults are made for application to pre-adult ages:

- The transfer rate from plasma to skeletal muscle at ages 100 d, 1 y, 5 y, and 10 y is assumed to be 0.5, 0.5, 0.7, and 0.85, respectively, times the transfer rate for the adult based on changes with age in muscle mass as a percentage of total-body mass.
- For infants and children through age 10 y, the transfer rates from plasma to bone surface compartments are set at twice the value for the adult to reflect a high blood flow rate to bone compared with adults.
- The transfer rate from plasma to the compartment Other is modified to maintain the same outflow rate from plasma at all ages, that is, to balance the changes in transfer from plasma to skeletal muscle and bone surface.

- For ages 100 d through 15 y, flow rates out of tissue compartments (Kidneys, Muscle, Cortical and Trabecular bone surface, Red marrow, Other) in the model for adults are increased by the following factors to approximate the age-specific biological half-times for the total-body retention times indicated above: 2.3 for age 100 d, 1.8 for age 1 y, 1.6 for age 5 y, 1.4 for age 10 y, and 1.1 for age 15 y. The observed (and modeled) half-time of K in the body depends to some extent on the observation period. The indicated values are based on the time required for the total-body content to decline from 50% to 25% of an acute input to blood.

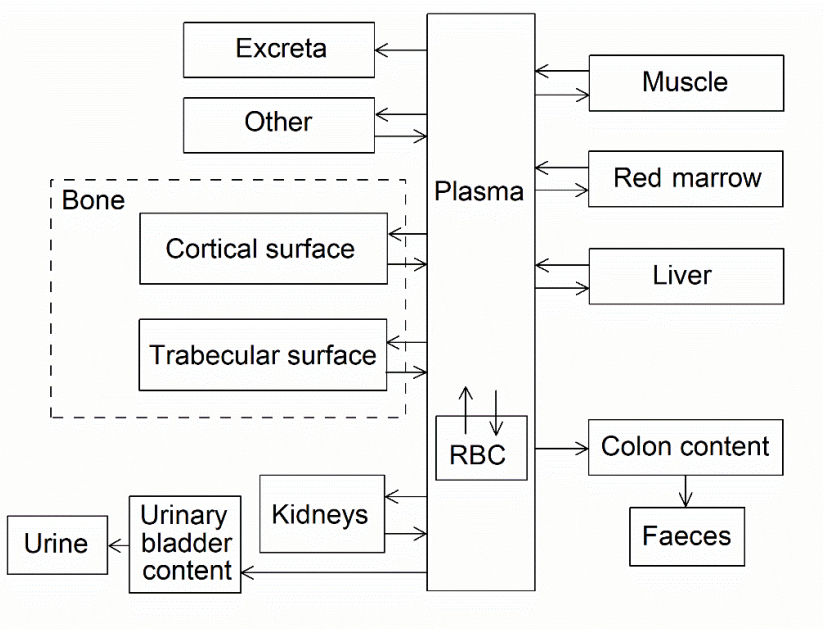

Fig. 9.1. Structure of the biokinetic model for systemic potassium.

Table 9.2. Age-specific transfer coefficients for potassium.

		Transfer coefficients (d^{-1})					
Pathway		100 d	1 y	5 y	10 y	15 y	Adult
Blood	RBC	6.00E+00	6.00E+00	6.00E+00	6.00E+00	6.00E+00	6.00E+00
Blood	Kidneys	2.57E+02	2.57E+02	2.57E+02	2.57E+02	2.57E+02	2.57E+02
Blood	Liver	2.30E+02	2.30E+02	2.30E+02	2.30E+02	2.30E+02	2.30E+02
Blood	Muscle	1.28E+02	1.28E+02	1.79E+02	2.17E+02	2.55E+02	2.55E+02
Blood	Trab surface	3.36E+01	3.36E+01	3.36E+01	3.36E+01	1.68E+01	1.68E+01
Blood	Cort surface	2.24E+01	2.24E+01	2.24E+01	2.24E+01	1.12E+01	1.12E+01
Blood	Red marrow	2.80E+01	2.80E+01	2.80E+01	2.80E+01	2.80E+01	2.80E+01
Blood	Other	5.70E+02	5.70E+02	5.19E+02	4.80E+02	4.70E+02	4.70E+02
Blood	UB content	5.50E+00	5.50E+00	5.50E+00	5.50E+00	5.50E+00	5.50E+00
Blood	RC content	8.30E-01	8.30E-01	8.30E-01	8.30E-01	8.30E-01	8.30E-01
Blood	Excreta	2.00E-01	2.00E-01	2.00E-01	2.00E-01	2.00E-01	2.00E-01
RBC	Blood	3.80E-01	3.80E-01	3.80E-01	3.80E-01	3.80E-01	3.80E-01
Kidneys	Blood	4.92E+02	3.85E+02	3.42E+02	3.00E+02	2.35E+02	2.14E+02
Liver	Blood	5.64E+01	4.41E+01	3.92E+01	3.43E+01	2.70E+01	2.45E+01
Muscle	Blood	3.11E+00	2.43E+00	2.16E+00	1.89E+00	1.49E+00	1.35E+00
Trab surface	Blood	6.14E+00	4.81E+00	4.27E+00	3.74E+00	2.94E+00	2.67E+00
Cort surface	Blood	6.14E+00	4.81E+00	4.27E+00	3.74E+00	2.94E+00	2.67E+00
Red marrow	Blood	6.14E+00	4.81E+00	4.27E+00	3.74E+00	2.94E+00	2.67E+00
Other	Blood	2.76E+01	2.16E+01	1.92E+01	1.68E+01	1.32E+01	1.20E+01

RBC, red blood cells; UB, urinary bladder; RC, right colon; Cort, cortical; Trab, trabecular.

9.1.3.3. Treatment of radioactive progeny

(104) The treatment of radioactive progeny produced in systemic compartments after intake of a radioisotope of potassium is described in Section 9.2.3.3. of *Publication 151* (ICRP, 2022).

9.2. Dosimetric data for potassium

Table 9.3. Committed effective dose coefficients (Sv Bq-1) for the inhalation or ingestion of ^{40}K compounds.

	Effective dose coefficients (Sv Bq^{-1})					
	3m	1y	5y	10y	15y	Adult
Inhaled particulate materials (1 μm AMAD aerosols)						
Type F	9.0E-09	7.6E-09	3.5E-09	2.3E-09	1.6E-09	1.4E-09
Type M, default	4.0E-08	3.6E-08	2.1E-08	1.4E-08	1.1E-08	1.1E-08
Type S	3.7E-07	3.9E-07	3.2E-07	2.6E-07	2.7E-07	2.8E-07
Ingested materials						
All compounds	1.7E-08	1.4E-08	7.8E-09	4.9E-09	3.8E-09	3.2E-09

AMAD, activity median aerodynamic diameter.

10. SCANDIUM (Z=21)

10.1. Routes of Intake

10.1.1. Inhalation

(105) For scandium, default parameter values were adopted on absorption to blood from the respiratory tract (ICRP, 2015). Absorption parameter values and types, and associated f_A values for particulate forms of scandium are given in Table 10.1 [taken from Section 10 of *Publication 151* (ICRP, 2022)].

Table 10.1. Absorption parameter values for inhaled and ingested scandium.

	Absorption parameter values*		
Inhaled particulate materials	f_r	s_r (d^{-1})	s_s (d^{-1})
Default parameter values†			
Absorption type			
F	1	30	–
M‡	0.2	3	0.005
S	0.01	3	1×10^{-4}

Ingested materials§	Age-dependent absorption from the alimentary tract, f_A					
Assigned forms	3 months	1 year	5 years	10 years	15 years	adult
All compounds	0.01	0.001	0.001	0.001	0.001	0.001

*It is assumed that the bound state can be neglected for scandium (i.e. $f_b = 0$). The values of s_r for Type F, M and S forms of scandium (30, 3 and 3 d^{-1} respectively) are the general default values.

†For inhaled material deposited in the respiratory tract and subsequently cleared by particle transport to the alimentary tract, the default f_A values for inhaled materials are applied: i.e. the product of f_r for the absorption type and the f_A value for ingested soluble forms of silicon applicable to the age-group of interest (e.g. 0.001 for adults).

‡Default Type M is recommended for use in the absence of specific information on which the exposure material can be assigned to an absorption type (e.g. if the form is unknown, or if the form is known but there is no information available on the absorption of that form from the respiratory tract).

§Activity transferred from systemic compartments into segments of the alimentary tract is assumed to be subject to reabsorption to blood. The default absorption fraction f_A for the secreted activity is the highest value for ingestion of the radionuclide applicable to the age-group of interest (e.g. 0.001 for adults).

10.1.2. Ingestion

10.1.2.1. Adults

(106) The limited information available indicates that the absorption of scandium is small, see *Publication 151* (ICRP, 2022) for details. In *Publications 30* and *72* (ICRP, 1981, 1995c), f_1 was taken to be 10^{-4} by analogy with yttrium. A value of $f_A = 10^{-3}$ was adopted in *Publication 151* for all chemical forms of scandium. The same value is used in this publication for ingestion of all forms of scandium by adult members the public.

10.1.2.2. Children

(107) Consistently with the approach of *Publication56* (ICRP, 1990), an $f_A = 0.01$ is adopted here for 3 month old infants and the adult value of $f_A = 10^{-3}$ is used for older children.

10.1.3. Systemic distribution, retention and excretion of scandium

10.1.3.1. Biokinetic data

(108) Scandium is the lightest of the rare earth elements, which also include yttrium and the 15 lanthanide elements. These elements have similar chemical properties and are generally found together in nature. The biokinetics of scandium has been studied in laboratory animals including rats, mice, and rabbits (Durbin, 1960; Rosoff et al., 1963; Taylor et al., 1966; Basse-Cathalinat et al., 1968; Zalikin et al., 1969; Hara and Freed, 1973; Freed et al., 1975; Lachine et al., 1976) and to a limited extent in human subjects (Rosoff et al., 1965). Identified sites of elevated deposition of scandium include liver, spleen, kidneys, bone, and bone marrow. The relative contents of scandium in those tissues as well as its rates of urinary and faecal excretion vary considerably among studies, presumably due to differences in study conditions including chemical form, level of colloid formation after administration, and animal species. Much of the available biokinetic information on scandium kinetics comes from interpretation of the behaviour of ^{47}Sc produced in the body after administration of ^{47}Ca or partly produced in the body after administration of a mixture of ^{47}Ca and ^{47}Sc. Overall, the biokinetics of scandium appears to be broadly similar to that of the adjacent element yttrium in the periodic table.

10.1.3.2. Biokinetic model for systemic scandium

(109) The biokinetic model for systemic scandium applied to workers in *Publication 151* (ICRP, 2022) is adopted for use in this report and is extended here to preadults.

(110) The model structure is shown in Fig. 10.1. Age-specific transfer coefficients are listed in Table 10.2.

(111) The model structure is a modification of the generic model structure for bone-surface-seeking radionuclides. Scandium is treated as a bone-surface seeker based on analogy with its chemical analogue yttrium. In *Publication 151* the spleen was added to the generic model structure for bone-surface seekers as this organ appears to be an important repository for scandium in laboratory animals. The generic structure was further modified regarding routes of transfer to and from bone marrow compartments based on indications from animal studies of relatively high transfer of scandium from plasma to marrow.

(112) The transfer coefficients describing outflow from bone tissue compartments are default age-specific values for bone-surface seekers. The remaining transfer coefficients were set as far as feasible for consistency with the biokinetic database for scandium. Where data for scandium were lacking, parameter values were based on analogy with yttrium.

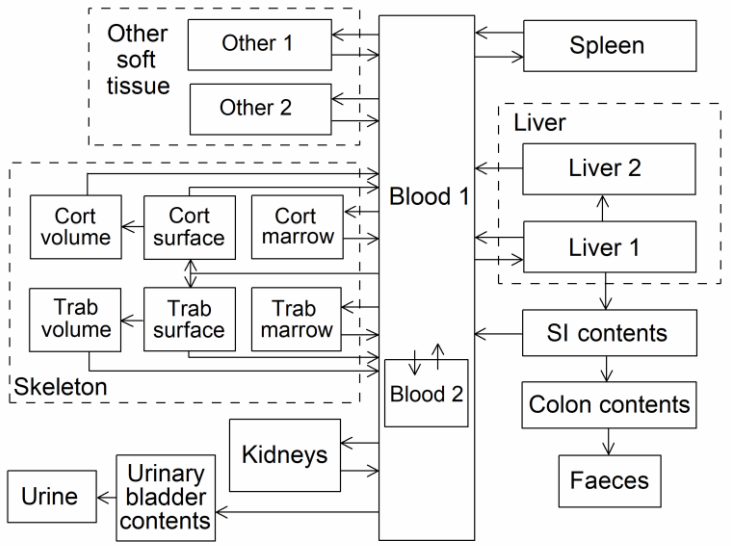

Fig. 10.1. Structure of the biokinetic model for systemic scandium.

Table 10.2. Age-specific transfer coefficients for scandium.

		Transfer coefficients (d^{-1})					
Pathway		100 d	1 y	5 y	10 y	15 y	Adult
Blood 1	Blood 2	4.25E-01	4.38E-01	4.38E-01	4.38E-01	4.38E-01	4.50E-01
Blood 1	UB content	5.10E-02	5.25E-02	5.25E-02	5.25E-02	5.25E-02	5.40E-02
Blood 1	Liver 1	5.67E-01	5.83E-01	5.83E-01	5.83E-01	5.83E-01	6.00E-01
Blood 1	Kidneys	8.50E-02	8.75E-02	8.75E-02	8.75E-02	8.75E-02	9.00E-02
Blood 1	Spleen	5.67E-02	5.83E-02	5.83E-02	5.83E-02	5.83E-02	6.00E-02
Blood 1	Trab marrow	1.42E-01	1.46E-01	1.46E-01	1.46E-01	1.46E-01	1.50E-01
Blood 1	Cort marrow	1.42E-01	1.46E-01	1.46E-01	1.46E-01	1.46E-01	1.50E-01
Blood 1	Trab surface	2.25E-01	1.88E-01	1.88E-01	1.88E-01	1.88E-01	1.50E-01
Blood 1	Cort surface	2.25E-01	1.88E-01	1.88E-01	1.88E-01	1.88E-01	1.50E-01
Blood 1	Other 1	5.67E-01	5.83E-01	5.83E-01	5.83E-01	5.83E-01	6.00E-01
Blood 1	Other 2	5.16E-01	5.31E-01	5.31E-01	5.31E-01	5.31E-01	5.46E-01
Blood 2	Blood 1	4.62E-01	4.62E-01	4.62E-01	4.62E-01	4.62E-01	4.62E-01
Liver 1	SI content	5.78E-02	5.78E-02	5.78E-02	5.78E-02	5.78E-02	5.78E-02
Liver 1	Liver 2	5.78E-02	5.78E-02	5.78E-02	5.78E-02	5.78E-02	5.78E-02
Liver 1	Blood 1	1.16E-01	1.16E-01	1.16E-01	1.16E-01	1.16E-01	1.16E-01
Liver 2	Blood 1	6.93E-03	6.93E-03	6.93E-03	6.93E-03	6.93E-03	6.93E-03
Kidneys	Blood 1	3.47E-02	3.47E-02	3.47E-02	3.47E-02	3.47E-02	3.47E-02
Spleen	Blood 1	1.90E-03	1.90E-03	1.90E-03	1.90E-03	1.90E-03	1.90E-03
Other 1	Blood 1	2.31E-01	2.31E-01	2.31E-01	2.31E-01	2.31E-01	2.31E-01
Other 2	Blood 1	6.93E-03	6.93E-03	6.93E-03	6.93E-03	6.93E-03	6.93E-03
Trab marrow	Blood 1	6.93E-03	6.93E-03	6.93E-03	6.93E-03	6.93E-03	6.93E-03
Cort marrow	Blood 1	6.93E-03	6.93E-03	6.93E-03	6.93E-03	6.93E-03	6.93E-03
Trab surface	Blood 1	8.22E-03	2.88E-03	1.81E-03	1.32E-03	9.59E-04	4.93E-04
Trab surface	T bone V	8.22E-03	2.88E-03	1.81E-03	1.32E-03	9.59E-04	2.47E-04
Trab volume	Blood 1	8.22E-03	2.88E-03	1.81E-03	1.32E-03	9.59E-04	4.93E-04
Cort surface	Blood 1	8.22E-03	2.88E-03	1.53E-03	9.04E-04	5.21E-04	8.21E-05
Cort surface	C bone V	8.22E-03	2.88E-03	1.53E-03	9.04E-04	5.21E-04	4.11E-05
Cort volume	Blood 1	8.22E-03	2.88E-03	1.53E-03	9.04E-04	5.21E-04	8.21E-05

UB, urinary bladder; SI, small intestine; Cort, cortical; Trab, trabecular.

10.1.3.3. Treatment of radioactive progeny

(113) The treatment of radioactive progeny produced in systemic compartments after intake of a radioisotope of scandium is described in Section 10.2.3.3. of *Publication 151* (ICRP, 2022).

10.2. Dosimetric date for scandium

Table 10.2. Committed effective dose coefficients (Sv Bq^{-1}) for the inhalation or ingestion of ^{44}Sc compounds.

	Effective dose coefficients (Sv Bq^{-1})					
	3m	1y	5y	10y	15y	Adult
Inhaled particulate materials (1 µm AMAD aerosols)						
Type F	6.0E-10	4.2E-10	1.9E-10	1.4E-10	8.4E-11	6.9E-11
Type M, default	7.2E-10	5.2E-10	2.5E-10	1.9E-10	1.3E-10	1.1E-10
Type S	7.3E-10	5.3E-10	2.6E-10	1.9E-10	1.3E-10	1.1E-10
Ingested materials						
All compounds	1.1E-09	9.1E-10	5.7E-10	4.1E-10	2.8E-10	2.3E-10

AMAD, activity median aerodynamic diameter.

11. TITANIUM (Z = 22)

11.1. Routes of Intake

11.1.1. Inhalation

(114) For titanium, default parameter values were adopted on absorption to blood from the respiratory tract (ICRP, 2015). Absorption parameter values and types, and associated f_A values for particulate forms of titanium are given in Table 11.1 [taken from Section 11 of *Publication 151* (ICRP, 2022)].

Table 11.1. Absorption parameter values for inhaled and ingested titanium.

	Absorption parameter values*		
Inhaled particulate materials	f_r	s_r (d^{-1})	s_s (d^{-1})
Default parameter values†			
Absorption type			
F	1	30	–
M‡	0.2	3	0.005
S	0.01	3	1×10^{-4}

Ingested materials§

	Age-dependent absorption from the alimentary tract, f_A					
Assigned forms	3 months	1 year	5 years	10 years	15 years	adult
All compounds	0.01	0.001	0.001	0.001	0.001	0.001

*It is assumed that the bound state can be neglected for titanium (i.e. $f_b = 0$). The values of s_r for Type F, M and S forms of titanium (30, 3 and 3 d^{-1}, respectively) are the general default values.
†For inhaled material deposited in the respiratory tract and subsequently cleared by particle transport to the alimentary tract, the default f_A values for inhaled materials are applied: i.e. the product of f_r for the absorption type and the f_A value for ingested soluble forms of titanium applicable to the age-group of interest (e.g. 0.001 for adults).
‡Default Type M is recommended for use in the absence of specific information on which the exposure material can be assigned to an absorption type (e.g. if the form is unknown, or if the form is known but there is no information available on the absorption of that form from the respiratory tract).
§Activity transferred from systemic compartments into segments of the alimentary tract is assumed to be subject to reabsorption to blood. The default absorption fraction f_A for the secreted activity is the highest value for any form of the radionuclide applicable to the age-group of interest (e.g. 0.001 for adults).

11.1.2. Ingestion

11.1.2.1. Adults

(115) Titanium compounds are poorly absorbed from the gastro-intestinal tract, see *Publication 151* (ICRP, 2022) for some more details. In *Publications 30* and *72* (ICRP, 1981, 1995c), a fractional absorption of 0.01 was retained for titanium. In *Publication 151*, f_A was taken to be 0.001 for all chemical forms of titanium at the workplace. The same value f_A = 0.001 is adopted here for titanium ingested by adult members of the public.

11.1.2.2. Children

(116) Consistently with the approach of *Publication56* (ICRP, 1990), an $f_A = 0.01$ is adopted here for 3 month old infants and the value $f_A = 0.001$ is used for older children.

11.1.3. Systemic distribution, retention and excretion of titanium

11.1.3.1. Biokinetic data

(117) Thomas and Archuleta (1980) studied the distribution and retention of ^{44}Ti in mice following its intraperitoneal (IP) or intravenous (IV) administration as chloride. The initial systemic distribution depended strongly on the exposure mode but did not vary noticeably over time after either IP or IV administration. Liver, spleen, kidneys, and gastrointestinal tract contained about 25%, 3.3%, 1.7%, and 3.6%, respectively, of the total-body content after intravenous injection and 8.4%, 2.1%, 2.0%, and 15%, respectively, after intraperitoneal injection. Differences in the distributions following IP and IV administration appeared to result largely from adherence of injected material to visceral organs near the injection site and elevated uptake by the RE system in the case of IV injection. A mean biological half-time of 642 d was estimated for the total body.

(118) Merritt et al. (1992, 1995) examined the behaviour of Ti in hamsters following repeated intraperitoneal or intramuscular injections of Ti salts over a few weeks. Transport from the site of injection was slow. One week after the end of six weekly injections of 100 µg of Ti tetrachloride, the following tissues showed Ti concentrations noticeably higher than found in control animals: spleen, 40.5 µg/g (above the control level); liver, 6.9 µg/g; bone matrix, 3.3 µg/g; bone mineral, 0.9 µg/g; kidney, 2.1 µg/g.

(119) Sarmiento-Gonzalez et al. (2009) determined Ti concentration in tissues of rats 18 months after implant of Ti wires in the femur, 1 week after intraperitoneal injection of soluble Ti as citrate, or 1 week after intraperitoneal injection of TiO_2 microparticles. The Ti concentrations in kidneys, spleen, lungs, and heart normalized to a concentration of 1.0 in the liver were, respectively, 2.7, 8.1, 7.4, and 2.1 for rats with implants; 6.5, 6.7, 1.8, and 0.74 for rats injected with Ti citrate; and 2.1, 2.1, 15, and 2.5 for rats injected with Ti dioxide.

(120) Golasik et al. (2016a, 2016b) studied the Ti distribution in selected tissues of rats following administration in ionic form, either as a single IV injection or daily oral administration for 30 d. During the first 24 h after IV injection or after the end of oral administration, the highest tissue concentration was found in the kidneys, followed by liver. Over this period the liver contained a greater portion of the administered Ti than the kidneys due to the larger mass of the liver. In the early hours after IV injection the biological half-time was about 3.3 h for the kidneys and 1.9 h for the liver. Much slower removal from these tissues was seen from 3 h to 24 h after the end of oral administration.

(121) Miller et al. (1976) determined the distribution of ^{44}Ti in lambs after oral or intravenous (IV) administration of $^{44}TiCl_4$. At 2 d after oral administration the mean activity concentration in systemic tissues, normalized to 1.0 for liver, decreased in the order liver (1.0) > kidneys (0.74) > pancreas (0.49) > spleen (0.28) > lung, heart, adrenals (< 0.15). At 2 d after IV administration the blood, skeleton, kidneys, liver, and remaining tissue contained about 18.4%, 24.8%, 2.1%, 1.3%, and 48.8%, respectively, of the administered activity; cumulative urinary excretion accounted for about 3%; and faecal excretion plus gastrointestinal (GI) tract contents accounted for about 1.6%. This distribution broadly resembles that predicted by the systemic model for Zr adopted in *Publication 34* (ICRP, 2016): blood, 38%; bone, 22.8%; kidneys, 0.4%; liver, 1.8%; other tissue, 33%, urine, 3%; faeces, 1%. Noticeable differences are that the Zr model predicts slower removal from blood, balanced by slower accumulation in "other tissue" and lower accumulation in the kidneys.

(122) Zhu et al. (2010) measured concentrations of 60 elements including Ti and Zr in 17 tissues obtained from autopsies of 68 Chinese men from four areas of China. All 68 subjects were considered healthy until the time of sudden accidental death. Concentrations of the elements were also measured in blood of living subjects from each of the four areas. The

concentration of an element in a tissue or blood was reported as a median and range of measured values. The results for Ti and Zr indicate considerable differences in their long-term distributions in the adult human body. For example, the median concentration of Zr in rib (the only bone addressed) was considerably greater than that in soft tissues other than liver, while the median concentration of Ti in rib (983 µg/kg) was lower than the median concentration in 8 soft tissues (e.g., liver, 3220 µg/kg; muscle, 2060 µg/kg; kidney, 1770 µg/kg). A relatively low median concentration (201 µg/kg) was determined for spleen. Blood, liver, kidneys, bone, and all other tissues combined contained about 0.4%, 6%, 0.6%, 11%, and 82%, respectively, of total-body Ti in these subjects based on median concentrations in tissues.

11.1.3.2. Biokinetic model for systemic titanium

(123) The biokinetic model for systemic titanium applied to workers in *Publication 151* (ICRP, 2022) is applied in this report to adult members of the public. As described in *Publication 151*, that model was based on reported data on Ti kinetics that did not appear to be greatly influenced by its accumulation in the RE system. The initial distribution of Ti in adults was based mainly on results of the study of Miller et al. (1976), which suggest that Ti distributes similarly to that of Zr. The long-term kinetics of Ti is based on relative concentrations of Ti in tissues indicated in the autopsy study of Zhu et al. (2010). The model for adults is extended to pre-adult ages by modification of transfer rates to reflect elevated deposition of Ti in immature bone and age-specific rates of removal from bone (ICRP, 2002). The bone model applied to Ti is analogous to that applied to Zr in Part 1 of this series of reports on doses to the public from environmental radionuclides [*Publication 158* (ICRP, 2024)].

(124) The structure of the systemic model for Ti is shown in Fig. 11.1. Transfer coefficients are listed in Table 11.2.

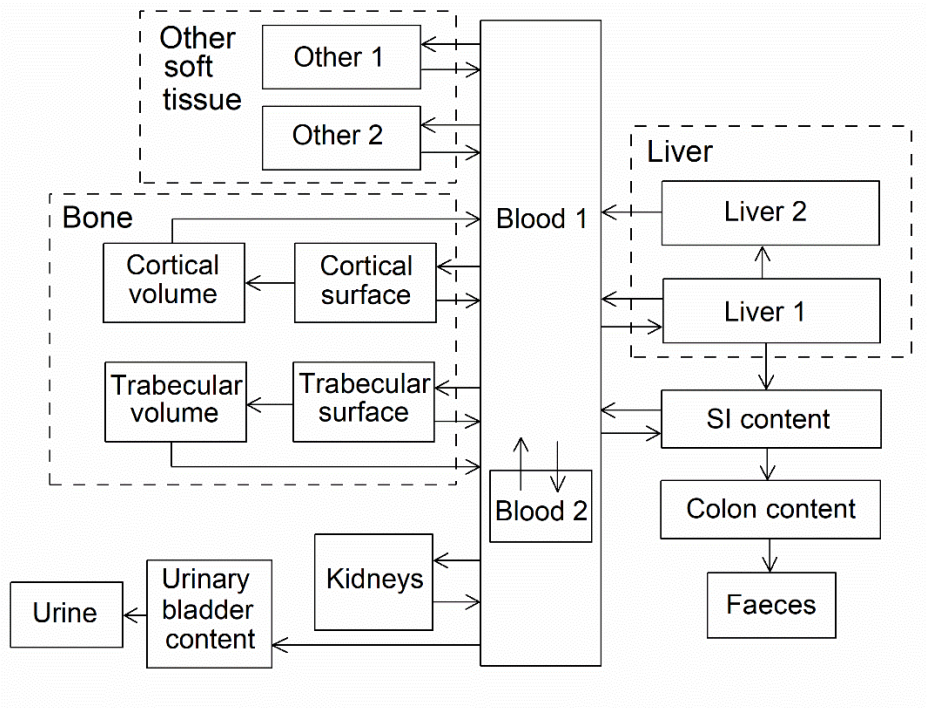

Fig. 11.1. Structure of the biokinetic model for systemic Ti. SI, small intestine.

Table 11.2. Age-specific transfer coefficients for titanium.

		Transfer coefficients (d^{-1})					
Pathway		100 d	1 y	5 y	10 y	15 y	Adult
Blood 1	Blood 2	1.82E+00	1.91E+00	1.91E+00	1.91E+00	1.91E+00	2.00E+00
Blood 1	Liver 1	4.56E-02	4.78E-02	4.78E-02	4.78E-02	4.78E-02	5.00E-02
Blood 1	Kidneys	6.84E-02	7.17E-02	7.17E-02	7.17E-02	7.17E-02	7.50E-02
Blood 1	Other 1	9.12E-01	9.56E-01	9.56E-01	9.56E-01	9.56E-01	1.00E+00
Blood 1	Other 2	9.12E-01	9.56E-01	9.56E-01	9.56E-01	9.56E-01	1.00E+00
Blood 1	UB content	9.12E-02	9.56E-02	9.56E-02	9.56E-02	9.56E-02	1.00E-01
Blood 1	SI content	2.28E-02	2.39E-02	2.39E-02	2.39E-02	2.39E-02	2.50E-02
Blood 1	Trab surface	5.63E-01	4.69E-01	4.69E-01	4.69E-01	4.69E-01	3.75E-01
Blood 1	Cort surface	5.63E-01	4.69E-01	4.69E-01	4.69E-01	4.69E-01	3.75E-01
Blood 2	Blood 1	1.60E+00	1.60E+00	1.60E+00	1.60E+00	1.60E+00	1.60E+00
Liver 1	SI content	1.16E-01	1.16E-01	1.16E-01	1.16E-01	1.16E-01	1.16E-01
Liver 1	Liver 2	4.62E-01	4.62E-01	4.62E-01	4.62E-01	4.62E-01	4.62E-01
Liver 1	Blood 1	1.16E-01	1.16E-01	1.16E-01	1.16E-01	1.16E-01	1.16E-01
Liver 2	Blood 1	1.05E-03	1.05E-03	1.05E-03	1.05E-03	1.05E-03	1.05E-03
Kidneys	Blood 1	2.10E-02	2.10E-02	2.10E-02	2.10E-02	2.10E-02	2.10E-02
Other 1	Blood 1	4.62E-01	4.62E-01	4.62E-01	4.62E-01	4.62E-01	4.62E-01
Other 2	Blood 1	2.00E-03	2.00E-03	2.00E-03	2.00E-03	2.00E-03	2.00E-03
T-bone-S	Blood 1	2.00E-02	2.00E-02	2.00E-02	2.00E-02	2.00E-02	2.00E-02
Trab surface	Trab volume	8.22E-03	2.88E-03	1.81E-03	1.32E-03	9.59E-04	2.47E-04
Trab volume	Blood 1	8.22E-03	2.88E-03	1.81E-03	1.32E-03	9.59E-04	4.93E-04
Cort surface	Blood 1	2.00E-02	2.00E-02	2.00E-02	2.00E-02	2.00E-02	2.00E-02
Cort surface	Cort volume	8.22E-03	2.88E-03	1.53E-03	9.04E-04	5.21E-04	4.11E-05
Cort volume	Blood 1	8.22E-03	2.88E-03	1.53E-03	9.04E-04	5.21E-04	8.21E-05

UB, urinary bladder; SI, small intestine; RC, right colon; Cort, cortical; Trab, trabecular.

11.1.3.3. Treatment of radioactive progeny

(125) The treatment of radioactive progeny produced in systemic compartments after intake of a radioisotope of titanium is described in Section 11.2.3.3. of *Publication 151* (ICRP, 2022).

11.2. Dosimetric data for titanium

Table 11.3. Committed effective dose coefficients (Sv Bq^{-1}) for the inhalation or ingestion of ^{44}Ti compounds.

	Effective dose coefficients (Sv Bq^{-1})					
	3m	1y	5y	10y	15y	Adult
Inhaled particulate materials (1 μm AMAD aerosols)						
Type F	6.0E-07	5.5E-07	3.6E-07	2.7E-07	2.4E-07	2.3E-07
Type M, default	2.7E-07	2.7E-07	1.9E-07	1.4E-07	1.3E-07	1.3E-07
Type S	5.9E-07	6.1E-07	4.9E-07	4.1E-07	4.2E-07	4.4E-07
Ingested materials						
All compounds	3.3E-08	6.4E-09	4.0E-09	3.0E-09	2.3E-09	2.2E-09

AMAD, activity median aerodynamic diameter.

12. VANADIUM (Z=23)

12.1. Routes of Intake

12.1.1. Inhalation

(126) For vanadium, default parameter values were adopted on absorption to blood from the respiratory tract (ICRP, 2015). Absorption parameter values and types, and associated f_A values for particulate forms of vanadium are given in Table 12.1 [taken from Section 12 of *Publication 151* (ICRP, 2022)].

Table 12.1. Absorption parameter values for inhaled and ingested vanadium.

	Absorption parameter values*		
Inhaled particulate materials	f_r	s_r (d^{-1})	s_s (d^{-1})
Default parameter values†			
Absorption type			
F	1	30	–
M‡	0.2	3	0.005
S	0.01	3	1×10^{-4}

Ingested materials§

	Age-dependent absorption from the alimentary tract, f_A					
Assigned forms	3 months	1 year	5 years	10 years	15 years	adult
Sodium metavanadate	0.4	0.2	0.2	0.2	0.2	0.2
All other chemical forms, including vanadium in diet	0.02	0.01	0.01	0.01	0.01	0.01

*It is assumed that the bound state can be neglected for vanadium (i.e. $f_b = 0$). The values of s_r for Type F, M and S forms of vanadium (30, 3 and 3 d^{-1} respectively) are the general default values.

†For inhaled material deposited in the respiratory tract and subsequently cleared by particle transport to the alimentary tract, the default f_A values for inhaled materials are applied: i.e. the product of f_r for the absorption type and the f_A value for ingested soluble forms of vanadium applicable to the age-group of interest (e.g. 0.2 for adults).

‡Default Type M is recommended for use in the absence of specific information on which the exposure material can be assigned to an absorption type (e.g. if the form is unknown, or if the form is known but there is no information available on the absorption of that form from the respiratory tract).

§Activity transferred from systemic compartments into segments of the alimentary tract is assumed to be subject to reabsorption to blood. The default absorption fraction f_A for the secreted activity is the highest value for any form of the radionuclide applicable to the age-group of interest (e.g. 0.2 for adults).

12.1.2. Ingestion

12.1.2.1. Adults

(127) The limited data available indicate a low absorption for vanadium, except in the sodium metavanadate form, see *Publication 151* (ICRP, 2022) for details.

(128) In *Publications 30* and *72* (ICRP, 1981, 1995c), f_1 was taken to be 0.01 for all compounds of vanadium. In *Publication 151*, the same value of $f_A = 0.01$ was retained for all chemical forms of vanadium, except sodium metavanadate for which a higher value of $f_A = 0.2$ was adopted. The same values are used here for ingestion of vanadium by adult members of the public. In particular, $f_A = 0.01$ is applied to vanadium in diet.

12.1.2.2. Children

(129) The comparison of vanadium levels in tissues of 21 d and 115 d old rats fed vanadium in water and diet suggested higher absorption in young animals (Edel et al., 1984). Consistently with the approach of *Publication56* (ICRP, 1990), an $f_A = 0.4$ is adopted here for ingestion of sodium metavanadate by 3-month-old infants. An $f_A = 0.02$ is used for ingestion of all other forms of vanadium by 3-month-old infants. The adult values are used for older children.

12.1.3. Systemic distribution, retention and excretion of vanadium

12.1.3.1. Biokinetic data

(130) The biokinetics of vanadium has been studied extensively in rodents (Strain et al 1964, Thomassen and Leicester, 1964; Sabbioni et al, 1978, 1981; Sharma et al, 1980; Roshchin et al, 1980; Hansen et al. 1982; Sharma, 1987; Merritt et al 1995; Amano et al, 1996; Setyawati et al, 1998; Barceloux and Barceloux, 1999; Hirunuma et al, 1999; Ando et al, 1989, 1990; Alimonti et al, 2000). Relatively high concentrations of injected or absorbed vanadium are seen in kidneys, bone, and liver. Bone eventually becomes the dominant repository. Endogenous excretion is primarily in urine (Barceloux and Barceloux, 1999). At least half of injected or absorbed vanadium is excreted within 3-4 d (Durbin, 1960, Hirunuma et al 1999, Barceloux and Barceloux, 1999).

(131) The Group VB elements vanadium, niobium, and tantalum share some biokinetic properties such as primary sites of deposition (Durbin, 1960, Ando et al, 1989, 1990), but vanadium is less firmly bound in tissues and is more rapidly excreted than niobium or tantalum. In a study described by Durbin (1960), less than 10% of absorbed vanadium was retained after 2 mo, compared with at least threefold higher retention of niobium or tantalum.

(132) The reader is referred to Leggett and O'Connell (2018) for a more detailed discussion of biokinetic data for systemic vanadium.

12.1.3.2. Biokinetic model for systemic vanadium

(133) The biokinetic model for systemic vanadium applied in *Publication 151* (ICRP, 2022) to workers is applied in this report to all ages.

(134) The model structure is shown in Fig. 12.1. The transfer coefficients are listed in Table 12.2.

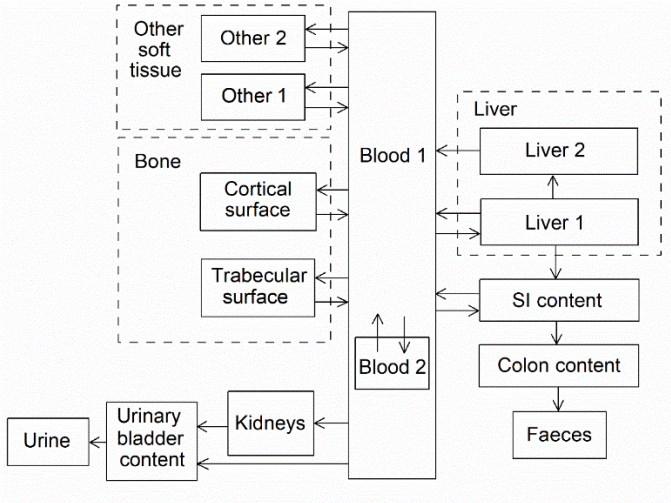

Fig. 12.1. Structure of the biokinetic model for systemic vanadium. SI, small intestine.

Table 12.2. Age-specific transfer coefficients for vanadium.

		Transfer coefficients (d^{-1})					
Pathway		100 d	1 y	5 y	10 y	15 y	Adult
Blood 1	Blood 2	2.80E+00	2.80E+00	2.80E+00	2.80E+00	2.80E+00	2.80E+00
Blood 1	Liver 1	2.40E-01	2.40E-01	2.40E-01	2.40E-01	2.40E-01	2.40E-01
Blood 1	Kidneys	4.00E-01	4.00E-01	4.00E-01	4.00E-01	4.00E-01	4.00E-01
Blood 1	Other 1	2.44E+00	2.44E+00	2.44E+00	2.44E+00	2.44E+00	2.44E+00
Blood 1	Other2	2.40E-01	2.40E-01	2.40E-01	2.40E-01	2.40E-01	2.40E-01
Blood 1	UB content	1.52E+00	1.52E+00	1.52E+00	1.52E+00	1.52E+00	1.52E+00
Blood 1	SI content	1.20E-01	1.20E-01	1.20E-01	1.20E-01	1.20E-01	1.20E-01
Blood 1	Trab surface	1.20E-01	1.20E-01	1.20E-01	1.20E-01	1.20E-01	1.20E-01
Blood 1	Cort surface	1.20E-01	1.20E-01	1.20E-01	1.20E-01	1.20E-01	1.20E-01
Blood 2	Blood 1	5.00E-01	5.00E-01	5.00E-01	5.00E-01	5.00E-01	5.00E-01
Liver 1	SI content	9.00E-02	9.00E-02	9.00E-02	9.00E-02	9.00E-02	9.00E-02
Liver 1	Blood 1	3.75E-01	3.75E-01	3.75E-01	3.75E-01	3.75E-01	3.75E-01
Liver 1	Liver 2	3.50E-02	3.50E-02	3.50E-02	3.50E-02	3.50E-02	3.50E-02
Liver 2	Blood 1	1.00E-02	1.00E-02	1.00E-02	1.00E-02	1.00E-02	1.00E-02
Kidneys	UB content	1.80E+00	1.80E+00	1.80E+00	1.80E+00	1.80E+00	1.80E+00
Other 1	Blood 1	1.40E-01	1.40E-01	1.40E-01	1.40E-01	1.40E-01	1.40E-01
Other 2	Blood 1	1.00E-02	1.00E-02	1.00E-02	1.00E-02	1.00E-02	1.00E-02
Trab surface	Blood 1	1.00E-02	1.00E-02	1.00E-02	1.00E-02	1.00E-02	1.00E-02
Cort surface	Blood 1	1.00E-02	1.00E-02	1.00E-02	1.00E-02	1.00E-02	1.00E-02

UB, Urinary bladder; SI, Small intestine; Cort, Cortical; Trab, Trabecular.

12.2. Dosimetric data for vanadium

Table 12.3. Committed effective dose coefficients (Sv Bq^{-1}) for the inhalation or ingestion of ^{48}V compounds.

	Effective dose coefficients (Sv Bq^{-1})					
	3m	1y	5y	10y	15y	Adult
Inhaled particulate materials (1 μm AMAD aerosols)						
Type F	6.1E-09	4.0E-09	2.0E-09	1.4E-09	9.0E-10	8.6E-10
Type M, default	8.6E-09	6.8E-09	3.7E-09	2.6E-09	1.8E-09	2.0E-09
Type S	9.8E-09	7.9E-09	4.4E-09	3.1E-09	2.2E-09	2.4E-09
Ingested materials						
Sodium metavanadate	8.9E-09	5.3E-09	3.0E-09	2.1E-09	1.5E-09	1.4E-09
All other chemical forms, including vanadium in diet	4.5E-09	4.0E-09	2.3E-09	1.6E-09	1.1E-09	1.1E-09

AMAD, activity median aerodynamic diameter.

13. CHROMIUM (Z=24)

13.1. Routes of Intake

13.1.1. Inhalation

(135) For chromium, default parameter values were adopted on absorption to blood from the respiratory tract (ICRP, 2015). Absorption parameter values and types, and associated f_A values for particulate forms of chromium are given in Table 13.1 [taken from Section 13 of *Publication 151* (ICRP, 2022)]

Table 13.1. Absorption parameter values for inhaled and ingested chromium.

	Absorption parameter values*		
Inhaled particulate materials	f_r	s_r (d^{-1})	s_s (d^{-1})
Default parameter values†			
Absorption type			
F	1	30	–
M‡	0.2	3	0.005
S	0.01	3	1×10^{-4}

Ingested materials§

	Age-dependent absorption from the alimentary tract, f_A					
Assigned forms	3 months	1 year	5 years	10 years	15 years	adult
Trivalent state Cr(III)	0.1	0.01	0.01	0.01	0.01	0.01
Hexavalent state Cr(VI)	0.1	0.05	0.05	0.05	0.05	0.05

*It is assumed that the bound state can be neglected for chromium (i.e. $f_b = 0$). The values of s_r for Type F, M and S forms of chromium (30, 3 and 3 d^{-1} respectively) are the general default values.

†For inhaled material deposited in the respiratory tract and subsequently cleared by particle transport to the alimentary tract, the default f_A values for inhaled materials are applied: i.e. the product of f_r for the absorption type and the f_A value for ingested soluble forms of chromium applicable to the age-group of interest (e.g. 0.05 for adults).

‡Default Type M is recommended for use in the absence of specific information on which the exposure material can be assigned to an absorption type (e.g. if the form is unknown, or if the form is known but there is no information available on the absorption of that form from the respiratory tract).

§Activity transferred from systemic compartments into segments of the alimentary tract is assumed to be subject to reabsorption to blood. The default absorption fraction f_A for the secreted activity is the highest value for any form of the radionuclide applicable to the age-group of interest (e.g. 0.05 for adults).

13.1.2. Ingestion

13.1.2.1. Adults

(136) As discussed *in Publication 151* (ICRP, 2022), chromium is poorly absorbed from the gastrointestinal tract. Ingested hexavalent chromium is absorbed to a slightly greater extent than trivalent chromium. The reduction of Cr (VI) to Cr (III) by gastric juices, or by mixture with orange juice or ascorbic acid thus appears to decrease its intestinal absorption.

(137) In *Publications 30* and *72* (ICRP, 1980, 1995c), f_1 was taken to be 0.01 for chromium in the trivalent state and 0.1 for chromium in the hexavalent state. In *Publication 151*, f_A values of 0.01 and 0.05 were retained respectively for Cr(III) and Cr(VI). The same values are used here for ingestion of chromium by adult members of the public.

13.1.2.2. Children

(138) In a study by Sullivan et al. (1984), 2-day old rats absorbed about ten times more Cr(III) chloride than adults (0.1 and 1.2% absorption respectively). Assuming the same age-dependent ratio in humans leads to the adoption of an f_A = 0.1 for ingestion of trivalent chromium by 3-month-old infants. Applying the approach of *Publication 56* (ICRP, 1990), f_A = 0.1 is also used for ingestion of hexavalent chromium by infants. The adult values are used for older children: f_A = 0.01 for ingestion of Cr(III) and f_A = 0.05 for ingestion of Cr(VI).

13.1.3. Systemic distribution, retention and excretion of chromium

13.1.3.1. Biokinetic data

(139) Chromium(III) is the most stable oxidation state of chromium and, in that form, is an essential nutrient in humans and several non-human species (Hambidge and Baum, 1972; Christensen et al., 1993; Mertz, 1993; Anderson, 1997). Chromium in other oxidation states tends to be converted to the trivalent oxide in the environment and in biological systems. The hexavalent form (Cr(VI)), which is the second most stable oxidation state, behaves differently from Cr(III) in the body and is categorized as a chemical toxin and carcinogen. The different behaviours and effects of Cr(VI) and Cr(III) in the body are associated with the fact that some Cr(VI) compounds can cross cell membranes, while Cr(III) is blocked by the membrane.

(140) Postmortem measurements of chromium concentrations in 17 tissues of up to 68 adult male subjects (Zhu et al., 2010) indicate a central total-body content of about 4 g chromium. Based on median chromium concentrations in tissues and reference tissues masses, about 55% of total-body chromium is contained in muscle and fat, 25% in bone, 4% in the liver, and 0.5% in the kidneys.

(141) Doisy et al. (1971) studied the blood kinetics and excretion of intravenously administered ^{51}Cr(III) in seven normal subjects. The blood content dropped to roughly 40% of the injected amount within a few minutes but decreased very slowly thereafter, with about 25% retained in blood after 7 d. Excretion of ^{51}Cr was primarily in urine.

(142) Sargent et al. (1979) measured the retention of intravenously administered ^{51}Cr(III) in five normal adult male humans. Total-body activity was measured externally for 8 mo, and activity in blood was measured for 40-80 d post injection. Data fits indicated three components of retention with mean half-times of 0.56 d (35%), 12.7 d (27%), and 192 d (38%). Blood clearance, apparently excluding a rapid phase of removal immediately after injection, was described in terms of four components of retention with mean half-times of 13 min, 6.3 h, 1.9 d, and 8.3 d.

(143) Lim et al. (1983) studied the behaviour of intravenously administered ^{51}Cr(III) in three normal subjects using external scanning and measurement of activity in plasma. Highest activity concentrations were seen in the liver, spleen, and bone.

(144) Chromium has been used to measure the volume and lifetime of red blood cells (RBC) in patients and normal subjects, based on tenacious retention of ^{51}Cr(III) in RBC after passage of intravenously administered ^{51}Cr(VI) across RBC membranes and reduction of ^{51}Cr(VI) to ^{51}Cr(III) within the RBC. Following administration of ^{51}Cr(VI) to normal subjects, the label disappeared from blood with a biological half-time of about 30 d (Korst, 1968).

(145) Hiller and Leggett (2020) reviewed information on the biokinetics of Cr(III) and Cr(VI) in human subjects (see above summaries) and laboratory animals (Hopkins, 1965; Mertz et al., 1965; Sayato et al., 1980; Weber, 1983; O'Flaherty, 1996; Kerger et al.. 1997; O'Flaherty et al., 2001). They proposed systemic models for both Cr(III) and Cr(VI). Parameter values for Cr(III) were based mainly on results of biokinetic and autopsy studies involving

human subjects. Data for laboratory animals were used to fill gaps in the data for human subjects. Cr(IV) was assumed to be reduced to Cr(III) over a period of hours to days.

13.1.3.2. Biokinetic model for systemic chromium

(146) The biokinetic model for systemic Cr(III) proposed by Hiller and Leggett (2020) was applied in *Publication 151* (2022) to intakes of chromium by workers and is adopted here for application to environmental intakes of chromium by all age groups. The structure of the model for Cr(III) is shown in Fig. 13.1. Transfer coefficients are listed in Table 13.2.

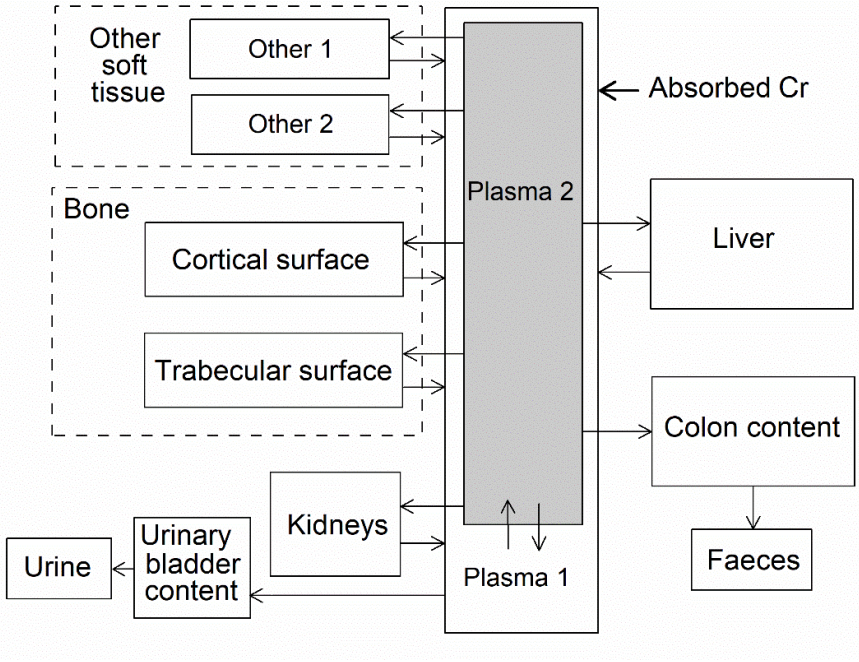

Fig. 13.1. Structure of the biokinetic model for systemic chromium.

Table 13.2. Age-specific transfer coefficients for chromium.

		Transfer coefficients (d^{-1})					
Pathway		100 d	1 y	5 y	10 y	15 y	Adult
Plasma 1	Plasma 2	2.20E+02	2.20E+02	2.20E+02	2.20E+02	2.20E+02	2.20E+02
Plasma 1	UB content	4.80E+00	4.80E+00	4.80E+00	4.80E+00	4.80E+00	4.80E+00
Plasma 2	Blood	1.00E+01	1.00E+01	1.00E+01	1.00E+01	1.00E+01	1.00E+01
Plasma 2	RC content	1.00E-01	1.00E-01	1.00E-01	1.00E-01	1.00E-01	1.00E-01
Plasma 2	Other 1	7.00E-01	7.00E-01	7.00E-01	7.00E-01	7.00E-01	7.00E-01
Plasma 2	Other 2	2.70E-02	2.70E-02	2.70E-02	2.70E-02	2.70E-02	2.70E-02
Plasma 2	Kidneys	1.50E-02	1.50E-02	1.50E-02	1.50E-02	1.50E-02	1.50E-02
Plasma 2	Liver	1.50E-01	1.50E-01	1.50E-01	1.50E-01	1.50E-01	1.50E-01
Plasma 2	Trab surface	1.50E-02	1.25E-02	1.25E-02	1.25E-02	1.25E-02	1.00E-02
Plasma 2	Cort surface	1.50E-02	1.25E-02	1.25E-02	1.25E-02	1.25E-02	1.00E-02
Other 1	Plasma 1	2.50E-01	2.50E-01	2.50E-01	2.50E-01	2.50E-01	2.50E-01
Other 2	Plasma 1	5.00E-05	5.00E-05	5.00E-05	5.00E-05	5.00E-05	5.00E-05
Liver	Plasma 1	1.00E-02	1.00E-02	1.00E-02	1.00E-02	1.00E-02	1.00E-02
Kidneys	Plasma 1	7.00E-03	7.00E-03	7.00E-03	7.00E-03	7.00E-03	7.00E-03
Trab surface	Plasma 1	4.93E-04	4.93E-04	4.93E-04	4.93E-04	4.93E-04	4.93E-04
Cort surface	Plasma 1	8.21E-05	8.21E-05	8.21E-05	8.21E-05	8.21E-05	8.21E-05

UB, urinary bladder; RC, right colon; Cort, cortical; Trab, trabecular.

13.1.3.3. Treatment of radioactive progeny

(147) The treatment of radioactive progeny produced in systemic compartments after intake of a radioisotope of chromium is described in Section 13.2.3.3. of *Publication 151* (ICRP, 2022).

13.2. Dosimetric data for chromium

Table 13.3. Committed effective dose coefficients (Sv Bq^{-1}) for the inhalation or ingestion of ^{51}Cr compounds.

	Effective dose coefficients (Sv Bq^{-1})					
	3m	1y	5y	10y	15y	Adult
Inhaled particulate materials (1 μm AMAD aerosols)						
Type F	1.4E-10	1.0E-10	5.2E-11	3.5E-11	2.4E-11	2.4E-11
Type M, default	1.7E-10	1.4E-10	7.3E-11	4.9E-11	3.5E-11	3.8E-11
Type S	2.0E-10	1.7E-10	9.0E-11	6.1E-11	4.3E-11	4.7E-11
Ingested materials						
Trivalent state Cr(III)	9.6E-11	4.8E-11	2.7E-11	2.0E-11	1.4E-11	1.3E-11
Hexavalent state Cr(VI)	9.6E-11	6.2E-11	3.5E-11	2.5E-11	1.7E-11	1.7E-11

AMAD, activity median aerodynamic diameter.

14. MANGANESE (Z=25)

14.1. Routes of Intake

14.1.1. Inhalation

(148) For manganese, default parameter values were adopted on absorption to blood from the respiratory tract (ICRP, 2015). Absorption parameter values and types, and associated f_A values for particulate forms of manganese are given in Table 14.1 [taken from Section 14 of *Publication 151* (ICRP, 2022)].

Table 14.1. Absorption parameter values for inhaled and ingested manganese.

	Absorption parameter values*		
Inhaled particulate materials	f_r	s_r (d^{-1})	s_s (d^{-1})
Default parameter values†			
Absorption type			
F	1	30	–
M‡	0.2	3	0.005
S	0.01	3	1×10^{-4}

Ingested materials§

	Age-dependent absorption from the alimentary tract, f_A					
Assigned forms	3 months	1 year	5 years	10 years	15 years	adult
All compounds	0.3	0.05	0.05	0.05	0.05	0.05

*It is assumed that the bound state can be neglected for manganese (i.e. $f_b = 0$). The values of s_r for Type F, M and S forms of manganese (30, 3 and 3 d^{-1} respectively) are the general default values.

†For inhaled material deposited in the respiratory tract and subsequently cleared by particle transport to the alimentary tract, the default f_A values for inhaled materials are applied: i.e. the product of f_r for the absorption type and the f_A value for ingested soluble forms of manganese applicable to the age-group of interest (e.g. 0.05 for adults).

‡Default Type M is recommended for use in the absence of specific information on which the exposure material can be assigned to an absorption type (e.g. if the form is unknown, or if the form is known but there is no information available on the absorption of that form from the respiratory tract).

§Activity transferred from systemic compartments into segments of the alimentary tract is assumed to be subject to reabsorption to blood. The default absorption fraction f_A for the secreted activity is the highest value for ingestion of the radionuclide applicable to the age-group of interest (e.g. 0.05 for adults).

14.1.2. Ingestion

(149) As discussed *in Publication 151* (ICRP, 2022), the fractional absorption of manganese averages around 3-5% in adults. It is under homoeostatic control and negatively correlated with total dietary manganese and iron intakes. The absorption is higher from water than from food. For all compounds of manganese, f_1 had been taken to be 0.1 in *Publications 30* and 72 (ICRP, 1979a, 1995c). In *Publication 151*, the value of $f_A = 0.05$ was applied to all chemical forms of manganese at the workplace. The same value of $f_A = 0.05$ is adopted here for all forms of manganese ingested by adult members of the public.

14.1.2.1. Children

(150) Mena (1981) noted that manganese homeostasis is achieved via the bile (not by renal excretion) and that most of Mn ingested with food is excreted unabsorbed. He reported, at an

age of 10 d, a total body retention of 15.7% in premature children (32-34 weeks of gestation), 8% in normal newborns and 1 - 3% in adults. Assuming a similar ratio with the adult f_A of 5% would suggest f_A about 25% for newborns. In another balance study by Dorner et al. (1989) in young infants and preterm infants, the apparent availability of Mn was highest in breast-milk (37% of intake) and lower in cow's milk formulas (16 to 21% of intake). In rats, the absorption decreased with age from 82 to 30% in 12-19 d old suckling (Keen et al. 1986). Consistently with these data, a higher $f_A = 0.3$ is adopted here for ingestion of manganese by 3-month-old infants, while the adult value $f_A = 0.05$ is used for older children.

14.1.3. Systemic distribution, retention and excretion of manganese

14.1.3.1. Biokinetic data

(151) Manganese is an essential element, but excessive intake can result in adverse health effects including progressive neurodegenerative damage with an associated motor dysfunction syndrome similar to Parkinson's disease. Dietary intake of manganese typically is about 2-6 mg d^{-1} for adult humans. The adult human body contains about 10-15 mg of manganese. The body's manganese is maintained at a nearly constant level by homeostatic controls involving regulation of gastrointestinal uptake and intestinal secretions. High dietary manganese enhances metabolism of manganese in the liver and increases secretion of systemic manganese into the gastrointestinal contents (Andersen et al., 1999; Dorman et al., 2001). Inhaled manganese initially bypasses the homeostatic control processes in the liver and becomes largely bound to transferrin. In persons chronically exposed to elevated mass concentrations of manganese in air, atypically high masses of manganese can accumulate in the brain and other tissues due to delivery by transferrin receptors.

(152) Autopsy data for adult male humans who suffered accidental deaths indicate that highest median concentrations of manganese in tissues, normalized to the concentration in liver, decrease in the order liver (1.0) > pancreas, kidney (~0.65) > gastrointestinal tissues (0.35-0.55) (Zhu et al., 2010). Lowest concentrations (0.02-0.05) were found in blood, fat, and skin. Based on median concentrations in tissues and reference tissue masses, about 34% of the body burden was contained in muscle, 24% in bone, 16% in liver, and 2% in kidneys.

(153) In laboratory animals, manganese tracers are rapidly removed from blood and initially concentrate mainly in tissues rich in mitochondria such as liver, pancreas, and kidneys (Chauncey et al., 1977; Dastur et al., 1971; Dorman et al., 2006; Kato, 1963). Brain, bone, and muscle and other tissues gradually accumulate increasing portions of retained manganese (Dastur et al., 1969, 1971; Furchner et al., 1966).

(154) Endogenous excretion of manganese is mainly in faeces and appears to arise mainly from biliary secretion, but substantial amounts are also secreted into the gastrointestinal tract in pancreatic juices and other intestinal fluids (Dorman et al., 2001; Mahoney and Small, 1968; Maynard and Fink, 1956). Urinary excretion typically accounts for at most a few percent of total excretion of manganese (Maynard and Fink, 1956; Mahoney and Small, 1968; Davidsson et al. 1989.

(155) Most of the manganese in blood is contained in red blood cells (Milne et al., 1990). The concentration of manganese in blood plasma typically is about 0.6-0.7 µg/L (Baruthio et al., 1988; Versieck and Cornelis, 1980; Versieck et al., 1988). Reported concentrations in whole blood of healthy adult subjects are typically on the order of 8-12 µg/L (Kristiansen et al., 1997; Milne et al., 1990; Pleban and Pearson, 1979).

(156) Mena et al. (1967) observed total-body retention of intravenously injected ^{54}Mn in 8 healthy adult humans (4 of each sex, age range 20-30 y), in 14 current manganese miners in good health (ages 23-60 y), and 10 former manganese miners with chronic manganese

poisoning (ages 18-56 y). Total-body removal half-times were 35.5 ± 8.4 d (mean ± standard deviation) in the control group, 12.5 ± 2.3 d in the healthy miners, and 26.5 ± 4.8 d in the subjects with manganese poisoning.

(157) Mahoney and Small (1968) measured retention of intravenously injected ^{54}Mn in six subjects including both sexes (age range 25-45 y) and studied factors affecting the rate of biological removal of the tracer from the body. About 30% of the injected amount was removed with a half-time of 4 d and 70% with a half-time of 39 d. Low manganese intake increased the size of the slow component to 84% and the retention half-time to 90 d but had no effect on the half-time of the fast component. Administration of a large mass of stable manganese two months after the start of the study substantially increased the rate of elimination of ^{54}Mn.

(158) Davidsson et al. (1989) measured retention and excretion of ^{54}Mn in 14 healthy adults after its ingestion in infant formula. The mean biological half-time of absorbed activity over the period 10-30 d post ingestion was 16.4 d with a range of 6-32 d. Following intravenous administration of ^{54}Mn to two subjects, the turnover rate during days 10-30 corresponded to biological half-times of 74 and 24 d, compared with 27 and 8 d, respectively, in the same subjects following oral administration.

(159) Finley and coworkers (1994, 1999) studied the effects of gender and other factors on absorption and retention of manganese in healthy adult human subjects. Retention data for absorbed manganese for days 10-20 indicated mean whole-body biological half-times of about 15 d for men and 12 d for women. Data for days 19 to 70 indicated mean half-times of about 48 d for men and 34 d for women.

14.1.3.2. Biokinetic model for systemic manganese

(160) The biokinetic model for systemic manganese applied to workers in *Publication 151* (2022) is applied here to adult members of the public. The same model is applied to preadult ages except that manganese reaching a bone volume compartment is assumed to be removed to blood at the reference age-specific rate of turnover of that bone type (ICRP, 2002).

(161) The model structure is shown in Fig. 14.1. Transfer coefficients are listed in Table 14.2.

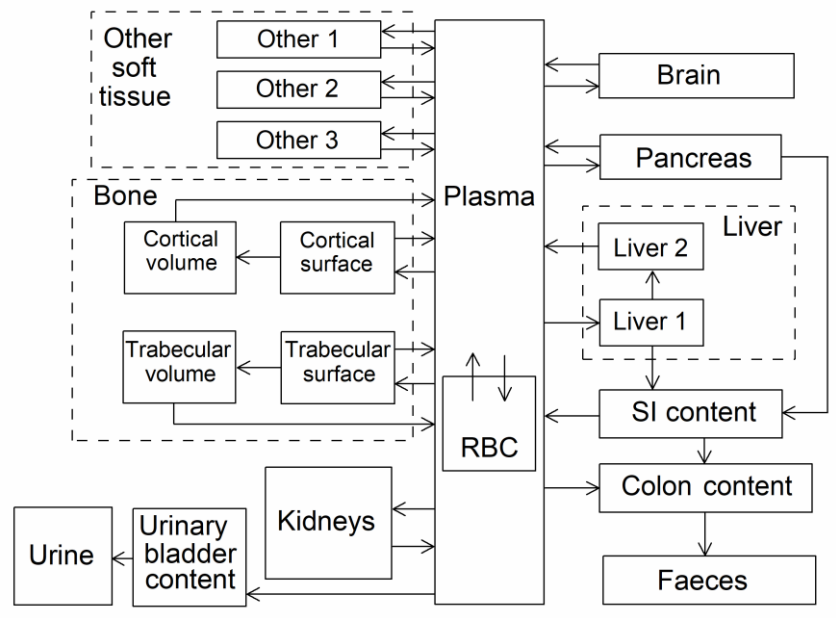

Fig. 14.1. Structure of the biokinetic model for systemic manganese. SI, small intestine; RBC, red blood cells.

Table 14.2. Age-specific transfer coefficients for manganese.

		Transfer coefficients (d^{-1})					
Pathway		100 d	1 y	5 y	10 y	15 y	Adult
Plasma	Liver 1	3.00E+02	3.00E+02	3.00E+02	3.00E+02	3.00E+02	3.00E+02
Plasma	Kidneys	5.00E+01	5.00E+01	5.00E+01	5.00E+01	5.00E+01	5.00E+01
Plasma	Pancreas	5.00E+01	5.00E+01	5.00E+01	5.00E+01	5.00E+01	5.00E+01
Plasma	UB content	2.00E+00	2.00E+00	2.00E+00	2.00E+00	2.00E+00	2.00E+00
Plasma	RC content	1.00E+01	1.00E+01	1.00E+01	1.00E+01	1.00E+01	1.00E+01
Plasma	Other 1	3.92E+02	3.92E+02	3.92E+02	3.92E+02	3.92E+02	3.92E+02
Plasma	Other 2	1.50E+02	1.50E+02	1.50E+02	1.50E+02	1.50E+02	1.50E+02
Plasma	Other 3	4.00E+01	4.00E+01	4.00E+01	4.00E+01	4.00E+01	4.00E+01
Plasma	Cort surface	2.50E+00	2.50E+00	2.50E+00	2.50E+00	2.50E+00	2.50E+00
Plasma	Trab surface	2.50E+00	2.50E+00	2.50E+00	2.50E+00	2.50E+00	2.50E+00
Plasma	Brain	1.00E+00	1.00E+00	1.00E+00	1.00E+00	1.00E+00	1.00E+00
Plasma	RBC	2.00E-01	2.00E-01	2.00E-01	2.00E-01	2.00E-01	2.00E-01
Liver 1	SI content	1.39E-01	1.39E-01	1.39E-01	1.39E-01	1.39E-01	1.39E-01
Liver 1	Liver 2	5.55E-01	5.55E-01	5.55E-01	5.55E-01	5.55E-01	5.55E-01
Liver 2	Plasma	3.47E-01	3.47E-01	3.47E-01	3.47E-01	3.47E-01	3.47E-01
Kidneys	Plasma	3.47E-01	3.47E-01	3.47E-01	3.47E-01	3.47E-01	3.47E-01
Pancreas	Plasma	3.47E-01	3.47E-01	3.47E-01	3.47E-01	3.47E-01	3.47E-01
Pancreas	SI content	3.47E-01	3.47E-01	3.47E-01	3.47E-01	3.47E-01	3.47E-01
Other 1	Plasma	3.33E+01	3.33E+01	3.33E+01	3.33E+01	3.33E+01	3.33E+01
Other 2	Plasma	3.47E-01	3.47E-01	3.47E-01	3.47E-01	3.47E-01	3.47E-01
Other 3	Plasma	1.73E-02	1.73E-02	1.73E-02	1.73E-02	1.73E-02	1.73E-02
Cort surface	Plasma	1.72E-02	1.72E-02	1.72E-02	1.72E-02	1.72E-02	1.72E-02
Cort surface	Cort volume	1.73E-04	1.73E-04	1.73E-04	1.73E-04	1.73E-04	1.73E-04
Trab surface	Plasma	1.72E-02	1.72E-02	1.72E-02	1.72E-02	1.72E-02	1.72E-02
Trab surface	Trab volume	1.73E-04	1.73E-04	1.73E-04	1.73E-04	1.73E-04	1.73E-04
Cort volume	Plasma	8.22E-03	2.88E-03	1.53E-03	9.04E-04	5.21E-04	8.21E-05
Trab volume	Plasma	8.22E-03	2.88E-03	1.81E-03	1.32E-03	9.59E-04	4.93E-04
Brain	Plasma	4.62E-03	4.62E-03	4.62E-03	4.62E-03	4.62E-03	4.62E-03
RBC	Plasma	8.33E-03	8.33E-03	8.33E-03	8.33E-03	8.33E-03	8.33E-03

UB, urinary bladder; RC, right colon; Cort, cortical; Trab, trabecular; RBC, red blood cells; SI, small intestine.

14.1.3.3. Treatment of radioactive progeny

(162) The treatment of radioactive progeny produced in systemic compartments after intake of a radioisotope of manganese is described in Section 14.2.3.3. of *Publication 151* (ICRP, 2022).

14.2. Dosimetric data for manganese

Table 14.3. Committed effective dose coefficients (Sv Bq^{-1}) for the inhalation or ingestion of ^{54}Mn compounds.

	Effective dose coefficients (Sv Bq^{-1})					
	3m	1y	5y	10y	15y	Adult
Inhaled particulate materials (1 µm AMAD aerosols)						
Type F	6.3E-09	3.5E-09	1.9E-09	1.3E-09	9.0E-10	9.3E-10
Type M, default	7.7E-09	6.3E-09	3.8E-09	2.6E-09	1.9E-09	2.3E-09
Type S	1.5E-08	1.4E-08	8.6E-09	5.9E-09	4.7E-09	5.6E-09
Ingested materials						
All compounds	6.9E-09	1.8E-09	1.0E-09	7.2E-10	5.1E-10	5.0E-10

AMAD, activity median aerodynamic diameter.

15. COPPER (Z=29)

15.1. Routes of Intake

15.1.1. Inhalation

(163) For copper, default parameter values were adopted on absorption to blood from the respiratory tract (ICRP, 2015). Absorption parameter values and types, and associated f_A values for particulate forms of copper are given in Table 15.1 [taken from Section 16 of *Publication 151* (ICRP, 2022)].

Table 15.1. Absorption parameter values for inhaled and ingested copper.

	Absorption parameter values*		
Inhaled particulate materials	f_r	s_r (d^{-1})	s_s (d^{-1})
Default parameter values†			
Absorption type			
F	1	30	–
M‡	0.2	3	0.005
S	0.01	3	1×10^{-4}

Ingested materials§

	Age-dependent absorption from the alimentary tract, f_A					
Assigned forms	3 months	1 year	5 years	10 years	15 years	adult
All compounds	1	0.5	0.5	0.5	0.5	0.5

*It is assumed that the bound state can be neglected for copper (i.e. $f_b = 0$). The values of s_r for Type F, M and S forms of copper (30, 3 and 3 d^{-1} respectively) are the general default values.
†For inhaled material deposited in the respiratory tract and subsequently cleared by particle transport to the alimentary tract, the default f_A values for inhaled materials are applied: i.e. the product of f_r for the absorption type and the f_A value for ingested soluble forms of copper applicable to the age-group of interest (e.g. 0.5 for adults).
‡Default Type M is recommended for use in the absence of specific information on which the exposure material can be assigned to an absorption type (e.g. if the form is unknown, or if the form is known but there is no information available on the absorption of that form from the respiratory tract).
§Activity transferred from systemic compartments into segments of the alimentary tract is assumed to be subject to reabsorption to blood. The default absorption fraction f_A for the secreted activity is the highest value for ingestion of the radionuclide applicable to the age-group of interest (e.g. 0.5 for adults).

15.1.2. Ingestion

15.1.2.1. Adults

(164) The average fractional absorption of copper ranges from 12% to 60%, see *Publication 151* (ICRP, 2022) for more details. In *Publications 30, 72* and *151* (ICRP, 1981, 1995c, 2022), the fractional absorption was taken to be 0.5 for all compounds of copper. In this publication, the same value of $f_A = 0.5$ is adopted for all chemical forms of copper ingested by adult members of the public.

15.1.2.2. Children

(165) Consistently with the approach of *Publication56* (ICRP, 1990), an $f_A = 1$ is adopted here for ingestion of all forms of copper by 3 month old infants and the adult value of 0.5 is used for older children.

15.1.3. Systemic distribution, retention and excretion of copper

15.1.3.1. Biokinetic data

(166) Copper (Cu) is a functional component of several enzymes in the human body and is necessary for normal iron metabolism and formation of red blood cells. The adult male human body contains about 70-80 mg of copper (Cartwright and Wintrobe, 1964; Zhu et al., 2010). Measured copper concentrations in postmortem tissues and in blood of living subjects indicate the following approximate distribution of copper in an adult male: blood 5%, skeletal muscle 48%, liver 18%, bone 8%, and other tissue 21% (Zhu et al., 2010).

(167) Absorption of copper from the small intestine is inversely related to the level of copper intake. Absorbed copper binds to two plasma proteins, albumin and transcuprein. Much of the bound copper is rapidly deposited in the liver, the key organ regarding copper metabolism and homeostasis. Most of the copper entering liver is incorporated into the enzyme ceruloplasmin, which is released to blood and transferred to tissues (Cartwright and Wintrobe, 1964; Cromwell, G. L., 1997; Linder and Hazegh-Azam, 1996; Turnland, 1998; Angelova et al., 2011; Osredkar and Sustar, 2011).

(168) Copper has two stable isotopes, ^{63}Cu and ^{65}Cu, with natural abundances of 69.2% and 30.8%, respectively. Scott and Turnland (1994) investigated the biokinetics of copper in healthy young adult male humans over a 90-day period in which the less abundant isotope ^{65}Cu was administered at different times. The time-dependent concentrations of ^{65}Cu were determined in blood components. Observed changes in the ^{65}Cu concentrations were interpreted in view of previously established characteristics of copper in the human body such as the typical mass, distribution, and faecal and urinary excretion rates of copper in adult humans and the roles of the liver in copper metabolism and storage. The data indicated that plasma contained about 4% of total-body copper, with ceruloplasmin containing 56-68% of plasma copper. The dietary copper level was judged to influence the flow rate from liver to plasma and from plasma to tissues other than liver. The investigators developed a biokinetic model depicting the observed behaviour of ^{65}Cu in blood plasma and the inferred time-dependent systemic distribution and excretion of ^{65}Cu. First-order transfer rates between compartments (or delay times, for two of the nine depicted transfers) were developed separately for each subject as fits to subject-specific data. Separate transfer coefficients were developed for oral intake and injection.

(169) Relative losses of copper along different excretion pathways were studied in dogs (Cartwright and Wintrobe, 1964). The results indicated that about 80% of excretion of systemic copper is due to biliary secretion into the small intestine, 16% is excreted after endogenous secretion directly across the intestinal wall, and 4% is excreted in urine.

(170) Following administration of ^{64}Cu as cupric acetate to rats, maximal activity concentrations were reached quickly in the liver, kidney, and gastrointestinal tract (Owen, 1965). Other tissues showed a progressive accumulation of ^{64}Cu after the disappearance of most of the non-ceruloplasmin ^{64}Cu from plasma and emergence of plasma ceruloplasmin ^{64}Cu, suggesting that ceruloplasmin may be the source of copper for tissues. The disappearance of ^{64}Cu from plasma tended to parallel that from the liver after 2 d.

(171) Dunn et al. (1991) developed a compartmental model of copper biokinetics in rats based on measurements of intravenously administered ^{64}Cu in plasma, tissues, and excreta over the first 3 d post injection. They interpreted the data in the context of a 16-compartment model that included 2 plasma compartments representing ceruloplasmin copper (Cp) and all other copper in plasma (NCp), 2 liver compartments, 2 compartments representing skin plus muscle (S-M), 2 compartments representing intestinal tissue, 2 compartments representing remaining tissue, and 6 compartments representing excretion pathways and excreta. Movement between

compartments was described by first-order transfers. Skin and muscle were treated as a single tissue because the data indicated virtually identical kinetics in these two tissues. The direct observations together with the results of the compartmental analysis indicated the following behaviour of ^{64}Cu. The injected activity entered the NCp fraction of plasma, cleared rapidly into the liver and S-M, and was initially removed at a high rate from liver in bile. The plasma content levelled out within the first hour, remained constant for about 10 h, and then began to decline gradually. This was attributed to a decreasing content of activity in NCp, offset by an increasing content in Cp. By 1 h post injection about 32% of the administered amount (after correction for physical decay) had accumulated in the liver. Activity was lost from the liver at a relatively high rate for a few hours and more slowly thereafter. Activity in S-M accounted for about 25% of the administered amount at 2 h, decreased slightly to about 10 h post administration, and then plateaued or slightly increased over the rest of the observation period, indicating a relatively long component of copper retention. About 25% of the administered amount was excreted in faeces in the first 24 h and about 45% by 72 h, apparently representing mainly biliary secretion of the tracer.

15.1.3.2. Biokinetic model for systemic copper

(172) The biokinetic model for copper developed by Scott and Turnland (1994) was modified for application to workers in *Publication 151* (ICRP, 2022). The model structure applied by those investigators was modified to depict the faecal and urinary excretion pathways applied in this report series. The mean transfer rates developed by Scott and Turnland for intravenous administration of ^{65}Cu during the period of adequate intake of copper were used as a starting point. Two delays depicted in their model were replaced with first-order transfer coefficients. The transfer rate from Liver 2 to Plasma 2 derived by Scott and Turnland was increased moderately for consistency with the long-term distribution of copper as indicated by autopsy data (Zhu et al., 2010). The transfer rate from Other to Plasma 1 was decreased to reflect longer retention in soft tissues indicated by data of Dunn et al. (1991) and for consistency with autopsy data.

(173) The biokinetic model for copper applied to workers in *Publication 151* is applied in this report to all age groups. The structure of the model used here is shown in Fig. 15.1. Transfer coefficients are listed in Table 15.2.

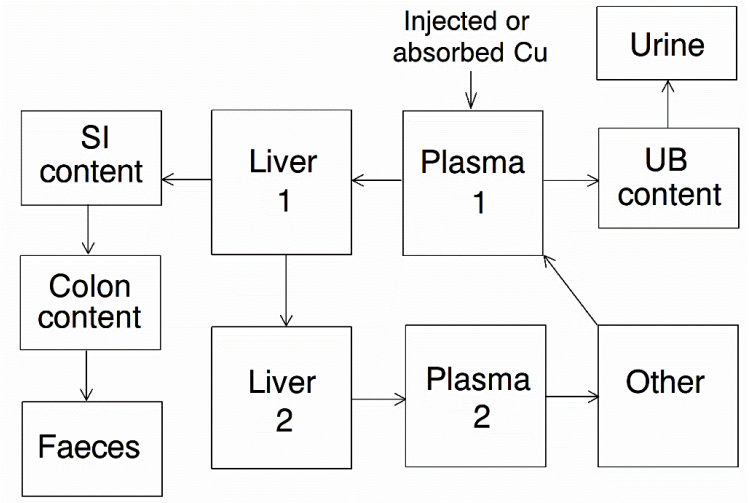

Fig. 15.1. Structure of the biokinetic model for systemic copper. UB, urinary bladder; SI, small intestine.

Table 15.2. Age-specific transfer coefficients for copper.

		Transfer coefficients (d^{-1})					
Pathway		100 d	1 y	5 y	10 y	15 y	Adult
Plasma 1	Liver 1	2.50E+01	2.50E+01	2.50E+01	2.50E+01	2.50E+01	2.50E+01
Plasma 1	UB content	1.40E-04	1.40E-04	1.40E-04	1.40E-04	1.40E-04	1.40E-04
Liver 1	SI content	1.90E+01	1.90E+01	1.90E+01	1.90E+01	1.90E+01	1.90E+01
Liver 1	Liver 2	2.00E+02	2.00E+02	2.00E+02	2.00E+02	2.00E+02	2.00E+02
Liver 2	Plasma 2	1.30E+00	1.30E+00	1.30E+00	1.30E+00	1.30E+00	1.30E+00
Plasma 2	Other	1.50E+01	1.50E+01	1.50E+01	1.50E+01	1.50E+01	1.50E+01
Other	Plasma 1	3.00E-01	3.00E-01	3.00E-01	3.00E-01	3.00E-01	3.00E-01

UB, urinary bladder; SI, small intestine.

15.2. Dosimetric data for copper

Table 15.3. Committed effective dose coefficients (Sv Bq^{-1}) for the inhalation or ingestion of ^{64}Cu compounds.

	Effective dose coefficients (Sv Bq^{-1})					
	3m	1y	5y	10y	15y	Adult
Inhaled particulate materials (1 µm AMAD aerosols)						
Type F	2.3E-10	1.5E-10	6.8E-11	4.8E-11	3.1E-11	2.6E-11
Type M, default	3.3E-10	2.4E-10	1.3E-10	9.0E-11	6.8E-11	5.9E-11
Type S	3.4E-10	2.5E-10	1.3E-10	9.5E-11	7.3E-11	6.4E-11
Ingested materials						
All compounds	3.8E-10	2.3E-10	1.4E-10	9.8E-11	6.5E-11	5.4E-11

AMAD, activity median aerodynamic diameter.

16. GALLIUM (Z=31)

16.1. Routes of Intake

16.1.1. Inhalation

(174) For gallium, default parameter values were adopted on absorption to blood from the respiratory tract (ICRP, 2015). Absorption parameter values and types, and associated f_A values for particulate forms of gallium are given in Table 16.1 [taken from Section 17 of *Publication 151* (ICRP, 2022)].

16.1.2. Ingestion

16.1.2.1. Adults

(175) Gallium is poorly absorbed from the gastro-intestinal tract, see *Publication 151* (ICRP, 2022) for more details. In *Publications 30*, *72* (ICRP, 1981, 1995c) and *151*, the fractional absorption was taken to be 0.001 for all compounds of the element. In this publication, the same value $f_A = 0.001$ is applied to all forms of gallium ingested by adult members of the public.

16.1.2.2. Children

(176) Consistently with the approach of *Publication56* (ICRP, 1990), an $f_A = 0.01$ is adopted here for 3 month old infants and the adult value of $f_A = 10^{-3}$ is used for older children.

Table 16.1. Absorption parameter values for inhaled and ingested gallium.

	Absorption parameter values*		
Inhaled particulate materials	f_r	s_r (d^{-1})	s_s (d^{-1})
Default parameter values†			
Absorption type			
F	1	30	–
M‡	0.2	3	0.005
S	0.01	3	1×10^{-4}

Ingested materials§

	Age-dependent absorption from the alimentary tract, f_A					
Assigned forms	3 months	1 year	5 years	10 years	15 years	adult
All compounds	0.01	0.001	0.001	0.001	0.001	0.001

*It is assumed that the bound state can be neglected for gallium (i.e. $f_b = 0$). The values of s_r for Type F, M and S forms of gallium (30, 3 and 3 d^{-1} respectively) are the general default values.

†For inhaled material deposited in the respiratory tract and subsequently cleared by particle transport to the alimentary tract, the default f_A values for inhaled materials are applied: i.e. the product of f_r for the absorption type and the f_A value for ingested soluble forms of gallium applicable to the age-group of interest (e.g. 0.001 for adults).

‡Default Type M is recommended for use in the absence of specific information on which the exposure material can be assigned to an absorption type (e.g. if the form is unknown, or if the form is known but there is no information available on the absorption of that form from the respiratory tract).

§Activity transferred from systemic compartments into segments of the alimentary tract is assumed to be subject to reabsorption to blood. The default absorption fraction f_A for the secreted activity is the highest value for ingestion of the radionuclide applicable to the age-group of interest (e.g. 0.001 for adults).

16.1.3. Systemic distribution, retention and excretion of gallium

16.1.3.1. Biokinetic data

(177) Nearly all of the gallium in blood is in plasma, where it is mainly bound to the iron-transport protein transferrin (Bernstein, 1998). Gallium has a strong affinity for growing and remodelling bone (Bernstein, 1998). In growing bone gallium is concentrated in the metaphysis, particularly the cartilaginous growth plate. It also accumulates on the endosteal and periosteal surfaces of diaphyseal bone (Bockman et al, 1986, 1990) and in some soft tissues including the liver, spleen, and kidneys (Bernstein, 1998).

(178) Clearance of gallium in blood can be described reasonably well as two phases of removal with half-times of about 0.25 d and 7 d (Kriegel, 1984). Roughly a third of the amount deposited in tissues is removed from the body over a relatively short period, mainly in urine, and the remainder is removed relatively slowly in urine and faeces (Kriegel, 1984).

(179) Priest et al. (1995) studied the biokinetics of ^{67}Ga ($T_{1/2}$ = 3.26 d) over a 21-d period following its intravenous administration to a healthy adult male volunteer. Retention $R(t)$ in blood at t days post injection ($t \geq 0.2$), expressed as a percentage of the injected amount corrected for decay, was described by the power function $R(t)=10.5t^{-0.75}$. Decay-corrected urinary and faecal excretion over the first 13 d represented about 27% and 10%, respectively, of administered activity.

(180) Nelson et al. (1972) measured activity concentrations in postmortem tissues of 23 patients administered ^{67}Ga intravenously at various times before death. Highest mean concentrations expressed as % kg^{-1} were found in spleen (4.1), kidney cortex (3.8), adrenals (3.8), bone marrow (3.6), liver (2.8), kidney (2.7), and bone (2.6). Some organs including the kidneys showed a rapid decrease in activity from high early values but a later slow decrease of retained activity. Considerable variation in tissue concentrations from patient to patient was observed.

(181) Zhu et al. (2010) measured concentrations of gallium in 17 tissues obtained from autopsies of up to 68 Chinese men from four areas of China. All subjects were considered healthy until the time of sudden accidental death. Based on median gallium concentrations in tissue and reference tissue masses, most of the total-body gallium was contained in fat (31%), bone (25%), and muscle (23%).

16.1.3.2. Biokinetic model for systemic gallium

(182) The biokinetic model for systemic gallium applied to workers in *Publication 151* (2022) is applied in this report to adult members of the public. In *Publication 151*, transfer coefficients were based largely on data summarized above on the observed kinetics and postmortem distribution of gallium in human subjects. Derivation of transfer coefficients focused on data for relatively early times after administration, as radioisotopes of gallium addressed by the ICRP have short half-lives (maximum, 3.26 d). For application to pre-adult ages, the flow rates from blood to bone surface compartments are increased by 50% above the values for adults, and the rate from blood to the fast-turnover soft-tissue compartment (Other 0) is decreased to yield the same total removal rate from blood at all ages.

(183) The structure of the biokinetic model for systemic gallium is shown in Fig. 16.1. Transfer coefficients are listed in Table 16.2.

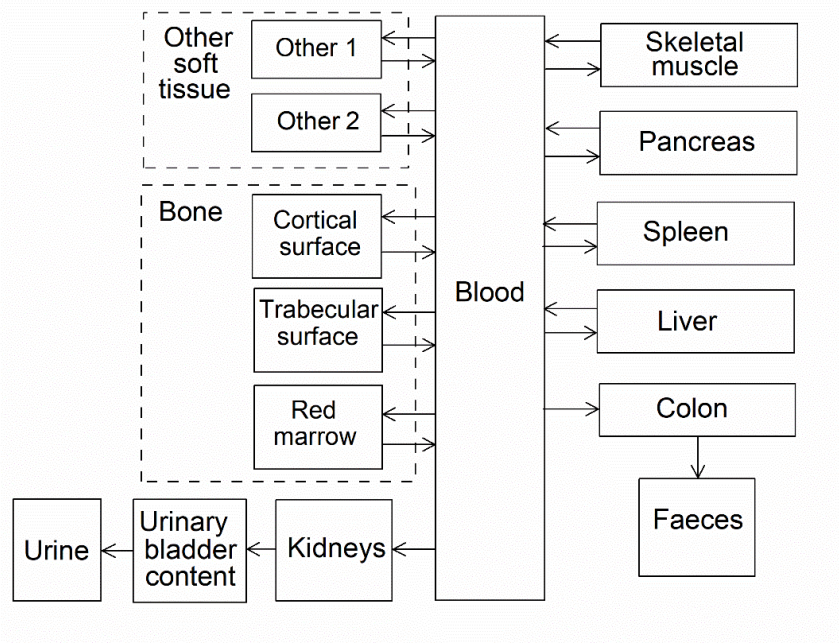

Fig. 16.1. Structure of the biokinetic model for systemic gallium.

Table 16.2. Age-specific transfer coefficients for gallium.

		Transfer coefficients (d^{-1})					
Pathway		100 d	1 y	5 y	10 y	15 y	Adult
Blood	RC content	1.50E-01	1.50E-01	1.50E-01	1.50E-01	1.50E-01	1.50E-01
Blood	Liver	3.00E-01	3.00E-01	3.00E-01	3.00E-01	3.00E-01	3.00E-01
Blood	Kidneys	4.00E-01	4.00E-01	4.00E-01	4.00E-01	4.00E-01	4.00E-01
Blood	Spleen	5.00E-02	5.00E-02	5.00E-02	5.00E-02	5.00E-02	5.00E-02
Blood	Trab surface	7.50E-01	7.50E-01	7.50E-01	7.50E-01	7.50E-01	5.00E-01
Blood	Cort surface	7.50E-01	7.50E-01	7.50E-01	7.50E-01	7.50E-01	5.00E-01
Blood	Red marrow	2.50E-01	2.50E-01	2.50E-01	2.50E-01	2.50E-01	2.50E-01
Blood	Muscle	2.00E-01	2.00E-01	2.00E-01	2.00E-01	2.00E-01	2.00E-01
Blood	Pancreas	5.00E-03	5.00E-03	5.00E-03	5.00E-03	5.00E-03	5.00E-03
Blood	Other 1	1.65E+00	1.65E+00	1.65E+00	1.65E+00	1.65E+00	2.15E+00
Blood	Other 2	5.00E-01	5.00E-01	5.00E-01	5.00E-01	5.00E-01	5.00E-01
Liver	Blood	1.39E-01	1.39E-01	1.39E-01	1.39E-01	1.39E-01	1.39E-01
Kidneys	UB content	1.39E+00	1.39E+00	1.39E+00	1.39E+00	1.39E+00	1.39E+00
Spleen	Blood	1.39E-01	1.39E-01	1.39E-01	1.39E-01	1.39E-01	1.39E-01
Trab surface	Blood	3.47E-01	3.47E-01	3.47E-01	3.47E-01	3.47E-01	3.47E-01
Cort surface	Blood	3.47E-01	3.47E-01	3.47E-01	3.47E-01	3.47E-01	3.47E-01
Red marrow	Blood	3.47E-01	3.47E-01	3.47E-01	3.47E-01	3.47E-01	3.47E-01
Muscle	Blood	1.39E-01	1.39E-01	1.39E-01	1.39E-01	1.39E-01	1.39E-01
Pancreas	Blood	1.39E-01	1.39E-01	1.39E-01	1.39E-01	1.39E-01	1.39E-01
Other 1	Blood	1.39E+00	1.39E+00	1.39E+00	1.39E+00	1.39E+00	1.39E+00
Other 2	Blood	1.90E-03	1.90E-03	1.90E-03	1.90E-03	1.90E-03	1.90E-03

UB, urinary bladder; RC, right colon; Cort, cortical; Trab, trabecular.

16.1.3.3. Treatment of radioactive progeny

(184) The treatment of radioactive progeny produced in systemic compartments after intake of a radioisotope of gallium is described in Section 17.2.3.3. of *Publication 151* (ICRP, 2022).

16.2. Dosimetric data for gallium

Table 16.3. Committed effective dose coefficients (Sv Bq^{-1}) for the inhalation or ingestion of ^{67}Ga compounds.

	Effective dose coefficients (Sv Bq^{-1})					
	3m	1y	5y	10y	15y	Adult
Inhaled particulate materials (1 μm AMAD aerosols)						
Type F	2.7E-10	2.0E-10	9.4E-11	6.2E-11	4.2E-11	3.9E-11
Type M, default	5.3E-10	4.0E-10	2.3E-10	1.6E-10	1.2E-10	1.2E-10
Type S	5.9E-10	4.5E-10	2.6E-10	1.8E-10	1.4E-10	1.3E-10
Ingested materials						
All compounds	2.3E-10	2.0E-10	1.1E-10	8.2E-11	5.7E-11	5.4E-11

AMAD, activity median aerodynamic diameter.

17. GERMANIUM (Z=32)

17.1. Routes of Intake

17.1.1. Inhalation

(185) For germanium, default parameter values were adopted on absorption to blood from the respiratory tract (ICRP, 2015). Absorption parameter values and types, and associated f_A values for particulate forms of germanium are given in Table 17.1 [taken from Section 18 of *Publication 151* (ICRP, 2022)].

17.1.2. Ingestion

(186) Dietary forms of germanium are well absorbed from the gastrointestinal tract of man, see *Publication 151* (ICRP, 2022) for details. In *Publications 30*, *72* and *151* (ICRP, 1981, 1995c, 2022), the fractional absorption was taken as 1 for all compounds of germanium. In this publication, the value $f_A = 1$ is also used for all chemical forms of germanium ingested by members of the public of all ages.

Table 17.1. Absorption parameter values for inhaled and ingested germanium.

	Absorption parameter values*		
Inhaled particulate materials	f_r	s_r (d^{-1})	s_s (d^{-1})
Default parameter values†			
Absorption type			
F	1	30	–
M‡	0.2	3	0.005
S	0.01	3	1×10^{-4}

Ingested materials§	Age-dependent absorption from the alimentary tract, f_A					
Assigned forms	3 months	1 year	5 years	10 years	15 years	adult
All compounds	1	1	1	1	1	1

*It is assumed that the bound state can be neglected for germanium (i.e. $f_b = 0$). The values of s_r for Type F, M and S forms of germanium (30, 3 and 3 d^{-1} respectively) are the general default values.

†For inhaled material deposited in the respiratory tract and subsequently cleared by particle transport to the alimentary tract, the default f_A values for inhaled materials are applied: i.e. the product of f_r for the absorption type and the f_A value for ingested soluble forms of germanium applicable to the age-group of interest (1).

‡Default Type M is recommended for use in the absence of specific information on which the exposure material can be assigned to an absorption type (e.g. if the form is unknown, or if the form is known but there is no information available on the absorption of that form from the respiratory tract).

§Activity transferred from systemic compartments into segments of the alimentary tract is assumed to be subject to reabsorption to blood. The default absorption fraction f_A for the secreted activity is the highest value for ingestion of the radionuclide applicable to the age-group of interest ($f_A = 1$).

17.1.3. Systemic distribution, retention and excretion of germanium

17.1.3.1. Biokinetic data

(187) Germanium is located just below silicon in Group IVA of the period table. In trace amounts, germanium mimics uptake and accumulation of silicon in laboratory animals. Mehard and Volcani (1975) compared the behaviours of ^{31}Si ($T_{1/2}$ = 157 min) and ^{68}Ge (271 d) in rats

following intravenous (IV) or intraperitoneal (IP) administration of $^{31}Si(OH)_4$ and $^{68}Ge(OH)_4$. Accumulation of ^{31}Si and ^{68}Ge in tissues increased for about 15-40 min, declined rapidly for ~30 min, and then declined more gradually. Faster depletion of ^{68}Ge than ^{31}Si was indicated. By 2 h after IV injection the concentration of ^{68}Ge in liver was about 65% higher than that of ^{31}Si. Concentrations of ^{68}Ge were measured in blood and 11 tissues at five times from 0.1-20 d after IV injection. Highest concentrations (normalized to 1.0 for kidney at each time) were seen in kidney (1.0), liver (0.29), and blood (0.19) at 0.1 d; kidney (1.0), spleen (0.31, and liver (0.28) at 4 d; and spleen (2.0), kidney (1.0), and urinary bladder (0.15) at 20 d.

(188) The concentration of germanium was measured in 17 tissues obtained from autopsies of up to 68 men from four areas of China and in blood of 10 volunteers from the same areas (Zhu et al., 2010). Highest median concentrations were found in rib (89 μg kg^{-1}) followed by blood, liver, and spleen (~45 μg kg^{-1} each); lung (33 μg kg^{-1}); kidney (19 μg kg^{-1}); and thyroid (18 μg kg^{-1}). Concentrations in the range 4-13 μg kg^{-1} were found in gastrointestinal tract tissues, skeletal muscle, heart, testes, thymus, fat, and skin. Based on median tissue concentrations and reference masses of tissues, bone contained about 50% of total-body germanium, blood 15%, liver 4.5%, kidney 0.4%, and other tissue 30%. The estimated total-body content based on median tissue concentrations was 1.4 mg, which is roughly the typical daily intake of germanium in food (Schauss, 1991; Scansetti, 1992). As germanium in food appears to be nearly completely absorbed from the gut (Rosenfeld, 1954; Scansetti, 1992), this suggests low systemic retention of germanium.

(189) During the early hours after parenteral administration of germanium compounds to rats or mice (Rosenfeld, 1954; Durbin, 1960; Mehard and Volcani, 1975; Shinoga et al., 1989), the concentration of germanium in the kidneys was much greater than in other tissues. Germanium was rapidly excreted in urine. At 4 d after intravenous administration of ^{71}Ge as $NaHGeO_3$ to rats, cumulative excretion accounted for about 98.5% of the administered amount, and the bone, liver, and kidney contents accounted for about 0.4%, 0.5%, and 1.1%, respectively (Durbin, 1960). At 3 h after intraperitoneal administration of Na_2GeO_3 to rats, the concentration of Ge in the kidneys was 2-20 times that in 14 other examined tissues and fluids (Rosenfeld, 1954). Germanium did not appear to be stored by any tissue after multiple weekly doses (Rosenfeld, 1954).

(190) Velikyan et al. (2013) investigated the organ distribution of ^{68}Ge in rats through day 7 following intravenous administration of $^{68}GeCl_4$. Activity was distributed somewhat uniformly among tissues beyond a few hours. Excretion was rapid and primarily in urine. About 90% of the injected activity was eliminated in urine with half-time < 1 h. A second, slower phase of retention was observed, with ~1.8% of the activity remaining in the animals after 1 wk. Velikyan and coworkers estimated absorbed doses to tissues for adult male and female humans based on the observed residence times in rat tissues. Highest dose estimates for females, expressed as μSv MBq^{-1}, were obtained for kidney (185), adrenals (83), liver (38), colon wall (~20), red marrow (13), osteogenic cells (11), and spleen (11). Lowest dose estimates were obtained for lungs (3.2), heart wall (2.6), muscle (2.0), pancreas (1.9), and brain (1.2). Dose estimates for 10 other tissues were in the range 7-10 μSv MBq^{-1}.

(191) Shinoga et al. (1989) studied uptake and retention of stable germanium in mice after a single peroral administration of GeO_2 solution. Germanium concentrations in blood, stomach, small intestine, and eight systemic soft tissues were measured from 1-24 h after administration. The maximum concentration in blood and systemic tissues was reached within 1 h. The kidneys showed the highest concentration from 1-24 h. The highest biological half-time was seen in brain (6.3 h). The half-time in blood was 1.2 h and in soft tissues other than brain was in the range 2.4-4.4 h. The area under the time-concentration curve, expressed as μg h g^{-1}, decreased in the order: kidney (51), liver (23), pancreas (13), blood and spleen (11), lung (10), heart (7), testis (6), brain (1.5). At 24 h germanium was detectable only in kidney, liver, spleen, and brain.

17.1.3.2. Biokinetic model for systemic germanium

(192) The biokinetic model for systemic germanium applied to workers in *Publication 151* (2022) is applied in this report to adult members of the public. The basis for the model is described in that report. The same model is applied to preadults except that increased rates of loss from bone compartments are assigned to preadults, as the rate of removal from bone is based on the bone turnover rate. The bone turnover rates applied in the model are reference values given in *Publication* 89 (ICRP, 2002).

(193) The structure of the biokinetic model for systemic germanium used in this report is shown in Fig. 17.1. Transfer coefficients are listed in Table 17.2.

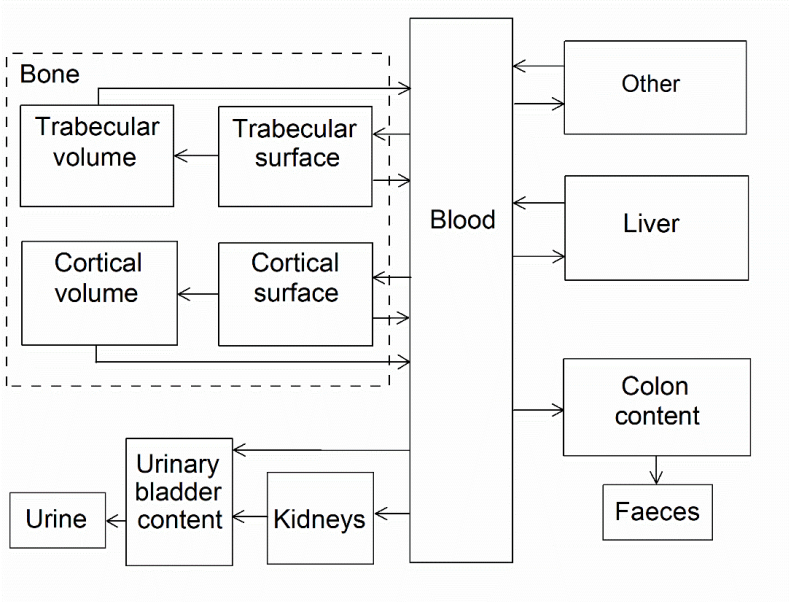

Fig. 17.1 Structure of the biokinetic model for systemic germanium.

Table 17.2. Age-specific transfer coefficients for germanium.

		Transfer coefficients (d^{-1})					
Pathway		100 d	1 y	5 y	10 y	15 y	Adult
Blood	Other	8.90E-01	8.90E-01	8.90E-01	8.90E-01	8.90E-01	8.90E-01
Blood	Kidneys	2.00E-01	2.00E-01	2.00E-01	2.00E-01	2.00E-01	2.00E-01
Blood	Liver	4.00E-01	4.00E-01	4.00E-01	4.00E-01	4.00E-01	4.00E-01
Blood	UB content	8.30E+00	8.30E+00	8.30E+00	8.30E+00	8.30E+00	8.30E+00
Blood	RC content	1.00E-02	1.00E-02	1.00E-02	1.00E-02	1.00E-02	1.00E-02
Blood	Trab surface	1.00E-01	1.00E-01	1.00E-01	1.00E-01	1.00E-01	1.00E-01
Blood	Cort suface	1.00E-01	1.00E-01	1.00E-01	1.00E-01	1.00E-01	1.00E-01
Other	Blood	3.00E-01	3.00E-01	3.00E-01	3.00E-01	3.00E-01	3.00E-01
Kidneys	UB contemt	1.20E+00	1.20E+00	1.20E+00	1.20E+00	1.20E+00	1.20E+00
Liver	Blood	9.00E-01	9.00E-01	9.00E-01	9.00E-01	9.00E-01	9.00E-01
Trab surface	Blood	3.00E-01	3.00E-01	3.00E-01	3.00E-01	3.00E-01	3.00E-01
Cort suface	Blood	3.00E-01	3.00E-01	3.00E-01	3.00E-01	3.00E-01	3.00E-01
Trab surface	Trab volume	1.50E-03	1.50E-03	1.50E-03	1.50E-03	1.50E-03	1.50E-03
Cort suface	Cort volume	1.50E-03	1.50E-03	1.50E-03	1.50E-03	1.50E-03	1.50E-03
Trab volume	Blood	8.22E-03	2.88E-03	1.81E-03	1.32E-03	9.59E-04	4.93E-04
Cort volume	Blood	8.22E-03	2.88E-03	1.53E-03	9.04E-04	5.21E-04	8.21E-05

UB, urinary bladder; RC, right colon; Cort, cortical; Trab, trabecular.

17.1.3.3. Treatment of radioactive progeny

(194) The treatment of radioactive progeny produced in systemic compartments after intake of a radioisotope of germanium is described in Section 18.2.3.3. of *Publication 151* (ICRP, 2022).

17.2. Dosimetric data for germanium

Table 17.3. Committed effective dose coefficients (Sv Bq^{-1}) for the inhalation or ingestion of ^{68}Ge compounds.

	Effective dose coefficients (Sv Bq^{-1})					
	3m	1y	5y	10y	15y	Adult
Inhaled particulate materials (1 μm AMAD aerosols)						
Type F	1.5E-09	1.0E-09	4.6E-10	3.2E-10	1.9E-10	1.4E-10
Type M, default	4.6E-08	4.1E-08	2.4E-08	1.6E-08	1.3E-08	1.3E-08
Type S	1.1E-07	1.0E-07	6.3E-08	4.2E-08	3.4E-08	3.5E-08
Ingested materials						
All compounds	1.9E-09	1.4E-09	8.3E-10	5.3E-10	3.6E-10	2.9E-10

AMAD, activity median aerodynamic diameter.

18. ARSENIC (Z=33)

18.1. Routes of Intake

18.1.1. Inhalation

(195) For arsenic, default parameter values were adopted on absorption to blood from the respiratory tract (ICRP, 2015). Absorption parameter values and types, and associated f_A values for particulate forms of arsenic are given in Table 18.1 [taken from Section 19 of *Publication 151* (ICRP, 2022)].

18.1.2. Ingestion

(196) Water soluble forms of arsenic are mostly absorbed from the gut, while insoluble forms appear to be less available for absorption, see *Publication 151* (ICRP, 2022) for details. Regarding organic forms, Buchet et al. (1981a) compared the urinary excretion of arsenic and its speciation over 4 days after ingestion of sodium arsenite, monomethylarsonate (MMA) and dimethylarsinate (DMA) by human volunteers. It represented 46, 78 and 75% of the ingested arsenic quantity in the respective chemical forms. About 84% of arsenic ingested by an individual as 0.1 mg/kg body weight of DMA (Marafante et al. 1987) was excreted in 48h-urine. Juhasz et al. (2006, 2008) evaluated the oral bioavailability in swine of arsenic present in rice either as organic DMA or inorganic sodium arsenate as 33 and 89% respectively; as 100% in mung beans and 50% in lettuce and chard grown using arsenic-contaminated water.

(197) Francesconi et al. (2002) monitored arsenic metabolites in human urine over 4 days after ingestion of arsenic-containing carbohydrates (arsenosugars), observing that approximately 80% of the ingested arsenic was excreted in urine. In a similar study, Raml et al. (2009) observed a large variation from 4 to 95% of arsenic urinary excretion among 6 volunteers correlated with a range of different metabolites in urine and blood.

(198) Early studies of arsenic in seafood indicated that arsenobetaine was efficiently absorbed and excreted unchanged (Chapman, 1926). Freeman et al. (1979) reported the urinary excretion of 76% arsenic over 8 days after ingestion in fish by 6 volunteers. Luten et al. (1982) showed that 69-85% of arsenic as organic arsenobetaine in ingested fish was excreted in urine within five days by 8 human volunteers. Tam et al. (1982) followed urinary and faecal excretion of arsenic in 15 healthy adult volunteers over 8 days after ingestion of arsenic-rich fish: 77% of fish-arsenic was excreted in urine while only 0.33% was recovered in faeces, demonstrating nearly complete absorption. Brown et al. (1990) administered ^{74}As-labelled arsenobetaine with fish to 6 volunteers and measured after one day a whole-body content of about half the ingested ^{74}As quantity, also suggesting nearly complete absorption.

(199) In *Publications 30* and *72* (ICRP, 1981, 1995c) an f_1 of 0.5 was recommended for all compounds of arsenic. In *Publication 151*, f_A values of 1 and 0.3 were used for water soluble compounds and for insoluble compounds, including and arsenic in soils, respectively. The same values of $f_A = 1$ for soluble arsenic forms, including arsenic in diet, and $f_A = 0.3$ for insoluble forms are adopted here for all ages.

Table 18.1. Absorption parameter values for inhaled and ingested arsenic.

	Absorption parameter values*		
Inhaled particulate materials	f_r	s_r (d^{-1})	s_s (d^{-1})
Default parameter values†			
Absorption type			
F	1	30	–
M‡	0.2	3	0.005
S	0.01	3	1×10^{-4}

Ingested materials§

	Age-dependent absorption from the alimentary tract, f_A					
Assigned forms	3 months	1 year	5 years	10 years	15 years	adult
Water soluble compounds, arsenic in diet	1	1	1	1	1	1
Water insoluble compounds and arsenic in soil	0.3	0.3	0.3	0.3	0.3	0.3

*It is assumed that the bound state can be neglected for arsenic (i.e. $f_b = 0$). The values of s_r for Type F, M and S forms of arsenic (30, 3 and 3 d^{-1} respectively) are the general default values.

†For inhaled material deposited in the respiratory tract and subsequently cleared by particle transport to the alimentary tract, the default f_A values for inhaled materials are applied: i.e. the product of f_r for the absorption type and the f_A value for ingested soluble forms of arsenic applicable to the age-group of interest (1).

‡Default Type M is recommended for use in the absence of specific information on which the exposure material can be assigned to an absorption type (e.g. if the form is unknown, or if the form is known but there is no information available on the absorption of that form from the respiratory tract).

§Activity transferred from systemic compartments into segments of the alimentary tract is assumed to be subject to reabsorption to blood. The default absorption fraction f_A for the secreted activity is the highest value for ingestion of the radionuclide applicable to the age-group of interest ($f_A = 1$).

18.1.3. Systemic distribution, retention and excretion of arsenic

18.1.3.1. Biokinetic data

(200) Arsenic (As) exists primarily in the trivalent state in the earth's crust but is largely oxidized to pentavalent arsenic (As(V)) in soil and water (Mochizuki, 2019). Absorbed or injected inorganic As(III) and As(V) initially have noticeably different systemic kinetics (Vahter and Norin, 1980; Lindgren et al., 1982). A substantial portion of absorbed As(V) is reduced to As(III) in the body (Vahter and Marafante, 1985; Vahter, 2002), resulting in more similar distributions of the initially different forms over time.

(201) Mealey et al. (1959) summarized observations of the systemic behaviour of ^{74}As in >100 patients administered ^{74}As(III) intravenously for brain tumor localization. In four patients followed up to 10 d, blood clearance $C(t)$ of ^{74}As expressed as % dosage L^{-1} blood at t hours ($t \geq 0.25$), was described by a sum of three exponential terms: $C(t) = 7.0e^{-1.54t} + 0.07e^{-0.025t} + 0.015e^{-0.003t}$. The activity concentration in red blood cells increased over time and was about 3 times the plasma concentration by 10 h post injection. Renal clearance of ^{74}As was estimated as 3.54 L plasma h^{-1}. Cumulative urinary activity was in the range 18-30% of the administered amount at 1 h post injection, 36-56% at 4 h, and 57-90% at 9 d. In a patient followed for 18 d, urinary activity accounted for ~97% of the injected amount. Only small amounts were recovered in faeces, e.g. 0.21% of the administered amount in one case during the first week, and 1.3% in a second case over 17 d. The concentration of ^{74}As in tissues was determined for 11 patients who died at times ranging from 1 h to 71 d after injection. In all cases the highest concentrations were found in the liver and kidneys. These two tissues contained roughly 20% and 10%, respectively, at 1 h after injection. The sequential data for the 11 cases indicated that

roughly 90% or more of the activity retained in the kidneys at 1 h was removed with a half-time of about 8 h, and the remainder declined with a half-time of 2-3 d. The indicated time-dependent behaviour of ^{74}As in the liver also suggested two components of retention, with half-times of roughly 1 d for 90% or more of the retained activity and 2 wk for the remainder.

(202) Pomroy et al. (1980) studied the biokinetics of ^{74}As(V) in six healthy adult male subjects (ages 28-60 y) following its oral administration as arsenic acid. Total-body retention was measured externally for periods up to 103 d, and losses in urine and faeces were measured up to 7 d. The pooled measurements of total-body retention were fit by a sum of three exponential terms indicating biological half-times of 2.1 d (65.9%), 9.5 d (30.4%), and 38.4 d (3.7%). Cumulative urinary and faecal excretion of ^{74}As over the first 7 d represented on average 62% and 6%, respectively, of the administered amount. The portions of faecal losses representing unabsorbed and endogenously secreted activity could not be determined. The excretion patterns are qualitatively consistent with findings of Mealey et al. (1959) for intravenously injected ^{74}As(III) in that most of the amount entering blood was largely excreted in urine over the next few days. However, the initial urinary excretion rate was higher in the subjects of Mealey et al.: 36-56% at 4 h, compared with 18-27% at 1 d observed by Pomroy et al.

(203) Activity concentrations were measured in post-mortem tissues of an adult female cancer patient who was administered ^{76}As intravenously 20 h before death (Ducoff et al., 1948). The highest concentration was found in the liver, followed by the kidneys. Normalized to a concentration of 1.0 in liver, the concentrations decreased in the order: kidneys (0.64) > spleen, heart, marrow, lymph nodes, stomach, pancreas, muscle, small intestine, and lung (0.23-0.35) > adrenals, ovary, thyroid, and skin (0.14-0.18) > brain and femoral cortical bone (0.05).

(204) Zhu et al. (2010) reported medians and ranges of arsenic concentration in 17 tissues collected at autopsy from up to 68 adult males from 4 regions of China, and in blood of 16 living subjects from the same regions. The highest median concentration was found in rib (102 μg kg^{-1} wet weight), followed by thyroid (53 μg kg^{-1}) and liver (41 μg kg^{-1}). Concentrations in blood and the remaining 14 tissues were in the range 19-38 μg kg^{-1}. Based on the observed median concentrations of arsenic in tissues and reference masses of tissues, about 38% of total-body arsenic was contained in bone, 29% in muscle, 11% in fat, 5% in blood, 4% in skin, 3% in liver, and 10% in remaining tissues.

(205) In biokinetic studies of inorganic arsenic in laboratory animals, the liver and kidneys usually show high concentrations of arsenic soon after administration of either As(III) or As(V) (Ducoff et al., 1948; Marafante et al., 1981; Lindgren et al., 1982). This is consistent with findings for human subjects (Ducoff et al., 1948; Mealey et al., 1959).

(206) Lindgren et al. (1982) examined the systemic distribution of intravenously injected ^{74}As as As(III) or As(V) in mice using whole-body autoradiography, external counting, and measurement of activity in dissected tissues. Comparison of autoradiograms at 1 h indicated higher uptake of As(III) in oral mucosa, stomach wall, and liver, and lower uptake in bone compared with As(V). The relatively high skeletal accumulation of As(V) was attributed to substitution of arsenate ions for the physiologically similar phosphate ions in bone crystal. Comparisons at 24 h indicated similar distributions of activity administered in the different forms except for higher skeletal uptake of activity administered as As(V).

18.1.3.2. Biokinetic model for systemic arsenic

(207) The biokinetic model for systemic arsenic applied in this report is the model applied in *Publication 151* (ICRP, 2022) to workers, except that activity reaching a bone volume compartment is assumed here to be removed to blood at the reference age-specific rate of bone turnover (ICRP, 2002). The model is assumed to apply to both As(III) and As(V). Where

differences in the kinetics of these two forms were suggested by human or animal studies, preference was given to data for As(V). The model formulated in *Publication 151* was designed for consistency of predictions with the central whole-body retention data determined in adult human subjects in the study by Pomroy et al. (1980) and reasonable consistency with the early systemic behaviour of inorganic arsenic in human subjects and laboratory animals. Reasonable consistency with the long-term systemic distribution of arsenic in adult humans indicated by autopsy data (Zhu et al., 2010) was also required. The model predicts high accumulation of arsenic in the kidneys and liver soon after uptake to blood but removal of the preponderance of accumulated arsenic from both organs over the next few days. Predicted long-term cumulative urinary and faecal losses represent about 95 and 5% of total excretion of arsenic.

(208) The structure of the biokinetic model for systemic arsenic applied in this report is shown in Fig. 18.1. Transfer coefficients are listed in Table 18.2.

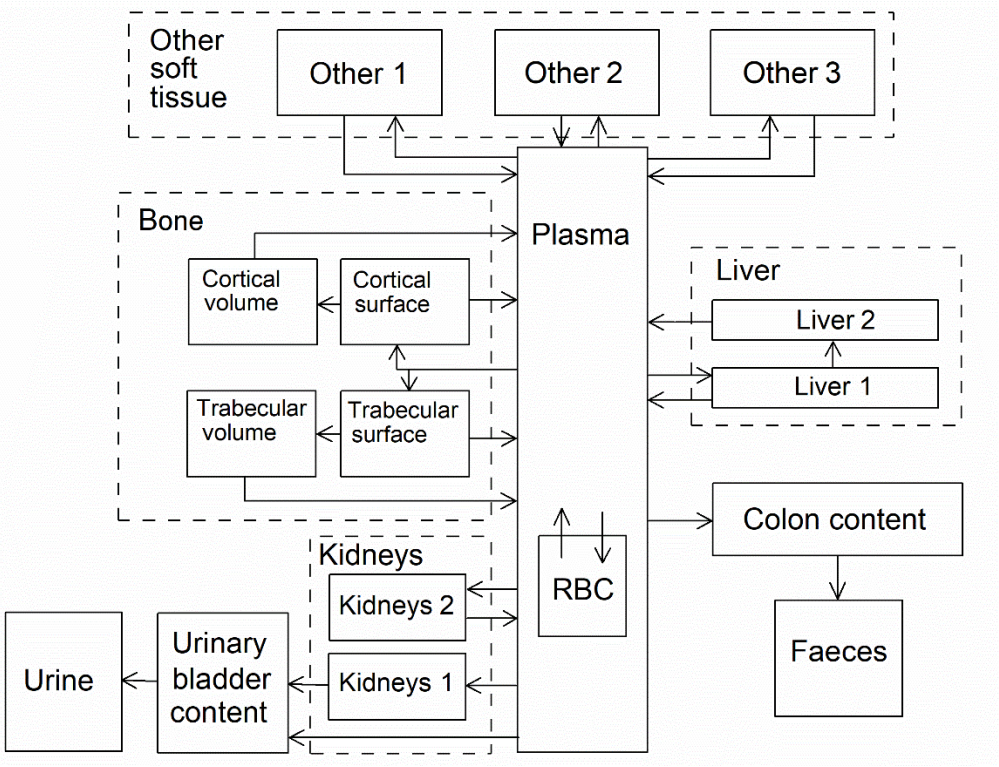

Fig. 18.1. Structure of the biokinetic model for systemic arsenic.

2138 Table 18.2. Age-specific transfer coefficients for arsenic.

		Transfer coefficients (d^{-1})					
Pathway		100 d	1 y	5 y	10 y	15 y	Adult
Plasma	RBC	2.00E+00	2.00E+00	2.00E+00	2.00E+00	2.00E+00	2.00E+00
Plasma	Other 1	2.00E+01	2.00E+01	2.00E+01	2.00E+01	2.00E+01	2.00E+01
Plasma	Other 2	1.52E+00	1.52E+00	1.52E+00	1.52E+00	1.52E+00	1.52E+00
Plasma	Other 3	2.80E-01	2.80E-01	2.80E-01	2.80E-01	2.80E-01	2.80E-01
Plasma	Liver 1	2.40E+00	2.40E+00	2.40E+00	2.40E+00	2.40E+00	2.40E+00
Plasma	Kidneys 1	2.52E+00	2.52E+00	2.52E+00	2.52E+00	2.52E+00	2.52E+00
Plasma	Kidneys 2	2.80E-01	2.80E-01	2.80E-01	2.80E-01	2.80E-01	2.80E-01
Plasma	Cort surface	1.00E+00	1.00E+00	1.00E+00	1.00E+00	1.00E+00	1.00E+00
Plasma	Trab surface	1.00E+00	1.00E+00	1.00E+00	1.00E+00	1.00E+00	1.00E+00
Plasma	UB content	8.40E+00	8.40E+00	8.40E+00	8.40E+00	8.40E+00	8.40E+00
Plasma	RC content	6.00E-01	6.00E-01	6.00E-01	6.00E-01	6.00E-01	6.00E-01
RBC	Plasma	3.00E-01	3.00E-01	3.00E-01	3.00E-01	3.00E-01	3.00E-01
Other 1	Plasma	6.00E-01	6.00E-01	6.00E-01	6.00E-01	6.00E-01	6.00E-01
Other 2	Plasma	8.00E-02	8.00E-02	8.00E-02	8.00E-02	8.00E-02	8.00E-02
Other 3	Plasma	1.80E-02	1.80E-02	1.80E-02	1.80E-02	1.80E-02	1.80E-02
Liver 1	Blood	9.50E-01	9.50E-01	9.50E-01	9.50E-01	9.50E-01	9.50E-01
Liver 1	Liver 2	5.00E-02	5.00E-02	5.00E-02	5.00E-02	5.00E-02	5.00E-02
Liver 2	Plasma	7.00E-02	7.00E-02	7.00E-02	7.00E-02	7.00E-02	7.00E-02
Kidneys 1	UB content	5.00E+00	5.00E+00	5.00E+00	5.00E+00	5.00E+00	5.00E+00
Kidneys 2	Plasma	7.00E-01	7.00E-01	7.00E-01	7.00E-01	7.00E-01	7.00E-01
Cort surface	Plasma	6.00E-01	6.00E-01	6.00E-01	6.00E-01	6.00E-01	6.00E-01
Trab surface	Plasma	6.00E-01	6.00E-01	6.00E-01	6.00E-01	6.00E-01	6.00E-01
Cort surface	Cort volume	3.00E-03	3.00E-03	3.00E-03	3.00E-03	3.00E-03	3.00E-03
Trab surface	Trab volume	6.00E-03	6.00E-03	6.00E-03	6.00E-03	6.00E-03	6.00E-03
Cort volume	Plasma	8.22E-03	2.88E-03	1.53E-03	9.04E-04	5.21E-04	8.21E-05
Trab volume	Plasma	8.22E-03	2.88E-03	1.81E-03	1.32E-03	9.59E-04	4.93E-04

2139 UB, urinary bladder; RC, right colon; Cort, cortical; Trab, trabecular.

2140 18.1.3.3. Treatment of radioactive progeny

2141 (209) The treatment of radioactive progeny produced in systemic compartments after intake
2142 of a radioisotope of arsenic is described in Section 19.2.3.3. of *Publication 151* (ICRP, 2022).
2143

18.2. Dosimetric data for arsenic

Table 18.3. Committed effective dose coefficients (Sv Bq^{-1}) for the inhalation or ingestion of ^{76}As compounds.

	Effective dose coefficients (Sv Bq^{-1})					
	3m	1y	5y	10y	15y	Adult
Inhaled particulate materials (1 µm AMAD aerosols)						
Type F	1.9E-09	1.3E-09	5.7E-10	4.0E-10	2.3E-10	1.7E-10
Type M, default	3.1E-09	2.3E-09	1.1E-09	8.0E-10	5.4E-10	4.9E-10
Type S	3.3E-09	2.4E-09	1.2E-09	8.7E-10	6.0E-10	5.4E-10
Ingested materials						
Water soluble compounds, arsenic in diet	3.2E-09	2.4E-09	1.4E-09	9.5E-10	6.3E-10	4.9E-10
Water insoluble compounds and arsenic in soil	3.3E-09	2.5E-09	1.5E-09	1.0E-09	6.9E-10	5.7E-10

AMAD, activity median aerodynamic diameter.

19. BROMINE (Z=35)

19.1. Routes of Intake

19.1.1. Inhalation

(210) For bromine, default parameter values were adopted for the absorption to blood from the respiratory tract (ICRP, 2015). Absorption parameter values and types, and associated f_A values for gas and vapour forms of bromine are given in Table 19.1 and for particulate forms in Table 19.2 [both taken from Section 21 of *Publication 151* (ICRP, 2022)]. By analogy with the halogen iodine, considered in detail in *Publication 137* (ICRP, 2017), default Type F is recommended for particulate forms in the absence of specific information on which the exposure material can be assigned to an absorption type.

(211) For bromine, and the other halogens, intakes could be in both particulate and gas and vapour forms, and it is therefore assumed that inhaled bromine is 50% particulate and 50% gas/vapour in the absence of information (ICRP, 2002b).

Table 19.1. Deposition and absorption for gas and vapour compounds of bromine.

	Percentage deposited (%)*						Absorption†	
Chemical form/origin	Total	ET_1	ET_2	BB	bb	AI	Type	Absorption from the alimentary tract, f_A‡,¶
Unspecified	100	0	20	10	20	50	F	1.0

ET_1, anterior nasal passage; ET_2, posterior nasal passage, pharynx and larynx; BB, bronchial; bb, bronchiolar; AI, alveolar-interstitial.

*Percentage deposited refers to how much of the material in the inhaled air remains in the body after exhalation. Almost all inhaled gas molecules contact airway surfaces but usually return to the air unless they dissolve in, or react with, the surface lining. The default distribution between regions is assumed: 20% ET_2, 10% BB, 20% bb, and 50% AI.

†It is assumed that the bound state can be neglected for bromine (i.e. $f_b = 0$).

‡For inhaled material deposited in the respiratory tract and subsequently cleared by particle transport to the alimentary tract, the default f_A values for inhaled materials are applied: i.e. the product of f_r for the absorption type and the f_A value for ingested soluble forms of bromine applicable to the age-group of interest (1.0).

¶The value of $f_A = 1.0$ is applicable to all age-groups.

Table 19.2. Absorption parameter values for inhaled and ingested bromine.

	Absorption parameter values*		
Inhaled particulate materials	f_r	s_r (d^{-1})	s_s (d^{-1})
Default parameter values†			
Absorption type			
F‡	1	30	–
M	0.2	3	0.005
S	0.01	3	1×10^{-4}

Ingested materials§

	Age-dependent absorption from the alimentary tract, f_A					
Assigned forms	3 months	1 year	5 years	10 years	15 years	adult
All compounds	1	1	1	1	1	1

*It is assumed that the bound state can be neglected for bromine (i.e. $f_b = 0$). The values of s_r for Type F, M and S forms of bromine (30, 3 and 3 d^{-1} respectively) are the general default values.

†For inhaled material deposited in the respiratory tract and subsequently cleared by particle transport to the alimentary tract, the default f_A values for inhaled materials are applied i.e. the product of f_r for the absorption type and the f_A value for ingested soluble forms of bromine applicable to the age-group of interest (1).

[ǂ]Default Type F is recommended for use in the absence of specific information on which the exposure material can be assigned to an absorption type (e.g. if the form is unknown, or if the form is known but there is no information available on the absorption of that form from the respiratory tract).

[§]Activity transferred from systemic compartments into segments of the alimentary tract is assumed to be subject to reabsorption to blood. The default absorption fraction f_A for the secreted activity is the highest value for ingestion of the radionuclide applicable to the age-group of interest ($f_A = 1$).

19.1.2. Ingestion

(212) After ingestion, bromine is completely absorbed in the gastrointestinal tract. In *Publications 30*, *72* and *151* (ICRP, 1980, 1995c, 2022), the fractional absorption was taken to be 1. In this publication, a $f_A = 1$ is also used for all chemical forms of bromine ingested by members of the public of any age.

19.1.3. Systemic distribution, retention and excretion of bromine

19.1.3.1. Biokinetic data

(213) The dominant form of bromine (Br) in the human body is inorganic bromide. The systemic kinetics of bromide closely resembles that of chloride (Reid et al., 1956; Pavelka, 2004). Ingested bromide is rapidly and nearly completely absorbed to blood and largely cleared from blood within a few minutes (Ray et al., 1952). It is distributed mainly in extracellular fluids where it replaces part of the extracellular chloride, with the molar sum of chloride and bromide remaining constant at about 110 mmol/L (Pavelka, 2004).

(214) The biological half-time of bromide in the human body is about 12 d (Söremark, 1960), compared with an estimated half-time of 8-15 d for chloride (Ray et al., 1952). The biological half-time of bromide or chloride in the body can be reduced considerably by elevated intake of chloride and increased considerably by a salt-deficient diet.

19.1.3.2. Biokinetic model for systemic bromine

(215) The biokinetic model for systemic bromine applied in *Publication 151* (ICRP, 2022) is applied here to all age groups. The systemic behaviour of bromine is assumed to be the same as that of chlorine. The relevant physiological forms of bromine and chlorine are assumed to be bromide and chloride, respectively. The common biokinetic model for bromide and chloride is based on the assumptions of rapid removal from blood ($T_{1/2}$ = 5 min), a uniform distribution in tissues, removal of 50% of absorbed bromide or chloride from the body in 12 d, and a urinary to faecal excretion ratio of 100:1. These conditions are approximated, using a first-order recycling model, with the transfer coefficients listed in Table 19.2.

Table 19.2. Age-specific transfer coefficients for bromine

		Transfer coefficients (d^{-1})					
Pathway		100 d	1 y	5 y	10 y	15 y	Adult
Blood	Other	2.00E+02	2.00E+02	2.00E+02	2.00E+02	2.00E+02	2.00E+02
Blood	UB content	8.30E-01	8.30E-01	8.30E-01	8.30E-01	8.30E-01	8.30E-01
Blood	RC content	8.30E-03	8.30E-03	8.30E-03	8.30E-03	8.30E-03	8.30E-03
Other	Blood	1.50E+01	1.50E+01	1.50E+01	1.50E+01	1.50E+01	1.50E+01

UB, urinary bladder; RC, right colon.

19.1.3.3. Treatment of radioactive progeny

(216) The treatment of radioactive progeny produced in systemic compartments after intake of a radioisotope of bromine is described in Section 21.2.3.3. of *Publication 151* (ICRP, 2022).

19.2. Dosimetric data for bromine

Table 19.3. Committed effective dose coefficients (Sv Bq^{-1}) for the inhalation or ingestion of ^{76}Br compounds.

	Effective dose coefficients (Sv Bq^{-1})					
Inhaled gases or vapours	3m	1y	5y	10y	15y	Adult
Unspecified	2.3E-09	1.6E-09	9.6E-10	6.2E-10	4.3E-10	3.9E-10
Inhaled particulate materials; (1 µm AMAD aerosols)						
Type F, default	1.5E-09	1.0E-09	4.7E-10	3.3E-10	2.0E-10	1.6E-10
Type M	2.2E-09	1.6E-09	8.1E-10	5.8E-10	3.8E-10	3.5E-10
Type S	2.3E-09	1.7E-09	8.6E-10	6.2E-10	4.1E-10	3.9E-10
Ingested materials						
All compounds	2.7E-09	2.0E-09	1.2E-09	8.0E-10	5.4E-10	4.5E-10

AMAD, activity median aerodynamic diameter.

20. RUBIDIUM (Z=37)

20.1. Routes of Intake

20.1.1. Inhalation

(217) For rubidium, default parameter values were adopted on absorption to blood from the respiratory tract (ICRP, 2015). Absorption parameter values and types, and associated f_A values for particulate forms of rubidium are given in Table 20.1 [taken from Section 22 of *Publication 151* (ICRP, 2022)].

20.1.2. Ingestion

(218) Ingested rubidium is almost completely absorbed from the gastrointestinal tract. In *Publications 30*, *72* and *151* (ICRP, 1980, 1994a), the fractional absorption was taken as 1 for all compounds of rubidium. In the present publication, the same value $f_A = 1$ is used for all chemical forms of rubidium ingested by members of the public of all ages.

Table 20.1. Absorption parameter values for inhaled and ingested rubidium.

	Absorption parameter values*		
Inhaled particulate materials	f_r	s_r (d^{-1})	s_s (d^{-1})
Default parameter values†			
Absorption type			
F	1	30	–
M‡	0.2	3	0.005
S	0.01	3	1×10^{-4}

Ingested materials§	Age-dependent absorption from the alimentary tract, f_A					
Assigned forms	3 months	1 year	5 years	10 years	15 years	adult
All compounds	1	1	1	1	1	1

*It is assumed that the bound state can be neglected for rubidium (i.e. $f_b = 0$). The values of s_r for Type F, M and S forms of rubidium (30, 3 and 3 d^{-1} respectively) are the general default values.

†For inhaled material deposited in the respiratory tract and subsequently cleared by particle transport to the alimentary tract, the default f_A values for inhaled materials are applied: i.e. the product of f_r for the absorption type and the f_A value for ingested soluble forms of rubidium applicable to the age-group of interest (1).

‡Default Type M is recommended for use in the absence of specific information on which the exposure material can be assigned to an absorption type (e.g. if the form is unknown, or if the form is known but there is no information available on the absorption of that form from the respiratory tract).

§Activity transferred from systemic compartments into segments of the alimentary tract is assumed to be subject to reabsorption to blood. The default absorption fraction f_A for the secreted activity is the highest value for any form of the radionuclide ($f_A = 1$).

20.1.3. Systemic distribution, retention and excretion of rubidium

20.1.3.1. Biokinetic data

(219) The alkali metal rubidium (Rb) is a physiological analogue of its neighboring alkali metals potassium (K) and caesium (Cs) in the periodic table. Rb and Cs compete with K for transport across cell membranes, with the rate of membrane transport generally decreasing in the order K > Rb > Cs. Cell membranes typically discriminate moderately between K and Rb

and to a greater extent between K and Cs (Relman, 1956; Sjodin, 1959; Kernan, 1969; Sheehan and Renkin, 1972).

(220) Measurements of stable Rb and K concentrations in tissues and fluids of human subjects indicate broadly similar distributions of these elements (Williams and Leggett, 1987; Zhu et al., 2010). In adult male humans, 60% or more of each of these elements is contained in skeletal muscle (Williams and Leggett, 1987; Zhu et al., 2010). Collected data for human subjects indicate that, on average, urinary excretion accounts for about 75% of total excretion of systemic Rb, compared with about 85% for systemic K (Leggett, 1983). Based on data for human subjects, ages 12-83 y (Ray et al., 1955; Kilpatrick et al., 1956; Tyor and Eldridge, 1956), and rabbits (Kilpatrick et al., 1956) injected with ^{42}K and ^{86}Rb, the early (through day 3) biological half-time of K in the body was about two-thirds that of Rb (assuming urinary losses were 85% and 75% of total losses for ^{42}K and ^{86}Rb, respectively). This is consistent with relative long-term half-times of K (30 d) and Rb (44 d) estimated for adults in *Publication 30* (Part 1, 1979, pp. 11 and 27).

(221) Love et al. (1954) compared the distributions of stable K and ^{86}Rb in 33 tissues or fluids following intravenous administration of ^{86}Rb to dogs. The distributions were compared in terms of a "relative Rb concentration" for individual tissues or fluids, intended to reflect the relative levels of accumulation of circulating Rb and K in these pools. The relative Rb concentration for a tissue or fluid was defined as the average ratio A:B for days 1, 3, and 7 post injection, where A is the concentration ratio of ^{86}Rb to K in the tissue or fluid sample and B is the analogous ratio for simultaneously sampled blood plasma. The relative rubidium ratio was in the range 1.02-1.91 with mean 1.4 ± 0.23 (SD) for 29 of the 33 pools and less than 1.0 for the other 4 (urine, 0.66; femur, 0.56; brain, 0.55; cerebrospinal fluid, 0.55).

(222) Lloyd et al. (1972, 1973) conducted a study of retention of simultaneously ingested ^{83}Rb and ^{137}Cs in 38 human subjects: 9 healthy male control subjects, ages 4-80 y; 5 healthy female control subjects, ages 14-52 y; 7 females, ages 14-50 y, thought to be carriers of Duchenne dystrophy or other muscle disease; and 14 males and 3 females, ages 5-62 y, with Duchenne dystrophy or other muscle disease. Total-body retention was measured externally for ~6 months for Rb and ~12 months for Cs. Total-body biological retention of each tracer could be fit closely by a sum of 2-3 exponential terms representing different phases of retention, or in some cases by a single exponential term. The biological half-time associated with the "long-term" component of retention (or the only component of retention in some cases) varied from several days to a few months, depending on age and state of health. Retention of the tracers generally was considerably lower in subjects with muscle disease than in controls of corresponding age or sex, particularly for Cs. In control subjects, retention of Rb initially was higher than that of Cs but fell below that of Cs after several days in most adults; a few weeks in subjects of age 10-19 y and in one adult; and 3 months in two 4-y-old boys, when little of the ingested amount remained in the body. An "equivalent" biological half-time Q for each tracer and subject was derived as the sum of component half-times weighted by the relative component sizes (fractions) in the fitted exponential expression. The equivalent half-times for Rb for control subjects generally decreased with decreasing age from mid-adulthood to age 4 y (Fig. 20.1). In control subjects the ratio Rb:Cs of the equivalent half-time in Rb to that in Cs was near 0.5 in adults but increased with decreasing age in pre-adults and exceeded 1.0 in two 4-y-old males (Fig. 20.2).

(223) A physiologically based biokinetic model for systemic Rb in adults was proposed by Leggett and Williams (1989). The model was built around a blood flow model depicting the distribution of cardiac output to 12 tissue compartments. Additional compartments were added to address transfer of Rb between plasma and red blood cells and between systemic pools and gastrointestinal content. Biological removal was assumed to be in urine, faeces, and sweat. Movement of Rb was depicted as a system of first-order processes. The transfer rate from

plasma into a tissue T was estimated as the product of the plasma flow rate to that tissue and a tissue-specific extraction fraction, E_T. The transfer rate from tissue T to plasma was estimated from the inflow rate and the relative contents of Rb in plasma and tissue T at equilibrium based mainly on autopsy data for stable Rb and typical concentrations of Rb in plasma and red blood cells. Transfer rates between plasma and red blood cells and between systemic compartments and gastrointestinal contents were based on empirical data. Model predictions of the blood clearance, uptake and loss by systemic tissues, total-body retention, and path-specific excretion rates of Rb were shown to be consistent with observations for human subjects.

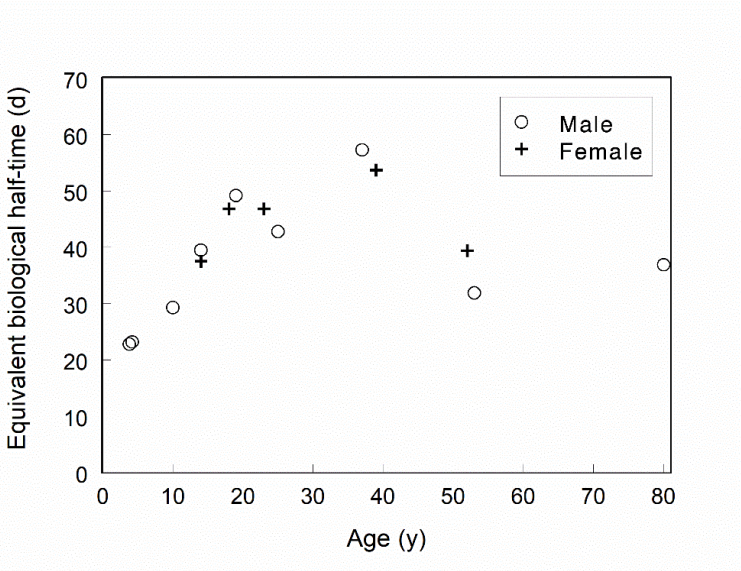

Fig. 20.1. Equivalent biological half-times for ingested ^{83}Rb in healthy human subjects, ages 4-80 y (data of Lloyd et al., 1972, 1973).

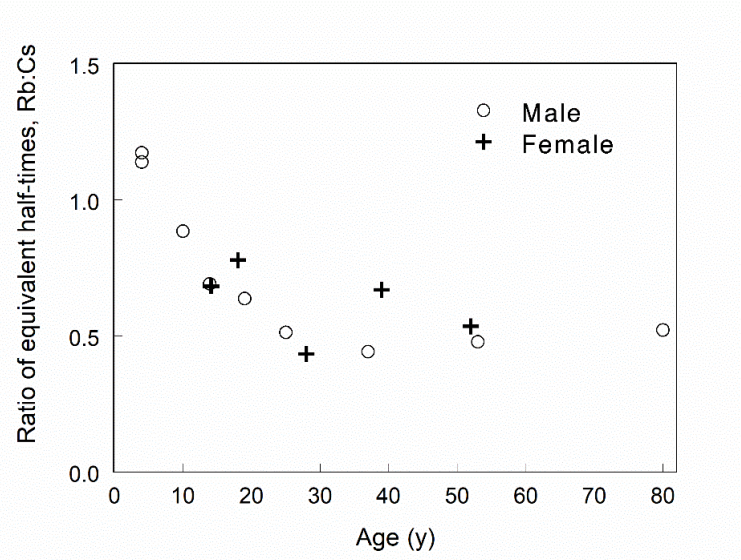

Fig. 20.2. Ratios Rb:Cs of equivalent biological half-times of ingested ^{83}Rb and ^{137}Cs in healthy human subjects, ages 4-80 y (based on data of Lloyd et al., 1972, 1973).

20.1.3.2. Biokinetic model for systemic rubidium

(224) The biokinetic model for systemic Rb in workers used in *Publication 151* (ICRP, 2022) is a simplification of the model of Leggett and Williams (1989) summarized above, with

a structure (Fig. 20.3) more consistent with the structures of other systemic models applied in this report series. The Rb model of *Publication 151* depicts a central blood compartment (plasma) in exchange with a set of peripheral tissue compartments representing specific tissues and a tissue named "Other" representing all tissues and fluids not explicitly identified in the model. Activity in Other is assumed to be uniformly distributed. In *Publication 151* the transfer coefficients were set for consistency with the original model regarding retention in the adult male body and in individual tissues depicted explicitly in both models.

(225) The biokinetic model for systemic Rb applied to workers in *Publication 151* (ICRP, 2022) is applied in this report to adult members of the public. The model is extended to pre-adult ages by adjustment of transfer coefficients to reflect pertinent anatomical or physiological changes during growth; age-specific total-body retention times of Rb measured by Lloyd et al. (1972, 1973) in healthy children, adolescents, and adults; and the similarity in retention times of Rb and Cs early in life as indicated by data of Lloyd and coworkers. The comparative data of Rb and Cs is particularly useful for modeling the kinetics of Rb in infants and toddlers because of the lack of biokinetic data for Rb but the existence of considerable data for Cs during this period of life.

(226) The following modifications of the Rb model for workers used in *Publication 151* (ICRP, 2022) are made for application to pre-adult ages:

(227) The transfer rate from plasma to skeletal muscle at ages 100 d, 1 y, 5 y, and 10 y is assumed to be 0.5, 0.5, 0.7, and 0.85, respectively, times the transfer rate for the adult based on changes with age in muscle mass as a percentage of total-body mass.

(228) For infants and children through age 10 y, the transfer rates from plasma to bone surface compartments are set at twice the value for the adult to reflect a high blood flow rate to bone compared with adults.

(229) The transfer rate from plasma to the compartment Other is modified to maintain the same outflow rate from plasma at all ages, that is, to balance the changes in transfer from plasma to skeletal muscle and bone surface.

(230) The model is required to reproduce the following long-term half-times: 17, 19, 25, 31, and 41 d for intake at age 100 d, 1 y, 5 y, 10 y, and 15 y, respectively. The long-term half-times for intake at age 100 d and 1 y are the values applied in the systemic model for Cs described in Part 1 of this series (ICRP, 2024). The application of these reasonably well supported long-term half-times for Cs to the less studied element Rb is based on indications in the results of the study of Lloyd et al. (1972, 1973) that long-term retention of Rb converges toward that of Cs with decreasing age of the pre-adult subjects. The half-times for the other intake ages are set to approximate the retention data for pre-adult controls in the study by Lloyd et al. (1972, 1973). All flow rates out of tissue compartments (Kidneys, Liver, Muscle, Cortical and Trabecular bone surface, Red marrow, Other) in the model for adults are multiplied by the following factors to approximate the assigned long-term half-times of Rb in pre-adults: 2.1 at age 100 d, 1.9 at age 1 y, 1.6 at age 5 y, 1.4 at age 10 y, and 1.1 at age 15 y.

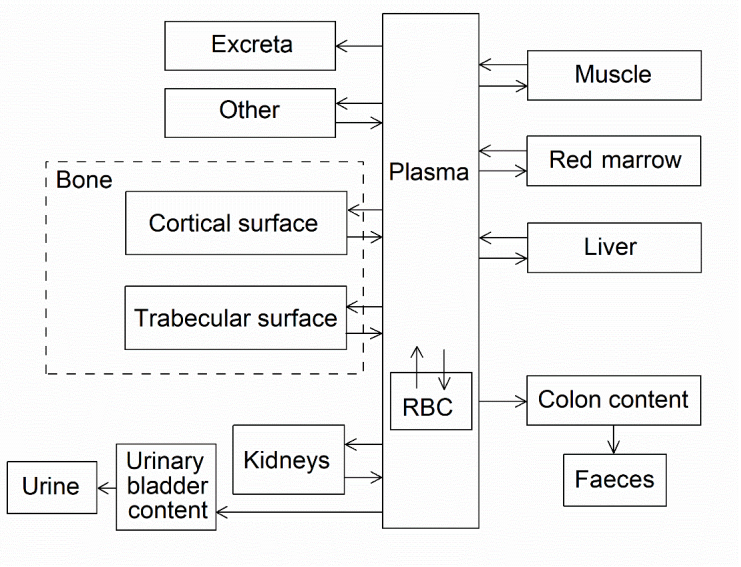

Fig. 20.3. Structure of the biokinetic model for systemic rubidium.

Table 20.2. Age-specific transfer coefficients for rubidium.

		Transfer coefficients (d^{-1})					
Pathway		100 d	1 y	5 y	10 y	15 y	Adult
Blood	RBC	6.00E+00	6.00E+00	6.00E+00	6.00E+00	6.00E+00	6.00E+00
Blood	Kidneys	2.40E+02	2.40E+02	2.40E+02	2.40E+02	2.40E+02	2.40E+02
Blood	Liver	1.53E+02	1.53E+02	1.53E+02	1.53E+02	1.53E+02	1.53E+02
Blood	Muscle	1.28E+02	1.28E+02	1.79E+02	2.17E+02	2.55E+02	2.55E+02
Blood	Trab surface	1.68E+01	1.68E+01	1.68E+01	1.68E+01	8.40E+00	8.40E+00
Blood	C-bone-S surface	1.12E+01	1.12E+01	1.12E+01	1.12E+01	5.60E+00	5.60E+00
Blood	Red marrow	1.40E+01	1.40E+01	1.40E+01	1.40E+01	1.40E+01	1.40E+01
Blood	Other	5.14E+02	5.14E+02	4.63E+02	4.24E+02	4.00E+02	4.00E+02
Blood	UB content	3.90E+00	3.90E+00	3.90E+00	3.90E+00	3.90E+00	3.90E+00
Blood	RC content	1.20E+00	1.20E+00	1.20E+00	1.20E+00	1.20E+00	1.20E+00
Blood	Excreta	1.00E-01	1.00E-01	1.00E-01	1.00E-01	1.00E-01	1.00E-01
RBC	Blood	3.50E-01	3.50E-01	3.50E-01	3.50E-01	3.50E-01	3.50E-01
Kidneys	Blood	2.52E+02	2.28E+02	1.92E+02	1.68E+02	1.32E+02	1.20E+02
Liver	Blood	2.10E+01	1.90E+01	1.60E+01	1.40E+01	1.10E+01	9.98E+00
Muscle	Blood	2.39E+00	2.17E+00	1.82E+00	1.60E+00	1.25E+00	1.14E+00
Trab surface	Blood	3.53E+00	3.19E+00	2.69E+00	2.35E+00	1.85E+00	1.68E+00
Cort surface	Blood	3.53E+00	3.19E+00	2.69E+00	2.35E+00	1.85E+00	1.68E+00
Red marrow	Blood	3.53E+00	3.19E+00	2.69E+00	2.35E+00	1.85E+00	1.68E+00
Other	Blood	1.53E+01	1.39E+01	1.17E+01	1.02E+01	8.03E+00	7.30E+00

RBC, red blood cells; UB, urinary bladder; RC, right colon; Cort, cortical; Trab, trabecular.

20.1.3.3. Treatment of radioactive progeny

(231) The treatment of radioactive progeny produced in systemic compartments after intake of a radioisotope of rubidium is described in Section 22.2.3.3. of *Publication 151* (ICRP, 2022).

20.2. Dosimetric data for rubidium

Table 20.3. Committed effective dose coefficients (Sv Bq^{-1}) for the inhalation or ingestion of ^{83}Rb compounds.

	Effective dose coefficients (Sv Bq^{-1})					
	3m	1y	5y	10y	15y	Adult
Inhaled particulate materials; (1 µm AMAD aerosols)						
Type F	2.7E-09	2.1E-09	1.3E-09	9.3E-10	7.1E-10	7.0E-10
Type M, default	3.6E-09	3.0E-09	1.8E-09	1.2E-09	9.2E-10	1.0E-09
Type S	5.1E-09	4.4E-09	2.6E-09	1.8E-09	1.3E-09	1.5E-09
Ingested materials						
All compounds	5.2E-09	4.0E-09	2.8E-09	2.0E-09	1.7E-09	1.6E-09

AMAD, activity median aerodynamic diameter.

Table 20.4. Committed effective dose coefficients (Sv Bq^{-1}) for the inhalation or ingestion of ^{84}Rb compounds.

	Effective dose coefficients (Sv Bq^{-1})					
	3m	1y	5y	10y	15y	Adult
Inhaled particulate materials; (1 µm AMAD aerosols)						
Type F	5.9E-09	4.4E-09	2.3E-09	1.6E-09	1.1E-09	1.0E-09
Type M, default	7.5E-09	6.2E-09	3.4E-09	2.3E-09	1.7E-09	1.8E-09
Type S	8.9E-09	7.4E-09	4.2E-09	2.9E-09	2.1E-09	2.3E-09
Ingested materials						
All compounds	1.1E-08	8.4E-09	5.2E-09	3.4E-09	2.6E-09	2.4E-09

AMAD, activity median aerodynamic diameter.

Table 20.5. Committed effective dose coefficients (Sv Bq^{-1}) for the inhalation or ingestion of ^{86}Rb compounds.

	Effective dose coefficients (Sv Bq^{-1})					
	3m	1y	5y	10y	15y	Adult
Inhaled particulate materials; (1 µm AMAD aerosols)						
Type F	8.4E-09	6.1E-09	2.7E-09	1.6E-09	9.0E-10	7.3E-10
Type M, default	1.2E-08	9.6E-09	5.2E-09	3.4E-09	2.6E-09	2.5E-09
Type S	1.4E-08	1.1E-08	6.3E-09	4.2E-09	3.2E-09	3.1E-09
Ingested materials						
All compounds	1.6E-08	1.1E-08	5.9E-09	3.4E-09	2.2E-09	1.7E-09

AMAD, activity median aerodynamic diameter.

21. RHODIUM (Z=45)

21.1. Routes of Intake

21.1.1. Inhalation

(232) For rhodium, default parameter values were adopted on absorption to blood from the respiratory tract (ICRP, 2015). Absorption parameter values and types, and associated f_A values for particulate forms of rhodium are given in Table 21.1 [taken from Section 23 of *Publication 151* (ICRP, 2022)].

21.1.2. Ingestion

21.1.2.1. Adults

(233) There appears to be no information concerning the uptake of rhodium from the gastrointestinal tract. Based on chemical analogy with ruthenium, the fractional absorption was taken to be 0.05 for all rhodium compounds in *Publications 30*, *72* and *151* (ICRP, 1980, 1995c, 2022). In this publication, f_A = 0.05 is also used for all forms of rhodium ingested by adult members of the public.

21.1.2.2. Children

(234) Consistently with the approach of *Publication56* (ICRP, 1990), an f_A = 0.1 is adopted here for ingestion of all forms of rhodium by 3 month old infants and the adult value of 0.05 is used for older children.

Table 21.1. Absorption parameter values for inhaled and ingested rhodium.

	Absorption parameter values*		
Inhaled particulate materials	f_r	s_r (d^{-1})	s_s (d^{-1})
Default parameter values†			
Absorption type			
F	1	30	–
M‡	0.2	3	0.005
S	0.01	3	1×10^{-4}

Ingested materials§						
	Age-dependent absorption from the alimentary tract, f_A					
Assigned forms	3 months	1 year	5 years	10 years	15 years	adult
All compounds	0.1	0.05	0.05	0.05	0.05	0.05

*It is assumed that the bound state can be neglected for rhodium (i.e. f_b = 0). The values of s_r for Type F, M and S forms of rhodium (30, 3 and 3 d^{-1} respectively) are the general default values.

†For inhaled material deposited in the respiratory tract and subsequently cleared by particle transport to the alimentary tract, the default f_A values for inhaled materials are applied: i.e. the product of f_r for the absorption type and the f_A value for ingested soluble forms of rhodium applicable to the age-group of interest (e.g. 0.05 for adults).

‡Default Type M is recommended for use in the absence of specific information on which the exposure material can be assigned to an absorption type (e.g. if the form is unknown, or if the form is known but there is no information available on the absorption of that form from the respiratory tract).

§Activity transferred from systemic compartments into segments of the alimentary tract is assumed to be subject to reabsorption to blood. The default absorption fraction f_A for the secreted activity is the highest value for ingestion of the radionuclide applicable to the age-group of interest (e.g. 0.05 for adults).

21.1.3. Systemic distribution, retention and excretion of rhodium

21.1.3.1. Biokinetic data

(235) Rhodium (Rh) is a member of the chemical family called the platinum group, which also includes platinum, iridium, ruthenium, palladium, and osmium. Biokinetic studies indicate broadly similar systemic behaviour across the platinum group (Durbin et al., 1957; Durbin, 1960).

(236) Durbin et al. (1957) summarized results of studies of rhodium in rats following administration of carrier-free ^{105}Rh. At 18 d after intramuscular injection about 46% had been eliminated in urine and 28% in faeces. Throughout the study the highest concentrations of activity were found in kidney, spleen, lymph glands, and skin.

21.1.3.2. Biokinetic model for systemic rhodium

(237) Due to the sparsity of biokinetic data for rhodium, the biokinetics of the adjacent platinum group member ruthenium in the period table has been applied to rhodium in previous ICRP reports on occupational or public intake of radionuclides (ICRP, 1980, 1994, 1996, 2022). The biokinetic model for systemic ruthenium described in Part 1 of this series of reports (ICRP, 2024) is applied in this report to rhodium.

(238) The model structure for rhodium is shown in Fig. 21.1. Transfer coefficients are listed in Table 21.2. These transfer coefficients are independent of age except that the ICRP's generic age-specific bone turnover rates are assigned to transfers from bone volume compartments to blood.

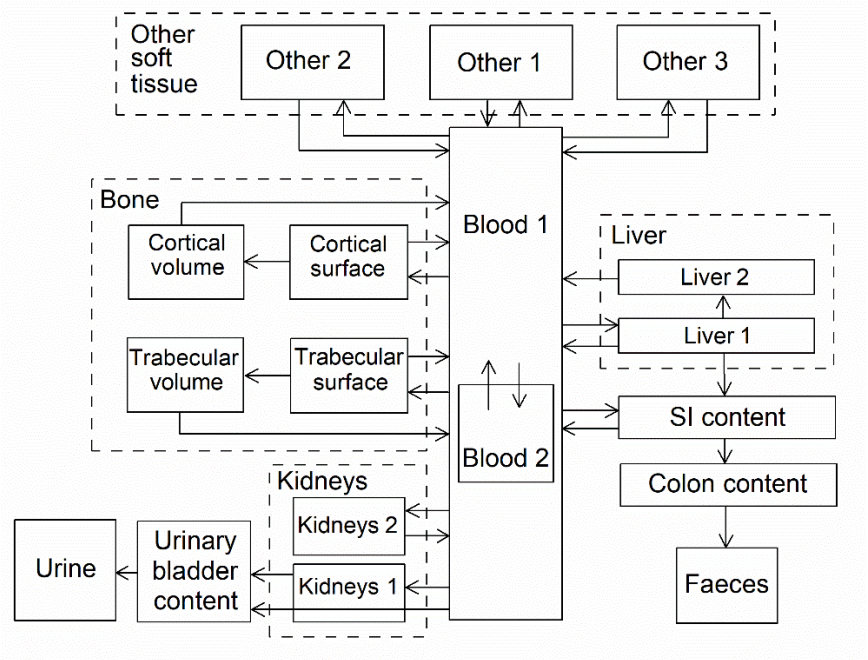

Fig. 21.1. Structure of the biokinetic model for systemic rhodium. SI, small intestine.

Table 21.2. Age-specific transfer coefficients for rhodium.

		Transfer coefficients (d^{-1})					
Pathway		100 d	1 y	5 y	10 y	15 y	Adult
Blood	SI content	3.00E+00	3.00E+00	3.00E+00	3.00E+00	3.00E+00	3.00E+00
Blood	UB content	1.70E+01	1.70E+01	1.70E+01	1.70E+01	1.70E+01	1.70E+01
Blood	Liver 1	1.20E+01	1.20E+01	1.20E+01	1.20E+01	1.20E+01	1.20E+01
Blood	Kidneys 1	7.76E+00	7.76E+00	7.76E+00	7.76E+00	7.76E+00	7.76E+00
Blood	Kidneys 2	2.40E-01	2.40E-01	2.40E-01	2.40E-01	2.40E-01	2.40E-01
Blood	Blood 2	2.70E+01	2.70E+01	2.70E+01	2.70E+01	2.70E+01	2.70E+01
Blood	Other 1	1.50E+01	1.50E+01	1.50E+01	1.50E+01	1.50E+01	1.50E+01
Blood	Other 2	5.00E+00	5.00E+00	5.00E+00	5.00E+00	5.00E+00	5.00E+00
Blood	Other 3	5.00E+00	5.00E+00	5.00E+00	5.00E+00	5.00E+00	5.00E+00
Blood	Cort surface	2.00E+00	2.00E+00	2.00E+00	2.00E+00	2.00E+00	2.00E+00
Blood	Trab surface	6.00E+00	6.00E+00	6.00E+00	6.00E+00	6.00E+00	6.00E+00
Blood 2	Blood	6.93E-01	6.93E-01	6.93E-01	6.93E-01	6.93E-01	6.93E-01
Liver 1	Blood	9.70E-02	9.70E-02	9.70E-02	9.70E-02	9.70E-02	9.70E-02
Liver 1	SI content	3.47E-02	3.47E-02	3.47E-02	3.47E-02	3.47E-02	3.47E-02
Liver 1	Liver 2	6.93E-03	6.93E-03	6.93E-03	6.93E-03	6.93E-03	6.93E-03
Liver 2	Blood	3.80E-03	3.80E-03	3.80E-03	3.80E-03	3.80E-03	3.80E-03
Kidneys 1	UB content	1.39E-01	1.39E-01	1.39E-01	1.39E-01	1.39E-01	1.39E-01
Kidneys 2	Blood	3.80E-03	3.80E-03	3.80E-03	3.80E-03	3.80E-03	3.80E-03
Other 1	Blood	9.90E-02	9.90E-02	9.90E-02	9.90E-02	9.90E-02	9.90E-02
Other 2	Blood	2.31E-02	2.31E-02	2.31E-02	2.31E-02	2.31E-02	2.31E-02
Other 3	Blood	9.50E-04	9.50E-04	9.50E-04	9.50E-04	9.50E-04	9.50E-04
Cort surface	Blood	7.92E-02	7.92E-02	7.92E-02	7.92E-02	7.92E-02	7.92E-02
Trab surface	Blood	7.92E-02	7.92E-02	7.92E-02	7.92E-02	7.92E-02	7.92E-02
Cort surface	Cort volume	1.98E-02	1.98E-02	1.98E-02	1.98E-02	1.98E-02	1.98E-02
Trab surface	Trab volume	1.98E-02	1.98E-02	1.98E-02	1.98E-02	1.98E-02	1.98E-02
Cort volume	Blood	8.22E-03	2.88E-03	1.53E-03	9.04E-04	5.21E-04	8.21E-05
Trab volume	Blood	8.22E-03	2.88E-03	1.81E-03	1.32E-03	9.59E-04	4.93E-04

UB, urinary bladder; SI, small intestine; Cort, cortical; Trab, trabecular.

21.1.3.3. Treatment of radioactive progeny

(239) The treatment of radioactive progeny produced in systemic compartments after intake of a radioisotope of rhodium is described in Section 23.2.3.3. of *Publication 151* (ICRP, 2022).

21.2. Dosimetric data for rhodium

Table 21.3. Committed effective dose coefficients (Sv Bq^{-1}) for the inhalation or ingestion of ^{101}Rh compounds.

	Effective dose coefficients (Sv Bq^{-1})					
	3m	1y	5y	10y	15y	Adult
Inhaled particulate materials; (1 µm AMAD aerosols)						
Type F	4.3E-09	3.6E-09	2.1E-09	1.4E-09	1.1E-09	1.1E-09
Type M, default	6.3E-09	5.6E-09	3.3E-09	2.2E-09	1.7E-09	1.9E-09
Type S	1.9E-08	1.8E-08	1.2E-08	8.3E-09	7.3E-09	8.0E-09
Ingested materials						
All compounds	2.3E-09	1.3E-09	7.6E-10	5.2E-10	3.9E-10	3.8E-10

AMAD, activity median aerodynamic diameter.

22. PALLADIUM (Z=46)

22.1. Routes of Intake

22.1.1. Inhalation

(240) For palladium, default parameter values were adopted on absorption to blood from the respiratory tract (ICRP, 2015). Absorption parameter values and types, and associated f_A values for particulate forms of palladium are given in Table 22.1 [taken from Section 24 of *Publication 151* (ICRP, 2022)].

22.1.2. Ingestion

22.1.2.1. Adults

(241) Palladium is poorly absorbed from the gastrointestinal tract. In *Publications 30*, *72* and *151* (ICRP, 1981, 1995c, 2022) the fractional absorption was taken to be 5×10^{-3} for all compounds of the element. In this publication the value of $f_A = 5 \times 10^{-3}$ is also used for all forms of palladium ingested by adult members of the public.

22.1.2.2. Children

(242) The fractional absorption from the gastrointestinal tract of palladium, administered as the chloride, appears to be ten times higher (about 5%) in suckling rats than in adult rats (less than 5 x 10^{-3}) (Moore et al., 1974, 1975b). Consistently with the approach of *Publication56* (ICRP, 1990), an $f_A = 0.05$ is adopted here for ingestion of all forms of palladium by 3 month old infants and the adult value of 0.005 is used for older children.

Table 22.1. Absorption parameter values for inhaled and ingested palladium.

	Absorption parameter values*		
Inhaled particulate materials	f_r	s_r (d^{-1})	s_s (d^{-1})
Default parameter values†			
Absorption type			
F	1	30	–
M‡	0.2	3	0.005
S	0.01	3	1×10^{-4}

Ingested materials§	Age-dependent absorption from the alimentary tract, f_A					
Assigned forms	3 months	1 year	5 years	10 years	15 years	adult
All compounds	0.05	0.005	0.005	0.005	0.005	0.005

*It is assumed that the bound state can be neglected for palladium (i.e. $f_b = 0$). The values of s_r for Type F, M and S forms of palladium (30, 3 and 3 d^{-1} respectively) are the general default values.

†For inhaled material deposited in the respiratory tract and subsequently cleared by particle transport to the alimentary tract, the default f_A values for inhaled materials are applied: i.e. the product of f_r for the absorption type and the f_A value for ingested soluble forms of palladium applicable to the age-group of interest (e.g. 0.005 for adults).

‡Default Type M is recommended for use in the absence of specific information on which the exposure material can be assigned to an absorption type (e.g. if the form is unknown, or if the form is known but there is no information available on the absorption of that form from the respiratory tract).

§Activity transferred from systemic compartments into segments of the alimentary tract is assumed to be subject to reabsorption to blood. The default absorption fraction f_A for the secreted activity is the highest value for ingestion of the radionuclide applicable to the age-group of interest (e.g. 0.005 for adults).

22.1.3. Systemic distribution, retention and excretion of palladium

22.1.3.1. Biokinetic data

(243) Following intravenous administration of $Na_2{}^{103}PdCl_4$, about 60% of intravenously injected ^{103}Pd was excreted in urine over the first 4 h, 71% after 1 d, and 76% after 7 d (after correction for radioactive decay) (Durbin et al., 1957; Durbin, 1960). Fecal excretion represented about 4% of the administered amount after 1 d and 13% after 7 d. At 1 d the liver, kidneys, muscle, bone, and blood contained 8.6%, 8.4%, 1.3%, 1.0%, and 0.8%, respectively, of the administered amount. At 7 d the liver contained about 4%, kidneys 5%, bone 0.2-0.3%, and spleen 0.2% of the administered amount.

(244) Moore et al. (1974, 1975) investigated the biokinetics of ^{103}Pd in rats following different modes of administration of $^{103}PdCl_2$. At 1 d after oral intake, activity was detectable only in the kidneys and liver. Intravenously injected ^{103}Pd initially was lost primarily in urine, mainly in faeces from 2 d to 2 wk, and mainly in urine after 2 wk. Male rats excreted about 30% of intravenously injected ^{103}Pd during the first day. At 1 d after intravenous injection, the highest concentrations were seen in the kidneys, followed by the spleen, liver, adrenal gland, lung, and bone. About 20% of the intravenously injected amount was retained in the body after 40 d, and about 10% was retained after 76 days. At 104 d after intravenous injection the highest concentrations of ^{103}Pd were found in the spleen, kidneys, liver, lung, and bone.

(245) Ando and coworkers (1989, 1994) determined the distribution of ^{103}Pd in rats at 3, 24, and 48 h after intravenous injection of $^{103}PdCl_2$. Cumulative urinary excretion at 3 h represented 6.4% of injected ^{192}Ir. At all three observation times the highest concentration was found in the kidneys: 20.2, 17.1, and 21.4% g^{-1} at 3, 24, and 48 h, respectively, followed by liver (14.1, 9.9, and 9.9%/g, respectively.

(246) Ducoulombier-Crépineau et al. (2007) examined the transfer of palladium to systemic tissues and milk following a single oral intake of $PdCl_2$ by lactating goats. The highest concentration was found in the kidneys. Little palladium was transferred to milk.

22.1.3.2. Biokinetic model for systemic palladium

(247) The biokinetic model for systemic palladium applied to workers in *Publication 151* (ICRP, 2022) is applied here to adult members of the public. The same model is applied to preadult ages except that palladium reaching a bone volume compartment is assumed to be removed to blood at the reference age-specific rate of turnover of that bone type (ICRP, 2002).

(248) The structure of the biokinetic model for systemic palladium is shown in Fig. 22.1. Transfer coefficients for palladium are listed in Table 22.2.

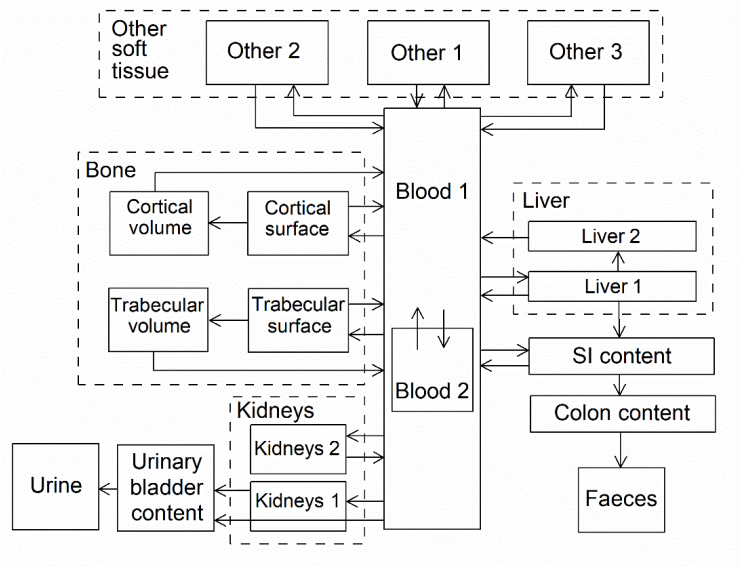

Fig. 22.1. Structure of the biokinetic model for systemic palladium. SI, small intestine.

Table 22.2. Age-specific transfer coefficients for palladium

		Transfer coefficients (d^{-1})					
Pathway		100 d	1 y	5 y	10 y	15 y	Adult
Blood 1	SI content	4.00E+00	4.00E+00	4.00E+00	4.00E+00	4.00E+00	4.00E+00
Blood 1	UB content	2.00E+01	2.00E+01	2.00E+01	2.00E+01	2.00E+01	2.00E+01
Blood 1	Liver 1	1.20E+01	1.20E+01	1.20E+01	1.20E+01	1.20E+01	1.20E+01
Blood 1	Kidneys 1	8.00E+00	8.00E+00	8.00E+00	8.00E+00	8.00E+00	8.00E+00
Blood 1	Kidneys 2	4.00E+00	4.00E+00	4.00E+00	4.00E+00	4.00E+00	4.00E+00
Blood 1	Blood 2	2.70E+01	2.70E+01	2.70E+01	2.70E+01	2.70E+01	2.70E+01
Blood 1	Other 1	1.00E+01	1.00E+01	1.00E+01	1.00E+01	1.00E+01	1.00E+01
Blood 1	Other 2	1.00E+01	1.00E+01	1.00E+01	1.00E+01	1.00E+01	1.00E+01
Blood 1	Other 3	1.00E+00	1.00E+00	1.00E+00	1.00E+00	1.00E+00	1.00E+00
Blood 1	Cort surface	1.00E+00	1.00E+00	1.00E+00	1.00E+00	1.00E+00	1.00E+00
Blood 1	Trab surface	3.00E+00	3.00E+00	3.00E+00	3.00E+00	3.00E+00	3.00E+00
Blood 2	Blood 1	2.77E+00	2.77E+00	2.77E+00	2.77E+00	2.77E+00	2.77E+00
Liver_1	Blood 1	4.62E-02	4.62E-02	4.62E-02	4.62E-02	4.62E-02	4.62E-02
Liver_1	SI content	9.24E-02	9.24E-02	9.24E-02	9.24E-02	9.24E-02	9.24E-02
Liver_1	Liver_2	1.39E-01	1.39E-01	1.39E-01	1.39E-01	1.39E-01	1.39E-01
Liver_2	Blood 1	1.39E-02	1.39E-02	1.39E-02	1.39E-02	1.39E-02	1.39E-02
Kidneys 1	UB content	2.77E-01	2.77E-01	2.77E-01	2.77E-01	2.77E-01	2.77E-01
Kidneys 2	Blood 1	1.39E-02	1.39E-02	1.39E-02	1.39E-02	1.39E-02	1.39E-02
Other 1	Blood 1	1.39E-01	1.39E-01	1.39E-01	1.39E-01	1.39E-01	1.39E-01
Other 2	Blood 1	1.39E-02	1.39E-02	1.39E-02	1.39E-02	1.39E-02	1.39E-02
Other 3	Blood 1	1.90E-03	1.90E-03	1.90E-03	1.90E-03	1.90E-03	1.90E-03
Cort surface	Blood 1	3.70E-02	3.70E-02	3.70E-02	3.70E-02	3.70E-02	3.70E-02
Trab surface	Blood 1	3.70E-02	3.70E-02	3.70E-02	3.70E-02	3.70E-02	3.70E-02
Cort surface	Cort volume	9.24E-03	9.24E-03	9.24E-03	9.24E-03	9.24E-03	9.24E-03
Trab surface	Trab volume	9.24E-03	9.24E-03	9.24E-03	9.24E-03	9.24E-03	9.24E-03
Cort volume	Blood 1	8.22E-03	2.88E-03	1.53E-03	9.04E-04	5.21E-04	8.21E-05
Trab volume	Blood 1	8.22E-03	2.88E-03	1.81E-03	1.32E-03	9.59E-04	4.93E-04

UB, urinary bladder; SI, small intestine; Cort, cortical; Trab, trabecular.

22.1.3.3. Treatment of radioactive progeny

(249) The treatment of radioactive progeny produced in systemic compartments after intake of a radioisotope of palladium is described in Section 24.2.3.3. of *Publication 151* (ICRP, 2022).

22.2. Dosimetric data for palladium

Table 22.3. Committed effective dose coefficients (Sv Bq^{-1}) for the inhalation or ingestion of ^{103}Pd compounds.

	Effective dose coefficients (Sv Bq^{-1})					
	3m	1y	5y	10y	15y	Adult
Inhaled particulate materials; (1 μm AMAD aerosols)						
Type F	3.5E-10	2.4E-10	1.1E-10	6.8E-11	4.4E-11	3.7E-11
Type M, default	1.0E-09	7.9E-10	4.4E-10	2.9E-10	2.2E-10	2.0E-10
Type S	1.3E-09	9.8E-10	5.5E-10	3.6E-10	2.8E-10	2.6E-10
Ingested materials						
All compounds	2.1E-10	1.4E-10	7.4E-11	5.3E-11	3.2E-11	2.5E-11

AMAD, activity median aerodynamic diameter.

Table 22.4. Committed effective dose coefficients (Sv Bq^{-1}) for the inhalation or ingestion of ^{107}Pd compounds.

	Effective dose coefficients (Sv Bq^{-1})					
	3m	1y	5y	10y	15y	Adult
Inhaled particulate materials; (1 μm AMAD aerosols)						
Type F	2.4E-10	1.7E-10	8.8E-11	5.2E-11	3.5E-11	3.1E-11
Type M, default	5.0E-10	4.4E-10	2.3E-10	1.4E-10	1.0E-10	9.2E-11
Type S	3.6E-09	3.6E-09	2.6E-09	2.0E-09	1.9E-09	1.9E-09
Ingested materials						
All compounds	5.4E-11	4.0E-12	2.2E-12	1.3E-12	8.8E-13	7.4E-13

AMAD, activity median aerodynamic diameter.

23. CADMIUM (Z=48)

23.1. Routes of Intake

23.1.1. Inhalation

(250) Information is available on the behaviour of cadmium after deposition in the respiratory tract from animal studies and limited empirical human data. For details see Section 26 of *Publication 151*, ICRP 2022. Absorption parameter values and types, and associated f_A values for particulate forms of cadmium are given in Table 23.1 [taken from Section 26 of *Publication 151* (ICRP, 2022)].

Table 23.1. Absorption parameter values for inhaled and ingested cadmium.

		Absorption parameter values*		
Inhaled particulate materials		f_r	s_r (d^{-1})	s_s (d^{-1})
Default parameter values†,‡				
Absorption type	Assigned forms			
F	-	1	30	–
M§	Oxide, chloride, sulphide, carbonate, telluride, all unspecified forms	0.2	3	0.005
S	-	0.01	3	1×10^{-4}

Ingested materials¶	Age-dependent absorption from the alimentary tract, f_A					
Assigned forms	3 months	1 year	5 years	10 years	15 years	Adult
All compounds	0.5	0.05	0.05	0.05	0.05	0.05

*It is assumed that the bound state can be neglected for cadmium (i.e. $f_b = 0$). The values of s_r for Type F, M and S forms of cadmium (30, 3 and 3 d^{-1} respectively) are the general default values.

†Materials (e.g. oxide) are generally listed here where there is sufficient information to assign to a default absorption type, but not to give specific parameter values [see Section 26 of *Publication 151* (ICRP, 2022)].

‡For inhaled material deposited in the respiratory tract and subsequently cleared by particle transport to the alimentary tract, the default f_A values for inhaled materials are applied: i.e. the product of f_r for the absorption type (or specific value where given) and the f_A value for ingested soluble forms of cadmium applicable to the age-group of interest (e.g. 0.05 for adults).

§Default Type M is recommended for use in the absence of specific information on which the exposure material can be assigned to an absorption type (e.g. if the form is unknown, or if the form is known but there is no information available on the absorption of that form from the respiratory tract).

¶Activity transferred from systemic compartments into segments of the alimentary tract is assumed to be subject to reabsorption to blood. The default absorption fraction f_A for the secreted activity is the highest value for ingestion of the radionuclide applicable to the age-group of interest (e.g. 0.05 for adults).

23.1.2. Ingestion

23.1.2.1. Adults

(251) From dietary balance studies, the average normal gastrointestinal absorption of ingested cadmium in humans ranged from 3 to 7% (WHO, 2011a; ATSDR, 2012a). The Joint Food and Agriculture Organization/World Health Organization of the United Nations Expert Committee on Food Additives (JEFCA, 2001) considered the overall point estimate of 5% for bioavailability to be appropriate. The bioavailability of cadmium from some foods in which it is bound to phytates, metallothionein, and other proteins may be reduced (ATSDR, 2012a; JECFA, 2001).

(252) In *Publications 30*, *72* and *151* (ICRP, 1980, 1995c and 2022) a fractional absorption of 0.05 was used. In this publication, the f_A value of 0.05 is also recommended for ingestion of cadmium by adult members of the public.

23.1.2.2. Children

(253) The absorption of cadmium in rats depends on age, with measured absorption decreasing from 12 to 5 to 0.5% at 2 hours, 24 hours, and 6 weeks after birth, respectively (Sasser and Jarboe 1977). Sasser and Jarboe (1980) also reported that absorption of cadmium in the gastrointestinal tract of young guinea pigs was 20-fold higher than in adult guinea pigs. Increases in absorption have also been observed in mice during gestation and lactation (ATSDR, 2012a).

(254) From these animal data, a 10 time increase in human infants vs. adult was assumed here, leading to an $f_A = 0.5$ that is adopted here for ingestion of all forms of cadmium by 3-month-old infants. The adult value of 0.05 is used for older children.

23.1.3. Systemic distribution, retention and excretion of cadmium

23.1.3.1. Biokinetic data

(255) Cadmium is in Group IIB of the periodic table, below the chemically similar element zinc (Zn). Cadmium is commonly found in zinc ores. Cadmium and zinc have the same valence (2+) in their stable form, but zinc is more stable in its divalent state and, unlike cadmium, does not undergo redox changes. Cadmium appears to have no essential physiological role but bears some biokinetic and physiological resemblance to zinc. In the mammalian body, cadmium and zinc bind to the same proteins and compete for uptake by many of the same cells, and cadmium can replace zinc in several biological processes. The toxic effects of cadmium appear to result in part from interactions with zinc at the stage of zinc biological function ((Cotzias et al., 1961; Brzoska and Moniuszko-Jakonuik, 2001).

(256) Systemic cadmium enters the urinary bladder and intestines much more slowly than zinc and hence has a much longer residence time than zinc in the body. A biological half-time on the order of 25 y has been estimated for cadmium (ICRP, 1980; Thorne et al., 1986).

(257) Zhu et al. (2010) measured concentrations of cadmium in 17 tissues obtained from autopsies of up to 68 Chinese men from four areas of China. All subjects were considered healthy until the time of sudden accidental death. Based on median cadmium concentrations in tissues and reference tissue masses, about 30% of total-body cadmium was contained in the kidneys, 24% in liver, 12% in muscle, 11% in bone, 9% in lung, and 14% in other tissues and fluids.

(258) The distribution of cadmium in laboratory animals resembles that found in humans, with highest concentrations in the liver and kidneys. Similar concentrations are found in liver and kidneys at early times, but during prolonged exposure the concentration in the kidneys exceeds that in the liver except for very high exposure (ATSDR, 2012).

(259) The kidney is the primary target organ for chronic exposure to cadmium. Long-term exposure to cadmium may result in various levels of kidney damage from minor tubular dysfunction to severe kidney impairment. Absorbed cadmium is transported to the liver, where it stimulates synthesis of metallothionein. Cadmium bound to metallothionein is subsequently transported to the kidneys. A portion of the cadmium filtered by the kidneys and a portion of cadmium stored in kidney tissue is excreted in urine. Over time urinary cadmium becomes closely related to the kidney content (Friberg, 1984).

(260) Järup et al. (1983) estimated the biological half-time of cadmium in blood based on measurements over 10-13 y of blood cadmium in five persons with previous occupational

exposure to cadmium. The collected data were fit by a bi-exponential function. The estimated half-times ranged from 75-128 d for the short-term component and 7.4-16 y for the long-term component.

23.1.3.2. Biokinetic model for systemic cadmium

(261) The biokinetic model for systemic cadmium applied in *Publication 151* (ICRP, 2022) to workers is applied here to adult members of the public. The transfer coefficients in the cadmium model for workers were designed to reproduce the following information or assumptions: the initial systemic distribution of cadmium as indicated by studies on laboratory animals; a retention half-time of ~25 y in the total body; the long-term distribution of stable cadmium in the body as indicated by results of a study of element contents in tissues of adult males (Zhu et al. 2010); and typical steady-state contents of stable cadmium in total body, blood, and urine of adult humans. Comparison of model predictions with the observed steady-state contents of stable cadmium in tissues was based on a reference gastrointestinal absorption fraction of 0.05 and a reference dietary intake of 15 µg Cd per day (ATSDR, 2012).

(262) By analogy with the age-specific treatment of zinc in *Publication* 130 (ICRP, 2016), the model for cadmium in adults is modified as follows for application to pre-adult ages: (1) the deposition fractions for trabecular and cortical bone surface are increased by 50% over the adult value for all pre-adult ages, (2) the deposition fraction for the soft-tissue compartment with the highest turnover rate (ST0 in Fig. 23.1) is reduced for pre-adult ages to balance the increased deposition on bone surface at those ages, and (3) activity is assumed to be removed from trabecular or cortical bone volume to blood at the age-specific rate of turnover of that bone type (ICRP, 2002).

(263) The structure of the biokinetic model for systemic cadmium applied in this report is shown in Fig. 23.1. Transfer coefficients are listed in Table 23.2.

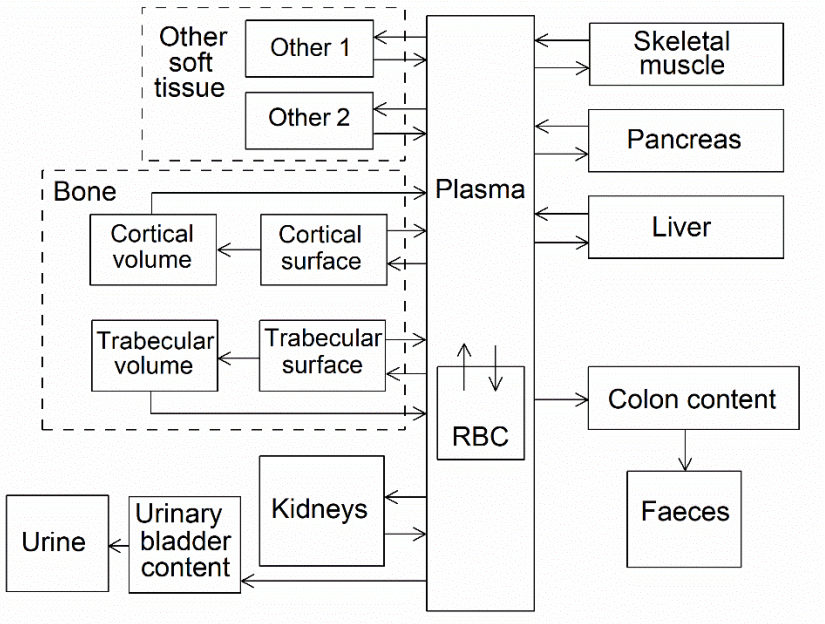

Fig. 23.1. Structure of the biokinetic model for systemic cadmium.

Table 23.2. Age-specific transfer coefficients for cadmium.

		Transfer coefficients (d^{-1})					
Pathway		100 d	1 y	5 y	10 y	15 y	Adult
Plasma	Liver	1.80E+02	1.80E+02	1.80E+02	1.80E+02	1.80E+02	1.80E+02
Plasma	Kidneys	1.20E+01	1.20E+01	1.20E+01	1.20E+01	1.20E+01	1.20E+01
Plasma	Pancreas	9.00E+00	9.00E+00	9.00E+00	9.00E+00	9.00E+00	9.00E+00
Plasma	Muscle	6.00E+00	6.00E+00	6.00E+00	6.00E+00	6.00E+00	6.00E+00
Plasma	RBC	1.00E-01	1.00E-01	1.00E-01	1.00E-01	1.00E-01	1.00E-01
Plasma	Other 1	1.19E+02	1.19E+02	1.19E+02	1.19E+02	1.19E+02	1.20E+02
Plasma	Other 2	9.45E+01	9.45E+01	9.45E+01	9.45E+01	9.45E+01	9.45E+01
Plasma	UB content	1.50E+00	1.50E+00	1.50E+00	1.50E+00	1.50E+00	1.50E+00
Plasma	RC content	1.50E+00	1.50E+00	1.50E+00	1.50E+00	1.50E+00	1.50E+00
Plasma	Trab surface	6.75E-01	6.75E-01	6.75E-01	6.75E-01	6.75E-01	4.50E-01
Plasma	Cort surface	1.35E+00	1.35E+00	1.35E+00	1.35E+00	1.35E+00	9.00E-01
Liver	Plasma	1.80E-02	1.80E-02	1.80E-02	1.80E-02	1.80E-02	1.80E-02
Kidneys	Plasma	8.00E-04	8.00E-04	8.00E-04	8.00E-04	8.00E-04	8.00E-04
Pancreas	Plasma	1.80E-02	1.80E-02	1.80E-02	1.80E-02	1.80E-02	1.80E-02
Muscle	Plasma	1.10E-03	1.10E-03	1.10E-03	1.10E-03	1.10E-03	1.10E-03
RBC	Plasma	8.33E-03	8.33E-03	8.33E-03	8.33E-03	8.33E-03	8.33E-03
Other 1	Plasma	5.00E-01	5.00E-01	5.00E-01	5.00E-01	5.00E-01	5.00E-01
Other 2	Plasma	1.70E-02	1.70E-02	1.70E-02	1.70E-02	1.70E-02	1.70E-02
Trab surface	Plasma	2.00E-04	2.00E-04	2.00E-04	2.00E-04	2.00E-04	2.00E-04
Cort surface	Plasma	2.00E-04	2.00E-04	2.00E-04	2.00E-04	2.00E-04	2.00E-04
Trab surface	Trab volume	1.00E-05	1.00E-05	1.00E-05	1.00E-05	1.00E-05	1.00E-05
Cort surface	Cort volume	1.00E-05	1.00E-05	1.00E-05	1.00E-05	1.00E-05	1.00E-05
Trab volume	Plasma	8.22E-03	2.88E-03	1.81E-03	1.32E-03	9.59E-04	4.93E-04
Cort volume	Plasma	8.22E-03	2.88E-03	1.53E-03	9.04E-04	5.21E-04	8.21E-05

RBC, red blood cells; UB, urinary bladder; RC, right colon; Cort, cortical; Trab, trabecular.

23.1.3.3. Treatment of radioactive progeny

(264) The treatment of radioactive progeny produced in systemic compartments after intake of a radioisotope of cadmium is described in Section 26.2.3.3. of *Publication 151* (ICRP, 2022).

23.2. Dosimetric data for cadmium

Table 23.3. Committed effective dose coefficients (Sv Bq^{-1}) for the inhalation or ingestion of ^{109}Cd compounds.

	Effective dose coefficients (Sv Bq^{-1})					
	3m	1y	5y	10y	15y	Adult
Inhaled particulate materials; (1 µm AMAD aerosols)						
Type F	3.2E-08	1.7E-08	9.9E-09	6.4E-09	4.4E-09	4.2E-09
Type M (default), oxide, chloride, sulphide, carbonate, telluride, all unspecified forms	1.6E-08	1.2E-08	6.9E-09	4.5E-09	3.5E-09	3.4E-09
Type S	1.8E-08	1.7E-08	9.7E-09	6.3E-09	5.0E-09	4.8E-09
Ingested materials						
All compounds	4.5E-08	3.9E-09	2.4E-09	1.6E-09	1.1E-09	1.0E-09

AMAD, activity median aerodynamic diameter.

24. INDIUM (Z=49)

24.1. Routes of Intake

24.1.1. Inhalation

(265) For indium, default parameter values were adopted on absorption to blood from the respiratory tract (ICRP, 2015). Absorption parameter values and types, and associated f_A values for particulate forms of indium are given in Table 24.1 [taken from Section 27 of *Publication 151* (ICRP, 2022)].

24.1.2. Ingestion

24.1.2.1. Adults

(266) The fractional absorption of indium from the gastrointestinal tract appears to be less than a few percent, see *Publication 151* (ICRP, 2022) for details. f_1 was taken to be 0.02 for all compounds of indium in *Publications 30* and *72* (ICRP, 1980, 1995c). An $f_A = 0.005$ was used in *Publication 151*, acknowledging it could be even lower for insoluble compounds. The value of $f_A = 0.005$ is also adopted here for indium ingestion by adult members of the public.

24.1.2.2. Children

(267) Consistently with the approach of *Publication56* (ICRP, 1990), an $f_A = 0.05$ is adopted here for ingestion of all forms of indium by 3 month old infants and the adult value of 0.005 is used for older children.

Table 24.1. Absorption parameter values for inhaled and ingested indium.

	Absorption parameter values*		
Inhaled particulate materials	f_r	s_r (d^{-1})	s_s (d^{-1})
Default parameter values†			
Absorption type			
F	1	30	–
M‡	0.2	3	0.005
S	0.01	3	1×10^{-4}

Ingested materials§	Age-dependent absorption from the alimentary tract, f_A					
Assigned forms	3 months	1 year	5 years	10 years	15 years	adult
All compounds	0.05	0.005	0.005	0.005	0.005	0.005

*It is assumed that the bound state can be neglected for indium (i.e. $f_b = 0$). The values of s_r for Type F, M and S forms of indium (30, 3 and 3 d^{-1} respectively) are the general default values.

†For inhaled material deposited in the respiratory tract and subsequently cleared by particle transport to the alimentary tract, the default f_A values for inhaled materials are applied: i.e. the product of f_r for the absorption type and the f_A value for ingested soluble forms of indium applicable to the age-group of interest (e.g. 0.005 for adults).

‡Default Type M is recommended for use in the absence of specific information on which the exposure material can be assigned to an absorption type (e.g. if the form is unknown, or if the form is known but there is no information available on the absorption of that form from the respiratory tract).

§Activity transferred from systemic compartments into segments of the alimentary tract is assumed to be subject to reabsorption to blood. The default absorption fraction f_A for the secreted activity is the highest value for ingestion of the radionuclide applicable to the age-group of interest (e.g. 0.005 for adults).

24.1.3. Systemic distribution, retention and excretion of indium

24.1.3.1. Biokinetic data

(268) Commonly studied chemical forms of indium bind with the iron-transport protein transferrin in blood, resulting in an initial distribution resembling that of iron. As a central estimate, transferrin-bound indium clears from human blood plasma with a half-time of ~10 h (Goodwin et all., 1971; Simonsen et al., 2009). Uptake of indium by red blood cells has been observed in dogs (Mclntyre et al., 1974) and rats (Jönsson, 1991). Results of human studies indicate relatively high accumulation of indium in the liver and bone marrow (McNiel et al., 1974; Sayle et al., 1982; Datz and Taylor, 1985; McNiel et al. (1974) found that neither the retention nor the distribution of indium in the liver changed between 1 and 2 d post injection. In studies on rats, mice, and hamsters, 11-14 % of the injected indium accumulated in the liver (Castronovo et al. 1973; Mclntyre et al 1974; Jönsson 1991; Yamauchi et al. 1992) and was gradually removed in faeces. About 10-12% of injected indium was retained in bone marrow (Smith et al. 1960; Beamish and Brown, 1974; Mclntyre et al. 1974; Jeffcoat et al. 1978; Jönsson 1991). Some indium is removed from the body in urine, but faecal excretion appears to be the dominant excretion pathway. Indium is removed slowly from the human body. Simonsen et al. (2009) estimated that only 1.8 ± 1.3% of indium entering blood was excreted over the first four days.

(269) The reader is referred to Andersson et al. (2017) for a more detailed description of the systemic behaviour of indium in human subjects and laboratory animals.

24.1.3.2. Biokinetic model for systemic indium

(270) A biokinetic model for systemic indium developed by Andersson et al. (2017) was adopted in *Publication 151* (ICRP, 2022) for application to workers. The same model is applied in this report to indium for all ages at intake.

(271) The model structure is shown in Fig. 24.1. Transfer coefficients are listed in Table 24.2.

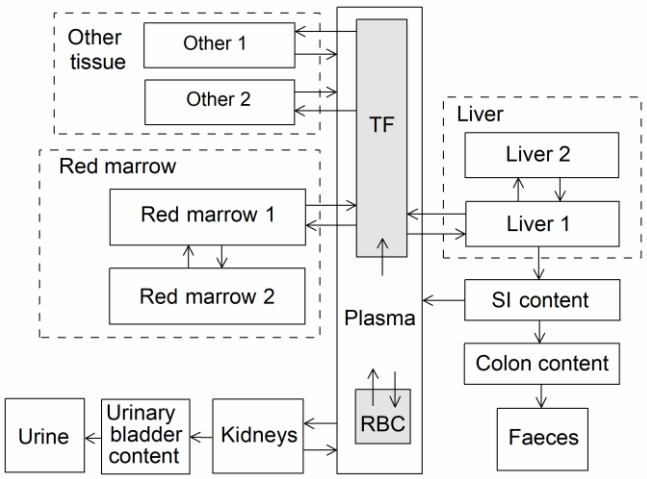

Fig. 24.1. The structure of the biokinetic model for systemic indium (from Andersson et al., 2017). TF, transferrin; RBC, red blood cells; SI, small intestine.

Table 24.2. Age-specific transfer coefficients for indium.

		Transfer coefficients (d^{-1})					
Pathway		100 d	1 y	5 y	10 y	15 y	Adult
Plasma	TF	8.30E+01	8.30E+01	8.30E+01	8.30E+01	8.30E+01	8.30E+01
Plasma	RBC	4.15E-01	4.15E-01	4.15E-01	4.15E-01	4.15E-01	4.15E-01
RBC	Plasma	5.54E-02	5.54E-02	5.54E-02	5.54E-02	5.54E-02	5.54E-02
TF	Red marrow 1	3.16E-01	3.16E-01	3.16E-01	3.16E-01	3.16E-01	3.16E-01
TF	Liver 1	2.53E-01	2.53E-01	2.53E-01	2.53E-01	2.53E-01	2.53E-01
TF	Other 1	4.27E-01	4.27E-01	4.27E-01	4.27E-01	4.27E-01	4.27E-01
TF	Other 2	5.86E-01	5.86E-01	5.86E-01	5.86E-01	5.86E-01	5.86E-01
Red marrow 1	TF	1.10E+00	1.10E+00	1.10E+00	1.10E+00	1.10E+00	1.10E+00
Red marrow 1	Red marrow 2	4.75E-01	4.75E-01	4.75E-01	4.75E-01	4.75E-01	4.75E-01
Red marrow 2	Red marrow 1	8.31E-03	8.31E-03	8.31E-03	8.31E-03	8.31E-03	8.31E-03
Liver 1	TF	4.75E-01	4.75E-01	4.75E-01	4.75E-01	4.75E-01	4.75E-01
Liver 1	SI content	1.10E-01	1.10E-01	1.10E-01	1.10E-01	1.10E-01	1.10E-01
Liver 1	Liver 2	5.54E-01	5.54E-01	5.54E-01	5.54E-01	5.54E-01	5.54E-01
Liver 2	Liver 1	8.31E-03	8.31E-03	8.31E-03	8.31E-03	8.31E-03	8.31E-03
Other 1	Plasma	2.37E+00	2.37E+00	2.37E+00	2.37E+00	2.37E+00	2.37E+00
Other 2	Plasma	4.75E-03	4.75E-03	4.75E-03	4.75E-03	4.75E-03	4.75E-03
Plasma	Kidneys	1.66E+00	1.66E+00	1.66E+00	1.66E+00	1.66E+00	1.66E+00
Kidneys	Plasma	1.66E-02	1.66E-02	1.66E-02	1.66E-02	1.66E-02	1.66E-02
Kidneys	UB content	2.68E-02	2.68E-02	2.68E-02	2.68E-02	2.68E-02	2.68E-02

TF, transferrin; RBC, red blood cells; SI, small intestine; UB, urinary bladder.

24.1.3.3. Treatment of radioactive progeny

(272) The treatment of radioactive progeny produced in systemic compartments after intake of a radioisotope of indium is described in Section 27.2.3.3. of *Publication 151* (ICRP, 2022).

24.2. Dosimetric data for indium

Table 24.3. Committed effective dose coefficients (Sv Bq^{-1}) for the inhalation or ingestion of ^{111}In compounds.

	Effective dose coefficients (Sv Bq^{-1})					
	3m	1y	5y	10y	15y	Adult
Inhaled particulate materials; (1 μm AMAD aerosols)						
Type F	5.4E-10	4.1E-10	1.9E-10	1.4E-10	8.7E-11	8.5E-11
Type M, default	6.5E-10	5.1E-10	2.7E-10	1.9E-10	1.3E-10	1.3E-10
Type S	6.8E-10	5.4E-10	2.8E-10	2.0E-10	1.4E-10	1.4E-10
Ingested materials						
All compounds	6.7E-10	5.7E-10	3.2E-10	2.3E-10	1.6E-10	1.5E-10

AMAD, activity median aerodynamic diameter.

25. TIN (Z=50)

25.1. Routes of Intake

25.1.1. Inhalation

(273) For tin, default parameter values were adopted on absorption to blood from the respiratory tract (ICRP, 2015). Absorption parameter values and types, and associated f_A values for particulate forms of tin are given in Table 24.1 [taken from Section 28 of *Publication 151* (ICRP, 2022)].

25.1.2. Ingestion

25.1.2.1. Adults

(274) The absorption of dietary or inorganic tin from the gastrointestinal tract is small, see *Publication 151* (ICRP, 2022) for details. In *Publications 30*, *72* (ICRP, 1981, 1995c) and *151*, the fractional absorption was taken as 0.02 for all compounds of tin. In this publication, the value of $f_A = 0.02$ is also adopted for all chemical forms of tin ingested by adult members of the public.

25.1.2.2. Children

(275) Consistently with the approach of *Publication56* (ICRP, 1990), an $f_A = 0.04$ is adopted here for ingestion of all forms of cadmium by 3 month old infants and the adult value of 0.02 is used for older children.

Table 25.1. Absorption parameter values for inhaled and ingested tin.

	Absorption parameter values*		
Inhaled particulate materials	f_r	s_r (d^{-1})	s_s (d^{-1})
Default parameter values†			
Absorption type			
F	1	30	–
M‡	0.2	3	0.005
S	0.01	3	1×10^{-4}

Ingested materials§	Age-dependent absorption from the alimentary tract, f_A					
Assigned forms	3 months	1 year	5 years	10 years	15 years	adult
All compounds	0.04	0.02	0.02	0.02	0.02	0.02

*It is assumed that the bound state can be neglected for tin (i.e. $f_b = 0$). The values of s_r for Type F, M and S forms of tin (30, 3 and 3 d^{-1} respectively) are the general default values.

†For inhaled material deposited in the respiratory tract and subsequently cleared by particle transport to the alimentary tract, the default f_A values for inhaled materials are applied: i.e. the product of f_r for the absorption type and the f_A value for ingested soluble forms of tin applicable to the age-group of interest (e.g. 0.02 for adults).

‡Default Type M is recommended for use in the absence of specific information on which the exposure material can be assigned to an absorption type (e.g. if the form is unknown, or if the form is known but there is no information available on the absorption of that form from the respiratory tract).

§Activity transferred from systemic compartments into segments of the alimentary tract is assumed to be subject to reabsorption to blood. The default absorption fraction f_A for the secreted activity is the highest value for ingestion of the radionuclide applicable to the age-group of interest (e.g. 0.02 for adults).

25.1.3. Systemic distribution, retention and excretion of tin

25.1.3.1. Biokinetic data

(276) The distribution of tin in the adult human body has been estimated from its measured concentration in tissues collected at autopsy, mainly from male subjects. Reported results vary considerable regarding the level of tin in the body and the relative concentrations in tissues. Zhu et al. (2010) reported the medians and ranges of concentrations of tin in 17 tissues of up to 68 adult males. Highest median values were determined for lung (0.031 mg kg^{-1} wet weight), liver (0.022), rib (0.013), and kidneys (0.012). Concentrations in stomach, small intestine, large intestine, heart, adrenals, testes, spleen, skin, fat, skeletal muscle, thyroid, pancreas, and thymus were in the range 0.005-0.009 mg kg^{-1}. The investigators estimated a central total-body content of 0.51 mg. Based on median concentrations and reference masses of tissues, about half of total-body tin was contained in muscle plus fat and 20-25% was in bone, assuming rib is representative of bone. Garcia et al. (2001) estimated mean tissue concentrations for 78 subjects of 0.47 (mg kg^{-1} wet weight) in bone, 0.27 in brain, 0.25 in kidney, 0.24 in lung, and 0.16 in liver. Chiba et al. (1991) estimated mean concentrations of 2.1 mg kg^{-1} dry weight in testes, 1.1 in liver, 0.83 in kidney cortex, 0.75 in heart, 0.45 in lung, and 0.61 in rib of 11-13 adult males. Hamilton et al. (1973) found highest concentrations in lymph nodes (1.5 mg kg^{-1} wet weight) and bone (1.1), followed by lungs (0.8), liver (0.4), and kidneys (0.2); relatively low concentrations were found in muscle (0.07) and brain (0.06).

(277) Hiles (1974) studied the biokinetics of inorganic tin in rats following oral or intravenous administration of ^{113}Sn(II) or ^{113}Sn(IV). About 2.85% and 0.64% of ^{113}Sn administered orally as Sn(II) and Sn(IV), respectively, was absorbed to blood. At 48 d after oral intake, the skeleton, liver, and kidneys contained about 1.0, 0.08, and 0.09%, respectively, of ^{113}Sn administered as Sn(II), and 0.24, 0.02, and 0.02%, respectively, of ^{113}Sn administered as Sn(IV), indicating similar systemic distributions of the absorbed activity for the two forms. At 48 h after intravenous injection, the bone, liver, and kidneys contained about 35, 2.0, and 5.9%, respectively, of ^{113}Sn administered as Sn(II), and 46, 0.2, and 5.3%, respectively, of ^{113}Sn administered as Sn(IV).

(278) Furchner and Drake (1976) examined the behaviour of ^{113}Sn in mice, Sprague-Dawley (S. D.) rats, African white-tailed rats (Mystromys), monkeys, and dogs following oral, intraperitoneal (IP), or intravenous (IV) administration as ^{113}Sn(II) chloride. The IP injection study involved only mice and rats. Mean total excretion over the first 3 d after IV injection was about 25% for mice, 38% for Mystromys, 45% for S. D. rats, 39% for monkeys, and 69% for dogs. Excretion over the first 3 d was primarily in urine, e.g., 84% of total excretion in monkeys and 91% in dogs. Total-body retention following IV injection was measured for periods of 291 d for rats, 319 d for Mystromys, 325 d for dogs, 338 d for mice, and 469 d for monkeys. Retention in each species could be described as a sum of four exponential terms. Retention was broadly similar across species and showed no relation to body size. As an average over the five studied species, the biological half-times of the four phases of retention for IV injection were about 0.5 d (50%), 4.3 d (13%), 28 d (9%), and 510 d (28%). The mean long-term half-time was about 760 d for mice, 580 d for Mystromys, 420 d for S. D. rats, 370 d for monkeys, and 430 d for dogs. The time-dependent distribution of systemic activity was measured in S. D. rats at 10 times from 1-141 d post IP injection. Bone contained 69% of total-body activity at 1 d, 71-76% at 6-113 d, and 65% at 141 d; muscle contained 12-20% at 1-141 d; liver contained 2.4-5.9% at 1-141 d; and kidneys contained 3.5% at 1 d, gradually decreasing to ~1% at 85-141 d.

25.1.3.2. Biokinetic model for systemic tin

(279) The biokinetic model for systemic tin applied in *Publication 151* (ICRP, 2022) is applied here to intake of tin at all ages. In that model, parameter values were set for reasonable consistency with total-body retention of tin observed in monkeys over the early months after acute input to blood, and with the early systemic distribution of tin observed in rats (Furchner and Drake, 1976). Parameter values determining the long-term distribution of tin were set for reasonable consistency with the central systemic distribution of tin indicated by results of an autopsy study by Zhu et al. (2010).

(280) The structure of the biokinetic model for systemic tin applied in this report is shown in Fig. 25.1. Transfer coefficients are listed in Table 25.2.

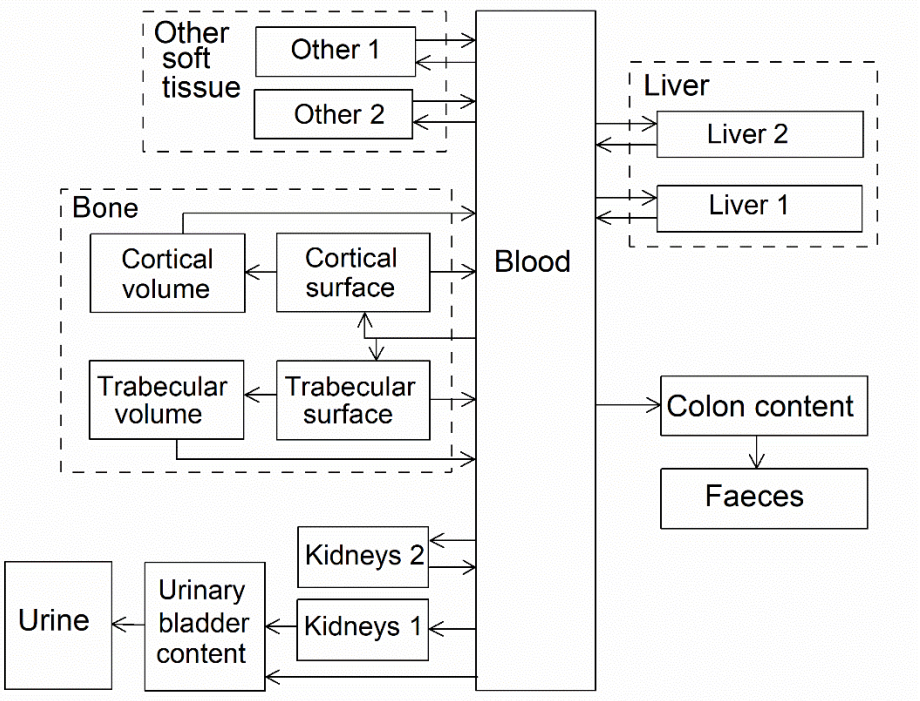

Fig. 25.1. Structure of the biokinetic model for systemic tin.

2809 Table 25.2. Age-specific transfer coefficients for tin.

		Transfer coefficients (d^{-1})					
Pathway		100 d	1 y	5 y	10 y	15 y	Adult
Blood	UB content	1.80E+00	1.80E+00	1.80E+00	1.80E+00	1.80E+00	1.80E+00
Blood	RC content	2.00E-01	2.00E-01	2.00E-01	2.00E-01	2.00E-01	2.00E-01
Blood	Trab surface	6.00E-01	6.00E-01	6.00E-01	6.00E-01	6.00E-01	6.00E-01
Blood	Cort surface	6.00E-01	6.00E-01	6.00E-01	6.00E-01	6.00E-01	6.00E-01
Blood	Other 1	6.00E-01	6.00E-01	6.00E-01	6.00E-01	6.00E-01	6.00E-01
Blood	Other 2	1.00E+00	1.00E+00	1.00E+00	1.00E+00	1.00E+00	1.00E+00
Blood	Liver 1	7.50E-02	7.50E-02	7.50E-02	7.50E-02	7.50E-02	7.50E-02
Blood	Liver 2	2.50E-02	2.50E-02	2.50E-02	2.50E-02	2.50E-02	2.50E-02
Blood	Kidneys 1	5.00E-02	5.00E-02	5.00E-02	5.00E-02	5.00E-02	5.00E-02
Blood	Kidneys 2	5.00E-02	5.00E-02	5.00E-02	5.00E-02	5.00E-02	5.00E-02
Trab surface	Blood	3.50E-02	3.50E-02	3.50E-02	3.50E-02	3.50E-02	3.50E-02
Cort surface	Blood	3.50E-02	3.50E-02	3.50E-02	3.50E-02	3.50E-02	3.50E-02
Trab surface	Trab volume	3.50E-02	3.50E-02	3.50E-02	3.50E-02	3.50E-02	3.50E-02
Cort surface	Cort volume	3.50E-02	3.50E-02	3.50E-02	3.50E-02	3.50E-02	3.50E-02
Trab volume	Blood	3.50E-03	3.50E-03	3.50E-03	3.50E-03	3.50E-03	3.50E-03
Cort volume	Blood	3.50E-03	3.50E-03	3.50E-03	3.50E-03	3.50E-03	3.50E-03
Liver 1	Blood	1.16E-02	1.16E-02	1.16E-02	1.16E-02	1.16E-02	1.16E-02
Liver 2	Blood	7.70E-04	7.70E-04	7.70E-04	7.70E-04	7.70E-04	7.70E-04
Kidneys 1	UB content	1.39E-01	1.39E-01	1.39E-01	1.39E-01	1.39E-01	1.39E-01
Kidneys 2	Blood	1.16E-02	1.16E-02	1.16E-02	1.16E-02	1.16E-02	1.16E-02
Other 1	Blood	1.39E-01	1.39E-01	1.39E-01	1.39E-01	1.39E-01	1.39E-01
Other 2	Blood	3.50E-03	3.50E-03	3.50E-03	3.50E-03	3.50E-03	3.50E-03

2810 UB, urinary bladder; RC, right colon; Cort, cortical; Trab, trabecular.

2811 25.1.3.3. Treatment of radioactive progeny

2812 (281) The treatment of radioactive progeny produced in systemic compartments after intake
2813 of a radioisotope of tin is described in Section 28.2.3.3. of *Publication 151* (ICRP, 2022).

2814 ## 25.2. Dosimetric data for tin

2815 Table 25.3. Committed effective dose coefficients (Sv Bq^{-1}) for the inhalation or ingestion of
2816 ^{113}Sn compounds.

	Effective dose coefficients (Sv Bq^{-1})					
	3m	1y	5y	10y	15y	Adult
Inhaled particulate materials; (1 µm AMAD aerosols)						
Type F	6.4E-09	5.0E-09	2.3E-09	1.3E-09	9.3E-10	7.7E-10
Type M, default	9.0E-09	7.8E-09	4.3E-09	2.8E-09	2.1E-09	2.1E-09
Type S	1.4E-08	1.2E-08	7.1E-09	4.7E-09	3.6E-09	3.6E-09
Ingested materials						
All compounds	1.9E-09	1.1E-09	6.1E-10	4.1E-10	2.7E-10	2.4E-10

2817 AMAD, activity median aerodynamic diameter.

26. HAFNIUM (Z=72)

26.1. Routes of Intake

26.1.1. Inhalation

(282) For hafnium, default parameter values were adopted on absorption to blood from the respiratory tract (ICRP, 2015). Absorption parameter values and types, and associated f_A values for particulate forms of hafnium are given in Table 26.1 [taken from Section 29 of *Publication 151* (ICRP, 2022)].

26.1.2. Ingestion

26.1.2.1. Adults

(283) There do not appear to be any relevant data available on the absorption of hafnium from the gastrointestinal tract. In *Publications 30*, *68* and *151* (ICRP, 1981, 1994a, 2022) the fractional absorption was taken to be 0.002 for all compounds of hafnium at the workplace based on chemical analogy with zirconium. A higher value of $f_1 = 0.01$ was used in *Publication 56* (ICRP, 1990) for ingestion of zirconium in diet by adult members of the public. The same value of $f_A = 0.01$ is adopted in this publication for ingestion of hafnium in diet; while the value $f_A = 0.002$ is used for all other forms of hafnium ingested by adult members of the public.

26.1.2.2 Children

(284) Consistently with the approach of *Publication56*, an $f_A = 0.02$ is adopted here for ingestion of all forms of hafnium by 3-month-old infants and the adult values of $f_A = 0.01$ (hafnium in diet) and $f_A = 0.002$ (other forms) are used for older children.

Table 26.1. Absorption parameter values for inhaled and ingested hafnium.

	Absorption parameter values*		
Inhaled particulate materials	f_r	s_r (d^{-1})	s_s (d^{-1})
Default parameter values†			
Absorption type			
F	1	30	–
M‡	0.2	3	0.005
S	0.01	3	1×10^{-4}

Ingested materials§	Age-dependent absorption from the alimentary tract, f_A					
Assigned forms	3 months	1 year	5 years	10 years	15 years	adult
hafnium in diet	0.02	0.01	0.01	0.01	0.01	0.01
all other forms	0.02	0.002	0.002	0.002	0.002	0.002

*It is assumed that the bound state can be neglected for hafnium (i.e. $f_b = 0$). The values of s_r for Type F, M and S forms of hafnium (30, 3 and 3 d^{-1} respectively) are the general default values.

†For inhaled material deposited in the respiratory tract and subsequently cleared by particle transport to the alimentary tract, the default f_A values for inhaled materials are applied: i.e. the product of f_r for the absorption type and the f_A value for ingested soluble forms of hafnium applicable to the age-group of interest (e.g. 0.002 for adults).

‡Default Type M is recommended for use in the absence of specific information on which the exposure material can be assigned to an absorption type (e.g. if the form is unknown, or if the form is known but there is no information available on the absorption of that form from the respiratory tract).

§Activity transferred from systemic compartments into segments of the alimentary tract is assumed to be subject to reabsorption to blood. The default absorption fraction f_A for the secreted activity is the highest value for ingestion of the radionuclide applicable to the age-group of interest (e.g. 0.01 for adults).

26.1.3. Systemic distribution, retention and excretion of hafnium

26.1.3.1. Summary of biokinetic data

(285) The chemical and physical properties of the Group IVB element Hf closely resemble those of the lighter IVB element zirconium. Comparisons of the behaviour of Hf and Zr in laboratory animals also indicate that they are close physiological analogues with virtually identical biokinetics (Leggett and Samuels, 2020).

(286) Taylor and coworkers (1983, 1985) studied the kinetics of ^{181}Hf or $^{175+181}$Hf in rats, hamsters, and marmosets over 6 months post administration by different routes. Total-body retention over 150 d was similar for the three animal types following parenteral administration of Hf as a citrate complex. Detailed studies of the distribution of activity in the body were conducted for hamsters and rats. The skeleton was the largest repository for Hf, containing ~29% of intravenously administered Hf in rats at 14 d post injection and ~43% at 21 d post subcutaneous administration to hamsters. In rats, the liver content peaked at 6.5% at 7 d and declined to 1.2% at 168 d. In hamsters the liver content peaked at 5% at 1 d and declined to 2.1% at 168 d. Limited tissue measurements on marmosets suggested a higher liver content than observed in rats and hamsters.

(287) Ando and Ando (1986) studied the behaviour of ^{181}Hf and ^{95}Zr in tumor-bearing rats over 2 d after intravenous injection of ^{181}Hf chloride, ^{95}Zr oxalate, and ^{95}Zr nitrate. The kinetics of Hf closely followed that of Zr in studied tissues other than liver and spleen. Higher accumulation of Hf than Zr in liver and spleen was attributed to formation of colloidal Hf in the injected solution and its removal from Blood 1 by phagocytic cells of liver and spleen.

(288) At 4 d after IV administration of 181Hf as citrate to rats, the median concentration ratios liver:femur and kidney:femur were ~0.5 (MacDonald and Bahner, 1953). At 14 d after IV administration of 175+181Hf as citrate, the total body, liver, and skeleton contained ~71%, 4.1%, and 29%, respectively, of the administered amount (Taylor et al., 1983). At 4 d after IV administration of 181Hf mandelate to rats, the median concentration ratios liver:femur and kidney:femur were ~6 and 1.4, respectively (MacDonald and Bahner, 1953). At 16 d after IV administration of 181Hf mandelate to rats, the total body, liver, and bone contained ~93%, 45%, and 13%, respectively, of the administered activity corrected for radioactive decay (Kittle et al., 1951).

26.1.3.2. Biokinetic model for systemic hafnium

(289) The age-specific biokinetic model for systemic zirconium adopted in Part 1 of this series on public intake of radionuclides (ICRP, 2024) is also applied to hafnium.

(290) The model structure is shown in Fig. 26.1. The transfer coefficients are listed in Table 26.2.

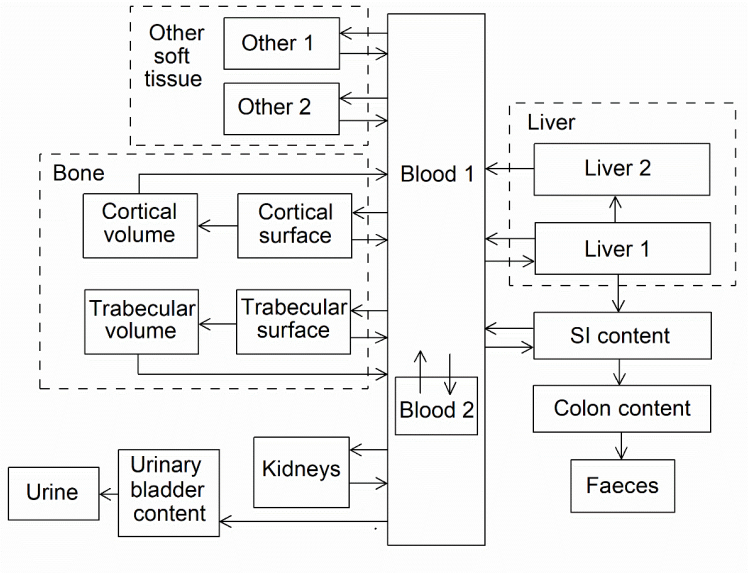

Fig. 26.1. Structure of the biokinetic model for systemic hafnium.

Table 26.2. Age-specific transfer coefficients for hafnium.

		Transfer coefficients (d^{-1})					
Pathway		100 d	1 y	5 y	10 y	15 y	Adult
Blood 1	Blood 2	1.82E+00	1.91E+00	1.91E+00	1.91E+00	1.91E+00	2.00E+00
Blood 1	Liver 1	6.84E-02	7.17E-02	7.17E-02	7.17E-02	7.17E-02	7.50E-02
Blood 1	Kidneys	1.14E-02	1.19E-02	1.19E-02	1.19E-02	1.19E-02	1.25E-02
Blood 1	Other 1	1.82E+00	1.91E+00	1.91E+00	1.91E+00	1.91E+00	2.00E+00
Blood 1	Other 2	3.42E-02	3.58E-02	3.58E-02	3.58E-02	3.58E-02	3.75E-02
Blood 1	UB content	9.12E-02	9.56E-02	9.56E-02	9.56E-02	9.56E-02	1.00E-01
Blood 1	SI content	2.28E-02	2.39E-02	2.39E-02	2.39E-02	2.39E-02	2.50E-02
Blood 1	Trab surface	5.63E-01	4.69E-01	4.69E-01	4.69E-01	4.69E-01	3.75E-01
Blood 1	Cort surface	5.63E-01	4.69E-01	4.69E-01	4.69E-01	4.69E-01	3.75E-01
Blood 2	Blood 1	4.62E-01	4.62E-01	4.62E-01	4.62E-01	4.62E-01	4.62E-01
Liver 1	SI content	1.16E-01	1.16E-01	1.16E-01	1.16E-01	1.16E-01	1.16E-01
Liver 1	Liver 2	4.62E-01	4.62E-01	4.62E-01	4.62E-01	4.62E-01	4.62E-01
Liver 1	Blood 1	1.16E-01	1.16E-01	1.16E-01	1.16E-01	1.16E-01	1.16E-01
Liver 2	Blood 1	1.00E-02	1.00E-02	1.00E-02	1.00E-02	1.00E-02	1.00E-02
Kidneys	Blood 1	1.00E-02	1.00E-02	1.00E-02	1.00E-02	1.00E-02	1.00E-02
Other 1	Blood 1	4.62E-01	4.62E-01	4.62E-01	4.62E-01	4.62E-01	4.62E-01
Other 2	Blood 1	2.00E-02	2.00E-02	2.00E-02	2.00E-02	2.00E-02	2.00E-02
Trab surface	Blood 1	8.22E-03	2.88E-03	1.81E-03	1.32E-03	9.59E-04	4.93E-04
Trab surface	Trab volume	8.22E-03	2.88E-03	1.81E-03	1.32E-03	9.59E-04	2.47E-04
Trab volume	Blood 1	8.22E-03	2.88E-03	1.81E-03	1.32E-03	9.59E-04	4.93E-04
Cort surface	Blood 1	8.22E-03	2.88E-03	1.53E-03	9.04E-04	5.21E-04	8.21E-05
Cort surface	Cort volume	8.22E-03	2.88E-03	1.53E-03	9.04E-04	5.21E-04	4.11E-05
Cort volume	Blood 1	8.22E-03	2.88E-03	1.53E-03	9.04E-04	5.21E-04	8.21E-05

UB, urinary bladder; SI, small intestine; Cort, cortical; Trab, trabecular.

26.1.3.3. Treatment of radioactive progeny

(291) The treatment of radioactive progeny produced in systemic compartments after intake of a radioisotope of hafnium is described in Section 29.2.3.3. of *Publication 151* (ICRP, 2022).

26.2. Dosimetric data for hafnium

Table 26.3. Committed effective dose coefficients (Sv Bq^{-1}) for the inhalation or ingestion of ^{182}Hf compounds.

	Effective dose coefficients (Sv Bq^{-1})					
	3m	1y	5y	10y	15y	Adult
Inhaled particulate materials; (1 µm AMAD aerosols)						
Type F	3.3E-07	3.4E-07	2.9E-07	2.9E-07	3.0E-07	3.0E-07
Type M, default	1.4E-07	1.5E-07	1.4E-07	1.3E-07	1.4E-07	1.5E-07
Type S	3.0E-07	3.2E-07	2.7E-07	2.2E-07	2.3E-07	2.4E-07
Ingested materials						
Hafnium in diet	3.2E-08	1.6E-08	1.5E-08	1.5E-08	1.5E-08	1.5E-08
All other forms	3.2E-08	3.5E-09	3.1E-09	3.1E-09	3.1E-09	3.0E-09

AMAD, activity median aerodynamic diameter.

27. TANTALUM (Z=73)

27.1. Routes of Intake

27.1.1. Inhalation

(292) For tantalum, default parameter values were adopted on absorption to blood from the respiratory tract (ICRP, 2015). Absorption parameter values and types, and associated f_A values for particulate forms of tantalum are given in Table 27.1 [taken from Section 30 of *Publication 151* (ICRP, 2022)].

27.1.2. Ingestion

27.1.2.1. Adults

(293) Data from animal experiments indicate that the fractional absorption of tantalum is small, see *Publication 151* (ICRP, 2022) for details. In *Publications 30, 72 and 151* (ICRP, 1981, 1995c, 2022), it was taken as 10^{-3} for all compounds of tantalum. In this publication, the value of $f_A = 10^{-3}$ is also used as the default for all forms of tantalum ingested by adult members of the public.

27.1.2.2. Children

(294) In young suckling rats, the absorption was several orders of magnitude greater than in adults (Rydzynski and Pakulska, 2012). Consistently with the approach of *Publication 56* (ICRP, 1990), an $f_A = 0.01$ is adopted here for 3-month-old infants and the adult value of $f_A = 10^{-3}$ is used for older children.

Table 27.1. Absorption parameter values for inhaled and ingested tantalum.

	Absorption parameter values*		
Inhaled particulate materials	f_r	s_r (d^{-1})	s_s (d^{-1})
Default parameter values†			
Absorption type			
F	1	30	–
M‡	0.2	3	0.005
S	0.01	3	1×10^{-4}

Ingested materials§	Age-dependent absorption from the alimentary tract, f_A					
Assigned forms	3 months	1 year	5 years	10 years	15 years	adult
All compounds	0.01	0.001	0.001	0.001	0.001	0.001

*It is assumed that the bound state can be neglected for tantalum (i.e. $f_b = 0$). The values of s_r for Type F, M and S forms of tantalum (30, 3 and 3 d^{-1} respectively) are the general default values.

†For inhaled material deposited in the respiratory tract and subsequently cleared by particle transport to the alimentary tract, the default f_A values for inhaled materials are applied: i.e. the product of f_r for the absorption type and the f_A value for ingested soluble forms of tantalum applicable to the age-group of interest (e.g. 0.001 for adults).

‡Default Type M is recommended for use in the absence of specific information on which the exposure material can be assigned to an absorption type (e.g. if the form is unknown, or if the form is known but there is no information available on the absorption of that form from the respiratory tract).

§Activity transferred from systemic compartments into segments of the alimentary tract is assumed to be subject to reabsorption to blood. The default absorption fraction f_A for the secreted activity is the highest value for any form of the radionuclide applicable to the age-group of interest (e.g. 0.001).

27.1.3. Systemic distribution, retention and excretion of tantalum

27.1.3.1. Biokinetic data

(295) The chemical and physical properties of the Group VB element tantalum (Ta) closely resemble those of the lighter Group VB element niobium (Nb). These two elements are found together in nature and are sometimes referred to as geochemical twins due to their nearly proportional mass ratios across most geological material (Muenker et al., 2003), attributed to a common valence state and virtually identical ionic radii.

(296) Ando et al (1989, 1990) studied the distribution and excretion of Ta and Nb following intravenous administration of these elements as oxalate to tumor-bearing rats. Activity concentrations were measured in blood, bone, ten different soft tissues, and an implanted sarcoma. The behaviour of Ta closely followed that of Nb at all studied sites.

(297) In rats administered ^{95}Nb and $^{182}Ta_2O_5$ in citrate solution via intramuscular injection, both radionuclides showed elevated concentrations in liver, kidney, and bone (Durbin, 1960). At 4 d post injection, cumulative excretion of activity accounted for 48.6% of administered ^{182}Ta and 39.4% of administered ^{95}Nb. At that time, activity in bone, liver, and kidneys represented roughly 23%. 14%, and 10%, respectively of retained ^{182}Ta and 27%, 14%, and 5%, respectively, of retained ^{95}Nb.

(298) Fleshman et al. (1971) investigated the biokinetics of ^{182}Ta in rats over 106 d after its oral administration as potassium tantalite to rats. Bone was the dominant long-term repository, followed by pelt. At 106 d, bone, liver, and kidneys contained about 46%, 3.4%, and 1.2% respectively, of the total-body content.

27.1.3.2. Biokinetic model for systemic tantalum

(299) In view of the close chemical and physical properties of Ta and Nb and their similar biokinetics in available comparative studies, the age-specific biokinetic model for Nb applied in Part 1 of this series of reports (ICRP 2024) is assigned to the less frequently studied element Ta.

(300) The structure of the systemic model for Ta is shown in Fig. 27.1. Transfer coefficients are listed in Table 27.2.

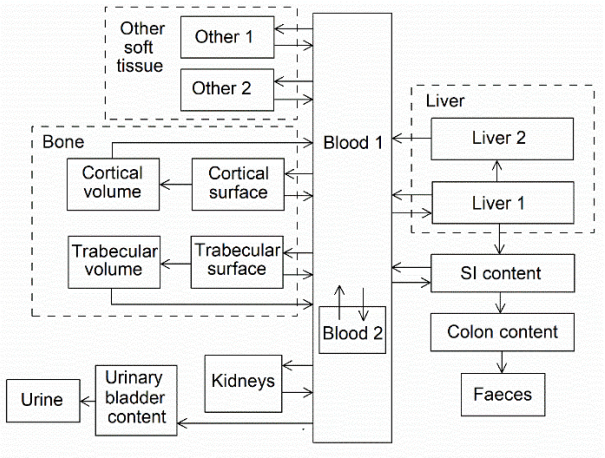

Fig. 27.1. Structure of the biokinetic model for systemic tantalum.

Table 27.2. Age-specific transfer coefficients for tantalum.

		Transfer coefficients (d^{-1})					
Pathway		100 d	1 y	5 y	10 y	15 y	Adult
Blood 1	Blood 2	3.15E+00	3.18E+00	3.18E+00	3.18E+00	3.18E+00	3.20E+00
Blood 1	Liver 1	2.36E-01	2.38E-01	2.38E-01	2.38E-01	2.38E-01	2.40E-01
Blood 1	Kidneys	3.94E-02	3.97E-02	3.97E-02	3.97E-02	3.97E-02	4.00E-02
Blood 1	Other 1	3.15E+00	3.18E+00	3.18E+00	3.18E+00	3.18E+00	3.20E+00
Blood 1	Other 2	1.18E-01	1.19E-01	1.19E-01	1.19E-01	1.19E-01	1.20E-01
Blood 1	UB content	8.66E-01	8.73E-01	8.73E-01	8.73E-01	8.73E-01	8.80E-01
Blood 1	SI content	7.88E-02	7.94E-02	7.94E-02	7.94E-02	7.94E-02	8.00E-02
Blood 1	Trab surface	1.80E-01	1.50E-01	1.50E-01	1.50E-01	1.50E-01	1.20E-01
Blood 1	Cort surface	1.80E-01	1.50E-01	1.50E-01	1.50E-01	1.50E-01	1.20E-01
Blood 2	Blood 1	1.39E+00	1.39E+00	1.39E+00	1.39E+00	1.39E+00	1.39E+00
Liver 1	SI content	5.78E-02	5.78E-02	5.78E-02	5.78E-02	5.78E-02	5.78E-02
Liver 1	Blood 1	5.78E-02	5.78E-02	5.78E-02	5.78E-02	5.78E-02	5.78E-02
Liver 1	Liver 2	2.31E-01	2.31E-01	2.31E-01	2.31E-01	2.31E-01	2.31E-01
Liver 2	Blood 1	5.00E-03	5.00E-03	5.00E-03	5.00E-03	5.00E-03	5.00E-03
Kidneys	Blood 1	5.00E-03	5.00E-03	5.00E-03	5.00E-03	5.00E-03	5.00E-03
Other 1	Blood 1	1.39E+00	1.39E+00	1.39E+00	1.39E+00	1.39E+00	1.39E+00
Other 2	Blood 1	1.00E-02	1.00E-02	1.00E-02	1.00E-02	1.00E-02	1.00E-02
Trab surface	Blood 1	8.22E-03	2.88E-03	1.81E-03	1.32E-03	9.59E-04	4.93E-04
Trab surface	Trab volume	8.22E-03	2.88E-03	1.81E-03	1.32E-03	9.59E-04	2.47E-04
Trab volume	Blood 1	8.22E-03	2.88E-03	1.81E-03	1.32E-03	9.59E-04	4.93E-04
Cort surface	Blood 1	8.22E-03	2.88E-03	1.53E-03	9.04E-04	5.21E-04	8.21E-05
Cort surface	Cort volume	8.22E-03	2.88E-03	1.53E-03	9.04E-04	5.21E-04	4.11E-05
Cort volume	Blood 1	8.22E-03	2.88E-03	1.53E-03	9.04E-04	5.21E-04	8.21E-05

UB, urinary bladder; SI, small intestine; RC, right colon; Cort, cortical; Trab, trabecular.

27.1.3.3. Treatment of radioactive progeny

(301) The treatment of radioactive progeny produced in systemic compartments after intake of a radioisotope of tantalum is described in Section 30.2.3.3. of *Publication 151* (ICRP, 2022).

27.2. Dosimetric data for tantalum

Table 27.3. Committed effective dose coefficients (Sv Bq^{-1}) for the inhalation or ingestion of ^{182}Ta compounds.

	Effective dose coefficients (Sv Bq^{-1})					
	3m	1y	5y	10y	15y	Adult
Inhaled particulate materials; (1 μm AMAD aerosols)						
Type F	1.1E-08	9.3E-09	4.7E-09	2.9E-09	2.2E-09	2.0E-09
Type M, default	1.9E-08	1.6E-08	9.2E-09	6.1E-09	4.7E-09	4.8E-09
Type S	2.9E-08	2.5E-08	1.5E-08	1.0E-08	7.7E-09	8.0E-09
Ingested materials						
All compounds	2.4E-09	1.9E-09	1.1E-09	7.6E-10	5.3E-10	5.0E-10

AMAD, activity median aerodynamic diameter.

28. TUNGSTEN (Z=74)

28.1. Routes of Intake

28.1.1. Inhalation

(302) For tungsten, default parameter values were adopted on absorption to blood from the respiratory tract (ICRP, 2015). Absorption parameter values and types, and associated f_A values for particulate forms of tungsten are given in Table 28.1 [taken from Section 31 of *Publication 151* (ICRP, 2022)].

28.1.2. Ingestion

28.1.2.1. Adults

(303) A large fraction of ingested tungsten is absorbed from the gut, with absorption from tungstic acid being less than from other compounds, see *Publication 151* (ICRP, 2022) for more details. In *Publications 30* and *72* (ICRP, 1981, 1994a), f_1 was taken as 0.01 for tungstic acid and 0.3 for all other compounds of the element. In *Publication 151*, a value of $f_A = 0.5$ was adopted for all forms other than tungstic acid. For ingestion of tungsten by adult members of the public the values adopted here are $f_A = 0.01$ for tungstic acid and $f_A = 0.5$ for all other forms of tungsten, including tungsten in diet.

28.1.2.2. Children

(304) Consistently with the approach of *Publication56* (ICRP, 1990), the values of $f_A = 0.02$ and $f_A = 1$, respectively, are adopted here for ingestion of tungstic acid and of all other forms of tungsten, respectively, by 3 month old infants. The adult values are used for older children.

Table 28.1. Absorption parameter values for inhaled and ingested tungsten.

	Absorption parameter values*		
Inhaled particulate materials	f_r	s_r (d^{-1})	s_s (d^{-1})
Default parameter values†			
Absorption type			
F	1	30	–
M‡	0.2	3	0.005
S	0.01	3	1×10^{-4}

Ingested materials§	Age-dependent absorption from the alimentary tract, f_A					
Assigned forms	3 months	1 year	5 years	10 years	15 years	adult
Tungstic acid	0.02	0.01	0.01	0.01	0.01	0.01
All other forms	1	0.5	0.5	0.5	0.5	0.5

*It is assumed that the bound state can be neglected for tungsten (i.e. $f_b = 0$). The values of s_r for Type F, M and S forms of tungsten (30, 3 and 3 d^{-1} respectively) are the general default values.

†For inhaled material deposited in the respiratory tract and subsequently cleared by particle transport to the alimentary tract, the default f_A values for inhaled materials are applied: i.e. the product of f_r for the absorption type and the f_A value for ingested soluble forms of tungsten applicable to the age-group of interest (e.g. 0.5 for adults).

‡Default Type M is recommended for use in the absence of specific information on which the exposure material can be assigned to an absorption type (e.g. if the form is unknown, or if the form is known but there is no information available on the absorption of that form from the respiratory tract).

[§]Activity transferred from systemic compartments into segments of the alimentary tract is assumed to be subject to reabsorption to blood. The default absorption fraction f_A for the secreted activity is the highest value for any form of the radionuclide applicable to the age group of interest (e.g. 0.5 for adults).

28.1.3. Systemic distribution, retention and excretion of tungsten

28.1.3.1. Biokinetic data

(305) The biokinetics of tungsten (W) has been studied in a variety of laboratory animals including: dogs receiving radio-tungsten by inhalation or injection (Aamodt, 1973, 1975); swine exposed to radionuclides produced by a nuclear explosion (Chertok and Lake 1971a, 1971b, 1971c); rodents administered radio-tungsten by different routes (Scott, 1952; Wase, 1956; Ballou, 1960; Fleshman et al., 1966; Kaye, 1968; Ando et al., 1989); and sheep, pigs, cows, and goats receiving radio-tungsten by injection or ingestion (Bell and Sneed, 1970; Mullen et al., 1976; Ekman et al., 1977). Direct information on the behaviour of absorbed tungsten in humans consists mainly of measurements of the concentration of tungsten in blood hair, nails, and excreta of living subjects (Wester 1973, 1974; Brune et al. 1980; Nicolaou et al. 1987).

(306) Important repositories for tungsten include the liver, kidneys, spleen, and bone. Results of animal studies indicate that a few percent of absorbed tungsten deposits in bone, a substantial portion of the deposited amount is retained for an extended period, and accumulation of tungsten is greater in growing than in mature bone (Fleshman et al., 1966; Kaye, 1968; Aamodt, 1975; Mullen et al., 1976; Ando et al., 1989). Similarities in the behaviour of tungstate, molybdate, and phosphate in biological systems have been observed. Tungsten is deposited and retained in bone, presumably due to substitution of tungstate for phosphate (Fleshman et al., 1966).

(307) Tungsten is considered a physiological analogue of molybdenum and can produce deficiency of molybdenum resulting from prevention of incorporation of molybdenum into certain enzymes (Cardin and Mason, 1976). Membrane transport may not distinguish between tungsten and molybdenum, although differences in the biokinetics of these elements may result from the fact that molybdenum compounds are more easily reduced in biological systems (Callis and Wentworth, 1977). An apparent difference in the systemic kinetics of these two elements is that the liver appears to accumulate considerably more molybdenum than tungsten.

28.1.3.2. Biokinetic model for systemic tungsten

(308) A biokinetic model for systemic tungsten proposed by Leggett (1997) was adopted in *Publication 151* (ICRP, 2022) for occupational intake of tungsten. That model is applied in this report to adult members of the public and is extended to pre-adults ages, primarily by introduction of age-specific transfer coefficients to and from bone compartments. For ages 15 y and lower, the transfer coefficients from plasma to cortical and trabecular bone surface are set at 2 times the values for adults. The transfer coefficients from plasma to all other destinations are decreased by ~6% to yield a removal half-time from plasma of 30 min (the same as the outflow rate from plasma in the model for adults) for all preadult ages. The age-specific bone model applied to phosphorus in Part 1 of this series is applied to tungsten that deposits in bone, based on the assumption that accumulation of tungsten in bone is due to replacement of phosphate with tungstate. The “bone model” refers here to all transfer coefficients describing outflow from any bone compartment.

(309) The structure of the biokinetic model for tungsten is shown in Fig. 28.1. Transfer coefficients are listed in Table 28.2.

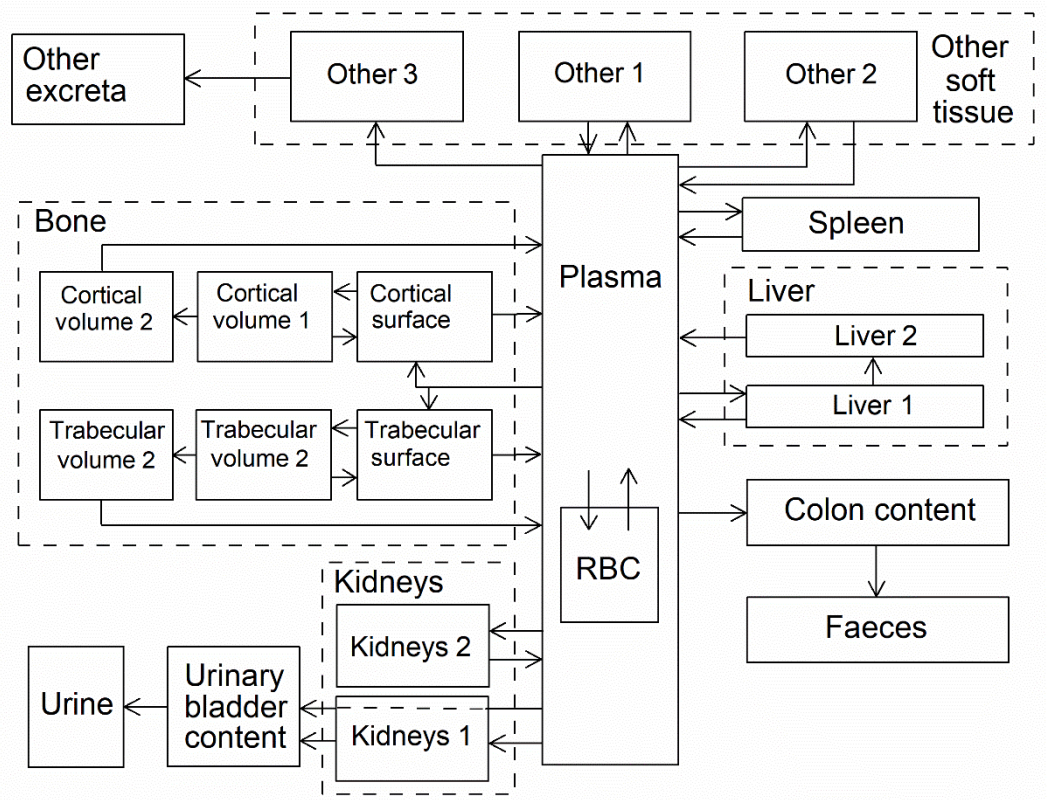

Fig. 28.1. Structure of the biokinetic model for systemic tungsten. RBC, red blood cells.

Table 28.2. Age-specific transfer coefficients for tungsten.

		Transfer coefficients (d^{-1})					
Pathway		100 d	1 y	5 y	10 y	15 y	Adult
Plasma	RBC	5.48E-02	5.48E-02	5.48E-02	5.48E-02	5.48E-02	5.82E-02
Plasma	UB content	8.22E+00	8.22E+00	8.22E+00	8.22E+00	8.22E+00	8.74E+00
Plasma	Kidneys 1	4.93E-01	4.93E-01	4.93E-01	4.93E-01	4.93E-01	5.24E-01
Plasma	Kidneys 2	5.48E-02	5.48E-02	5.48E-02	5.48E-02	5.48E-02	5.82E-02
Plasma	RC content	5.48E-01	5.48E-01	5.48E-01	5.48E-01	5.48E-01	5.82E-01
Plasma	Spleen	5.48E-03	5.48E-03	5.48E-03	5.48E-03	5.48E-03	5.82E-03
Plasma	Liver 1	4.38E-01	4.38E-01	4.38E-01	4.38E-01	4.38E-01	4.66E-01
Plasma	Other 1	4.69E+00	4.69E+00	4.69E+00	4.69E+00	4.69E+00	4.99E+00
Plasma	Other 2	2.47E-01	2.47E-01	2.47E-01	2.47E-01	2.47E-01	2.62E-01
Plasma	Other 3	2.19E-02	2.19E-02	2.19E-02	2.19E-02	2.19E-02	2.33E-02
Plasma	Trab surface	1.04E+00	1.04E+00	1.04E+00	1.04E+00	1.04E+00	5.18E-01
Plasma	Cort surface	8.28E-01	8.28E-01	8.28E-01	8.28E-01	8.28E-01	4.14E-01
RBC	Plasma	3.47E-01	3.47E-01	3.47E-01	3.47E-01	3.47E-01	3.47E-01
Kidneys 1	UB content	1.39E+00	1.39E+00	1.39E+00	1.39E+00	1.39E+00	1.39E+00
Kidneys 2	Plasma	1.90E-03	1.90E-03	1.90E-03	1.90E-03	1.90E-03	1.90E-03
Liver 1	Plasma	3.12E-01	3.12E-01	3.12E-01	3.12E-01	3.12E-01	3.12E-01
Liver 1	Liver 2	3.47E-02	3.47E-02	3.47E-02	3.47E-02	3.47E-02	3.47E-02
Liver 2	Plasma	1.90E-03	1.90E-03	1.90E-03	1.90E-03	1.90E-03	1.90E-03
Other 1	Plasma	8.32E+00	8.32E+00	8.32E+00	8.32E+00	8.32E+00	8.32E+00
Other 2	Plasma	6.93E-02	6.93E-02	6.93E-02	6.93E-02	6.93E-02	6.93E-02
Other 3	Excreta	1.90E-03	1.90E-03	1.90E-03	1.90E-03	1.90E-03	1.90E-03
Spleen	Plasma	1.90E-03	1.90E-03	1.90E-03	1.90E-03	1.90E-03	1.90E-03
Trab surface	Plasma	5.78E-01	5.78E-01	5.78E-01	5.78E-01	5.78E-01	5.78E-01
Trab surface	Trab volume 1	1.16E-01	1.16E-01	1.16E-01	1.16E-01	1.16E-01	1.16E-01
Cort surface	Plasma	5.78E-01	5.78E-01	5.78E-01	5.78E-01	5.78E-01	5.78E-01
Cort surface	Cort volume 1	1.16E-01	1.16E-01	1.16E-01	1.16E-01	1.16E-01	1.16E-01
Trab volume 1	Trab surface	2.77E-03	2.77E-03	2.77E-03	2.77E-03	2.77E-03	2.77E-03
Trab volume 1	Trab volume 2	4.16E-03	4.16E-03	4.16E-03	4.16E-03	4.16E-03	4.16E-03
Cort volume 1	Cort surface	2.77E-03	2.77E-03	2.77E-03	2.77E-03	2.77E-03	2.77E-03
Cort volume 1	Cort volume 2	4.16E-03	4.16E-03	4.16E-03	4.16E-03	4.16E-03	4.16E-03
Trab volume 2	Plasma	8.22E-03	2.88E-03	1.81E-03	1.32E-03	9.59E-04	4.93E-04
Cort volume 2	Plasma	8.22E-03	2.88E-03	1.53E-03	9.04E-04	5.21E-04	8.21E-05

UB, urinary bladder; RC, right colon; Cort, cortical; Trab, trabecular; RBC, red blood cells.

28.1.3.3. Treatment of radioactive progeny

(310) The treatment of radioactive progeny produced in systemic compartments after intake of a radioisotope of tungsten is described in Section 31.2.3.3. of *Publication 151* (ICRP, 2022).

28.2. Dosimetric data for tungsten

Table 28.3. Committed effective dose coefficients (Sv Bq^{-1}) for the inhalation or ingestion of ^{181}W compounds.

	Effective dose coefficients (Sv Bq^{-1})					
	3m	1y	5y	10y	15y	Adult
Inhaled particulate materials; (1 µm AMAD aerosols)						
Type F	1.3E-10	8.9E-11	4.4E-11	2.9E-11	1.8E-11	1.6E-11
Type M, default	8.2E-10	7.0E-10	3.8E-10	2.5E-10	1.8E-10	1.8E-10
Type S	1.5E-09	1.3E-09	7.2E-10	4.8E-10	3.5E-10	3.6E-10
Ingested materials						
Tungstic acid	9.9E-11	9.1E-11	5.0E-11	3.6E-11	2.4E-11	2.4E-11
All other forms	2.6E-10	1.4E-10	8.1E-11	5.4E-11	3.8E-11	3.2E-11

AMAD, activity median aerodynamic diameter.

29. RHENIUM (Z=75)

29.1. Routes of Intake

29.1.1. Inhalation

(311) For rhenium, default parameter values were adopted on absorption to blood from the respiratory tract (ICRP, 2015). Absorption parameter values and types, and associated f_A values for particulate forms of rhenium are given in Table 29.1 [taken from Section 32 of *Publication 151* (ICRP, 2022)].

29.1.2. Ingestion

29.1.2.1. Adults

(312) In *Publications 30* and *72* (ICRP, 1980, 1995c), a fractional absorption value of 0.8 was recommended for all chemical forms of rhenium based on the chemical analogy with technetium. In *Publication 134* (ICRP, 2016), an f_A value of 0.9 was used for all chemical forms of technetium in the workplace. The same value of $f_A = 0.9$ was consequently adopted in *Publication 151* (ICRP, 2022) for all forms of rhenium. In *Publication 158*(ICRP, 2024), a value of $f_A = 0.5$ was adopted for ingestion by adults of technetium in food, while for ingestion of pertechnetate an $f_A = 0.9$ was used. In this publication, values of $f_A = 0.5$ for rhenium in food and $f_A = 0.9$ for all other forms of rhenium are adopted for ingestion by adult members of the public.

29.1.2.2. Children

(313) The same values as used in *Publication 158* for ingestion of technetium by children are adopted for rhenium in this publication. So, for ingestion by 3-month-old infants, an $f_A = 1$ is used here for all forms of rhenium. For older children, the adult f_A values are used.

Table 29.1. Absorption parameter values for inhaled and ingested rhenium.

	Absorption parameter values*		
Inhaled particulate materials	f_r	s_r (d^{-1})	s_s (d^{-1})
Default parameter values†			
Absorption type			
F	1	30	–
M‡	0.2	3	0.005
S	0.01	3	1×10^{-4}

Ingested materials§	Age-dependent absorption from the alimentary tract, f_A					
Assigned forms	3 months	1 year	5 years	10 years	15 years	adult
Rhenium in food	1	0.5	0.5	0.5	0.5	0.5
All other forms	1	0.9	0.9	0.9	0.9	0.9

*It is assumed that the bound state can be neglected for rhenium (i.e. $f_b = 0$). The values of s_r for Type F, M and S forms of rhenium (30, 3 and 3 d^{-1} respectively) are the general default values.

†For inhaled material deposited in the respiratory tract and subsequently cleared by particle transport to the alimentary tract, the default f_A values for inhaled materials are applied: i.e. the product of f_r for the absorption type and the f_A value for ingested soluble forms of rhenium applicable to the age-group of interest (e.g. 0.9 for adults).

[‡]Default Type M is recommended for use in the absence of specific information on which the exposure material can be assigned to an absorption type (e.g. if the form is unknown, or if the form is known but there is no information available on the absorption of that form from the respiratory tract).
[§]Activity transferred from systemic compartments into segments of the alimentary tract is assumed to be subject to reabsorption to blood. The default absorption fraction f_A for the secreted activity is the highest value for any form of the radionuclide applicable to the age-group of interest (e.g. 0.9 for adults).

29.1.3. Systemic distribution, retention and excretion of rhenium

29.1.3.1. Biokinetic data

(314) Rhenium (Re) is the heaviest naturally occurring element in Group VIIB of the period table. It is a close physiological analogue of the Group VIIB element technetium, presumably due to the combination of the similar ionic radii and chemical properties of these elements (Deutsch et al., 1986; Dadachova et al., 2002; Zuckier et al., 2004). Rhenium and technetium have similar coordination chemistry, often resulting in isostructural rhenium and technetium complexes. These elements become covalently bound with oxide ions to form the structurally similar anions perrhenate (ReO_4^-) and pertechnetate (TcO_4^-) in the body, which have medical applications as physiological analogues of iodide (Dadachova et al., 2002).

29.1.3.2. Biokinetic model for systemic rhenium

(315) The age-specific biokinetic model for systemic technetium applied in Part 1 of this report series on dose coefficients for members of the public (ICRP, 2024) is also applied to rhenium. The model structure is shown in Fig. 29.1. Transfer coefficients are listed in Table 29.2. These transfer coefficients are independent of age except that the ICRP's generic age-specific bone turnover rates are assigned to transfers from bone volume compartments to blood.

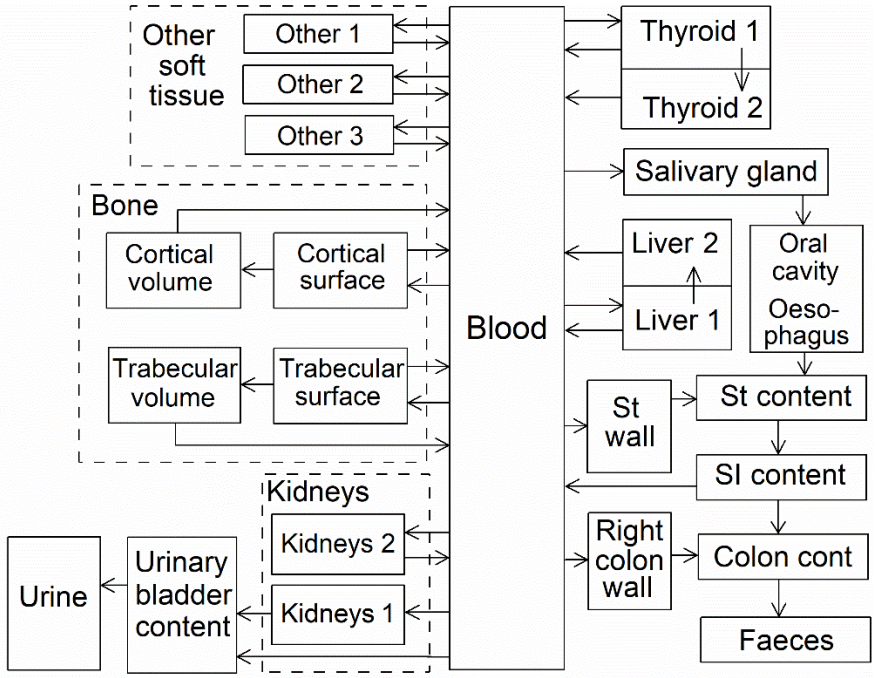

Fig. 29.1. Structure of the biokinetic model for systemic rhenium. St, stomach; SI, stomach wall; cont, content.

Table 29.2. Age-specific transfer coefficients for rhenium.

		Transfer coefficients (d^{-1})					
Pathway		100 d	1 y	5 y	10 y	15 y	Adult
Blood	Thyroid 1	7.00E+00	7.00E+00	7.00E+00	7.00E+00	7.00E+00	7.00E+00
Blood	Other 1	7.19E+01	7.19E+01	7.19E+01	7.19E+01	7.19E+01	7.19E+01
Blood	Other 2	3.00E+00	3.00E+00	3.00E+00	3.00E+00	3.00E+00	3.00E+00
Blood	Other 3	1.80E-01	1.80E-01	1.80E-01	1.80E-01	1.80E-01	1.80E-01
Blood	UB content	1.70E+00	1.70E+00	1.70E+00	1.70E+00	1.70E+00	1.70E+00
Blood	S-glands	2.60E+00	2.60E+00	2.60E+00	2.60E+00	2.60E+00	2.60E+00
Blood	Stomach wall	4.30E+00	4.30E+00	4.30E+00	4.30E+00	4.30E+00	4.30E+00
Blood	Kidneys 1	7.00E-01	7.00E-01	7.00E-01	7.00E-01	7.00E-01	7.00E-01
Blood	Kidneys 2	4.00E-02	4.00E-02	4.00E-02	4.00E-02	4.00E-02	4.00E-02
Blood	Liver 1	4.50E+00	4.50E+00	4.50E+00	4.50E+00	4.50E+00	4.50E+00
Blood	RC wall	3.40E+00	3.40E+00	3.40E+00	3.40E+00	3.40E+00	3.40E+00
Blood	Cort surface	3.50E-01	3.50E-01	3.50E-01	3.50E-01	3.50E-01	3.50E-01
Blood	Trab surface	3.50E-01	3.50E-01	3.50E-01	3.50E-01	3.50E-01	3.50E-01
Thyroid 1	Blood	1.00E+02	1.00E+02	1.00E+02	1.00E+02	1.00E+02	1.00E+02
Thyroid 1	Thyroid 2	1.00E+00	1.00E+00	1.00E+00	1.00E+00	1.00E+00	1.00E+00
Thyroid 2	Blood	1.00E+00	1.00E+00	1.00E+00	1.00E+00	1.00E+00	1.00E+00
Other 1	Blood	5.00E+01	5.00E+01	5.00E+01	5.00E+01	5.00E+01	5.00E+01
Other 2	Blood	4.62E-01	4.62E-01	4.62E-01	4.62E-01	4.62E-01	4.62E-01
Other 3	Blood	3.47E-02	3.47E-02	3.47E-02	3.47E-02	3.47E-02	3.47E-02
S-glands	Oral cavity	5.00E+01	5.00E+01	5.00E+01	5.00E+01	5.00E+01	5.00E+01
Stomach wall	St content	5.00E+01	5.00E+01	5.00E+01	5.00E+01	5.00E+01	5.00E+01
Kidneys 1	UB content	8.32E+00	8.32E+00	8.32E+00	8.32E+00	8.32E+00	8.32E+00
Kidneys 2	Blood	3.47E-02	3.47E-02	3.47E-02	3.47E-02	3.47E-02	3.47E-02
Liver 1	Blood	8.23E+00	8.23E+00	8.23E+00	8.23E+00	8.23E+00	8.23E+00
Liver 1	Liver 2	8.32E-02	8.32E-02	8.32E-02	8.32E-02	8.32E-02	8.32E-02
Liver 2	Blood	3.47E-02	3.47E-02	3.47E-02	3.47E-02	3.47E-02	3.47E-02
RC wall	RC content	1.39E+00	1.39E+00	1.39E+00	1.39E+00	1.39E+00	1.39E+00
Cort surface	Blood	4.57E-01	4.57E-01	4.57E-01	4.57E-01	4.57E-01	4.57E-01
Cort surface	Cort volume	4.62E-03	4.62E-03	4.62E-03	4.62E-03	4.62E-03	4.62E-03
Trab surface	Blood	4.57E-01	4.57E-01	4.57E-01	4.57E-01	4.57E-01	4.57E-01
Trab surface	Trab volume	4.62E-03	4.62E-03	4.62E-03	4.62E-03	4.62E-03	4.62E-03
Cort volume	Blood	8.22E-03	2.88E-03	1.53E-03	9.04E-04	5.21E-04	8.21E-05
Trab volume	Blood	8.22E-03	2.88E-03	1.81E-03	1.32E-03	9.59E-04	4.93E-04

UB, urinary bladder; RC, right colon; Cort, cortical; Trab, trabecular; S-glands, salivary glands.

29.1.3.3. Treatment of radioactive progeny

(316) The treatment of radioactive progeny produced in systemic compartments after intake of a radioisotope of rhenium is described in Section 32.2.3.3. of *Publication 151* (ICRP, 2022).

29.2. Dosimetric data for rhenium

Table 29.3. Committed effective dose coefficients (Sv Bq^{-1}) for the inhalation or ingestion of ^{186}Re compounds.

	Effective dose coefficients (Sv Bq^{-1})					
	3m	1y	5y	10y	15y	Adult
Inhaled particulate materials; (1 μm AMAD aerosols)						
Type F	3.0E-09	2.1E-09	8.8E-10	5.1E-10	3.1E-10	2.4E-10
Type M, default	2.6E-09	1.9E-09	9.9E-10	6.6E-10	4.9E-10	4.4E-10
Type S	2.4E-09	1.8E-09	1.0E-09	6.9E-10	5.3E-10	4.8E-10
Ingested materials						
Rhenium in food	5.6E-09	2.3E-09	1.2E-09	7.2E-10	4.8E-10	3.7E-10
All other forms	5.6E-09	3.7E-09	1.9E-09	1.1E-09	7.3E-10	5.5E-10

AMAD, activity median aerodynamic diameter.

Table 29.4. Committed effective dose coefficients (Sv Bq^{-1}) for the inhalation or ingestion of ^{188}Re compounds.

	Effective dose coefficients (Sv Bq^{-1})					
	3m	1y	5y	10y	15y	Adult
Inhaled particulate materials; (1 μm AMAD aerosols)						
Type F	2.5E-09	1.8E-09	8.1E-10	5.1E-10	3.2E-10	2.4E-10
Type M, default	2.0E-09	1.4E-09	7.0E-10	4.9E-10	3.4E-10	2.8E-10
Type S	1.8E-09	1.3E-09	6.6E-10	4.7E-10	3.3E-10	2.9E-10
Ingested materials						
Rhenium in food	4.9E-09	2.5E-09	1.4E-09	9.2E-10	6.2E-10	4.7E-10
All other forms	4.9E-09	3.6E-09	2.0E-09	1.2E-09	8.4E-10	6.2E-10

AMAD, activity median aerodynamic diameter.

30. OSMIUM (Z=76)

30.1. Routes of Intake

30.1.1. Inhalation

(317) For osmium, default parameter values were adopted on absorption to blood from the respiratory tract (ICRP, 2015). Absorption parameter values and types, and associated f_A values for particulate forms of osmium are given in Table 30.1 [taken from Section 33 of *Publication 151* (ICRP, 2022)].

30.1.2. Ingestion

30.1.2.1. Adults

(318) In *Publications 30*, *72* and *151* (ICRP, 1980, 1995c, 2022), a fractional absorption value of 0.01 was recommended for ingestion of all forms of osmium based on the chemical analogy with iridium. The same value of $f_A = 0.01$ is adopted here for all chemical forms of osmium ingested by adult members of the public.

30.1.2.2. Children

(319) The same values as used in *Publication 158* (ICRP, 2024) for ingestion of iridium by children are adopted for osmium in this publication. So, for ingestion by 3-month-old infants, an $f_A = 0.02$ is used here for all forms of osmium. For older children, the adult value of $f_A = 0.01$ is used.

Table 30.1. Absorption parameter values for inhaled and ingested osmium.

	Absorption parameter values*		
Inhaled particulate materials	f_r	s_r (d^{-1})	s_s (d^{-1})
Default parameter values†			
Absorption type			
F	1	30	–
M‡	0.2	3	0.005
S	0.01	3	1×10^{-4}

Ingested materials§	Age-dependent absorption from the alimentary tract, f_A					
Assigned forms	3 months	1 year	5 years	10 years	15 years	adult
All compounds	0.02	0.01	0.01	0.01	0.01	0.01

*It is assumed that the bound state can be neglected for osmium (i.e. $f_b = 0$). The values of s_r for Type F, M and S forms of osmium (30, 3 and 3 d^{-1} respectively) are the general default values.

†For inhaled material deposited in the respiratory tract and subsequently cleared by particle transport to the alimentary tract, the default f_A values for inhaled materials are applied: i.e. the product of f_r for the absorption type and the f_A value for ingested soluble forms of osmium applicable to the age-group of interest (e.g. 0.01 for adults).

‡Default Type M is recommended for use in the absence of specific information on which the exposure material can be assigned to an absorption type (e.g. if the form is unknown, or if the form is known but there is no information available on the absorption of that form from the respiratory tract).

§Activity transferred from systemic compartments into segments of the alimentary tract is assumed to be subject to reabsorption to blood. The default absorption fraction f_A for the secreted activity is the highest value for any form of the radionuclide applicable to the age-group of interest (e.g. 0.01 for adults).

30.1.3. Systemic distribution, retention and excretion of osmium

30.1.3.1. Biokinetic data

(320) Osmium (Os) is a member of the platinum group, which also includes platinum, iridium, ruthenium, rhodium, and palladium. Results of studies on rodents indicate similar systemic behaviour across the platinum group following administration of relatively soluble forms (Durbin et al., 1957; Durbin, 1960; Moore et al., 1975a, 1975b, 1975c; Weininger et al., 1990; Jamre et al., 2011). Limited comparative data indicate that the systemic kinetics of osmium is particularly close to that of platinum. Relatively high concentrations of the platinum elements are seen in the kidneys and liver at early times after injection (Durbin et al., 1957; Durbin, 1960; Weininger et al., 1990; Jamre et al., 2011). Excretion is mainly in urine.

30.1.3.2. Biokinetics model for systemic osmium

(321) The biokinetic model for systemic osmium applied to workers in *Publication 151* (2022) is applied here to adult members of the public. The same model is applied to preadults except that osmium reaching a bone volume compartment is assumed to be removed to blood at the reference age-specific rate of turnover of that bone type (ICRP, 2002).

(322) The model structure is shown in Fig. 30.1. Transfer coefficients are listed in Table 30.2.

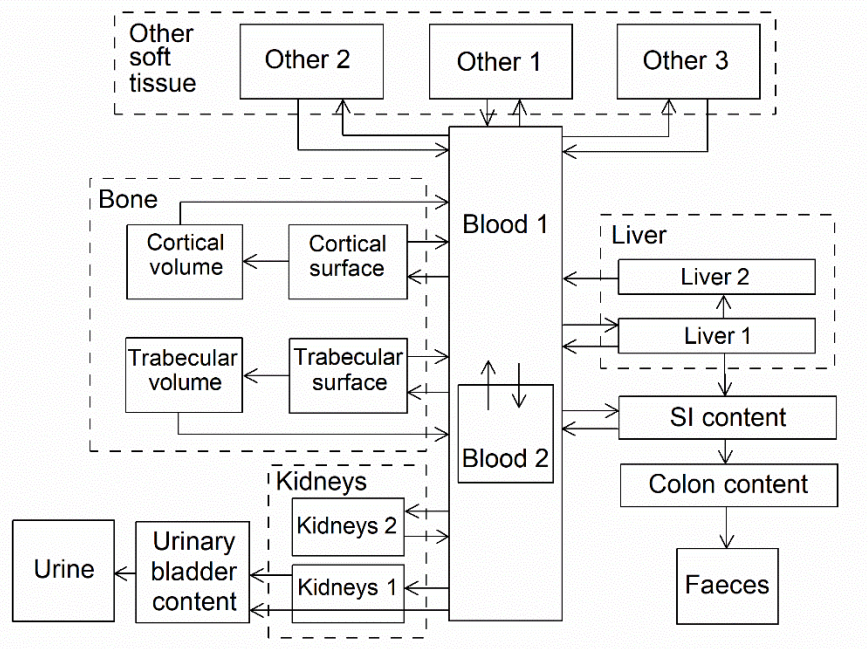

Fig. 30.1. Structure of the biokinetic model for systemic osmium. SI, small intestine.

Table 30.2. Age-specific transfer coefficients for osmium.

		Transfer coefficients (d^{-1})					
Pathway		100 d	1 y	5 y	10 y	15 y	Adult
Blood 1	SI content	3.00E+00	3.00E+00	3.00E+00	3.00E+00	3.00E+00	3.00E+00
Blood 1	UB content	2.30E+01	2.30E+01	2.30E+01	2.30E+01	2.30E+01	2.30E+01
Blood 1	Liver 1	1.20E+01	1.20E+01	1.20E+01	1.20E+01	1.20E+01	1.20E+01
Blood 1	Kidneys 1	1.07E+01	1.07E+01	1.07E+01	1.07E+01	1.07E+01	1.07E+01
Blood 1	Kidneys 2	3.30E-01	3.30E-01	3.30E-01	3.30E-01	3.30E-01	3.30E-01
Blood 1	Blood 2	2.70E+01	2.70E+01	2.70E+01	2.70E+01	2.70E+01	2.70E+01
Blood 1	Other 1	1.50E+01	1.50E+01	1.50E+01	1.50E+01	1.50E+01	1.50E+01
Blood 1	Other 2	2.50E+00	2.50E+00	2.50E+00	2.50E+00	2.50E+00	2.50E+00
Blood 1	Other 3	2.50E+00	2.50E+00	2.50E+00	2.50E+00	2.50E+00	2.50E+00
Blood 1	Cort surface	1.00E+00	1.00E+00	1.00E+00	1.00E+00	1.00E+00	1.00E+00
Blood 1	Trab surface	3.00E+00	3.00E+00	3.00E+00	3.00E+00	3.00E+00	3.00E+00
Blood 2	Blood 1	6.93E-01	6.93E-01	6.93E-01	6.93E-01	6.93E-01	6.93E-01
Liver_1	Blood 1	9.70E-02	9.70E-02	9.70E-02	9.70E-02	9.70E-02	9.70E-02
Liver_1	SI content	3.47E-02	3.47E-02	3.47E-02	3.47E-02	3.47E-02	3.47E-02
Liver_1	Liver_2	6.93E-03	6.93E-03	6.93E-03	6.93E-03	6.93E-03	6.93E-03
Liver_2	Blood 1	3.80E-03	3.80E-03	3.80E-03	3.80E-03	3.80E-03	3.80E-03
Kidneys 1	UB content	1.39E-01	1.39E-01	1.39E-01	1.39E-01	1.39E-01	1.39E-01
Kidneys 2	Blood 1	3.80E-03	3.80E-03	3.80E-03	3.80E-03	3.80E-03	3.80E-03
Other 1	Blood 1	9.90E-02	9.90E-02	9.90E-02	9.90E-02	9.90E-02	9.90E-02
Other 3	Blood 1	2.31E-02	2.31E-02	2.31E-02	2.31E-02	2.31E-02	2.31E-02
Other 2	Blood 1	9.50E-04	9.50E-04	9.50E-04	9.50E-04	9.50E-04	9.50E-04
Cort surface	Blood 1	7.92E-02	7.92E-02	7.92E-02	7.92E-02	7.92E-02	7.92E-02
Trab surface	Blood 1	7.92E-02	7.92E-02	7.92E-02	7.92E-02	7.92E-02	7.92E-02
Cort surface	Cort volume	1.98E-02	1.98E-02	1.98E-02	1.98E-02	1.98E-02	1.98E-02
Trab surface	Trab volume	1.98E-02	1.98E-02	1.98E-02	1.98E-02	1.98E-02	1.98E-02
Cort volume	Blood 1	8.22E-03	2.88E-03	1.53E-03	9.04E-04	5.21E-04	8.21E-05
Trab volume	Blood 1	8.22E-03	2.88E-03	1.81E-03	1.32E-03	9.59E-04	4.93E-04

UB, urinary bladder; SI, small intestine; Cort, cortical; Trab, trabecular.

30.1.3.3. Treatment of radioactive progeny

(323) The treatment of radioactive progeny produced in systemic compartments after intake of a radioisotope of osmium is described in Section 33.2.3.3. of *Publication 151* (ICRP, 2022).

30.2. Dosimetric data for osmium

Table 30.3. Committed effective dose coefficients (Sv Bq^{-1}) for the inhalation or ingestion of ^{194}Os compounds.

	Effective dose coefficients (Sv Bq^{-1})					
	3m	1y	5y	10y	15y	Adult
Inhaled particulate materials; (1 µm AMAD aerosols)						
Type F	1.7E-08	1.5E-08	8.4E-09	5.2E-09	4.2E-09	3.8E-09
Type M, default	6.1E-08	5.7E-08	3.3E-08	2.2E-08	1.8E-08	1.8E-08
Type S	2.8E-07	2.8E-07	1.9E-07	1.4E-07	1.3E-07	1.4E-07
Ingested materials						
All compounds	2.8E-09	1.8E-09	1.1E-09	7.0E-10	4.8E-10	4.6E-10

AMAD, activity median aerodynamic diameter.

31. PLATINUM (Z=78)

31.1. Routes of Intake

31.1.1. Inhalation

(324) For platinum, default parameter values were adopted on absorption to blood from the respiratory tract (ICRP, 2015). Absorption parameter values and types, and associated f_A values for particulate forms of platinum are given in Table 31.1 [taken from Section 34 of *Publication 151* (ICRP, 2022)].

31.1.2. Ingestion

31.1.2.1. Adults

(325) The gastro-intestinal absorption of soluble platinum in human and animal studies appears to be in the order of a percent, see *Publication 151* (ICRP, 2022) for details. In *Publications 30* and *72* (ICRP, 1981, 1995c), a fractional absorption value of 0.01 was recommended for all chemical forms of platinum. The same value was used in *Publication 151* for soluble forms of platinum. For metallic, oxide and hydroxide platinum compounds, *Publication 151* used a lower $f_A = 0.001$. The values of $f_A = 0.01$ for soluble forms of platinum and for platinum in diet, and $f_A = 0.001$ for platinum metal, oxide and hydroxide are adopted here for ingestion by adult members of the public.

31.1.2.2. Children

(326) In a study by Moore et al (1975a), a twice higher retention was observed in suckling rats than in adult rats only for one day after oral administration. For one week thereafter, the fractional retention was similar in suckling and adult rats. Consistently with these data and with the approach of *Publication 56* (ICRP, 1990), an $f_A = 0.02$ is adopted here for ingestion of soluble platinum forms by 3-month-old infants while the value $f_A = 0.01$ is used for older children. The values of $f_A = 0.002$ and $f_A = 0.001$ are used for ingestion of platinum metal, oxide and hydroxide by 3-month-old infants and by older children, respectively.

Table 31.1. Absorption parameter values for inhaled and ingested platinum.

	Absorption parameter values*		
Inhaled particulate materials	f_r	s_r (d^{-1})	s_s (d^{-1})
Default parameter values†			
Absorption type			
F	1	30	–
M‡	0.2	3	0.005
S	0.01	3	1×10^{-4}

Ingested materials§	Age-dependent absorption from the alimentary tract, f_A					
Assigned forms	3 months	1 year	5 years	10 years	15 years	adult
Soluble forms and platinum in diet	0.02	0.01	0.01	0.01	0.01	0.01
Metal, oxide and hydroxide	0.002	0.001	0.001	0.001	0.001	0.001

*It is assumed that the bound state can be neglected for platinum (i.e. $f_b = 0$). The values of s_r for Type F, M and S forms of platinum (30, 3 and 3 d^{-1} respectively) are the general default values.

[†]For inhaled material deposited in the respiratory tract and subsequently cleared by particle transport to the alimentary tract, the default f_A values for inhaled materials are applied: i.e. the product of f_r for the absorption type and the f_A value for ingested soluble forms of platinum applicable to the age-group of interest (e.g. 0.01 for adults).
[‡]Default Type M is recommended for use in the absence of specific information on which the exposure material can be assigned to an absorption type (e.g. if the form is unknown, or if the form is known but there is no information available on the absorption of that form from the respiratory tract).
[§]Activity transferred from systemic compartments into segments of the alimentary tract is assumed to be subject to reabsorption to blood. The default absorption fraction f_A for the secreted activity is the highest value for any form of the radionuclide applicable to the age-group of interest (e.g. 0.01 for adults).

31.1.3. Systemic distribution, retention and excretion of platinum

31.1.3.1. Biokinetic data

(327) The chemically similar elements platinum, iridium, ruthenium, rhodium, palladium, and osmium are found together in nature and are referred to as the platinum group. Biokinetic studies indicate broadly similar systemic behaviour across the platinum group (Durbin et al., 1957; Durbin, 1960; Moore et al., 1975b; Weininger et al., 1990; Jamre et al., 2011). These elements typically show a high urinary excretion rate and high deposition in the kidneys and liver at early times after injection or absorption into blood.

(328) The systemic behaviour of platinum has been studied in laboratory animals and to some extent in human subjects (Durbin et al., 1957; Durbin, 1960; Lange et al., 1973; Smith and Taylor, 1974; Litterst et al., 1976; Yoakum et al., 1975; Moore et al., 1975a,b,c; Hirunuma et al., 1997). Following intravenous administration of radio-platinum to rats, highest concentrations generally were found in the kidneys, followed by the liver (Durbin et al., 1957; Moore et al., 1975a,b,c). At 1 mo the rats contained roughly 10-15% of the intravenously injected activity (corrected for decay).

(329) The biokinetics of platinum has been studied in human subjects following administration of the antitumor agent cis-$Pt(NH_3)_2Cl_2$ labeled with ^{195m}Pt (Lange et al., 1973; Smith and Taylor, 1974). The systemic behaviour of the platinum label resembled that of other forms of platinum administered to laboratory animals. In the study by Smith and Taylor (1974), about 35% of the injected activity was excreted in urine during the first 3.5 d. Fecal excretion of the label was estimated as <10% over 4 d. A high rate of urinary excretion also was seen in the study by Lange et al. (1973). The liver accumulated an estimated 10% of the injected activity during the first day. The estimated biological half-times of the label in the liver and total body during days 1-7 were 8 d and 10 d, respectively.

31.1.3.2. Biokinetic model for systemic platinum

(330) The biokinetic model for systemic platinum applied to workers in *Publication 151* (ICRP, 2022) is applied here to adult members of the public. The same model is applied to preadult ages except that platinum reaching a bone volume compartment is assumed to be removed to blood at the reference age-specific rate of turnover of that bone type (ICRP, 2002).

(331) The model structure is shown in Fig. 31.1. Transfer coefficients are listed in Table 31.2.

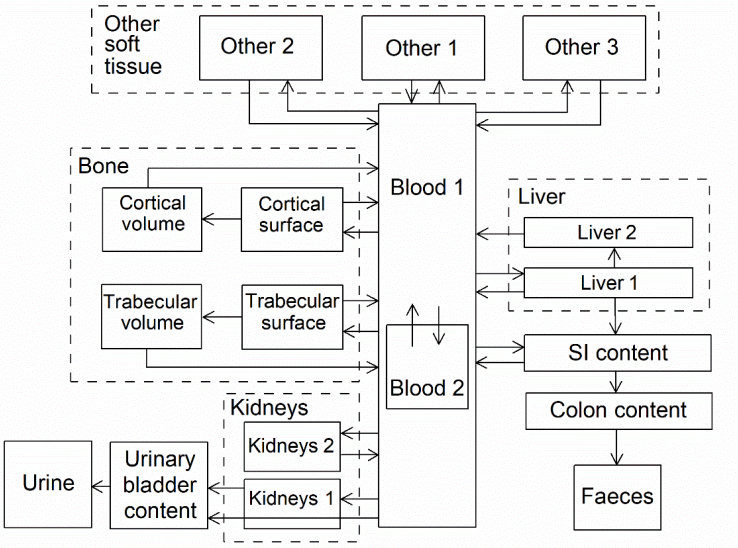

Fig. 31.1. Structure of the biokinetic model for systemic platinum. SI, small intestine.

Table 31.2. Age-specific transfer coefficients for platinum.

		Transfer coefficients (d^{-1})					
Pathway		100 d	1 y	5 y	10 y	15 y	Adult
Blood 1	SI content	3.00E+00	3.00E+00	3.00E+00	3.00E+00	3.00E+00	3.00E+00
Blood 1	UB content	2.30E+01	2.30E+01	2.30E+01	2.30E+01	2.30E+01	2.30E+01
Blood 1	Liver 1	1.20E+01	1.20E+01	1.20E+01	1.20E+01	1.20E+01	1.20E+01
Blood 1	Kidneys 1	1.07E+01	1.07E+01	1.07E+01	1.07E+01	1.07E+01	1.07E+01
Blood 1	Kidneys 2	3.30E-01	3.30E-01	3.30E-01	3.30E-01	3.30E-01	3.30E-01
Blood 1	Blood 2	2.70E+01	2.70E+01	2.70E+01	2.70E+01	2.70E+01	2.70E+01
Blood 1	Other 1	1.50E+01	1.50E+01	1.50E+01	1.50E+01	1.50E+01	1.50E+01
Blood 1	Other 2	2.50E+00	2.50E+00	2.50E+00	2.50E+00	2.50E+00	2.50E+00
Blood 1	Other 3	2.50E+00	2.50E+00	2.50E+00	2.50E+00	2.50E+00	2.50E+00
Blood 1	Cort surface	1.00E+00	1.00E+00	1.00E+00	1.00E+00	1.00E+00	1.00E+00
Blood 1	Trab surface	3.00E+00	3.00E+00	3.00E+00	3.00E+00	3.00E+00	3.00E+00
Blood 2	Blood 1	6.93E-01	6.93E-01	6.93E-01	6.93E-01	6.93E-01	6.93E-01
Liver 1	Blood 1	9.70E-02	9.70E-02	9.70E-02	9.70E-02	9.70E-02	9.70E-02
Liver 1	SI content	3.47E-02	3.47E-02	3.47E-02	3.47E-02	3.47E-02	3.47E-02
Liver 1	Liver 2	6.93E-03	6.93E-03	6.93E-03	6.93E-03	6.93E-03	6.93E-03
Liver 2	Blood 1	3.80E-03	3.80E-03	3.80E-03	3.80E-03	3.80E-03	3.80E-03
Kidneys 1	UB content	1.39E-01	1.39E-01	1.39E-01	1.39E-01	1.39E-01	1.39E-01
Kidneys 2	Blood 1	3.80E-03	3.80E-03	3.80E-03	3.80E-03	3.80E-03	3.80E-03
Other 1	Blood 1	9.90E-02	9.90E-02	9.90E-02	9.90E-02	9.90E-02	9.90E-02
Other 2	Blood 1	2.31E-02	2.31E-02	2.31E-02	2.31E-02	2.31E-02	2.31E-02
Other 3	Blood 1	9.50E-04	9.50E-04	9.50E-04	9.50E-04	9.50E-04	9.50E-04
Cort surface	Blood 1	7.92E-02	7.92E-02	7.92E-02	7.92E-02	7.92E-02	7.92E-02
Trab surface	Blood 1	7.92E-02	7.92E-02	7.92E-02	7.92E-02	7.92E-02	7.92E-02
Cort surface	Cort volume	1.98E-02	1.98E-02	1.98E-02	1.98E-02	1.98E-02	1.98E-02
Trab surface	Trab volume	1.98E-02	1.98E-02	1.98E-02	1.98E-02	1.98E-02	1.98E-02
Cort volume	Blood 1	8.22E-03	2.88E-03	1.53E-03	9.04E-04	5.21E-04	8.21E-05
Trab volume	Blood 1	8.22E-03	2.88E-03	1.81E-03	1.32E-03	9.59E-04	4.93E-04

UB, urinary bladder; SI, small intestine; Cort, cortical; Trab, trabecular.

31.1.3.3. Treatment of radioactive progeny

(332) The treatment of radioactive progeny produced in systemic compartments after intake of a radioisotope of platinum is described in Section 34.2.3.3. of *Publication 151* (ICRP, 2022).

31.2. Dosimetric data for platinum

Table 31.3. Committed effective dose coefficients (Sv Bq^{-1}) for the inhalation or ingestion of ^{193}Pt compounds.

	Effective dose coefficients (Sv Bq^{-1})					
	3m	1y	5y	10y	15y	Adult
Inhaled particulate materials (1 μm AMAD aerosols)						
Type F	2.2E-10	1.8E-10	9.7E-11	5.9E-11	4.1E-11	4.0E-11
Type M, default	5.8E-10	5.1E-10	2.7E-10	1.7E-10	1.2E-10	1.1E-10
Type S	3.8E-09	3.8E-09	2.7E-09	2.0E-09	2.0E-09	2.0E-09
Ingested materials						
Soluble forms and platinum in diet	3.8E-11	2.3E-11	1.2E-11	8.1E-12	4.8E-12	3.5E-12
Metal, oxide and hydroxide	2.0E-11	1.6E-11	7.7E-12	5.5E-12	3.0E-12	1.8E-12

AMAD, activity median aerodynamic diameter.

32. GOLD (Z=79)

32.1. Routes of Intake

32.1.1. Inhalation

(333) Information is available from experimental studies on the behaviour of gold nanoparticles (particles with at least one dimension < 100 nm) and gold-labelled insoluble particles after deposition in the respiratory tract. For details see Section 35 of *Publication 151,* ICRP 2022. Absorption parameter values and types, and associated f_A values for particulate forms of gold are given in Table 32.1 [taken from Section 35 of *Publication 151* (ICRP, 2022)].

Table 32.1. Absorption parameter values for inhaled and ingested gold.

		Absorption parameter values*		
Inhaled particulate materials		f_r	s_r (d^{-1})	s_s (d^{-1})
Default parameter values†,‡				
Absorption type	Assigned forms			
F	–	1	30	–
M§	–	0.2	3	0.005
S	Elemental gold, gold-labelled Teflon	0.01	3	1×10^{-4}

Ingested materials¶

	Age-dependent absorption from the alimentary tract, f_A					
Assigned forms	3 months	1 year	5 years	10 years	15 years	adult
Gold in diet	0.4	0.2	0.2	0.2	0.2	0.2
All other forms	0.2	0.1	0.1	0.1	0.1	0.1

*It is assumed that the bound state can be neglected for gold (i.e. f_b=0). The values of s_r for Type F, M, and S forms of gold (30, 3, and 3 d^{-1}, respectively) are the general default values.
†Materials (e.g. elemental gold) are listed here where there is sufficient information to assign to a default absorption type, but not to give specific parameter values [see Section 35 of *Publication 151* (ICRP 2022)].
‡For inhaled material deposited in the respiratory tract and subsequently cleared by particle transport to the alimentary tract, the default f_A values for inhaled materials are applied: i.e. the product of f_r for the absorption type and the f_A value for ingested soluble forms of gold applicable to the age-group of interest (e.g. 0.1 for adults).
§Default Type M is recommended for use in the absence of specific information on which the exposure material can be assigned to an absorption type; for example, if the form is unknown, or if the form is known but there is no information available on the absorption of that form from the respiratory tract.
¶Activity transferred from systemic compartments into segments of the alimentary tract is assumed to be subject to reabsorption to blood. The default absorption fraction f_A for the secreted activity is the highest value for any form of the radionuclide applicable to the age-group of interest (e.g. 0.2 for adults).

32.1.2. Ingestion

32.1.2.1. Adults

(334) Based on human and animal studies, the value of $f_A = 0.1$ was used for all chemical forms of gold in *Publications 72* (ICRP, 1995c) and *151* (ICRP, 2022). In *Publication 100* (ICRP, 2006, Table D.23) a value of 0.4 was considered for organic compounds. Since the available studies indicate significant variability of gastro-intestinal absorption, an intermediate value of $f_A = 0.2$ is adopted here for gold in diet and the value of $f_A = 0.1$ is used for all other forms of gold ingested by adult members of the public.

32.1.2.2. Children

(335) Applying the approach of *Publication 56* (ICRP, 1990), $f_A = 0.4$ is used for ingestion of dietary gold by infants and $f_A = 0.2$ is used for ingestion of other forms of gold by infants. The adult values are used for older children: $f_A = 0.2$ for ingestion of dietary gold and $f_A = 0.1$ for ingestion of all other chemical forms.

32.1.3. Systemic distribution, retention and excretion of gold

32.1.3.1. Biokinetic data

(336) The biokinetics of gold has been investigated in human subjects and laboratory animals in studies related to its medical applications, particularly the use of stable gold for treating rheumatoid arthritis and short-lived radioactive gold as an imaging agent (Freyberg, et al., 1942; Block, et al., 1942, 1944; Jeffrey et al., 1958; Lawrence, 1961; Rubin et al., 1967; McQueen and Dykes, 1969; Mascarenhas et al., 1972; Sugawa-Katayama et al., 1975; Gottlieb, 1983; Jellum et al., 1980; Massarella and Pearlman, 1987; Andersson et al., 1988; Bacso et al., 1988; Brihaye and Guillaume, 1990). Other studies have addressed the biological behaviour of gold as a radioactive contaminant in the workplace or environment (Durbin, 1960; Fleshman et al., 1966; Chertok and Lake, 1971a, 1971b, 1971c; Silva et al., 1973).

(337) Development of a representative biokinetic model for systemic gold in the human body is complicated by the strong dependence in the distribution and residence times on several factors including mode of administration, chemical form, and administered mass.

(338) For gold administered in low mass and relatively soluble form, it appears that much of the absorbed or injected amount is excreted in the first week or two, but a nontrivial portion may be retained up to several months or possibly years. Excretion is primarily in urine. Much of the retained amount generally is found in the blood, liver, and kidneys. Most of the gold found in blood is bound to plasma proteins.

32.1.3.2. Biokinetic model for systemic gold

(339) The biokinetic model for systemic gold applied in *Publication 30*, Part 2 (ICRP, 1980) and *Publication* 68 (ICRP, 1994) depicts a uniform distribution of absorbed gold (other than an elevated concentration in the urinary bladder content) and a biological half-time of 3 d. *Publication 151* (ICRP, 2022) introduced a more conservative biokinetic model for gold in view of the widely varying systemic distributions and retention times for gold reported in the literature. The biokinetic model for gold applied to workers in *Publication 151* (ICRP, 2022) depicts a nonuniform distribution of absorbed gold with relatively high concentrations in blood, liver, and kidneys, and a relatively long retention time compared with the previous ICRP model. For example, for the relatively long-lived isotope ^{195}Au ($T_{1/2}$ = 186.1 d), the model of *Publication 151* predicts a total-body content of about 24% of administered activity 30 d after injection to blood, with about one-third of the retained amount in blood, liver, and kidneys.

(340) The biokinetic model for systemic gold applied to workers in *Publication 151* (ICRP, 2022) is applied in this report intake at any age. The structure of the biokinetic model for systemic gold used in this report is shown in Fig. 32.1. Transfer coefficients are listed in Table 32.2.

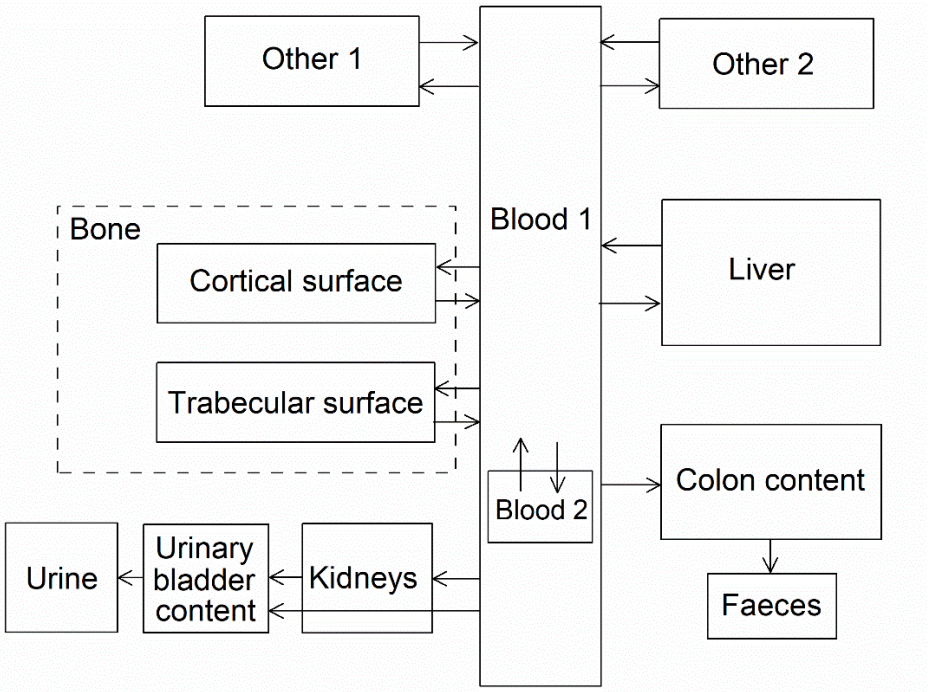

Fig. 32.1. Structure of the biokinetic model for systemic gold.

Table 32.2. Age-specific transfer coefficients for gold.

		Transfer coefficients (d^{-1})					
Pathway		100 d	1 y	5 y	10 y	15 y	Adult
Blood 1	Blood 2	1.00E-01	1.00E-01	1.00E-01	1.00E-01	1.00E-01	1.00E-01
Blood 1	Kidneys	1.00E-01	1.00E-01	1.00E-01	1.00E-01	1.00E-01	1.00E-01
Blood 1	Liver	1.00E-01	1.00E-01	1.00E-01	1.00E-01	1.00E-01	1.00E-01
Blood 1	Other 1	1.80E-01	1.80E-01	1.80E-01	1.80E-01	1.80E-01	1.80E-01
Blood 1	Other 2	1.00E-01	1.00E-01	1.00E-01	1.00E-01	1.00E-01	1.00E-01
Blood 1	UB content	3.00E-01	3.00E-01	3.00E-01	3.00E-01	3.00E-01	3.00E-01
Blood 1	RC content	1.00E-01	1.00E-01	1.00E-01	1.00E-01	1.00E-01	1.00E-01
Blood 1	Trab surface	1.00E-02	1.00E-02	1.00E-02	1.00E-02	1.00E-02	1.00E-02
Blood 1	Cort surface	1.00E-02	1.00E-02	1.00E-02	1.00E-02	1.00E-02	1.00E-02
Blood 2	Blood 1	1.39E-01	1.39E-01	1.39E-01	1.39E-01	1.39E-01	1.39E-01
Kidneys	UB content	6.93E-02	6.93E-02	6.93E-02	6.93E-02	6.93E-02	6.93E-02
Liver	Blood 1	6.93E-02	6.93E-02	6.93E-02	6.93E-02	6.93E-02	6.93E-02
Other 1	Blood 1	6.93E-02	6.93E-02	6.93E-02	6.93E-02	6.93E-02	6.93E-02
Other 2	Blood 1	1.39E-02	1.39E-02	1.39E-02	1.39E-02	1.39E-02	1.39E-02
Trab surface	Blood 1	6.93E-02	6.93E-02	6.93E-02	6.93E-02	6.93E-02	6.93E-02
Cort surface	Blood 1	6.93E-02	6.93E-02	6.93E-02	6.93E-02	6.93E-02	6.93E-02

UB, urinary bladder; SI, small intestine; Cort, cortical; Trab, trabecular.

32.1.3.3. Treatment of radioactive progeny

(341) The treatment of radioactive progeny produced in systemic compartments after intake of a radioisotope of gold is described in Section 35.2.3.3. of *Publication 151* (ICRP, 2022).

32.2. Dosimetric data for gold

Table 32.3. Committed effective dose coefficients (Sv Bq^{-1}) for the inhalation or ingestion of ^{195}Au compounds.

	Effective dose coefficients (Sv Bq^{-1})					
	3m	1y	5y	10y	15y	Adult
Inhaled particulate materials (1 µm AMAD aerosols)						
Type F	1.2E-09	7.8E-10	3.8E-10	2.4E-10	1.6E-10	1.5E-10
Type M, default	3.4E-09	2.8E-09	1.6E-09	1.0E-09	7.5E-10	7.4E-10
Type S, elemental gold, gold-labelled Teflon	6.4E-09	5.7E-09	3.2E-09	2.1E-09	1.5E-09	1.5E-09
Ingested materials						
Gold in diet	1.8E-09	7.3E-10	3.9E-10	2.6E-10	1.7E-10	1.5E-10
All other forms	9.8E-10	4.6E-10	2.5E-10	1.6E-10	1.1E-10	1.0E-10

AMAD, activity median aerodynamic diameter.

33. MERCURY (Z=80)

33.1. Routes of Intake

33.1.1. Inhalation

(342) Comprehensive information on the behaviour of inhaled mercury vapour is available from both volunteer experiments and animal studies. Some information is also available from experimental studies of volatile organic compounds and particulate forms. Several studies have been reported following accidental intakes of mercury radioisotopes. For details see Section 36 of *Publication 151* (ICRP, 2022). Absorption parameter values and Types, and associated f_A values for gas and vapour forms of mercury are given in Table 33.1 and for particulate forms in Table 33.2 [both taken from Section 36 of *Publication 151* (ICRP, 2022)].

(343) Exposures to both gas/vapour and particulate forms of mercury have occurred, and it is therefore recommended in this series of documents that 50% particulate and 50% gas/vapour should be assumed in the absence of information (ICRP, 2002a).

Table 33.1. Deposition and absorption for gas and vapour compounds of mercury.

	Percentage deposited (%)*						Absorption†		
Chemical form/origin	Total	ET_1	ET_2	BB	Bb	AI	f_r	s_r (d^{-1})	s_s (d^{-1})
Mercury Vapour	80	0	2	1	2	75	0.94	1000	0.14

	Age-dependent absorption from the alimentary tract, f_A‡					
Chemical form/origin	3 months	1 year	5 years	10 years	15 years	Adult
Mercury Vapour	0.47	0.094	0.094	0.094	0.094	0.094

ET_1, anterior nasal passage; ET_2, posterior nasal passage, pharynx and larynx; BB, bronchial; bb, bronchiolar; AI, alveolar-interstitial.

*Percentage deposited refers to how much of the material in the inhaled air remains in the body after exhalation. Almost all inhaled gas molecules contact airway surfaces but usually return to the air unless they dissolve in, or react with, the surface lining. The distribution between regions is material specific: 2% ET_2, 1% BB, 2% bb, and 75% AI.

†For mercury, it is assumed that a bound fraction $f_b = 0.24$ with an uptake rate $s_b = 2.1\ d^{-1}$ is applied throughout the respiratory tract except in the ET_1 region.

‡For inhaled material deposited in the respiratory tract and subsequently cleared by particle transport to the alimentary tract, the default f_A values for inhaled materials are applied: i.e. the product of f_r for the absorption type (or specific value where given) and the f_A value for ingested soluble forms of mercury (e.g. 0.1 for adults and 0.5 for infants).

Table 33.2. Absorption parameter values for inhaled and ingested mercury.

Inhaled particulate materials		Absorption parameter values* f_r	s_r (d^{-1})	s_s (d^{-1})
Default parameter values†,‡				
Absorption type	Assigned forms			
F	–	1	30	–
M§	Mercuric oxide	0.2	3	0.005
S	–	0.01	3	1×10^{-4}

Ingested materials¶	Age-dependent absorption from the alimentary tract, f_A					
Assigned forms	3 months	1 year	5 years	10 years	15 years	adult
All inorganic forms	0.5	0.1	0.1	0.1	0.1	0.1
Methyl mercury	1	1	1	1	1	1
Other organic forms and mercury in diet	0.8	0.4	0.4	0.4	0.4	0.4

*For mercury, it is assumed that a bound fraction $f_b = 0.24$ with an uptake rate $s_b = 2.1$ d^{-1} is applied throughout the respiratory tract except in the ET_1 region. The values of s_r for Type F, M and S forms of mercury (30, 3 and 3 d^{-1} respectively) are the general default values.

†Materials (e.g. mercuric oxide) are generally listed here where there is sufficient information to assign to a default absorption type, but not to give specific parameter values [see Section 36 of *Publication 151* (ICRP, 2022)].

‡For inhaled material deposited in the respiratory tract and subsequently cleared by particle transport to the alimentary tract, the default f_A values for inhaled materials are applied: i.e. the product of f_r for the absorption type (or specific value where given) and the f_A value for ingested soluble forms of mercury applicable to the age-group of interest (e.g. 0.1 for adults).

§Default Type M is recommended for use in the absence of specific information on which the exposure material can be assigned to an absorption type (e.g. if the form is unknown, or if the form is known but there is no information available on the absorption of that form from the respiratory tract).

¶Activity transferred from systemic compartments into segments of the alimentary tract is assumed to be subject to reabsorption to blood. The default absorption fraction f_A for the secreted activity is the highest value for any form of the radionuclide applicable to the age-group of interest (1).

33.1.2. Ingestion

33.1.2.1. Adults

(344) Conversion to methyl mercury by marine organism is an important step of the population exposure to mercury (Nelson et al., 1971). Human and animal studies indicate that elemental mercury is virtually unabsorbed; inorganic salts exhibit absorption in the order of 8–15%, and the absorption of methyl mercury from the gastrointestinal tract appears to be almost complete in humans and animals (Cooper, 1985; Nordberg and Sherfving, 1972; Kojima and Fujita, 1973, ATSDR, 1999; EFSA, 2012). The fractional absorption of mercuric acetate is about 0.2 and that of phenyl mercury salts is typically 0.4 or higher. Methyl mercury shows some absorption from the stomach (Sasser et al., 1978).

(345) In *Publication 151* (ICRP, 2022), a value of $f_A = 0.1$ was used for all forms of mercury ingested at the workplace. In *Publication 72* (ICRP, 1995c), fractional absorptions of 0.02, 1 and 0.4 were used respectively for ingestion of inorganic forms of mercury, methyl mercury and other organic forms of mercury. In this publication, f_A values of 0.1, 1 and 0.4 are adopted respectively for ingestion of inorganic forms of mercury, methyl mercury and other organic forms of mercury by adult members of the public.

33.1.2.2. Children

(346) In one-week suckling mice, the fractional absorption of mercuric chloride was increased to 38%, compared with 1% in adults (7% for adult mice fed milk diet; Kostial et al., 1978). The 1-h duodenal absorption of mercuric chloride was also significantly greater in 6-d-old neonatal rats (18.1%) as compared to 23-d weanling (7.3%) or mature animals (3.6%; Walsh, 1982). These data indicate an increase of gastrointestinal absorption of inorganic mercury in the order of a factor of five at youngest ages. Consistently, f_A values of 0.5, 1 and 0.8 are adopted here respectively for ingestion of inorganic forms of mercury, methyl mercury and other organic forms of mercury by infants. For older children, the adult values of f_A = 0.1, 1 and 0.4 respectively are adopted.

33.1.3. Systemic distribution, retention and excretion of mercury

33.1.3.1. Biokinetic data

(347) This section summarizes data on the systemic behaviour of three environmentally important forms of mercury and describes the models applied to these forms in this report: divalent inorganic mercury (Hg^{2+}), mercury vapor (Hg^0 vapor), and methyl mercury (CH_3Hg^+, also written as $MeHg^+$). These forms initially exhibit distinct kinetics in the body, but Hg^0 (always used below to refer to mercury vapor) and $MeHg^+$ are both converted to Hg^{2+} in the body. The conversion occurs quickly for Hg^0 but over a period of several weeks for $MeHg^+$. The biokinetic models for Hg^0 and $MeHg^+$ depict their initial distributions in systemic repositories and their subsequent movement into compartments of the systemic model for Hg^{2+}, after which the behaviour of Hg is governed by the biokinetic model for systemic Hg^{2+}.

(a) Data for mercury vapor and divalent inorganic mercury

(348) Data on the systemic kinetics of Hg^0 and Hg^{2+} are discussed together because their systemic behaviours are often investigated in the same studies, as Hg^0 taken up by RBC or tissues is soon oxidized to Hg^{2+}.

(349) Blood clearance of Hg has been investigated in controlled studies of human subjects who inhaled Hg^0 for a brief period (Hursh et al., 1976, 1980; Cherian et al., 1978; Sandborgh-Englund et al., 1998; Jonsson et al., 1999) and in studies of workers after their removal from chronic exposure to Hg^0 (Barregård et al., 1992; Sallsten et al., 1993). A substantial portion of inhaled Hg^0 moves rapidly into blood, and a smaller portion is oxidized to Hg^{2+}in the lungs, followed by slower absorption to blood. Hg^0 that enters blood is rapidly taken up by red blood cells (RBC) or tissues, or exhaled (Teisinger and Fiserova-Bergerova, 1965; Magos et al., 1989). The portion entering RBC and tissues is soon oxidized to Hg^{2+}.

(350) Data for human subjects acutely exposed to Hg^0 under controlled conditions and data for workers just removed from exposure to Hg^0 indicate an initial removal half-time of Hg^{2+} from blood of about 3 d. A relatively long-term component of blood retention (half-time, 18-45 d) has been observed in workers removed from chronic exposure to Hg. Studies of animals administered Hg^{2+} salts indicate an initially rapid (minutes to hours) disappearance of mercury from blood and longer retention of a substantial portion of the amount entering blood (Rothstein and Hayes, 1960; Clarkson and Rothstein, 1964).

(351) The kidneys have a high affinity for mercury. In laboratory animals exposed briefly to Hg^0 via inhalation, the kidneys gradually accumulated as much as 25-35% of the initial body burden over a period of days. The kidneys initially took up only a few percent of inhaled Hg^0 but continued to accumulate Hg^{2+} that was absorbed more slowly from the lungs to blood or returned from relatively short-term systemic repositories to blood. External measurements on

human subjects acutely exposed to Hg^0 or Hg^{2+} compounds also show considerable accumulation of mercury in the kidneys (Hursh et al., 1976, 1980; Newton and Fry, 1978). Autopsy data from studies of persons environmentally or occupationally exposed to mercury showed a much higher concentration of Hg in the kidneys than in the rest of the body (Barregard et al., 1999; Zhu et al., 2010).

(352) External measurements on human subjects following brief inhalation of Hg^0 indicate a mean biological half-time of 52 d (range, 35-90 d) for mercury in the kidneys (Hursh et al. 1976, 1980). External measurements on subjects accidentally exposed to aerosols of mercury indicate a mean half-time of 49 d (range, 37-60 d) (Newton and Fry, 1978).

(353) In laboratory animals exposed briefly to Hg^0 in air, the liver typically accumulated 3-6% (range, 2-18%) of the initial body burden shortly after intake. The collective data suggest a slight rise in the liver content over the first few days after inhalation of Hg^0. Higher initial uptake by the liver was seen after intravenous injection with Hg^{2+} than after inhalation of Hg^0 (Hayes and Rothstein, 1962; Magos et al., 1989). Mercury was generally removed from the liver with a half-time of a few days.

(354) Hg^0 carried in plasma to the brain readily crosses the blood-brain barrier. Hg^0 that enters the brain is converted to Hg^{2+}, which moves slowly across the blood-brain barrier to blood. After acute inhalation of Hg^0 by squirrel monkeys, rats, mice, rabbits, and guinea pigs, the peak mercury content in the brain typically was 1-2% of the initial body burden, which is considerably higher than uptake of circulating Hg^{2+} (Berlin et al., 1966, 1969). The subsequent pattern of uptake and retention by brain is broadly consistent across species, despite the large variation in brain size as a fraction of total-body weight. Data for laboratory animals indicate a biological half-time on the order of 10 d for the preponderance of Hg^{2+} deposited in the brain. External measurements over the head in human subjects suggest half-times in the range 14-29 d (Hursh et al., 1976, 1980; Newton and Fry, 1978). Long-term retention of a small portion of mercury entering the brain could not be dismissed in human or laboratory animal studies.

(355) More than half of Hg^0 or Hg^{2+} entering blood is deposited in massive soft tissues such as muscle, skin, and fat. The mercury that accumulates in these tissues declines over days or weeks as it redistributes largely to the kidneys and to a lesser extent to the liver. After inhalation of Hg^0 by rats for a period of 5 h, the kidneys and liver accounted for about 20% of retained mercury at the end of exposure, 40% after 1 d, 50% after 5 d, and 67% after 15 d (Hayes and Rothstein, 1962). In rats injected with Hg^{2+}, kidneys and liver accounted for about 10% of the systemic burden after 4 h, 40% after 1 d, 70% after 6 d, 88% after 15 d, and 91% after 52 d (Rothstein and Hayes, 1960). External measurements on human subjects exposed to Hg^{2+} also indicate that much of the mercury deposited in soft tissues other than kidneys is removed over a few weeks.

(356) Urinary mercury appears to originate predominantly from Hg^{2+} stored in the kidneys (Barregård, 1993; Clarkson, 1997). In human subjects, the peak concentration of mercury in urine occurs 2-3 weeks after short-term inhalation of Hg^0 (Barregård, 1993), in parallel with the peak kidney content. Following inhalation of Hg^0, more than half of absorbed Hg^{2+} is removed from the body in urine. Initially, the rate of faecal excretion is much higher than that of urinary excretion, but this relation reverses over a few weeks. At times remote from exposure, daily urinary losses are considerably larger than faecal losses (Hursh et al., 1976, 1980; Newton and Fry, 1978; Jonsson et al., 1999). Analysis of excretion data for human subjects who inhaled Hg^0 for a short period (Jonsson et al., 1999) indicate that cumulative faecal excretion represented roughly 25-30% of the initial body burden. Results of animal studies indicate that faecal excretion of mercury may arise from a combination of biliary secretion and other secretions across the intestinal wall that are most prominent in the small intestine (Gregus and Klaassen, 1986; Zalups, 1998).

(357) In addition to losses in urine and faeces, mercury is removed from the systemic fluids and tissues by exhalation of Hg^0, and small amounts are lost through sweat, hair, and other routes. Exhalation of Hg^0 occurs over a period of at least several days, either after administration of mercuric salts or inhalation of Hg^0 (Clarkson and Rothstein, 1964; Hursh et al., 1976; Cheria et al., 1978; Berlin, 1986; Jonsson et al., 1999). Hursh et al. (1976) estimated that approximately 7% of the initial body burden was exhaled in expired air over the first few days after acute inhalation of Hg^0 by human subjects. The rate of exhalation of mercury was highest soon after intake and declined with a half-time of 1-2 d.

(358) Rahola et al. (1972) administered Hg^{2+} orally to 10 healthy adult humans (5 males and 5 females). Two subjects were given $^{203}Hg(NO_3)_2$ in water, and the other eight subjects were given ^{203}Hg bound to calf-liver paste. On average about 15% of the administered activity was absorbed to blood. The mean biological half-life of the absorbed mercury as measured from about 10-15 d to about 70 d post intake was 42 ± 3 (SD) d. Estimated mean half-lives in females and males were 37 ± 3 d and 48 ± 5 d, respectively. Little activity was retained in blood beyond the first day after intake. During the first 50 d the ratio of the tracer in RBC to that in plasma was about 0.4.

(b) Data for methyl mercury

(359) Aberg et al. (1969) studied the distribution and excretion of ^{203}Hg following its oral administration as $CH_3{}^{203}HgNO_3$ to three healthy males, ages 37-44 y. Urine and faeces were collected up to 10 d from Subject A, 49 d from Subjects B and C, and occasionally from Subject B from 50-71 d post administration. Blood samples were collected occasionally from all three subjects in the first two days. Hair samples were collected from Subjects B and C at regular haircuts. External measurements of activity in the total body and selected regions of the body were performed on all subjects up to ~ 8 mo. The concentration of activity in RBC was roughly 10 times that in blood plasma from 15 min to 24 d post administration. The blood content peaked at 3-6 h. Excretion was primarily via faeces and represented 13.0, 13.6, and 14.2% of the administered tracer (adjusted for radioactive decay) through 10 d for the 3 subjects and 33.4 and 34.7% through 49 d for Subjects B and C, respectively. An estimated average of 6% of the ingested activity was not absorbed to blood or soon secreted back into the intestines. Loss in urine represented <0.3% of the administered amount through 10 d for the 3 subjects and about 3.3% through 49 d for each of the subjects B and C. A maximum concentration in hair of 0.12% per g hair was found 40-50 d post ingestion. The liver accumulated roughly half and the head (including hair) roughly a tenth of the administered amount. Activity was lost more slowly from the head than other body regions. Total-body retention after the first few days was closely fit by a single exponential term for each subject. The indicated biological half-times for the 3 subjects were 70.4, 73.7 d, and 74.2 d. The authors pointed out that the observed half-times were consistent with values estimated in studies involving fish-eating subjects who changed to diets without fish.

(360) Miettinen et al. (1971) studied the kinetics of ^{203}Hg-labeled $MeHg^+$ in 15 healthy adults (9 males and 6 females, ages 27-48 y) over ~8 mo after a single ingestion in fish. During the first week after intake, daily faecal and urinary excretion averaged about 1.9% and 0.01%, respectively, of the ingested activity. Activity in blood represented about 9-10% of the ingested amount in the early days after intake, with ~90% of the blood content in RBC. The biological half-time of ^{203}Hg in RBC averaged ~50 d in 5 men and 1 woman. Mean total-body half-times were 71 d (range, 52-88 d) for females and 79 d (range, 70-93 d) for males.

(361) Smith et al. (1994) studied the biokinetics of $MeHg^+$ separately from that of its metabolite, Hg^{2+}, over a period of 70 d after intravenous administration of ^{203}Hg-labeled $MeHg^+$ to 7 healthy young adult males. Activity was measured in urine, faeces, and blood in

$MeHg^+$ separated chemically from Hg^{2+}. Total-body retention of ^{203}Hg representing both Hg^{2+} and $MeHg^+$ was measured externally. The mean biological half-time of activity in blood was ~45 d. The mean biological half-time of $MeHg^+$ in the total body was estimated as 44 d. Over the 70-d study ~31% of the injected activity was excreted in faeces, and ~4% was excreted in urine. The authors concluded that "whole-body $MeHg^+$ behaves as a single kinetic compartment."

(362) Smith and Farris (1996) examined implications of data of Aberg et al. (1969) and Miettinen et al. (1971) summarized above, considering both a one-compartment and a two-compartment model of retention and excretion pathways of $MeHg^+$ and its metabolite, Hg^{2+}. They concluded that a two-compartment model yielded the better fit to the data, particularly the rising daily percentage of mercury in urine over time. Using the two-compartment model, they estimated the biological half-time of whole-body $MeHg^+$ alone as 51 d based on the data of Aberg et al. (1969) and 56 d based on the data of Miettinen et al. (1971), compared with the half-time of 44 d determined by Smith et al. (1994).

33.1.3.2. Biokinetic model for systemic mercury

(363) The biokinetic models for systemic mercury adopted in this report address mercury entering blood as Hg^0 (vapor), Hg^{2+}, or $MeHg^+$. Inhalation is the only mode of intake of Hg^0 addressed in this report. Ingestion is the only mode of intake of $MeHg^+$ addressed. The model for Hg^{2+} is applied to intake of Hg^{2+} via either ingestion or inhalation.

(364) The models depict initially distinct kinetics of Hg^0, Hg^{2+}, and $MeHg^+$ following their entry into the systemic circulation but convergence of kinetics over time due to conversion of Hg^0 and $MeHg^+$ to Hg^{2+}. The conversion is assumed to happen rapidly for Hg^0 but over a period of several weeks for $MeHg^+$. For all three forms of mercury, the transfer coefficients developed for adults are applied to all ages due to a paucity of age-specific biokinetic data.

(365) The models for Hg^0 and Hg^{2+} were taken from *Publication 151* (ICRP, 2022) but were modified by removal of explicitly identified bone compartments, in view of uncertainties in the level and locations of mercury accumulation in bone (Ciosek et al., 2023; Zafar et al., 2024). In the present versions of the models for Hg^0 and Hg^{2+} (and $MeHg^+$), activity in bone is treated as a mass fraction of "Other".

(a) Biokinetic models for divalent inorganic mercury and mercury vapor

(366) The structure of the systemic model for divalent inorganic mercury is shown in Fig. 33.1. The same structure (arranged differently), with an added blood compartment named Plasma 0 and several arrows representing flow to or from Plasma 0, is applied to mercury vapor (Fig. 33.2). Transfer coefficients for divalent inorganic mercury that enters the systemic circulation are listed in Table 33.3. Transfer coefficients for mercury vapor that enters the systemic circulation are listed in Table 33.4. The last 18 transfer coefficients in Table 33.3 (beginning with the transfer from Plasma 1 to RBC) are the transfer coefficients for divalent inorganic mercury listed in Table 33.3. The models for both forms of mercury were based primarily on data for human subjects including data on blood clearance, uptake and retention in major repositories or total body following acute intake of a mercury tracer, and the distribution of mercury in occupationally or non-occupationally exposed persons. The data for human subjects were supplemented with data for laboratory animals where information for humans was sparse.

(367) In the model for mercury vapor, blood is divided into three plasma compartments and a fourth compartment representing red blood cells. Two plasma compartments, called Plasma 0 and Plasma 1, are used to account for differences in the rates of disappearance of absorbed mercury vapor and absorbed divalent mercury from plasma and differences in their initial

distributions. Mercury vapor absorbed from the respiratory tract to blood is assigned to Plasma 0, and absorbed divalent mercury absorbed to blood from the respiratory or alimentary tract is assigned to Plasma 1. A third compartment, called Plasma 2, is used to account for a relatively long-term component of retention of divalent inorganic mercury in plasma associated with binding to plasma proteins.

(368) The fractions of inhaled mercury vapor that are assumed to enter the systemic circulation as mercury vapor and as divalent inorganic mercury are described in terms of two absorption parameters, f_r (highly mobile activity) and f_b ("bound" activity) used in the ICRP's Human Respiratory Tract Model. The fraction of inhaled mercury vapor that is absorbed rapidly into blood is $f_r \times (1\text{-}f_b)$. This fraction enters the systemic circulation as mercury vapor depositing in the compartment named Plasma 0. The bound fraction, f_b, and another slowly absorbed fraction, $(1\text{-}f_r) \times (1\text{-}f_b)$, enter the systemic circulation as Hg^{2+} by depositing in the compartment named Plasma 1; these two fractions represent divalent inorganic mercury formed in lung tissues by oxidation of mercury vapor.

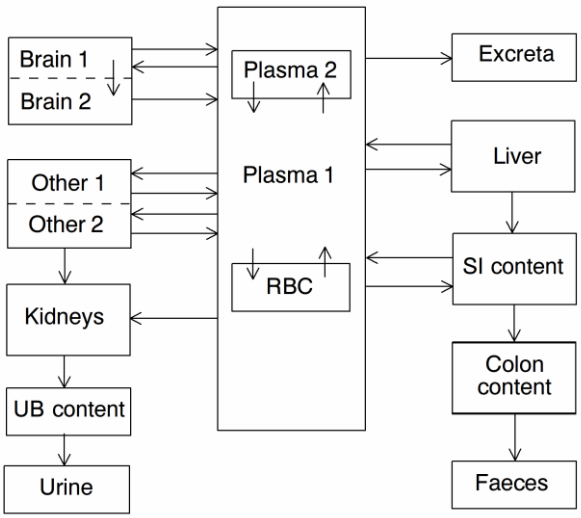

Fig. 33.1. Structure of the systemic biokinetic model for mercury inhaled or ingested as divalent inorganic mercury. Absorbed activity is assigned to Plasma 1. RBC, red blood cells; UB, urinary bladder; SI, small intestine.

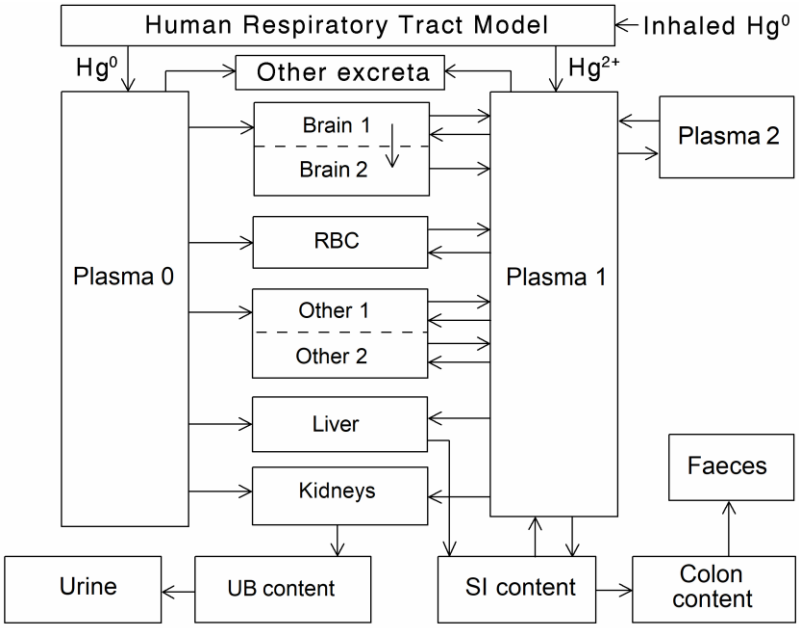

Fig. 33.2. Structure of the systemic biokinetic model for mercury inhaled as vapor. Absorbed activity is assigned to Plasma 0. RBC, red blood cells; UB, urinary bladder; SI, small intestine.

Table 33.3. Transfer coefficients for mercury inhaled or ingested as divalent inorganic mercury.

		Transfer coefficients (d^{-1})					
Pathway		100 d	1 y	5 y	10 y	15 y	Adult
Plasma 1	RBC	4.80E-01	4.80E-01	4.80E-01	4.80E-01	4.80E-01	4.80E-01
Plasma 1	Plasma 2	2.40E+00	2.40E+00	2.40E+00	2.40E+00	2.40E+00	2.40E+00
Plasma 1	Kidneys	7.20E+00	7.20E+00	7.20E+00	7.20E+00	7.20E+00	7.20E+00
Plasma 1	Liver	4.80E+00	4.80E+00	4.80E+00	4.80E+00	4.80E+00	4.80E+00
Plasma 1	Brain 1	4.80E-02	4.80E-02	4.80E-02	4.80E-02	4.80E-02	4.80E-02
Plasma 1	Other 1	5.23E+00	5.23E+00	5.23E+00	5.23E+00	5.23E+00	5.23E+00
Plasma 1	Other 2	7.26E-01	7.26E-01	7.26E-01	7.26E-01	7.26E-01	7.26E-01
Plasma 1	SI content	1.92E+00	1.92E+00	1.92E+00	1.92E+00	1.92E+00	1.92E+00
Plasma 1	Excreta	1.20E+00	1.20E+00	1.20E+00	1.20E+00	1.20E+00	1.20E+00
RBC	Plasma 1	3.30E-01	3.30E-01	3.30E-01	3.30E-01	3.30E-01	3.30E-01
Plasma 2	Plasma 1	6.00E-01	6.00E-01	6.00E-01	6.00E-01	6.00E-01	6.00E-01
Kidneys	UB content	1.98E-02	1.98E-02	1.98E-02	1.98E-02	1.98E-02	1.98E-02
Liver	SI content	1.73E-01	1.73E-01	1.73E-01	1.73E-01	1.73E-01	1.73E-01
Brain 1	Plasma 1	3.29E-02	3.29E-02	3.29E-02	3.29E-02	3.29E-02	3.29E-02
Brain 1	Brain 2	1.73E-03	1.73E-03	1.73E-03	1.73E-03	1.73E-03	1.73E-03
Brain 2	Plasma 1	3.80E-04	3.80E-04	3.80E-04	3.80E-04	3.80E-04	3.80E-04
Other 1	Plasma 1	3.47E-02	3.47E-02	3.47E-02	3.47E-02	3.47E-02	3.47E-02
Other 2	Plasma 1	6.93E-03	6.93E-03	6.93E-03	6.93E-03	6.93E-03	6.93E-03

RBC, red blood cells; UB, urinary bladder; SI, small intestine.

Table 33.4. Transfer coefficients for mercury inhaled as vapor

		Transfer coefficients (d^{-1})					
Pathway		100 d	1 y	5 y	10 y	15 y	Adult
Plasma 0	RBC	1.00E+02	1.00E+02	1.00E+02	1.00E+02	1.00E+02	1.00E+02
Plasma 0	Brain 1	2.00E+01	2.00E+01	2.00E+01	2.00E+01	2.00E+01	2.00E+01
Plasma 0	Kidneys	1.00E+02	1.00E+02	1.00E+02	1.00E+02	1.00E+02	1.00E+02
Plasma 0	Liver	6.00E+01	6.00E+01	6.00E+01	6.00E+01	6.00E+01	6.00E+01
Plasma 0	Other 1	6.50E+02	6.50E+02	6.50E+02	6.50E+02	6.50E+02	6.50E+02
Plasma 0	Excreta	7.00E+01	7.00E+01	7.00E+01	7.00E+01	7.00E+01	7.00E+01
Plasma 1	RBC	4.80E-01	4.80E-01	4.80E-01	4.80E-01	4.80E-01	4.80E-01
Plasma 1	Plasma 2	2.40E+00	2.40E+00	2.40E+00	2.40E+00	2.40E+00	2.40E+00
Plasma 1	Kidneys	7.20E+00	7.20E+00	7.20E+00	7.20E+00	7.20E+00	7.20E+00
Plasma 1	Liver	4.80E+00	4.80E+00	4.80E+00	4.80E+00	4.80E+00	4.80E+00
Plasma 1	Brain 1	4.80E-02	4.80E-02	4.80E-02	4.80E-02	4.80E-02	4.80E-02
Plasma 1	Other 1	5.23E+00	5.23E+00	5.23E+00	5.23E+00	5.23E+00	5.23E+00
Plasma 1	Other 2	7.26E-01	7.26E-01	7.26E-01	7.26E-01	7.26E-01	7.26E-01
Plasma 1	SI content	1.92E+00	1.92E+00	1.92E+00	1.92E+00	1.92E+00	1.92E+00
Plasma 1	Excreta	1.20E+00	1.20E+00	1.20E+00	1.20E+00	1.20E+00	1.20E+00
RBC	Plasma 1	3.30E-01	3.30E-01	3.30E-01	3.30E-01	3.30E-01	3.30E-01
Plasma 2	Plasma 1	6.00E-01	6.00E-01	6.00E-01	6.00E-01	6.00E-01	6.00E-01
Kidneys	UB content	1.98E-02	1.98E-02	1.98E-02	1.98E-02	1.98E-02	1.98E-02
Liver	SI content	1.73E-01	1.73E-01	1.73E-01	1.73E-01	1.73E-01	1.73E-01
Brain 1	Plasma 1	3.29E-02	3.29E-02	3.29E-02	3.29E-02	3.29E-02	3.29E-02
Brain 1	Brain 2	1.73E-03	1.73E-03	1.73E-03	1.73E-03	1.73E-03	1.73E-03
Brain 2	Plasma 1	3.80E-04	3.80E-04	3.80E-04	3.80E-04	3.80E-04	3.80E-04
Other 1	Plasma 1	3.47E-02	3.47E-02	3.47E-02	3.47E-02	3.47E-02	3.47E-02
Other 2	Plasma 1	6.93E-03	6.93E-03	6.93E-03	6.93E-03	6.93E-03	6.93E-03

RBC, red blood cells; UB, urinary bladder; SI, small intestine.

(b) Biokinetic model for systemic methyl mercury

(369) The structure of the biokinetic model for methyl mercury following its absorption to blood is shown in Fig. 33.3. Transfer coefficients are listed in Table Hg-3. The last 18 transfer coefficients in Table 33.5 (beginning with the transfer from Plasma 1 to RBC) are the transfer coefficients for systemic Hg^{2+} listed in Table 33.3. The transfer coefficients describing the behaviour of absorbed $MeHg^{+}$ in the body, before it is converted to Hg^{2+}, are set for reasonable agreement with the generally consistent results of the human studies for ingested or intravenously injected $MeHg^{+}$ summarized above. These data include tracer (^{203}Hg) studies of total-body retention, blood clearance, systemic distribution, urinary and faecal excretion rates, cumulative excretion estimates, and levels of accumulation in hair for periods up to ~8 months following oral administration to a total of 18 healthy adult human subjects (Aberg et al., 1969; Miettinen et al. (1971); and a 70-d study of the kinetics of $MeHg^{+}$, separately from that of its metabolite, Hg^{2+}, following intravenous administration to 7 healthy adult subjects (Smith et al., 1994; Smith and Farris, 1996).

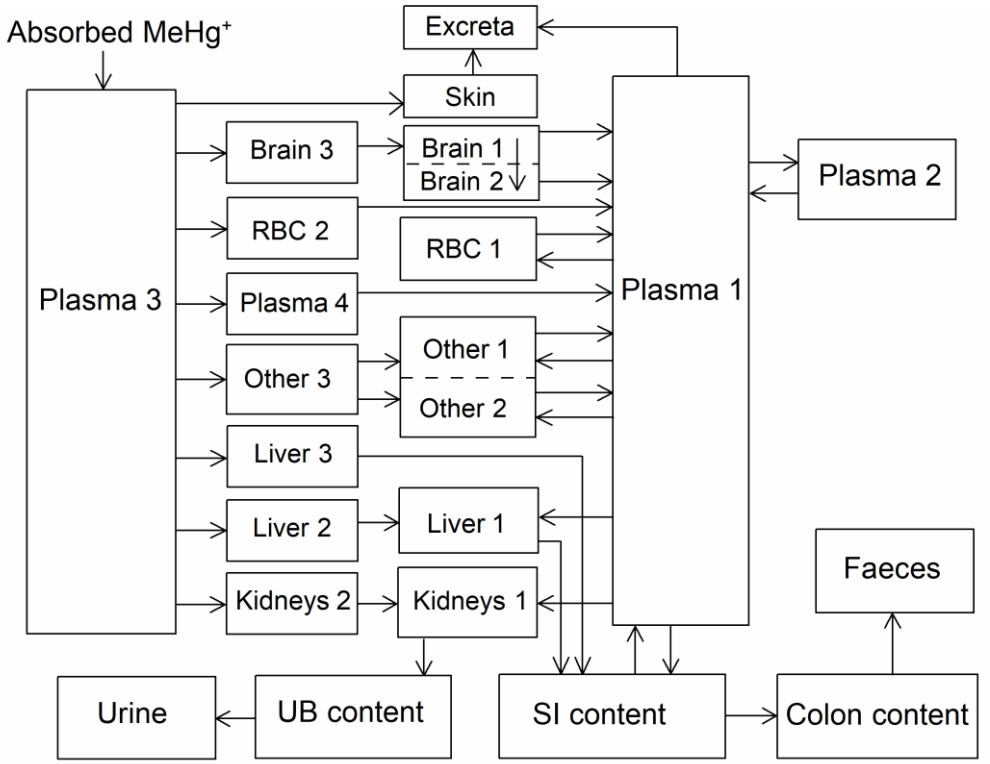

Fig. 33.3. Structure of the systemic biokinetic model for mercury inhaled or ingested as methyl mercury. RBC, red blood cells; UB, urinary bladder; SI, small intestine.

3655 Table 33.5. Transfer coefficients for mercury inhaled or ingested as methyl mercury.

		Transfer coefficients (d^{-1})					
Pathway		100 d	1 y	5 y	10 y	15 y	Adult
Plasma 3	Brain 3	1.60E+01	1.60E+01	1.60E+01	1.60E+01	1.60E+01	1.60E+01
Plasma 3	RBC 2	2.00E+01	2.00E+01	2.00E+01	2.00E+01	2.00E+01	2.00E+01
Plasma 3	Plasma 4	2.00E+00	2.00E+00	2.00E+00	2.00E+00	2.00E+00	2.00E+00
Plasma 3	Other 3	2.40E+01	2.40E+01	2.40E+01	2.40E+01	2.40E+01	2.40E+01
Plasma 3	Liver 3	1.50E+01	1.50E+01	1.50E+01	1.50E+01	1.50E+01	1.50E+01
Plasma 3	Liver 2	9.50E+01	9.50E+01	9.50E+01	9.50E+01	9.50E+01	9.50E+01
Plasma 3	Kidneys 2	2.00E+01	2.00E+01	2.00E+01	2.00E+01	2.00E+01	2.00E+01
Plasma 3	Skin	8.00E+00	8.00E+00	8.00E+00	8.00E+00	8.00E+00	8.00E+00
Plasma 4	Plasma 1	1.40E-02	1.40E-02	1.40E-02	1.40E-02	1.40E-02	1.40E-02
Brain 3	Brain 1	1.40E-02	1.40E-02	1.40E-02	1.40E-02	1.40E-02	1.40E-02
RBC 2	Plasma 1	1.40E-02	1.40E-02	1.40E-02	1.40E-02	1.40E-02	1.40E-02
Kidneys 2	Kidneys	1.40E-02	1.40E-02	1.40E-02	1.40E-02	1.40E-02	1.40E-02
Other 3	Other 1	1.23E-02	1.23E-02	1.23E-02	1.23E-02	1.23E-02	1.23E-02
Other 3	Other 2	1.70E-03	1.70E-03	1.70E-03	1.70E-03	1.70E-03	1.70E-03
Liver 2	Liver	1.40E-02	1.40E-02	1.40E-02	1.40E-02	1.40E-02	1.40E-02
Liver 3	SI content	2.31E-01	2.31E-01	2.31E-01	2.31E-01	2.31E-01	2.31E-01
Skin	Excreta*	5.00E-02	5.00E-02	5.00E-02	5.00E-02	5.00E-02	5.00E-02
Plasma 1	RBC	4.80E-01	4.80E-01	4.80E-01	4.80E-01	4.80E-01	4.80E-01
Plasma 1	Plasma 2	2.40E+00	2.40E+00	2.40E+00	2.40E+00	2.40E+00	2.40E+00
Plasma 1	Kidneys	7.20E+00	7.20E+00	7.20E+00	7.20E+00	7.20E+00	7.20E+00
Plasma 1	Liver	4.80E+00	4.80E+00	4.80E+00	4.80E+00	4.80E+00	4.80E+00
Plasma 1	Brain 1	4.80E-02	4.80E-02	4.80E-02	4.80E-02	4.80E-02	4.80E-02
Plasma 1	Other 1	5.23E+00	5.23E+00	5.23E+00	5.23E+00	5.23E+00	5.23E+00
Plasma 1	Other 2	7.26E-01	7.26E-01	7.26E-01	7.26E-01	7.26E-01	7.26E-01
Plasma 1	SI content	1.92E+00	1.92E+00	1.92E+00	1.92E+00	1.92E+00	1.92E+00
Plasma 1	Excreta	1.20E+00	1.20E+00	1.20E+00	1.20E+00	1.20E+00	1.20E+00
RBC	Plasma 1	3.30E-01	3.30E-01	3.30E-01	3.30E-01	3.30E-01	3.30E-01
Plasma 2	Plasma 1	6.00E-01	6.00E-01	6.00E-01	6.00E-01	6.00E-01	6.00E-01
Kidneys	UB content	1.98E-02	1.98E-02	1.98E-02	1.98E-02	1.98E-02	1.98E-02
Liver	SI content	1.73E-01	1.73E-01	1.73E-01	1.73E-01	1.73E-01	1.73E-01
Brain 1	Plasma 1	3.29E-02	3.29E-02	3.29E-02	3.29E-02	3.29E-02	3.29E-02
Brain 1	Brain 2	1.73E-03	1.73E-03	1.73E-03	1.73E-03	1.73E-03	1.73E-03
Brain 2	Plasma 1	3.80E-04	3.80E-04	3.80E-04	3.80E-04	3.80E-04	3.80E-04
Other 1	Plasma 1	3.47E-02	3.47E-02	3.47E-02	3.47E-02	3.47E-02	3.47E-02
Other 2	Plasma 1	6.93E-03	6.93E-03	6.93E-03	6.93E-03	6.93E-03	6.93E-03

3656 RBC, red blood cells, UB, urinary bladder; SI, small intestine.
3657 *Excreta is primarily loss in hair.

3658 33.1.3.3. Treatment of radioactive progeny

3659 (370) The treatment of radioactive progeny produced in systemic compartments after intake
3660 of a radioisotope of mercury is described in Section 36.2.3.3. of *Publication 151* (ICRP, 2022).

33.2. Dosimetric data for mercury

Table 33.6. Committed effective dose coefficients (Sv Bq^{-1}) for the inhalation or ingestion of ^{203}Hg compounds.

	Effective dose coefficients (Sv Bq^{-1})					
Inhaled gases or vapours	3m	1y	5y	10y	15y	Adult
Mercury vapour	1.0E-08	7.6E-09	4.2E-09	2.6E-09	1.8E-09	1.7E-09
Inhaled particulate materials (1 µm AMAD aerosols)						
Type F	4.8E-09	2.5E-09	1.3E-09	8.1E-10	5.6E-10	5.6E-10
Type M (default), mercuric oxide	5.0E-09	3.8E-09	2.2E-09	1.4E-09	1.1E-09	1.1E-09
Type S	6.0E-09	5.0E-09	2.8E-09	1.9E-09	1.5E-09	1.5E-09
Ingested materials						
All inorganic forms	6.4E-09	1.2E-09	7.0E-10	4.5E-10	3.2E-10	3.0E-10
Methyl mercury	1.9E-08	1.4E-08	8.1E-09	5.5E-09	3.7E-09	3.6E-09
Other organic forms and mercury in diet	1.6E-08	6.1E-09	3.4E-09	2.3E-09	1.6E-09	1.5E-09

AMAD, activity median aerodynamic diameter.

34. THALLIUM (Z=81)

34.1. Routes of Intake

34.1.1. Inhalation

(371) For thallium, default parameter values were adopted on absorption to blood from the respiratory tract (ICRP, 2015). Absorption parameter values and types, and associated f_A values for particulate forms of thallium are given in Table 34.1 [taken from Section 37 of *Publication 151* (ICRP, 2022)].

34.1.2. Ingestion

(372) Thallium is readily absorbed from the gastrointestinal tract, see *Publication 151* (ICRP, 2022) for details. In *Publications 72* (ICRP, 1995c) and *151*, a fractional absorption of 1 was used for all compounds of the element. In this publication, $f_A = 1$ is also adopted as the default for all chemical forms of thallium ingested by members of the public of any age.

Table 34.1. Absorption parameter values for inhaled and ingested thallium.

	Absorption parameter values*		
Inhaled particulate materials	f_r	s_r (d^{-1})	s_s (d^{-1})
Default parameter values†			
Absorption type			
F	1	30	–
M‡	0.2	3	0.005
S	0.01	3	1×10^{-4}

Ingested materials§	Age-dependent absorption from the alimentary tract, f_A					
Assigned forms	3 months	1 year	5 years	10 years	15 years	adult
All compounds	1	1	1	1	1	1

*It is assumed that the bound state can be neglected for thallium (i.e. $f_b = 0$). The values of s_r for Type F, M and S forms of thallium (30, 3 and 3 d^{-1} respectively) are the general default values.

†For inhaled material deposited in the respiratory tract and subsequently cleared by particle transport to the alimentary tract, the default f_A values for inhaled materials are applied: i.e. the product of f_r for the absorption type and the f_A value for ingested soluble forms of thallium applicable to the age-group of interest (1).

‡Default Type M is recommended for use in the absence of specific information on which the exposure material can be assigned to an absorption type (e.g. if the form is unknown, or if the form is known but there is no information available on the absorption of that form from the respiratory tract).

§Activity transferred from systemic compartments into segments of the alimentary tract is assumed to be subject to reabsorption to blood. The default absorption fraction f_A for the secreted activity is the highest value for any form of the radionuclide applicable to the age-group of interest (1).

34.1.3. Systemic distribution, retention and excretion of thallium

34.1.3.1. Biokinetic data

(373) The biokinetics of thallium has been investigated extensively in human subjects and laboratory animals due to the importance of radio-thallium in nuclear medicine and its uses as a poisonous substance (Gettler and Weiss, 1943; Barclay et al., 1953; Lie et al., 1960; Gehring and Hammond, 1967; Potter et al., 1971; Bradley-Moore et al., 1975; Strauss et al., 1975;

Atkins et al., 1977; Suzuki et al., 1978; Berger et al., 1983; Nakamura et al., 1985; Gregus and Klaassen, 1986; Krahwinkel et al., 1988; Lathrop et al., 1989; Blanchardon et al., 2005; Thomas et al., 2005). Its systemic behaviour resembles that of the alkali metals potassium and rubidium (Gehring and Hammond, 1967; Strauss et al., 1975), but the residence time of thallium in the body is less than that of potassium or rubidium due to a higher rate of clearance from plasma to excretion pathways. Most reported removal half-times of thallium from the adult human body are in the range 9-13 d (Atkins et al., 1977; Krahwinkel et al., 1988; Blanchardon et al., 2005). Chen et al. (1983) reported two components of retention of thallium: 7d for 63% and 28 d for 37% of the injected amount. It appears that faecal excretion typically represents more than half of cumulative excretion of thallium over a period of weeks following its acute intake, although some relatively short-term human studies have suggested that excretion of thallium is primarily in urine (Barclay et al., 1953; Lathrop et al., 1975; Atkins et al., 1977; Blanchardon et al., 2005).

34.1.3.2. Biokinetic model for systemic thallium

(374) The biokinetic model for systemic thallium applied to workers in *Publication 151* (ICRP, 2022) is applied in this report to all ages. The model structure is shown in Fig. 37.1. The transfer coefficients are listed in Table 37.3.

(375) It is assumed that thallium leaves the central blood compartment (Plasma) with a half-time of 5 min and is distributed as follows: 2.5% goes to red blood cells (RBC), 0.75% to the urinary bladder content, 1.75% to the right colon content, 5% to kidneys, 5% to the liver, 7.5% to trabecular bone surface, 7.5% to cortical bone surface, and 70% to the remaining tissues (Other). Thallium is assumed to return from RBC to plasma at the rate 3.7 d^{-1} and from tissue compartments to plasma at the rate 2.5 d^{-1}.

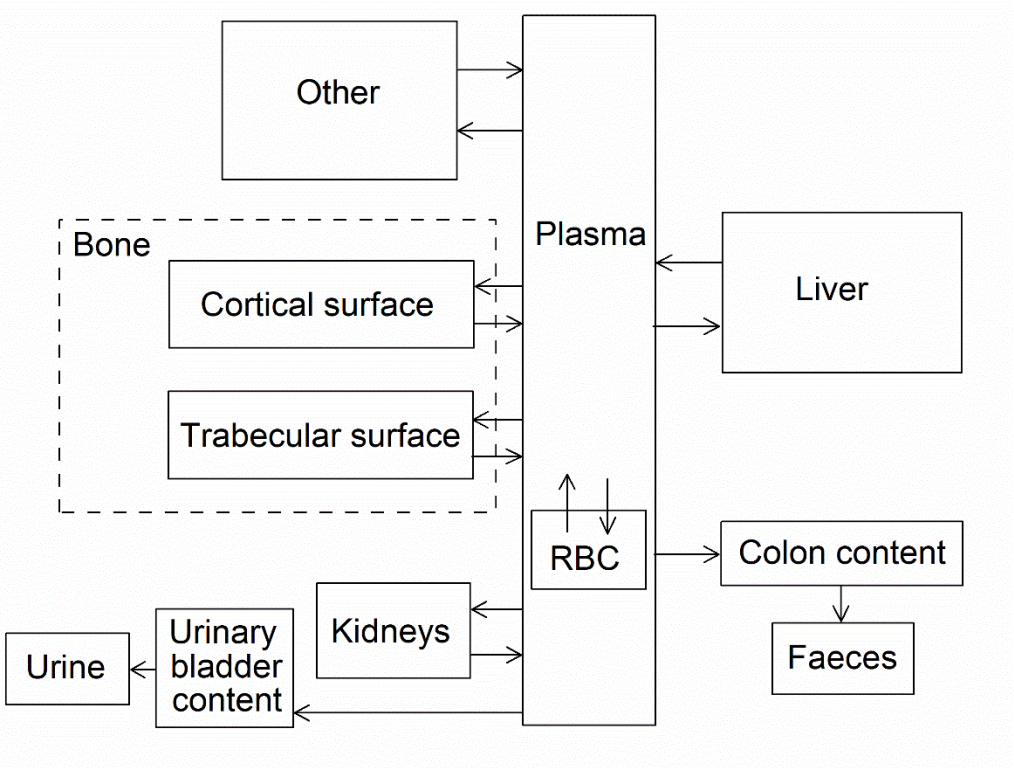

Fig. 37.1. Structure of the biokinetic model for systemic thallium.

Table 34.2. Age-specific transfer coefficients for thallium.

		Transfer coefficients (d^{-1})					
Pathway		100 d	1 y	5 y	10 y	15 y	Adult
Plasma	Liver	1.00E+01	1.00E+01	1.00E+01	1.00E+01	1.00E+01	1.00E+01
Plasma	Kidneys	1.00E+01	1.00E+01	1.00E+01	1.00E+01	1.00E+01	1.00E+01
Plasma	RBC	5.00E+00	5.00E+00	5.00E+00	5.00E+00	5.00E+00	5.00E+00
Plasma	Trab surface	1.50E+01	1.50E+01	1.50E+01	1.50E+01	1.50E+01	1.50E+01
Plasma	Cort surface	1.50E+01	1.50E+01	1.50E+01	1.50E+01	1.50E+01	1.50E+01
Plasma	Other	1.40E+02	1.40E+02	1.40E+02	1.40E+02	1.40E+02	1.40E+02
Plasma	UB content	1.50E+00	1.50E+00	1.50E+00	1.50E+00	1.50E+00	1.50E+00
Plasma	RC content	3.50E+00	3.50E+00	3.50E+00	3.50E+00	3.50E+00	3.50E+00
RBC	Plasma	3.70E+00	3.70E+00	3.70E+00	3.70E+00	3.70E+00	3.70E+00
Liver	Plasma	2.50E+00	2.50E+00	2.50E+00	2.50E+00	2.50E+00	2.50E+00
Kidneys	Plasma	2.50E+00	2.50E+00	2.50E+00	2.50E+00	2.50E+00	2.50E+00
Trab surface	Plasma	2.50E+00	2.50E+00	2.50E+00	2.50E+00	2.50E+00	2.50E+00
Cort surface	Plasma	2.50E+00	2.50E+00	2.50E+00	2.50E+00	2.50E+00	2.50E+00
Other	Plasma	2.50E+00	2.50E+00	2.50E+00	2.50E+00	2.50E+00	2.50E+00

RBC, red blood cells; UB, urinary bladder; RC, right colon; Cort, cortical; Trab, trabecular.

34.1.3.3. Treatment of radioactive progeny

(376) The treatment of radioactive progeny produced in systemic compartments after intake of a radioisotope of thallium is described in Section 37.2.3.3. of *Publication 151* (ICRP, 2022).

34.2. Dosimetric data for thallium

Table 34.3. Committed effective dose coefficients (Sv Bq^{-1}) for the inhalation or ingestion of ^{200}Tl compounds.

	Effective dose coefficients (Sv Bq^{-1})					
	3m	1y	5y	10y	15y	Adult
Inhaled particulate materials (1 µm AMAD aerosols)						
Type F	5.5E-10	4.0E-10	2.0E-10	1.4E-10	8.6E-11	8.3E-11
Type M, default	7.6E-10	6.0E-10	3.0E-10	2.2E-10	1.4E-10	1.4E-10
Type S	8.0E-10	6.4E-10	3.2E-10	2.3E-10	1.5E-10	1.5E-10
Ingested materials						
All compounds	1.1E-09	7.9E-10	4.7E-10	3.1E-10	2.2E-10	2.1E-10

AMAD, activity median aerodynamic diameter.

Table 34.4. Committed effective dose coefficients (Sv Bq^{-1}) for the inhalation or ingestion of ^{201}Tl compounds.

	Effective dose coefficients (Sv Bq^{-1})					
	3m	1y	5y	10y	15y	Adult
Inhaled particulate materials (1 μm AMAD aerosols)						
Type F	3.1E-10	2.1E-10	9.5E-11	5.9E-11	3.7E-11	3.3E-11
Type M, default	4.7E-10	3.5E-10	2.0E-10	1.3E-10	1.1E-10	9.8E-11
Type S	5.1E-10	3.8E-10	2.2E-10	1.5E-10	1.2E-10	1.1E-10
Ingested materials						
All compounds	5.8E-10	3.9E-10	2.0E-10	1.2E-10	8.3E-11	7.2E-11

AMAD, activity median aerodynamic diameter.

Table 34.5. Committed effective dose coefficients (Sv Bq^{-1}) for the inhalation or ingestion of ^{202}Tl compounds.

	Effective dose coefficients (Sv Bq^{-1})					
	3m	1y	5y	10y	15y	Adult
Inhaled particulate materials (1 μm AMAD aerosols)						
Type F	1.2E-09	9.4E-10	4.7E-10	3.1E-10	2.0E-10	1.9E-10
Type M, default	1.4E-09	1.1E-09	5.9E-10	4.1E-10	2.8E-10	3.0E-10
Type S	1.5E-09	1.2E-09	6.4E-10	4.4E-10	3.1E-10	3.4E-10
Ingested materials						
All compounds	2.4E-09	1.8E-09	1.0E-09	6.7E-10	4.8E-10	4.5E-10

AMAD, activity median aerodynamic diameter.

35. ASTATINE (Z=85)

35.1. Routes of Intake

35.1.1. Inhalation

(377) For astatine, default parameter values were adopted for the absorption to blood from the respiratory tract (ICRP, 2015). Absorption parameter values and types, and associated f_A values for gas and vapour forms of astatine are given in Table 35.1 and for particulate forms in Table 35.2 [both taken from Section 38 of *Publication 151* (ICRP, 2022)]. By analogy with the halogen iodine, considered in detail in *Publication 137* (ICRP, 2017), default Type F is recommended for particulate forms in the absence of specific information on which the exposure material can be assigned to an absorption type.

(378) For astatine, and the other halogens, intakes could be in both particulate and gas and vapour forms, and it is therefore assumed that inhaled astatine is 50% particulate and 50% gas/vapour in the absence of information (ICRP, 2002b).

Table 35.1. Deposition and absorption for gas and vapour compounds of astatine.

	Percentage deposited (%)*						Absorption†	
Chemical form/origin	Total	ET_1	ET_2	BB	bb	AI	Type	Absorption from the alimentary tract, f_A‡,¶
Unspecified	100	0	20	10	20	50	F	1.0

ET_1, anterior nasal passage; ET_2, posterior nasal passage, pharynx and larynx; BB, bronchial; bb, bronchiolar; AI, alveolar-interstitial.

*Percentage deposited refers to how much of the material in the inhaled air remains in the body after exhalation. Almost all inhaled gas molecules contact airway surfaces, but usually return to the air unless they dissolve in, or react with, the surface lining. The default distribution between regions is assumed: 20% ET_2, 10% BB, 20% bb, and 50% AI.

†It is assumed that the bound state can be neglected for astatine (i.e. $f_b = 0$).

‡For inhaled material deposited in the respiratory tract and subsequently cleared by particle transport to the alimentary tract, the default f_A values for inhaled materials are applied [i.e. the product of f_r for the absorption Type (or specific value where given) and the f_A value for ingested soluble forms of astatine (1)].

¶The value of $f_A = 0.094$ is applicable to all age-groups.

Table 35.2. Absorption parameter values for inhaled and ingested astatine.

	Absorption parameter values*		
Inhaled particulate materials	f_r	s_r (d^{-1})	s_s (d^{-1})
Default parameter values†			
Absorption type			
F‡	1	30	–
M	0.2	3	0.005
S	0.01	3	1×10^{-4}

Ingested materials§

	Age-dependent absorption from the alimentary tract, f_A					
Assigned forms	3 months	1 year	5 years	10 years	15 years	adult
All compounds	1	1	1	1	1	1

*It is assumed that the bound state can be neglected for astatine (i.e. $f_b = 0$). The values of s_r for Type F, M and S forms of astatine (30, 3 and 3 d^{-1} respectively) are the general default values.

[†]For inhaled material deposited in the respiratory tract and subsequently cleared by particle transport to the alimentary tract, the default f_A values for inhaled materials are applied: i.e. the product of f_r for the absorption type and the f_A value for ingested soluble forms of astatine applicable to the age-group of interest (1).

[‡]Default Type F is recommended for use in the absence of specific information on which the exposure material can be assigned to an absorption type (e.g. if the form is unknown, or if the form is known but there is no information available on the absorption of that form from the respiratory tract).

[§]Activity transferred from systemic compartments into segments of the alimentary tract is assumed to be subject to reabsorption to blood. The default absorption fraction f_A for the secreted activity is the highest value for any form of the radionuclide applicable to the age-group of interest (1).

35.1.2. Ingestion

(379) There appears to be no data on the gastrointestinal absorption of astatine. In *Publications 72* and *151* (ICRP, 1995c, 2022), the fractional absorption was taken to be 1 for all compounds of astatine by analogy with the lighter halides, chlorine, bromine and iodine. The same value of $f_A = 1$ is adopted in this publication for all chemical forms of astatine ingested by members of the public of any age.

35.1.3. Systemic distribution, retention and excretion of astatine

35.1.3.1. Biokinetic data

(380) Astatine (At) is the heaviest member of the halogen group of elements (Group VIIA of the periodic table). Its kinetics resembles that of the next heaviest halogen, iodine in several ways, particularly regarding selective uptake by the thyroid gland and stomach wall, blood clearance rates, and excretion patterns. A notable difference between astatine and iodine is that accumulation of astatine in the thyroid is generally much lower than that of iodine, as indicated by data for human subjects, monkeys, guinea pigs, rats, and mice (Hamilton et al., 1953; Shellabarger and Godwin, 1954; Cobb et al., 1988; Garg et al., 1990). Also, astatine shows longer retention than iodine in the stomach wall and in most other soft tissues (Hamilton et al., 1953; Garg et al., 1990).

(381) Following parenteral administration to guinea pigs, the thyroidal content and cumulative urinary and faecal excretion at 4 h represented 8.5%, 12%, and 0.8%, respectively, of the administered amount of iodine, and 3.4%, 8.8%, and 0.4%, respectively, of administered astatine (Hamilton and Soley, 1940). Corresponding values at 18 h were 17%, 37%, and 17% for iodine and 5.4%, 36%, and 13% for astatine.

(382) Hamilton et al. (1953) compared the biokinetics of intravenously administered ^{211}At and ^{131}I in rats. Plasma clearance was rapid for both radionuclides, with clearance of ^{131}I slightly faster than that of ^{211}At. At 24 h, plasma contained about 0.9% of injected ^{211}At and 0.6% of injected ^{131}I (after correction for radioactive decay). At 1 h the thyroid and stomach wall contained on average 5.6% and 6.1%, respectively, of injected ^{131}I, and 1.1% and 5.2% respectively, of injected ^{211}At. The stomach content of ^{131}I decreased steadily to about 0.5% of the injected amount at 24 h, while the stomach content of ^{211}At increased to 9.9% of the injected amount at 4 h and then decreased gradually to 5.9% at 24 h. The thyroid content of both radionuclides peaked at 24 h, at which time the thyroid contained about 1.5% of injected ^{211}At and 12% of injected ^{131}I. The ^{211}At content of the thyroid decreased by about a factor of 2 from 24-48 h and showed little if any change from 48-72 d. The ^{131}I content decreased more slowly than that of ^{211}At after 24 h, declining by about one-fourth from 24-72 h. Non-thyroidal tissues generally contained a larger portion of injected ^{211}At than injected ^{131}I from 4-24 h. For example, the mean ^{211}At content (% injected activity) of the liver, kidneys, and muscle were, respectively, about 4.6, 5.6, and 3.6 times the content of ^{131}I.

(383) Hamilton et al. (1953, 1954a, 1954b) observed higher thyroidal accumulation of ^{211}At in limited studies on monkeys and human subjects than was observed in rats. In two monkeys, the thyroid contained 9 and 20% of administered ^{211}At at 24 h. In human subjects with various forms of thyroid pathology, 4.6-17.8% of administered astatine was contained in the thyroid at 24 h, compared with 12-30% of administered ^{131}I (Hamilton et al., 1954a).

(384) Harrison and Royle (1984) measured the content of ^{211}At in blood, thyroid, kidneys, and testes of mice over the first 28.5 h after intravenous injection. The blood content (corrected for decay) declined to ~0.5% of the injected amount by ~12 h post injection and remained at that level through 28.5 h. The thyroid content peaked at ~3.5% of the injected amount within 3-4 h post injection, declined to roughly 40% of the peak content by 12-15 h, and remained near that level through 28.5 h. The pattern of uptake and retention by the testes was broadly similar to that of the thyroid. The kidneys contained about 5-6% of the injected amount at 0.5-1 h, 3% at 4-5 h, and 1.0-1.5% from 12-28.5 h.

(385) Larsen et al. (1998) compared the biokinetics of intravenously administered [^{131}I]iodide and [^{211}At]astatide in mice. Activity concentrations were determined in 12 tissues and in blood. High concentrations of ^{131}I were measured in thyroid and stomach at 1 and 4 h, with relatively low concentrations found in other tissues at 4 h. The thyroid showed high concentrations of ^{211}At at 1 and 4 h but only about one-half of that of ^{131}I at 1 h and one-fourth at 4 h. The two radionuclides showed similar uptake by the stomach wall at 1 h. By 4 h the concentration of ^{131}I in the stomach had decreased considerably while the ^{211}At concentration showed little change. On average, the ^{211}At concentration in individual tissues (% dosage g^{-1}) was 2.2 and 3.0 times the ^{131}I concentration at 1 h and 4 h, respectively.

35.1.3.2. Biokinetic model for systemic astatine

(386) The biokinetic model for systemic astatine applied in this report to all ages is the model for astatine applied to workers in *Publication 151* (ICRP, 2022). The model structure for astatine is shown in Fig. 35.1. Transfer coefficients are listed in Table 35.3.

(387) The biokinetic model for astatine in adults is based on observed similarities and differences in the systemic behaviours of astatine and iodine. The structure of the model for iodine is simplified in some ways for application to astatine, e.g., by representing each of the tissues liver, kidneys, and "Other" as single rather than multiple compartments, but additional tissues are treated explicitly in the astatine model based on apparent differences of the level of accumulation of iodine and astatine or its progeny in these tissues. Flow rates from plasma to urinary bladder content, right colon content, and all other excretion pathways combined are assumed to be the same for astatine and iodine. Fractional uptake of astatine from plasma to the thyroid is assumed to be 40% of the value for iodine. A greater accumulation of astatine than iodine in tissues of laboratory animals other than thyroid is assumed to result from slower return of astatine from these tissues to plasma.

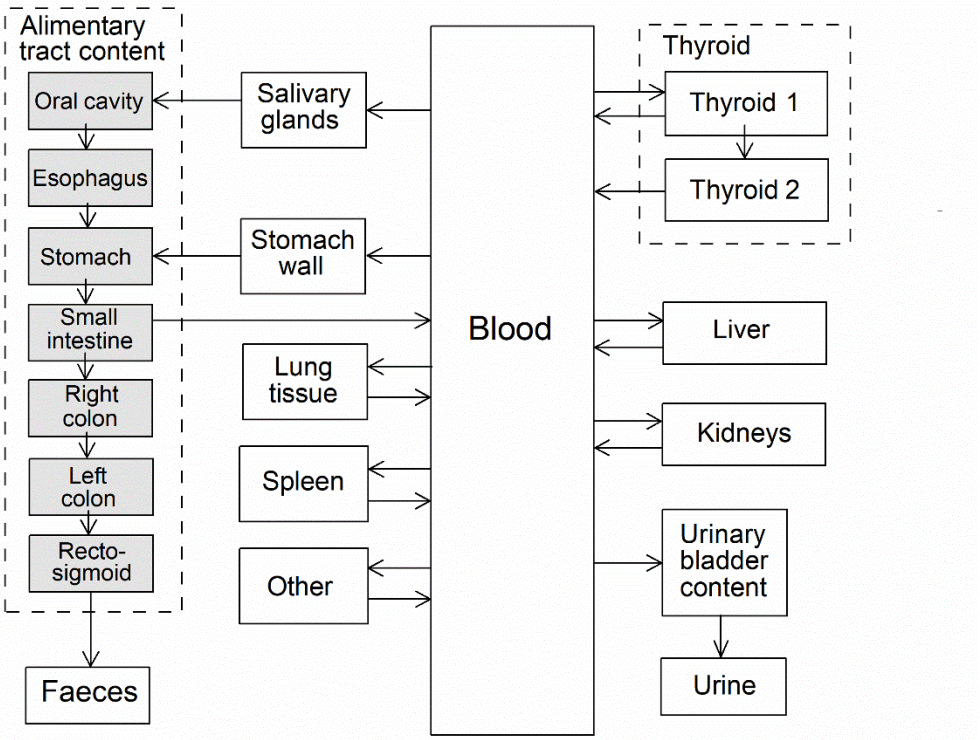

Fig. 35.1. Structure of the biokinetic model for systemic astatine.

Table 35.3. Age-specific transfer coefficients for astatine.

		Transfer coefficients (d^{-1})					
Pathway		100 d	1 y	5 y	10 y	15 y	Adult
Blood	Thyroid 1	2.90E+00	2.90E+00	2.90E+00	2.90E+00	2.90E+00	2.90E+00
Blood	UB content	1.18E+01	1.18E+01	1.18E+01	1.18E+01	1.18E+01	1.18E+01
Blood	Salivary glands	5.16E+00	5.16E+00	5.16E+00	5.16E+00	5.16E+00	5.16E+00
Blood	Stomach wall	8.60E+00	8.60E+00	8.60E+00	8.60E+00	8.60E+00	8.60E+00
Blood	Kidneys	2.50E+01	2.50E+01	2.50E+01	2.50E+01	2.50E+01	2.50E+01
Blood	Liver	5.00E+01	5.00E+01	5.00E+01	5.00E+01	5.00E+01	5.00E+01
Blood	Lung tissue	5.00E+01	5.00E+01	5.00E+01	5.00E+01	5.00E+01	5.00E+01
Blood	Spleen	1.30E+01	1.30E+01	1.30E+01	1.30E+01	1.30E+01	1.30E+01
Blood	Other	5.06E+02	5.06E+02	5.06E+02	5.06E+02	5.06E+02	5.06E+02
Thyroid 1	Blood	3.60E+01	3.60E+01	3.60E+01	3.60E+01	3.60E+01	3.60E+01
Thyroid 1	Thyroid 2	9.50E+01	9.50E+01	9.50E+01	9.50E+01	9.50E+01	9.50E+01
Thyroid 2	Blood	2.31E-01	2.31E-01	2.31E-01	2.31E-01	2.31E-01	2.31E-01
Salivary glands	Oral cavity	2.50E+01	2.50E+01	2.50E+01	2.50E+01	2.50E+01	2.50E+01
Stomach wall	Stomach content	2.50E+01	2.50E+01	2.50E+01	2.50E+01	2.50E+01	2.50E+01
Kidneys	Blood	5.00E+01	5.00E+01	5.00E+01	5.00E+01	5.00E+01	5.00E+01
Liver	Blood	5.00E+01	5.00E+01	5.00E+01	5.00E+01	5.00E+01	5.00E+01
Lung tissue	Blood	5.00E+01	5.00E+01	5.00E+01	5.00E+01	5.00E+01	5.00E+01
Spleen	Blood	5.00E+01	5.00E+01	5.00E+01	5.00E+01	5.00E+01	5.00E+01
Other	Blood	5.00E+01	5.00E+01	5.00E+01	5.00E+01	5.00E+01	5.00E+01

UB, urinary bladder; RC, right colon.

35.1.3.3. Treatment of radioactive progeny

(389) The treatment of radioactive progeny produced in systemic compartments after intake of a radioisotope of astatine is described in Section 38.2.3.3. of *Publication 151* (ICRP, 2022).

35.2. Dosimetric data for astatine

Table 35.4. Committed effective dose coefficients (Sv Bq^{-1}) for the inhalation or ingestion of ^{210}At compounds.

	Effective dose coefficients (Sv Bq^{-1})					
Inhaled gases and vapours	3m	1y	5y	10y	15y	Adult
Unspecified	9.2E-08	7.3E-08	4.0E-08	2.4E-08	1.1E-08	7.5E-09
Inhaled particulate materials (1 µm AMAD aerosols)						
Type F, default	3.9E-08	3.1E-08	1.5E-08	8.9E-09	3.7E-09	2.6E-09
Type M	2.6E-08	2.1E-08	1.2E-08	7.8E-09	5.3E-09	4.7E-09
Type S	3.1E-08	2.7E-08	1.6E-08	1.0E-08	7.9E-09	7.4E-09
Ingested materials						
All compounds	8.6E-08	6.8E-08	3.7E-08	2.2E-08	1.0E-08	6.9E-09

AMAD, activity median aerodynamic diameter.

36. FRANCIUM (Z=87)

36.1. Routes of Intake

36.1.1. Inhalation

(390) For francium, default parameter values were adopted on absorption to blood from the respiratory tract (ICRP, 2015). Absorption parameter values and types, and associated f_A values for particulate forms of francium are given in Table 36.1 [taken from Section 39 of *Publication 151* (ICRP, 2022)].

Table 36.1. Absorption parameter values for inhaled and ingested francium.

	Absorption parameter values*		
Inhaled particulate materials	f_r	s_r (d^{-1})	s_s (d^{-1})
Default parameter values†			
Absorption type			
F	1	30	–
M‡	0.2	3	0.005
S	0.01	3	1×10^{-4}

Ingested materials§	Age-dependent absorption from the alimentary tract, f_A					
Assigned forms	3 months	1 year	5 years	10 years	15 years	adult
All compounds	1	1	1	1	1	1

*It is assumed that the bound state can be neglected for francium (i.e. $f_b = 0$). The values of s_r for Type F, M and S forms of francium (30, 3 and 3 d^{-1} respectively) are the general default values.

†For inhaled material deposited in the respiratory tract and subsequently cleared by particle transport to the alimentary tract, the default f_A values for inhaled materials are applied: i.e. the product of f_r for the absorption type and the f_A value for ingested soluble forms of francium applicable to the age-group of interest (1).

‡Default Type M is recommended for use in the absence of specific information on which the exposure material can be assigned to an absorption type (e.g. if the form is unknown, or if the form is known but there is no information available on the absorption of that form from the respiratory tract).

§Activity transferred from systemic compartments into segments of the alimentary tract is assumed to be subject to reabsorption to blood. The default absorption fraction f_A for the secreted activity is the highest value for any form of the radionuclide applicable to the age-group of interest (1).

36.1.2. Ingestion

(391) There appear to be no data on the gastrointestinal absorption of francium. In *Publications 72* and *151* (ICRP, 1995c, 2022), the fractional absorption was taken to be 1 for all compounds of francium, by analogy with potassium, rubidium and caesium. In this publication, $f_A = 1$ is also applied to all chemical forms of francium ingested by members of the public of any age.

36.1.3. Systemic distribution, retention and excretion of francium

36.1.3.1. Biokinetic model for systemic francium

(392) Francium is the heaviest member of the alkali metal family. Its systemic behaviour has not been determined but is assumed to resemble that of caesium, which is located just above francium in the periodic table. A much simpler biokinetic model is applied to francium than to

caesium (ICRP, 2017), however, in view of the short half-life of francium radioisotopes (≤ 22 min) and uncertainty in the accuracy of the caesium analogy.

(393) At all ages, francium is assumed to leave blood at the rate 200 d^{-1} (half-time ~5 min), with 5% going to the urinary bladder content, 1% going to the right colon content, and 94% uniformly distributed in all tissues. Francium deposited in tissues is assumed to transfer to blood at the rate 0.1 d^{-1}. The same model was applied to workers in *Publication 151* (ICRP, 2022).

(394) Transfer coefficients for francium are listed in Table 36.2.

Table 36.2. Age-specific transfer coefficients for francium.

		Transfer coefficients (d^{-1})					
Pathway		100 d	1 y	5 y	10 y	15 y	Adult
Blood	Other	1.88E+02	1.88E+02	1.88E+02	1.88E+02	1.88E+02	1.88E+02
Blood	UB content	1.00E+01	1.00E+01	1.00E+01	1.00E+01	1.00E+01	1.00E+01
Blood	RC content	2.00E+00	2.00E+00	2.00E+00	2.00E+00	2.00E+00	2.00E+00
Other	Blood	1.00E-01	1.00E-01	1.00E-01	1.00E-01	1.00E-01	1.00E-01

UB, Urinary bladder; SI, Small intestine.

36.1.3.2. Treatment of radioactive progeny

(395) The treatment of radioactive progeny produced in systemic compartments after intake of a radioisotope of francium is described in Section 39.2.3.3. of *Publication 151* (ICRP, 2022).

36.2. Dosimetric data for francium

Table 36.3. Committed effective dose coefficients (Sv Bq^{-1}) for the inhalation or ingestion of ^{223}Fr compounds.

	Effective dose coefficients (Sv Bq^{-1})					
	3m	1y	5y	10y	15y	Adult
Inhaled particulate materials (1 µm AMAD aerosols)						
Type F	3.8E-09	1.5E-09	5.9E-10	3.8E-10	3.3E-10	1.5E-10
Type M, default	1.7E-08	1.2E-08	7.6E-09	5.0E-09	4.3E-09	3.8E-09
Type S	2.0E-08	1.5E-08	9.5E-09	6.3E-09	5.3E-09	4.8E-09
Ingested materials						
All compounds	6.2E-09	1.9E-09	8.3E-10	5.3E-10	4.8E-10	1.5E-10

AMAD, activity median aerodynamic diameter.

REFERENCES

Aamodt, R.L., 1973. Retention and. excretion of. injected 181W labeled sodium tungstate by. beagles. Health Phys. 24, 519-524.

Aamodt, R.L., 1975. Inhalation of. 181W labeled tungstic oxide. by. six. beagle dogs. Health Phys. 28, 733-742.

Abdel-Rahman, M.S., Couri, D. and Bull, R.J., 1982. Metabolism and. pharmacokinetics of. alternate drinking water. disinfectants. Environmental Health Perspectives 46: 19–23.

Abdel-Rahman, M.S., Waldron, D.M. and Bull, R.J., 1983. A. comparative kinetics study. of. monochloramine and. hypochlorous acid. in. the. rat. Journal of. Applied Toxicology 3(4): 175–179.

Abert, B., Ekman, L., Falk, R., Persson, G., Snihs, J. 0., 1969. Metabolism of. methyl mercury (203Hg) compounds in. man. Arch. Environ. Health 19:478-484.

Adachi, A., Ogawa, K., Tsushi, Y., et al., 2000. Balance, excretion and. tissue distribution of. vanadium in. rats. after. short-term ingestion. Journal of. Health Science 46(1): 59–62.

Adeyemi, A., Garelick, H. and Priest, N.D., 2010. A. biokinetic model. to. describe the. distribution and. excretion of. arsenic by. man. following acute. and. chronic intakes of. arsenite/arsenate compounds by. ingestion. Human. Expl. Toxicol 29: 891–902.

Adler, A.J., Etzion, Z. and Berlyne, G.M., 1986. Uptake, distribution, and. excretion of. 31silicon in. rats. Am. J. Physiol: 251 670– 673.

Aikawa, J. K., Gordon, G. S., Rhoades, E. L. 1960. Magnesium metabolism in. human. beings: studies with. 28Mg. J. Appl. Physiol 15:503-507.

Alaimo, K., McDowell, M. A., Briefel, R. D., Bischof, A. M., Caughman, C. R., Loria, C. M. and Johnson, C. L. 1994. Dietary Intake of. Vitamins, Mineral, and. Fiber. of. Persons Ages. 2 Months and. Over. in. the. United States: Third. National Health and. Nutrition Examination Survey, Phase. 1, 1988-91, Advance Data. 258 (U. S. Dept. of. Health and. Human. Services).

Alimonti, A., Petrucci F., Krachler M., Bocca B. and Caroli S. 2000 Reference values for. chromium, nickel and. vanadium in. urine. of. youngsters from. the. urban. area. of. Rome. J. Environ Monit. 2: 351-354

Alvioli, L. V., Berman, M. 1966. 28Mg kinetics in. man. J. Appl. Physiol 21:1688-1694.

Amano, R., Enomoto S., Nobuta M., Sakamoto M., Tsujioka R. and Ambe F. 1996 Bone. uptake of. vanadium in. mice. Simultaneous tracing of. V. Se, Sr, Y. Zr, Ru. and. Rh. using. a. radioactive multitracer J. Trace. Elem. Med. Biol. 10: 145-148

Andersen, J.C.Ø., Cropp, A. and Paradise, D.C., 2017. Solubility of. indium-tin oxide. in. simulated lung. and. gastric fluids: Pathways for. human. intake. Science of. the. Total. Environment 579: 628–636. DOI: 10.1016/j.scitotenv.2016.11.047.

Andersen, M.E., Gearhart, J.M. and Clewell, H.J., 1999. Pharmacokinetic data. needs. to. support risk. assessment for. inhaled and. ingested manganese. NeuroToxicology 20: 161–72.

Anderson, R.A., 1997. Chromium as. an. Essential Nutrient for. Humans. Regulatory Toxicology and. Pharmacology. 26: S35-S41.

Andersson, L., Hallstadius, L. and Strand, S-E., 1988. Biokinetics and. dosimetry for. 195Au, evaluated in. an. animal model. Eur. J. Nucl. Med. 14: 393–399.

Andersson, M., Mattsson, S., Johansson, L., Leide-Svegborn, S. 2017. A. biokinetic and. dosimetric model. for. ionic. indium in. humans. Phys. Med. Biol. 62: 6397.

Ando, A., Ando I., 1994. Biodistributions of. radioactive bipositive metal. ions. in. tumor-bearing animals. Biometals 7:185–192.

Ando, A., Ando I. 1990. Biodistribution of. 95Nb and. 182Ta in. tumor-bearing animals and. mechanisms for. accumulation in. tumor. and. liver. J. Radiat. Res. 31:97–109.

Ando, A., Ando I., Hiraki T., Hisada K. 1989. Relation between the. location of. elements in. the. periodic table. and. various organ-uptake rates. Int. J. Rad. Appl. Instrum. B. Nucl. Med. Biol. 16:57–80.

Ando, A., Ando I., 1986. Distribution of. 95Zr and. 181Hf in. tumor-bearing animals and. mechanism for. accumulation in. tumor. and. liver. Nucl. Med. Biol. 13:21–29.

3966 Ando, A., Ando I., Hiraki T., Hisada K., 1989. Relation between the. location of. elements in. the.
3967 periodic table. and. various organ-uptake rates. Nucl. Med. Biol. 16:57–69.
3968 Angelova, M., Asenova, S., Nedkova, V., et al., 2011. Copper in. the. human. organism. Trakia J. Sci.
3969 9: 88–98.
3970 Archimbaud, Y., Grillon, G., Poncy, J.L., et al., 1992. 75Se transfer via. placenta and. milk, distribution
3971 and. retention in. fetal, young. and. adult. rat. Radiation Protection Dosimetry 41: 147–151.
3972 Artelt, S., Creutzenberg, O., Kock, H., et al., 1999. Bioavailability of. fine. dispersed platinum as.
3973 emitted from. automotive catalytic converters: a. model. study. Science of. the. Total. Environment
3974 228: 219 –242.
3975 Artelt, S., Koch, H., Nachtigall, D., et al., 1998. Bioavailability of. platinum emitted from. automobile
3976 exhaust. Toxicology Letters 96/97: 163 –167.
3977 Asakura, K., Satoh, H., Chiba, M., et al., 2008. Oral. toxicity of. indium in. rats: Single and. 28-day
3978 repeated administration studies. Journal of. Occupational Health 50(6): 471–478.
3979 Atkins, H.L., Budinger, T.F., Lebowitz, E., et al., 1977. Thallium-201 for. medical use, 3. Human.
3980 distribution and. physical imaging properties. J. Nucl. Med. 18: 133–140.
3981 ATSDR, 1988. Toxicological Profile for. Beryllium. Prepared by. Syracuse Research Corporation under.
3982 Contract 68-C8-0004. Agency for. Toxic. Substances and. Disease Registry (ATSDR). Atlanta,
3983 Georgia: U.S. Public Health Service.
3984 ATSDR, 1999. Toxicological Profile for. Mercury. Agency for. Toxic. Substances and. Disease
3985 Registry (ATSDR). Atlanta, Georgia: U.S. Department of. Health and. Human. Services. Public
3986 Health Service.
3987 ATSDR, 2002. Toxicological Profile for. Beryllium. Agency for. Toxic. Substances and. Disease
3988 Registry (ATSDR). Atlanta, Georgia: U.S. Department of. Health and. Human. Services. Public
3989 Health Service.
3990 ATSDR, 2004. Toxicological Profile for. Copper. Agency for. Toxic. Substances and. Disease Registry
3991 (ATSDR). Atlanta, Georgia: U.S. Department of. Health and. Human. Services. Public Health
3992 Service.
3993 ATSDR, 2005b. Toxicological Profile for. Tin. Agency for. Toxic. Substances and. Disease Registry
3994 (ATSDR). Atlanta, Georgia: U.S. Department of. Health and. Human. Services. Public Health
3995 Service.
3996 ATSDR, 2005c. Toxicological Profile for. Tungsten. Agency for. Toxic. Substances and. Disease
3997 Registry (ATSDR). Atlanta, Georgia: U.S. Department of. Health and. Human. Services. Public
3998 Health Service.
3999 ATSDR, 2007. Toxicological Profile for. Arsenic. Agency for. Toxic. Substances and. Disease Registry
4000 (ATSDR). Atlanta, Georgia: U.S. Department of. Health and. Human. Services. Public Health
4001 Service.
4002 ATSDR, 2008. Toxicological Profile for. Perchlorates. Agency for. Toxic. Substances and. Disease
4003 Registry (ATSDR). Atlanta, Georgia: U.S. Department of. Health and. Human. Services. Public
4004 Health Service.
4005 ATSDR, 2012a. Toxicological Profile for. Cadmium. Agency for. Toxic. Substances and. Disease
4006 Registry (ATSDR). Atlanta, Georgia: U.S. Department of. Health and. Human. Services. Public
4007 Health Service.
4008 ATSDR, 2012b. Toxicological Profile for. Chromium. Agency for. Toxic. Substances and. Disease
4009 Registry (ATSDR). Atlanta, Georgia: U.S. Department of. Health and. Human. Services. Public
4010 Health Service.
4011 ATSDR, 2012c. Toxicological Profile for. Manganese. Agency for. Toxic. Substances and. Disease
4012 Registry (ATSDR). Atlanta, Georgia: U.S. Department of. Health and. Human. Services. Public
4013 Health Service.
4014 ATSDR, 2017. Toxicological Profile for. Silica. Agency for. Toxic. Substances and. Disease Registry
4015 (ATSDR). Atlanta, Georgia: U.S. Department of. Health and. Human. Services. Public Health
4016 Service.
4017 Azay, J., Bres, J., Krosniak, M., et al., 2001. Vanadium pharmacokinetics and. oral. bioavailability upon.
4018 single-dose administration of. vanadyl sulfate to. rats. Fundamental & Clinical Pharmacology 15(5):
4019 313–324.

4020 Bachler, G., Losert, S., Umehara, Y., et al., 2015. Translocation of. gold. nanoparticles across the. lung.
4021 epithelial tissue barrier: Combining in. vitro. and. in. silico methods to. substitute in. vivo.
4022 experiments. Particle and. Fibre. Toxicology 12(1).
4023 Bacso, J., Uzonyi, I., Dezso, B., 1988. Determination of. gold. accumulation in. human. tissues caused
4024 by. gold. therapy using. x-ray fluorescence analysis. Appl. Radiat. Isot. 39:323-326.
4025 Bair, W.J., 1961. Deposition, retention, translocation and. excretion of. radioactive particles. In: Davies
4026 CN. (ed.) Inhaled Particles and. Vapours. Oxford: Pergamon Press, pp. 192–208.
4027 Baisch, B.L., Corson, N.M., Wade-Mercer, P., et al., 2014. Equivalent titanium dioxide nanoparticle
4028 deposition by. intratracheal instillation and. whole-body inhalation: The. effect of. dose. rate. on.
4029 acute. respiratory trace. inflammation. Particle and. Fibre. Toxicology 11: 5–16.
4030 Balasubramanian, S.K., Poh, K-W., Ong, C-N., et al., 2013. The. effect of. primary particle size. on.
4031 biodistribution of. inhaled gold. nano-agglomerates. Biomaterials 34(22): 5439–5452.
4032 Ballou, J.E., 1960. Metabolism of. 185W in. the. rat. AEC. Research and. Development Report HW-
4033 64112. Durham, NC: Hanford Laboratory.
4034 Barceloux, D. G. and Barceloux D. 1999 Vanadium J. Toxicol Clin. Toxicol 37 265-278
4035 Barclay, R.K., Peacock, W.C. and Karnofsky, D.A., 1953. Distribution and. excretion of. radioactive
4036 thallium in. the. chick. embryo, rat, and. man. Journal of. Pharmacology and. Experimental
4037 Therapeutics 107(2): 178–187.
4038 Barnes, J.M. and Stoner, H.B., 1959. The. toxicology of. tin. compounds. Pharmacological Reviews
4039 11(2, Part. 1): 211–231.
4040 Barregård, L. 1993. Biological monitoring of. exposure to. mercury vapor. Scand. J. Work. Environ.
4041 Health 19, suppl. 1:45-49.
4042 Barregård, L., Sallsten, G., Conradi, N., 1999. Tissue levels of. mercury determined in. a. deceased
4043 worker after. occupational exposure. Int. Arch. Occup. Environ. Health 72:169-173.
4044 Barregård, L., Sallsten, G., Schutz, A., Attewell, R., Skerfving, S., Jarvholm, B., 1992. Kinetics of.
4045 mercury in. blood. and. urine. after. brief. occupational exposure. Arch. Environ. Health 47:176-184.
4046 Barrett, H.M., Irwin, D.A. and Semmons, E., 1947. Studies on. the. toxicity of. inhaled cadmium. I. The.
4047 acute. toxicity of. cadmium oxide. by. inhalation. J. Ind. Hyg. Toxicol 29: 279–285.
4048 Baruthio, F., Guillard, O., Arnaud, J., Pierre, F., Zawislak, R. 1988. Determination of. manganese in.
4049 biological materials by. electrothermal atomic absorption spectrometry: A. review. Clin. Chem. 34,
4050 227-34.
4051 Basse-Cathalinat, B., Blanquet, P., Collignon, G., Mirande-Iriberry, J., 1968. Bone. scintigraphy with.
4052 47Sc and. the. scintillation camera. J. Nucl. Med. 9, 436-438.
4053 Bau, M. and Dulski, P., 1995. Comparative study. of. yttrium and. rare-earth element behaviours in.
4054 fluorine-rich hydrothermal fluids. Contributions to. Mineralogy and. Petrology 119: 213–223.
4055 Beamish, M.R. and Brown, E.B., 1974. The. metabolism of. transferrin-bound 111In and. 59Fe in. rat.
4056 Blood. 43: 693–701.
4057 Becker, K., Schulz, C., Kaus, S., et al., 2003. German Environmental Survey 1998 (GerES III):
4058 Environmental pollutants in. the. urine. of. the. German population. International Journal of.
4059 Hygiene and. Environmental Health 206(1): 15–24. DOI: 10.1078/1438-4639-00188.
4060 Begerow, J., Neuendorf, J., Turfeld, M., et al., 1999. Long-term urinary platinum, palladium, and. gold.
4061 excretion of. patients after. insertion of. noble-metal dental alloys. Biomarkers 4(1): 27–36. DOI:
4062 10.1080/135475099230976.
4063 Begerow, J., Sensen, U., Wiesmüller, G.A., et al., 1999. Internal platinum, palladium, and. gold.
4064 exposure in. environmentally and. occupationally exposed persons. Zentralblatt für Hygiene und.
4065 Umweltmedizin = International journal of. hygiene and. environmental medicine 202(5): 411–424.
4066 Bell, M.C. and Sneed, N.N., 1970. Metabolism of. tungsten by. sheep. and. swine. In: Mills. CF. (ed.)
4067 Trace. Element Metabolism in. Animals. E&S. Livingstone. Edinburgh, pp. 70–72.
4068 Bello, D. and Warheit, D.B., 2017. Biokinetics of. engineered nano-TiO2 in. rats. administered by.
4069 different exposure routes: Implications for. human. health. Nanotechnology 11: 431–433.
4070 Benoy, C.J., Hooper, P.A. and Schneider, R., 1971. The. toxicity of. tin. in. canned fruit. juices and.
4071 solid. foods. Food. and. Cosmetics Toxicology 9: 645–656.
4072 Beresford, N.A., Mayes, R.W., Crout, N.M.J., et al., 1994. Dynamic behaviour of. 110mAg in. sheep.
4073 tissues. Health Physics 66: 420–426.

4074 Berg, H.F., 1951. Localization of. radioactivity of. colloidal gold198 (a preliminary report. AMA. Arch.
4075 Surg. 63: 545–553.
4076 Berg, H.F., Christopherson, W.M. and Bryant, J.R., 1954. Time. and. site. study. for. optimum lymph.
4077 node. concentration of. radiogold following intrabronchial injection. Cancer Res. 4. Berg, H.F.
4078 Christopherson, W.M. Bryant, J.,R: 775–779.
4079 Berger, C. D., Lane, B. H., Hamrick, T., 1983. Clearance of. 202Tl contaminate following intravenous
4080 injection of. 201Tl. Health Phys. 45:999-1001.
4081 Berger, C.D., Lane, B.H. and Hamrick, T., 1983. Clearance of. 202Tl contaminate following
4082 intravenous injection of. 201Tl. Health Phys. 45: 999–1001.
4083 Bergstrom, W. H. 1955. The. participation of. bone. in. total. body. sodium metabolism in. the. rat. J.
4084 Clin. Invest. 34:997-1004.
4085 Bergstrom, W.H., 1955. The. participation of. bone. in. total. body. sodium metabolism in. the. rat. J.
4086 Clin. Invest 34: 997–1004.
4087 Berlin, M. 1986. Mercury. In: Friberg, L. Nordberg, G. F. Vouk, V. B. eds. Handbook of. the.
4088 toxicology of. metals, Vol. II. New. York: Elsevier, pp. 387-445.
4089 Berlin, M., 1986. Mercury. In: Friberg L. Nordberg GF, and. Vouk. VB. (eds) Handbook of. the.
4090 toxicology of. metals. New. York: Elsevier, pp. 387–445.
4091 Berlin, M., Fazackerley, J. and Nordberg, G., 1969. The. uptake of. mercury in. the. brains of. mammals
4092 exposed to. mercury vapour and. to. mercuric salts. Arch. Environ. Health 18: 719–729.
4093 Berlin, M., Jerksell, L.G. and Ubisch, H., 1966. Uptake and. retention of. mercury in. the. mouse. brain.
4094 Arch. Environ. Health 12: 33–42.
4095 Berlin, M., Fazackerley, J., Nordberg, G., 1969. The. uptake of. mercury in. the. brains of. mammals
4096 exposed to. mercury vapor. and. to. mercuric salts. Arch. Environ. Health 18:719-729.
4097 Berlin, M., Jerksell, L. G., von Ubisch, H., 1966. Uptake and. retention of. mercury in. the. mouse. brain.
4098 Arch. Environ. Health 12:33-42.
4099 Berlin, M.H., Nordberg, G.F. and Serenium, F., 1969. On. the. site. and. mechanism of. mercury vapour
4100 resorption in. the. lung. A. study. in. the. guinea pig. using. mercuric nitrate Hg-203. Arch. Environ.
4101 Health 18: 43–50.
4102 Berlyne, G. M., Ben Ari, J., Knopf, E., Yagil, R., Weinberger, G., Danovitch, G. M., 1972. Aluminium
4103 toxicity in. rats. Lancet 299: 564-568.
4104 Berlyne, G.M., Ben, Ari, J., Knopf, E., et al., 1972. Aluminium toxicity in. rats. Lancet 299: 564–568.
4105 Berlyne, G.M., Shainkin-Kestenbaum, R., Yagil, R., Alfassi, Z., Kushelevsky, A., Etzion, Z., 1986.
4106 Distribution of. 31silicon-labeled silicic acid. in. the. rat. Biol. Trace. Elem. Res. 10, 159-162.
4107 Berlyne, G.M., Shainkin-Kestenbaum, R., Yagil, R., et al., 1986. Distribution of. 31silicon-labeled
4108 silicic acid. in. the. rat. Biol. Trace. Elem. Res. 10: 159–162.
4109 Bernstein, L.R., 1998. Mechanisms of. therapeutic activity for. gallium. Pharmacological Reviews 50,
4110 665-682.
4111 Bernstein, L.R., 1998. Mechanisms of. therapeutic activity for. gallium. Pharmacological Reviews 50:
4112 665–682.
4113 Berry, J.P. and Galle, P., 1992. Preferential localization of. hafnium in. nodular lymphatic cells. Study.
4114 by. electron microprobe. Journal of. Submicroscopic Cytology and. Pathology 24: 15–18.
4115 Bertinato, J., Plouffe, L.J., Lavergne, C., et al., 2014 Bioavailability of. magnesium from. inorganic and.
4116 organic compounds is. not. affected in. rats. fed. a. high. phytic acid. diet. Magnes Res. 27(4): 175–
4117 85.
4118 Bettley, F.R. and O'Shea, J.A., 1975. The. absorption of. arsenic and. its. relation to. carcinoma. British
4119 Journal of. Dermatology 92: 563–568.
4120 Bianco, A., Bassi, P., Belvisi, M., et al., 1980. Inhalation of. a. radioactively labelled monodisperse
4121 aerosol in. rats. for. the. assessment of. regional deposition and. clearance. Am. Ind. Hyg. Ass. J.
4122 41(8): 563–567.
4123 Black, D. A. K., Davies, H. E. F., Emery, E. W., 1955. The. disposal of. radioactive potassium injected
4124 intravenously. Lancet 265:1097-1099.
4125 Blanchardon, E., Challeton-de Vathaire, C., Boisson, P., Celier, D., Martin, J. C., Casso, S., Herbelet,
4126 G., Franck, D., Jourdain, J. R., Biau, A., 2005. Long. term. retention and. excretion of. 201Tl in. a.
4127 patient after. myocardial perfusion imagingRadiat. Prot. Dosim. 113:47-53.

Block, W. D., Buchanan, O. H., Freyberg, R. H., 1942. Metabolism, toxicity and. manner of. action of. gold. compounds used. in. the. treatment of. arthritis. IV. Studies of. the. absorption, distribution and. excretion of. gold. following the. intramuscular injection of. gold. thioglucose and. gold. calcium thiomalate. J. Pharmacol. Exp. Ther. 76:355-357.

Block, W. D., Buchanan, O. H., Freyberg, R. H., 1944. Metabolism, toxicity and. manner of. action of. gold. compounds used. in. the. treatment of. arthritis. V. A. comparative study. of. the. rate. of. absorption, the. retention, and. the. rate. of. excretion of. gold. administered in. different compounds. J. Pharmacol. Exp. Ther. 82:391-398.

Bockman, R. S., Boskey, A. L., Blumenthal, N. C. Alcock, N. W., Walrrell, R. P., 1986. Gallium increases bone. calcium and. crystallite perfection of. hydroxyapatite. Calcif. Tissue Int. 39:376-381.

Bockman, R. S., Repo, M. A., Warrell, R. P., Pounds, J. G., Schidlovsky, G., Gordon, B. M., Jones, K. W., 1990. Distribution of. trace. levels of. therapeutic gallium in. bone. as. mapped by. synchroton x-ray microscopy. Proc. Natl. Acad. Sci. 87:4149-4153.

Böckmann, J., Lahl, H., Eckert, T., et al., 2000. Titan-Blutspiegel vor. und. nach. Belastungsversuchen mit. Titandioxid. Pharmazie 55: 140–143.

Bogden, J.D., Higashino, H., Lavenhar, M.A., et al., 1982. Balance and. tissue distribution of. vanadium after. short-term ingestion of. vanadate. Journal of. Nutrition 112: 2279–2285.

Boisset, M., Girard, F., Godin, J., et al., 1978. Cadmium content of. lung, liver, and. kidney in. rats. exposed to. cadmium oxide. fumes. Int. Arch. Occup. Environ. Health 41: 41–53.

Bornmann, G., Henke, G., Alfes, H., et al., 1970. Uber. die. Enterlae Resorption von. Metallischem Quecksilber. Archiv für Toxikologie: 203–209.

Bradley-Moore, P. R., Lebowitz, E., Greene, M. W., Atkins, H. L., Ansari, A. N., 1975. Thallium-201 for. medical use, 2. Biologic behaviour. J. Nucl. Med. 16:156-160.

Brandt, J. L., Glaser, W., Jones, A., 1958. Soft-tissue distribution and. plasma disappearance of. intravenously administered isotopic magnesium with. observations on. uptake in. bone. Metab. Clin. Exp.7:355-363.

Breiter, K. and Škoda, R., 2017. Zircon and. whole-rock Zr/Hf ratios as. markers of. the. evolution of. granitic magmas: Examples from. the. Teplice caldera (Czech Republic/Germany). Mineralogy and. Petrology 111(4): 435–457. DOI: 10.1007/s00710-017-0509-z.

Brihaye, C. and Guillaume, M., 1990. 195Au biokinetics and. dosimetry. Eur. J. Nucl. Med. 16: 369–371.

Brown, R. M., Newton, D., Pickford, C. J., Sherlock, J. C., 1990. Human. metabolism of. arsenobetaine ingested with. fish. Human. Exper. Toxicol. 9, 41-46.

Brune, D., Nordberg, G. and Wester, P.O., 1980. Distribution of. 23 elements in. the. kidney, liver. and. lungs. of. workers from. a. smeltery and. refinery in. North. Sweden exposed to. a. number of. elements and. of. a. control group. Sci. Total. Environ 16: 13–35.

Bryant, J.R., Berg, H.F. and Christopherson, W.M., 1953. Localization of. radioactivity in. the. lung. and. the. lymph. nodes. J. Thorac. Surg. 26. Bryant, J.R. Berg, H.F. Christophersen, W.,M: 221–232.

Brzoska, M.M. and Moniuszko-Jakoniuk, J., 2001. Interactions between cadmium and. zinc. in. the. organism. Food. Chem. Toxicol 39: 967–980.

Buchet, J.P., Lauwerys, R. and Roels, H., 1981a. Comparison of. the. urinary excretion of. arsenic metabolites after. a. single oral. dose. of. sodium arsenite, monomethylarsonate, or. dimethylarsinate in. man. Int. Arch. Occup. Environ. Health 48: 71–79.

Buchet, J.P., Lauwerys, R. and Roels, H., 1981b. Urinary excretion of. inorganic arsenic and. its. metabolites after. repeated ingestion of. sodium metaarsenite by. volunteers. International Archives of. Occupational and. Environmental Health 48: 111–118.

Bugryshev, P.F., Moskalev, Y.I. and Nozarova, V.A., 1974. Effect of. an. isotope carrier (9Be) on. the. distortion of. the. 7Be in. the. organs and. tissues of. rats. Gig. Sanit. 6: 43–47.

Bugryshev, P.F., Zaikina, T.I. and Moskalev, I.I., 1984. Absorption of. beryllium from. the. gastrointestinal tract. of. rats. [Vsasyvanie berilliia iz. zheludochno-kishechnogo trakta krysy. Meditsina Truda. I. Promyshlennaya Ekologiya 6: 52–53.

Burch, G.E., Threefoot, S.A. and Ray, C.T., 1955. The. rate. of. disappearance of. Rb-86 from. the. plasma, the. biologic decay. rates. of. Rb-86, and. the. applicability of. Rb-86 as. a. tracer of. potassium in. man. with. and. without chronic congestive heart. failure. J. Lab. Clin. Med. 45: 371–394.

4183 Burkstaller, M.A., Weissman, S.H. and Cuddihy, R.G., 1977. Generation of. selenious acid. aerosols.
4184 In: Inhalation Toxicology Research Institute Annual Report 1976–1977. Albuquerque, New.
4185 Mexico: Lovelace Biomedical and. Environmental Research Institute, pp. 285–288.
4186 Burrill, M.W., Freeman, S. and Ivy, A.C., 1945. Sodium potassium and. chloride excretion of. human.
4187 subjects exposed to. a. simulated altitude of. eighteen thousand feet. Journal of. Biological Chemistry
4188 157: 297–302.
4189 Byrne, A.R. and Kosta, L., 1978. Vanadium in. foods. and. in. human. body. fluids and. tissues. Science
4190 of. the. Total. Environment 10: 17–30.
4191 Calamosca, M. and Pagano, P., 1991. Nasopharyngeal deposition and. retention of. an. insoluble aerosol
4192 by. rats. Radiat. Prot. Dosim. 38(1/3): 35–39.
4193 Callis, G.E. and Wentworth, R.A., 1977. Tungsten vs. molybdenum in. models for. biological system.
4194 Bioinorg. Chem. 7: 57–70.
4195 Callis, G.E., Wentworth, R.A., 1977. Tungsten vs. molybdenum in. models for. biological system.
4196 Bioinorg. Chem. 7, 57-70.
4197 Camner, P., Hellström, P.A. and Lundborg, M., 1973. Coating 5µ particles with. carbon and. metals for.
4198 lung. clearance studies. Archives of. Environmental Health 27: 331–333.
4199 Camner, P.E., Lundborg, M. and Philipson, M.K., 1977. Lung. clearance of. 4-µm particles coated with.
4200 silver, carbon, or. beryllium. Archives of. Environmental Health 32(2): 58–62.
4201 Campbell, B.J., Reinhold, J.G., Cannell, J.J., et al., 1976. The. effects of. prolonged consumption of.
4202 wholemeal bread. upon. metabolism of. calcium, magnesium, zinc. and. phosphorus of. two. young.
4203 American adults. Pahlavi Medical Journal 7: 1–17.
4204 Cardin, C.J. and Mason, J., 1976. Molybdate and. tungstate transfer by. rat. ileum. competitive
4205 inhibition by. sulphate. Biochim. Biophys. Acta. 455: 937–946.
4206 Caroli, S., Alimonti, A., Petrucci, F., et al., 2001. Assessment of. exposure to. platinum-group metals
4207 in. urban. children. Spectrochim Acta. Part. B. 56: 1241 –1248.
4208 Cartwright, G.E. and Wintrobe, M.M., 1964 Copper Metabolism in. Normal Subjects. The. American
4209 Journal of. Clinical Nutrition 14(4). Oxford Academic: 224–232.
4210 Carvalho, S.M. and Ziemer, P.L., 1982. Distribution and. clearance of. 63Ni administered in. the. rat:
4211 intratracheal study. Archives of. environmental contamination and. toxicology 11: 245–248.
4212 Castronovo, F.P. and Wagner, H.N., 1971. Factors affecting the. toxicity of. the. element indium. British
4213 Journal of. Experimental Pathology 52: 543–559.
4214 Castronovo, Jr. F.P. and Wagner, Jr. H.N., 1973. Comparative toxicity and. pharmacodynamics of. ionic.
4215 indium chloride and. hydrated indium oxide. Journal of. Nuclear Medicine 14(9): 677–682.
4216 Chapman, AC, 1926. On. the. presence of. compounds of. arsenic in. marine crustaceans and. shellfish.
4217 Analyst 51, 548-563.
4218 Charkes, N.D., Makler, P.T. and Philips, C., 1978. Studies of. skeletal tracer kinetics. I. digital-computer
4219 solution of. a. five-compartment model. of. [18F] fluoride kinetics in. humans. Journal of. Nuclear
4220 Medicine 19: 1301–1309.
4221 Chauncey, D.M., Schelbert, H.R., Halpern, S.E., Delano, F., McKegney, M.L., Ashburn, W.L., Hagan,
4222 P.L. 1977. Tissue distribution studies with. radioactive manganese: A. potential agent. for.
4223 myocardial imaging. J. Nucl. Med. 18, 933-6.
4224 Chen, C. T., Lathrop, K. A., Harper, P. V., Bartlett, R. D., Stark V. J., Fultz, K. R., Faulhaber, P. F.,
4225 1983. Quantitative measurement of. long-term in. vivo. thallium distribution in. the. human. J. Nucl.
4226 Med. 24:50.
4227 Cherian, M. G., Hursh, J. B., Clarkson, T. W., Allen, J., 1978. Radioactive mercury distribution in.
4228 biological fluids and. excretion in. human. subjects after. inhalation of. mercury vapor. Arch.
4229 Environ. Health 33:109-114.
4230 Chertok, R. J., Lake, S., 1971a. Availability in. the. peccary pig. of. radionuclides in. nuclear debris
4231 from. the. plowshare excavation buggy. Health Phys. 20:313-316.
4232 Chertok, R. J., Lake, S. 1971b. Biological availability of. radionuclides produced by. the. plowshare
4233 event. schooner I. Body. distribution in. domestic pigs. exposed in. the. field. Health Phys. 20:317-
4234 324.
4235 Chertok, R. J., Lake, S., 1971c. Biological availability of. radionuclides produced by. the. plowshare
4236 event. schooner II. Retention and. excretion rates. in. peccaries after. a. single oral. dose. of. debris.
4237 Health Phys. 20:325-330.

4238 Chertok, R.J. and Lake, S., 1971d. Biological availability of. radionuclides produced by. the. plowshare
4239 event. schooner-III. Accumulation, excretion rates. and. body. distribution in. peccaries after. daily.
4240 ingestion of. debris. Health Physics 20: 577–584.
4241 Cheryan, M., 1980. Phytic acid. interactions in. food. systems. Critical Reviews in. Food. Science and.
4242 Nutrition 13: 297–335.
4243 Chiba, M., Shinohara, A. and Ujiie, C., 1991. Tin. concentrations in. various organs in. humans, dogs,
4244 and. mice. Biomed. Trace. Element Res. 2: 257–258.
4245 Chou, T. and Adolph, W.H., 1935. Copper metabolism in. man. Biochem J. 29: 476–479.
4246 Christensen, J.M., Holst, E., Bonde, J.P., Knudsen, L., 1993. Determination of. Chromium in. Blood.
4247 and. Serum: Evaluation of. Quality Control Procedures and. Estimation of. Reference Values in.
4248 Danish Subjects. Science of. the. Total. Environment. 132(1), 11-25.
4249 Christie, H., MacKay, R.J. and Fisher, A.M., 1963. Pulmonary effects of. inhalation of. aluminium by.
4250 rats. and. hamsters. Am. Ind. Hyg. J. 24: 47–56.
4251 Cima, F., 2011. Tin: Environmental pollution and. health effects. In: Nriagu JO. (ed.) Encylopedia of.
4252 Environmental Health. London: Elsevier, pp. 351–359.
4253 Ciosek,, Z., Kot, K., Rotter, I. 2023. Iron, zinc, copper, cadmium, mercury, and. bone. tissue. Int. J.
4254 Environ. Res. Public Health 20:2197.
4255 Clarkson, T. and Rothstein, A., 1964. The. excretion of. volatile mercury by. rats. injected with.
4256 mercuric salts. Health Phys. 10: 1115–1121.
4257 Clarkson, T. W., 1997. The. toxicology of. mercury. Critical Rev. Clin. Lab. Sci. 34:369-403.
4258 Clarkson, T., Rothstein, A., 1964. The. excretion of. volatile mercury by. rats. injected with. mercuric
4259 salts. Health Phys. 10:1115-1121.
4260 Clarkson, T.W., 1997. The. toxicology of. mercury. Critical Rev. Clin. Lab. Sci. 34: 369–403.
4261 Coates, G., Gilday, D.L., Cradduck, T.D., et al., 1973. Measurement of. the. rate. of. stomach emptying
4262 using. Indium-113m and. a. 10-crystal rectilinear scanner. Canadian Medical Association Journal
4263 108: 180–183.
4264 Cobb, L.M., Harrison, A. and Butler, S.A., 1988. Toxicity of. 211At in. the. mouse. Human. Toxicol 7:
4265 529–534.
4266 Cochran, K.W., Doull, J., Mazur, M., et al., 1950. Acute. toxicity of. zirconium, columbium, strontium,
4267 lanthanum, caesium, tantalum and. yttrium. Archives of. Industrial Hygiene and. Occupational
4268 Medicine 1(6): 637–50.
4269 Colombo, C., Monhemius, A.J. and Plant, J.A., 2008. The. estimation of. the. bioavailabilities of.
4270 platinum, palladium and. rhodium in. vehicle exhaust catalysts and. road. dusts. using. a.
4271 physiologically based. extraction test. Science of. the. Total. Environment 389(1): 46–51.
4272 Conklin, A.W., Skinner, S.C., Felten, T.L., et al., 1982. Clearance and. distribution of. intratracheally
4273 instilled vanadium-48 compounds in. the. rat. Toxicology Letters 11: 199–203.
4274 Cooper, J.R., 1985. The. influence of. speciation on. the. gastrointestinal absorption of. elements. In:
4275 Bulman RA. and. Cooper JR. (eds) Speciation of. Fission and. Activation Products in. the.
4276 Environment. London: Elsevier, pp. 162–174.
4277 Corsa, L., Olney, J.M., Steenburg, R.W., et al., 1950. The. measurement of. exchangeable potassium in.
4278 man. by. isotope dilution. J. Clin. Invest 29: 1280–1295.
4279 Costeas, R., Woodard, H.Q. and Laughlin, J.S., 1970. Depletion of. 18F from. blood. flowing through
4280 bone. Journal of. Nuclear Medicine 11: 43–45.
4281 Cotzias, G.C., Borg, D.C. and Selleck, B., 1961. Virtual absence of. turnover in. cadmium metabolism:
4282 109Cd studies in. the. mouse. Am. J. Physiol 201: 927–930.
4283 Coudray, C., Rambeau M., Feillet-Coudray C., et al. 2005. Study. of. magnesium bioavailability from.
4284 ten. organic and. inorganic Mg. salts. in. Mg-depleted rats. using. a. stable isotope approach.
4285 Magnesium Res. 18(4):215–223.
4286 Crecelius, E.A., 1977. Changes in. the. chemical speciation of. arsenic following ingestion by. man.
4287 Environ. Health Perspect. 19:147–150.
4288 Cromwell, G.L. 1997. Copper as. a. nutrient for. animals. In: Richardson H.W. editor. Handbook of.
4289 Copper Compounds and. Applications. New. York: Marcel Dekker. p. 177–202.
4290 Curran, G.L., Costello R.L. 1956. Reduction of. excess cholesterol in. the. rabbit aorta. by. inhibition
4291 of. endogenous cholesterol synthesis. J. Exp. Med. 103:49–56.

4292 Curran, G.L., Azarnoff D.L., Bolinger R.E. 1959. Effect of. cholesterol synthesis inhibition in.
4293 normocholesteremic young. men. J. Clin. Invest. 38:1251–1261.
4294 Dadachova, E., Bouzahzah B., Zuckier L.S., Pestell R.G., 2002. Rhenium-188 as. an. alternative to.
4295 iodine-131 for. treatment of. breast tumors expressing the. sodium/iodide symporter (NIS). Nucl.
4296 Med. Biol. 29:13–18.
4297 Dainty, J.R., 2001. Use. of. stable isotopes and. mathematical modelling to. investigate human. mineral
4298 metabolism. Nutr. Res. Rev. 14:295–315.
4299 Dastur, D.K., Manghani D.K., Raghavendran K.V. 1969. Distribution and. fate. of. 54Mn in. the. rat,
4300 with. special reference to. the. CNS. Q. J. Exp. Physiol. 54:322–331.
4301 Dastur, D.K., Manghani D.K., Raghavendran K.V. 1971. Distribution and. fate. of. 54Mn in. the.
4302 monkey: studies of. different parts. of. the. central nervous system and. other. organs. J. Clin. Invest.
4303 50:9–20.
4304 Datz, F., Taylor A., 1985. The. clinical use. of. radionuclide bone. marrow imaging. Semin. Nucl. Med.
4305 15(3).
4306 Davidsson, L., Cederblad Å., Lönnerdal B., et al. 1989. Manganese retention in. man: a. method for.
4307 estimating manganese absorption in. man. Am. J. Clin. Nutr. 49(1):170–179.
4308 Demigné C., Sabboh H., Rémésy C., et al. 2004. Protective effects of. high. dietary potassium:
4309 nutritional and. metabolic aspects. J. Nutr. 134:2903–2906.
4310 Deutsch, E., Libson K., Vanderheyden J.L., Ketring A.R., Maxon H.R. 1986. The. chemistry of.
4311 rhenium and. technetium as. related to. the. use. of. isotopes of. these. elements in. therapeutic and.
4312 diagnostic nuclear medicine. Int. J. Radiat. Appl. Instrum. B. 13:465–477.
4313 DeVoto, E., Yokel R.A., 1994. The. biological speciation and. toxicokinetics of. aluminum. Environ.
4314 Health Perspect. 102:940–951.
4315 Dimond, E.G., Caravaca J., Benchimol A. 1963. Vanadium: excretion, toxicity, lipid. effect in. man.
4316 Am. J. Clin. Nutr. 12:49–53.
4317 Doisy, R.J., Streeten D.H.P., Souma M.L., et al. 1971. Metabolism of. 51Chromium in. human. subjects
4318 / normal, elderly, and. diabetic subjects. In: Newer. Trace. Elements in. Nutrition. p. 155–168.
4319 Dorman, D.C., Struve M.F., Wong B.A., 2001. Factors that. influence manganese delivery to. the. brain.
4320 Centers Health Res. CIIT. Activities 21(7–8).
4321 Dorman, D.C., Struve M.F., Marshall M.W., Parkinson C.U., James R.A., Wong B.A., 2006. Tissue
4322 manganese concentrations in. young. male. rhesus monkeys following subchronic manganese sulfate
4323 inhalation. Toxicol. Sci. 92:201–210.
4324 Dorner, K., Dziadzka S., Hohn A., et al. 1989. Longitudinal manganese and. copper balances in. young.
4325 infants and. preterm infants fed. on. breast-milk and. adapted cow's milk. formulas. Br. J. Nutr.
4326 61:559–572.
4327 Doull, J., Dubois K.P., 1949. Metabolism and. toxicity of. radioactive tantalum, Part. 2. In: Quarterly
4328 Progress Report Number Two. University of. Chicago Toxicity Laboratory. p. 12.
4329 Downey, H.F., Bashour F.A., 1975. Dynamics of. tissue distribution of. radiopotassium as. affected by.
4330 simulated differences in. regional extraction. Cardiovasc. Res. 9:607–612.
4331 Drasch, G., Muss C., Roider G. 2000. Gold. and. palladium burden from. dental restoration materials.
4332 J. Trace. Elem. Med. Biol. 14(2):71–75.
4333 Ducoff, H.S., Neal W.B., Straube R.L., Jacobson L.O., Brues A.M., 1948. Biological studies with.
4334 arsenic-76. II. Excretion and. tissue localization. Proc. Soc. Exp. Biol. Med. 69(3):548–554.
4335 Ducoulombier-Crépineau C., Feidt C., Rychen G., 2007. Platinum and. palladium transfer to. milk,
4336 organs and. tissues after. a. single oral. administration to. lactating goats. Chemosphere 68:712–715.
4337 Dudley, H.C., Levine M.D. 1949. Studies of. the. toxic. action of. gallium. J. Pharmacol. Exp. Ther.
4338 95:487–493.
4339 Dunn, M.A., Green M.H., Leach R.M. 1991. Kinetics of. copper metabolism in. rats: a. compartmental
4340 model. Am. J. Physiol. 261:E115–E125.
4341 Durbin, P.W., 1960. Metabolic characteristics within a. chemical family. Health Phys. 2:225–238.
4342 Durbin, P.W., Scott K.G., Hamilton J.G., 1957. Distribution of. radioisotopes of. some. heavy. metals
4343 in. the. rat. Univ. Calif. Publ. Pharmacol. 3(1):1–34.
4344 Edvardsson, K.A., 1971. Case. studies of. elimination of. radioactive contaminants observed at.
4345 Studsvik between 1963 and. 1970. In: Assessment of. Radioactive Contamination in. Man. Proc.
4346 Symp. Stockholm 22–26 November 1971, Stockholm, IAEA. Vienna.

EFSA. 2009. Scientific opinion of. the. Panel. on. Food. Additives and. Nutrient Sources added. to. Food. on. choline-stabilised orthosilicic acid. added. for. nutritional purposes to. food. supplements following a. request from. the. European Commission. EFSA. Journal. 948:1–23.
EFSA. 2011. On. the. evaluation of. a. new. study. related to. the. bioavailability of. aluminium in. food. EFSA. Journal. 9(5):2157.
EFSA. 2012. Scientific opinion on. the. risk. for. public health related to. the. presence of. mercury and. methylmercury in. food. EFSA. Journal. 10(12):2985. https://doi.org/10.2903/j.efsa.2012.2985
EFSA. 2013. Scientific opinion on. dietary reference values for. manganese. EFSA. Journal. 11(11):3419. https://doi.org/10.2903/j.efsa.2013.3419
EFSA. 2014. Scientific opinion on. the. risks. to. public health related to. the. presence of. chromium in. food. and. drinking water. EFSA. Journal. 12(3):3595.
EFSA. 2015a. Scientific opinion on. dietary reference values for. copper. EFSA. Journal. 13(10):4253.
EFSA. 2015b. Scientific opinion on. dietary reference values for. magnesium. EFSA. Journal. 13(7):4186. https://doi.org/10.2903/j.efsa.2015.4186
EFSA. 2015c. Scientific opinion on. risks. for. public health related to. the. presence of. chlorate in. food. EFSA. Journal. 13(6):4135. https://doi.org/10.2903/j.efsa.2015.4186
EFSA. 2016. Scientific opinion on. the. re-evaluation of. titanium dioxide (E. 171) as. a. food. additive. EFSA. Journal. 14(9):4253.
EFSA. 2018a. Scientific opinion on. the. re-evaluation of. calcium silicate. EFSA. Journal. 16(8):5375.
EFSA. 2018b. Scientific opinion on. the. re-evaluation of. silicon dioxide (E. 551) as. a. food. additive. EFSA. Journal. 16(1):5088.
Ekman, L., Figueiras HD, Jones BEV, et al. 1977. Metabolism of. 181W-labelled sodium tungstate in. goats. FOA. Report C. 40070 A3. Sundbyberg, Sweden: Foersvarets Forskningsanstalt.
Elgrabli, D., Beaudouin R., Jbilou N., et al. 2015. Biodistribution and. clearance of. TiO2 nanoparticles in. rats. after. intravenous injection. PLoS. One. 10(5):e0124490.
Elin, RJ. 1987. Assessment of. magnesium status. Clin. Chem. 33(11):1965–1970.
Elinder, CG, Ahrengart L., Lidums V., et al. 1991. Evidence of. aluminium accumulation in. aluminium welders. Br. J. Ind. Med. 48(11):735–738.
Elinder, CG, Friberg L., Lind B., et al. 1983. Lead. and. cadmium levels in. blood. samples from. the. general population Sweden. Environ Res. 30(2):233–253.
Elinder, CG, Kjellström T., Friberg L., et al. 1976. Cadmium in. kidney cortex, liver. and. pancreas, from. Swedish autopsies. Arch. Environ Health. 31(6):292–302.
El-Masri, HA, Kenyon EM. 2008. Development of. a. human. physiologically based. pharmacokinetic (PBPK) model. for. inorganic arsenic and. its. mono- and. di-methylated metabolites. J. Pharmacokinet Pharmacodyn. 35(1):31–68
Emery, EW, Holmes R., Davies HE, et al. 1955. Renal. uptake of. radioactive potassium. Clin. Sci. 14(2):241–244.
Ensslin, AS, Huber R., Pethran A., et al. 1997. Biological monitoring of. hospital pharmacy personnel occupationally exposed to. cytostatic drugs: urinary excretion and. cytogenetics studies. Int. Arch. Occup. Environ Health. 70(3):205–208.
Erck, A., Sherwood E., Bear JL, et al. 1976. The. metabolism of. rhodium(II) acetate in. tumor-bearing mice. Cancer Res. 36:2204–2209.
Fabian, E., Landsiedel R., Ma-Hock L., et al. 2008. Tissue distribution and. toxicity of. intravenously administered titanium dioxide nanoparticles in. rats. Arch. Toxicol. 82:151–157.
Farrar, G., Morton AP, Blair JA. 1987. The. intestinal absorption and. tissue distribution of. aluminium, gallium and. scandium: a. comparative study. Biochem Soc. Trans. 15(6):1164–1165.
Finch, GL, Mewhinney JA, Hoover MD, Eidson AF, Haley PJ, Bice DE. 1990. Clearance, translocation, and. excretion of. beryllium following acute. inhalation of. beryllium oxide. by. beagle dogs. Fundam Appl. Toxicol. 15(2):231–241. https://doi.org/10.1016/0272-0590(90)90050-T.
Finley, JW. 1999. Manganese absorption and. retention by. young. women. is. associated with. serum. ferritin concentration. Am. J. Clin. Nutr. 70:37–43.
Finley, JW, Johnson PE, Johnson LK. 1994. Sex. affects manganese absorption and. retention by. humans from. a. diet. adequate in. manganese. Am. J. Clin. Nutr. 60:949–955.
Firoz, M., Graber M., 2001. Bioavailability of. US. commercial magnesium preparations. Magnes Res. 14:257–262.

4402 Fleshman, D., Krotz S., Silva A., 1966. The. metabolism of. elements of. high. atomic number. UCRL.
4403 14739:69–86.
4404 Fleshman, DG, Silva AJ, Shore B., 1971. The. metabolism of. tantalum in. the. rat. Health Phys. 21:385–
4405 392.
4406 Flynn, MA, Woodruff C., Clark J., Chase G., 1972. Total. body. potassium in. normal children. Pediatr
4407 Res. 6:239–245.
4408 Food, and Agriculture Organization of the United Nations, World Health Organization, FAO Panel of
4409 Experts on Pesticide Residues in Food and the Environment, et al. 1989. Bromide ion. In: Pesticide
4410 Residues in. Food: 1988 Evaluations (Toxicology, Part. 2). Rome: FAO. Available at:
4411 https://apps.who.int/iris/handle/10665/38225
4412 Forbes, GB, McCoord A., 1969. Long-term behaviour of. radiosodium in. bone: comparison with.
4413 radiocalcium and. effects of. various procedures. Calcif Tissue Res. 4:113–128.
4414 Francesconi, KA, Tanggaard R., McKenzie CJ, Goessler W., 2002. Arsenic metabolites in. human.
4415 urine. after. ingestion of. an. arsenosugar. Clin. Chem. 48(1):92–101.
4416 Freed, BR, Woodard HQ, Laughlin JS. 1975. Kinetics of. 47Sc generated by. decay. of. 47Ca in. vivo.
4417 Health Phys. 29:90.
4418 Freeman, HC, Uthe JF, Fleming RB, Odense PH, Ackman RG, Landry G., Musial C., 1979. Clearance
4419 of. arsenic ingested by. man. from. arsenic contaminated fish. Bull. Environ Contam Toxicol.
4420 22:224–229.
4421 Freyberg, RH, Block WD, Levey S., 1942. Metabolism, toxicity and. manner of. action of. gold.
4422 compounds used. in. the. treatment of. arthritis. III. Complete excretion studies and. comparison of.
4423 intravenous and. intramuscular administration of. some. gold. salts. Ann. Rheum. Dis. 3:77–89.
4424 Friberg, L., 1984. Cadmium and. the. kidney. Environ Health Perspect. 54:1–11.
4425 Friberg, L., Piscator M., Nordberg GF, et al. 1974. Cadmium in. the. Environment, 2nd ed. Boca. Raton,
4426 FL: CRC. Press.
4427 Fritsch, P., de Saint Blanquat G., Derache R., 1977. Effect of. various dietary components on. absorption
4428 and. tissue distribution of. orally administered inorganic tin. in. rats. Food. Cosmet Toxicol. 15:147–
4429 149.
4430 Froment, DH, Buddington B., Miller NL, et al. 1989. Effect of. solubility on. the. gastrointestinal
4431 absorption of. aluminum from. various aluminum compounds in. the. rat. J. Lab. Clin. Med.
4432 114:237–242.
4433 Fukayama, MY, Tan H., Wheeler WB, et al. 1986. Reactions of. aqueous chlorine and. chlorine dioxide
4434 with. model. food. compounds. Environ Health Perspect. 69:267–274.
4435 Furchner, JE, Drake GA. 1976. Comparative metabolism of. radionuclides in. mammals – XI. Retention
4436 of. 113Sn in. the. mouse, rat, monkey and. dog. Health Phys. 31:219–224.
4437 Furchner, JE, Richmond CR, London JE. 1973. Comparative metabolism of. radionuclides in. mammals.
4438 VIII. Retention of. beryllium in. the. mouse, rat, monkey and. dog. Health Phys. 24:293–300.
4439 Furchner, JE, London JE, Wilson JS. 1975. Comparative metabolism of. radionuclides in. mammals–
4440 IX. Retention of. 7SSe in. the. mouse, rat, monkey and. dog. Health Phys. 29:641–648.
4441 Furchner, JE, Richmond CR, Drake GA. 1966. Comparative metabolism of. radionuclides in. mammals
4442 – III. Retention of. manganese-54 in. the. mouse, rat, monkey and. dog. Health Phys. 12:1415–1423.
4443 Furchner, JE, Richmond CR, Drake GA. 1971. Comparative metabolism of. radionuclides in.
4444 mammals—V. Retention of. 192Ir in. the. mouse, rat, monkey and. dog. Health Phys. 20:375–382.
4445 Gabler, WL. Absorption of fluoride through the oral mucosa of rats. Arch Oral Biol. 1968,13:619–623.
4446 Garcia, F., Ortega A., Domingo JL, et al. Accumulation of metals in autopsy tissues of subjects living
4447 in Tarragona country, Spain. J. Environ Sci Health A., 2001,36:1767–1786.
4448 Garg, PK, Harrison CL, Zalutsky MR. Comparative tissue distribution in mice of the α-emitter 211At
4449 and. 131I as. labels of. monoclonal antibody and. F(ab')2 fragment. Cancer Res. 1990,50:3514–
4450 3520.
4451 Gehring, PJ, Hammond PB. The interrelationship between thallium and potassium in animals. J.,
4452 Pharmacol Exp Ther. 1967,155:187–201.
4453 Geraets, L., Oomen A., Krystek P., et al. Tissue distribution and elimination after oral and intravenous
4454 administration of different titanium dioxide nanoparticles in rats. Part Fibre Toxicol. 2014,11:30.
4455 Gettler, AO, Weiss L. Thallium poisoning III. Clinical toxicology of thallium. Am J., Clin Pathol.
4456 1943,13:422–429.

4457 Ginsburg, JM, Wilde WS. Distribution kinetics of intravenous radiopotassium. Am J., Physiol.
4458 1954,179:63–75.
4459 Ginsburg, JM. Equilibration of potassium in blood and tissues. Dig Dis Sci. 1962,7:34–42.
4460 Gitelman, HJ. Aluminum exposure and excretion. Sci Total Environ. 1995,163:129–135.
4461 Gitelman, HJ, Alderman FR, Kurs-Lasky M., et al. Serum and urinary aluminium levels of workers in
4462 the aluminium industry. Ann Occup Hyg. 1995,39:181–191.
4463 Glaser, U., Kloppel H., Hochrainer D., Bioavailability indicators of inhaled cadmium compounds.
4464 Ecotoxicol Environ Saf. 1986,11:261–271.
4465 Golasik, M., Herman M., Olbert M., et al. Toxicokinetics and tissue distribution of titanium in ionic
4466 form after intravenous and oral administration. Toxicol Lett. 2016a,24:56–61.
4467 Golasik, M., Wrobel P., Olbert M., et al. Does titanium in ionic form display a tissue-specific
4468 distribution? Biometals. 2016b,29:487–494.
4469 Gongora, G., Roy M., Gongora R., et al. Méthode utilisée pour l'étude de la réparation de l'épuration
4470 pulmonaire chez l'homme normal, après administration d'aérosols radioactifs. J., Biol Med Nucl.
4471 1973,102:19–26.
4472 Gongora, G., Roy M., Gongora R., et al. Techniques de mesure à long terme de l'épuration pulmonaire
4473 chez l'homme et premiers résultats. In: Réactions bronchopulmonaires aux polluants
4474 atmosphériques: compte rendu du colloque tenu les 18 et. 19 janvier 1974 à Pont-à-Mousson. Paris:
4475 Editions INSERM, 1974. p. 183–192.
4476 Goodwin, DA, Goode R., Brown L., 111-In-labeled transferrin for. the. detection of. tumors. Radiology.
4477 1971,100:175–179.
4478 Gottlieb, NL. Comparison of the kinetics of parenteral and oral gold. Scand J., Rheumatol. 1983,12:10–
4479 14.
4480 Graham, LA, Veatch RL, Kaplan E. Distribution of 75Se-selenomethionine as. influenced by. the. route.
4481 of. administration. J. Nucl. Med. 1971,12:566–569.
4482 Greger, JL. Aluminium metabolism. Annu Rev Nutr. 1993,13:43–63.
4483 Gregus, Z., Klaassen CD. Disposition of metals in rats: a comparative study of faecal, urinary, and
4484 biliary excretion and tissue distribution of eighteen metals. Toxicol Appl Pharmacol. 1986,85:24–
4485 38.
4486 Griffiths, N., Stewart R., Robinson M. The metabolism of seienomethionine in four women. Br J., Nutr.
4487 1976,35:373–383.
4488 Hadley, JG, Conklin AW, Sanders CL. Rapid solubilization and translocation of 109CdO following
4489 pulmonary deposition. Toxicol Appl. Pharmacol. 1980,54:156–160.
4490 Hall, LL, Kilpper RW, Smith FA, et al. Kinetic model of fluoride metabolism in the rabbit. Environ
4491 Res. 1977,14:285–302.
4492 Hambidge, KM, Baum JD. Hair chromium concentrations of human newborn and changes during
4493 infancy. Am J., Clin Nutr. 1972,25:376–379.
4494 Hamilton, EI, Minski MJ, Cleary JJ. The concentration and distribution of some stable elements in
4495 healthy human tissues from the United Kingdom. An environmental study. Sci Total Environ.
4496 1973,1:341–374.
4497 Hamilton, JG, Asling CW, Garrison WM, Scott KG. The accumulation, metabolism and biological
4498 effects of astatine in rats and monkeys. Univ Calif Publ Pharmacol. 1953,2:283–343.
4499 Hamilton, JG, Durbin PW, Parrott ML. Accumulation of 211Astatine by. thyroid gland. in. man. Exp.
4500 Biol. Med. 1954a,86:366–369.
4501 Hamilton, JG, Durbin PW, Parrott ML. The accumulation and destructive action of astatine- 211 (eka-
4502 iodine) in. the. thyroid gland. of. rats. and. monkeys. J. Clin. Endocrinol Metab. 1954b,14:1161–
4503 1178.
4504 Hamilton, JG, Soley MH. A., comparison of the metabolism of iodine and of element 85 (eka-iodine).
4505 Proc. Natl. Acad. Sci. USA. 1940,26:483–489.
4506 Hamilton, JG, Asling CW, Garrison WM, et al. 1953. The. accumulation, metabolism and. biological
4507 effects of. astatine in. rats. and. monkeys. Univ. Calif. Publ. Pharmacol 2:283–343.
4508 Hamilton, JG, Durbin PW, Parrott ML. 1954a. Accumulation of. 211Astatine by. thyroid gland. in. man.
4509 Exp. Biol. Med. 86:366–369.

4510 Hamilton, JG, Durbin PW, Parrott ML. 1954b. The. accumulation and. destructive action of. astatine-
4511 211 (eka-iodine) in. the. thyroid gland. of. rats. and. monkeys. J. Clin. Endocrinol Metab. 14:1161–
4512 1178.
4513 Han, SG, Lee JS, Ahn K., et al. 2015. Size-dependent clearance of. gold. nanoparticles from. lungs. of.
4514 Sprague–Dawley rats. after. short-term inhalation exposure. Arch. Toxicol 89(7):1083–1094.
4515 Hansen, TV, Aaseth J., Alexander J., 1982. The. effect of. chelating agents on. vanadium distribution
4516 in. the. rat. body. and. on. uptake by. human. erythrocytes. Arch. Toxicol 50:195–202.
4517 Hara, T., Freed BR. 1973. Preparation of. carrier-free 47Sc by. chemical separation from. 47Ca and. its.
4518 distribution in. tumor. bearing mice. Int. J. Appl. Radiat Isot. 24:373–376.
4519 Haram, EM, Weberg R., Berstad A. 1987. Urinary excretion of. aluminum after. ingestion of. sucralfate
4520 and. an. aluminum-containing antacid in. man. Scand. J. Gastroenterol 22:615–618.
4521 Harrison, A., Royle L., 1984. Determination of. absorbed dose. to. blood, kidneys, testes and. thyroid
4522 in. mice. injected with. 211At and. comparison of. testes mass. and. sperm. number in. X-irradiated
4523 and. 211At treated mice. Health Phys. 46:377–383.
4524 Harrison, HE, Buting H., Ordway NK, et al. 1947. The. effects and. treatment of. inhalation of. cadmium
4525 chloride in. the. dog. J. Ind. Hyg. Toxicol 29(5):302–314.
4526 Harrison, HN. 1979. Pharmacology of. sulfadiazine silver. Its. attachment to. burned human. and. rat.
4527 skin. and. studies of. gastrointestinal absorption and. extension. Arch. Surg. 114:281–285.
4528 Hart, EB, Steenbock J., Waddell J., et al. 1928. Iron. in. nutrition. VII. Copper as. a. supplement to. iron.
4529 for. hemoglobin building in. the. rat. J. Biol. Chem. 77:797–812.
4530 Hawkins, RA, Sung-Cheng Huang YC, Hoh CK, et al. 1992. Evaluation of. the. skeletal kinetics of.
4531 fluorine-18-fluoride ion. with. PET. J. Nucl. Med. 33:633–642.
4532 Hayes, AD, Rothstein A. 1962. The. metabolism of. inhaled mercury vapor. in. the. rat. studied by.
4533 isotope techniques. J. Pharmacol 38:1–10.
4534 Heck, JD, Costa M., 1982. Surface reduction of. amorphous NiS. particles potentiates their.
4535 phagocytosis and. subsequent induction of. morphological transformation in. Syrian hamster embryo
4536 cells. Cancer Lett. 15:19–26.
4537 Henderson, RF, Reba AH, Pickrell JA. 1979. Early. damage indicators in. the. lung. III. Biochemical
4538 and. cytological response of. the. lung. to. inhaled metal. salts. Toxicol Appl. Pharmacol 50:123–
4539 136.
4540 Higgins, ES, Richert DA, Westerfeld WW. 1956. Molybdenum deficiency and. tungstate inhibition
4541 studies. J. Nutr. 59(4):539–559.
4542 Hiles, RA. 1974. Absorption, distribution and. excretion of. inorganic tin. in. rats. Toxicol Appl.
4543 Pharmacol 27:366–379.
4544 Hill, CH. 1980. Interactions of. vitamin C. with. lead. and. mercury. Ann. NY. Acad. Sci. 355:262–266.
4545 Hiller, MM, Leggett RW. 2020. A. biokinetic model. for. trivalent or. hexavalent chromium in. adult.
4546 humans. J. Radiol Prot. 40:19–39.
4547 Hinderling, PH. 2016. The. pharmacokinetics of. potassium in. humans is. unusual. J. Clin. Pharmacol
4548 56:1212–1220.
4549 Hirunuma, R., Endo K., Enomoto S., et al. 1999. Study. on. the. distribution of. radioactive trace.
4550 elements in. vitamin D-overloaded rats. using. the. multitracer technique. Appl. Radiat Isot. 50:843–
4551 849.
4552 Hirunuma, R., Endo K., Yanaga M., et al. 1997. The. use. of. a. multitracer technique for. the. studies
4553 of. the. uptake and. retention of. trace. elements in. rats. Appl. Radiat Isot. 48:727–733.
4554 Hochrainer, D., Oberdoerster G., Mihm U. 1980. Generation of. NiO. aerosols for. studying lung.
4555 clearance of. Ni. and. its. effect on. lung. function. In: Stöber W. Hochrainer D. editors. Aerosols in.
4556 Science, Medicine and. Technology—Physical and. Chemical Properties of. Aerosols. Gesellschaft
4557 für Aerosolforschung, pp. 259–264.
4558 Hohl, C., Gerisch P., Korschinek G., et al. 1994. Medical application of. 26Al. Nucl. Instrum Methods
4559 Phys. Res. B. 92:478–482.
4560 Holbrook, DJ Jr, Washington ME, Leake HB, et al. 1975. Studies on. the. evaluation of. the. toxicity of.
4561 various salts. of. lead, manganese, platinum, and. palladium. Environ Health Perspect 10:95–101.
4562 Hopkins, LL Jr. 1965. Distribution in. the. rat. of. physiological amounts of. injected 51Cr(III) with.
4563 time. Am. J. Physiol 209(4):731–735.

4564 Hoy, MK, Goldman JD. 2012. Potassium intake of. the. U.S. population: What. we. eat. in. America,
4565 NHANES 2009–2010. Food. Surveys Research Group. Dietary Data. Brief. No. 10. Available at:
4566 http://ars.usda.gov/Services/docs.htm?docid=19476
4567 Hughes, MF. 2002. Arsenic toxicity and. potential mechanisms of. action. Toxicol Lett. 133:1–16.
4568 Hunt, CD, Meacham SL. 2001. Aluminum, boron, calcium, copper, iron, magnesium, manganese,
4569 molybdenum, phosphorus, potassium, sodium, and. zinc: concentrations in. common western foods.
4570 and. estimated daily. intakes by. infants, toddlers, male. and. female adolescents, adults, and. seniors
4571 in. the. United States. J. Am. Diet. Assoc. 101:1058–1060.
4572 Hursh, JB, Clarkson TW, Cherian MG, et al. 1976. Clearance of. mercury (Hg-197, Hg-203) vapor.
4573 inhaled by. human. subjects. Arch. Environ Health 31:302–309.
4574 Hursh, JB, Greenwood MR, Clarkson TW, et al. 1980. The. effect of. ethanol on. the. fate. of. mercury
4575 vapor. inhaled by. man. J. Pharmacol Exp. Ther. 214:520–527.
4576 IARC. 1990. IARC. monographs on. the. evaluation of. carcinogenic risks. to. humans of. chromium,
4577 nickel, and. welding. Lyon, France: World. Health Organization.
4578 ICRP. 1975. Report of. the. Task. Group. on. Reference Man. ICRP. Publication 23. Oxford: Pergamon
4579 Press.
4580 ICRP. 1979a. Limits for. intakes of. radionuclides by. workers, ICRP. Publication 30, Part. 1. Ann.
4581 ICRP. 2(3/4).
4582 ICRP. 1979b. Limits for. intakes of. radionuclides by. workers, ICRP. Publication 30, Supplement to.
4583 Part. 1. Ann. ICRP. 3(1–4).
4584 ICRP. 1980. Limits for. intakes of. radionuclides by. workers, ICRP. Publication 30, Part. 2. Ann. ICRP.
4585 4(3/4).
4586 ICRP. 1981. Limits for. intakes of. radionuclides by. workers, ICRP. Publication 30, Part. 3. Ann. ICRP.
4587 6(2/3).
4588 ICRP. 1988. Limits for. intakes of. radionuclides by. workers: an. addendum. ICRP. Publication 30,
4589 Part. 4. Ann. ICRP. 19(4).
4590 ICRP. 1989. Individual monitoring for. intakes of. radionuclides by. workers. ICRP. Publication 54.
4591 Ann. ICRP. 19(1–3).
4592 ICRP. 1990. Age-dependent doses. to. members of. the. public from. intake of. radionuclides - Part. 1.
4593 ICRP. Publication 56. Ann. ICRP. 20(2).
4594 ICRP. 1993. Age-dependent doses. to. members of. the. public from. intake of. radionuclides: Part. 2,
4595 ingestion dose. coefficients. ICRP. Publication 67. Ann. ICRP. 23(3/4).
4596 ICRP. 1994a. Dose. coefficients for. intakes of. radionuclides by. workers. ICRP. Publication 68. Ann.
4597 ICRP. 24(4).
4598 ICRP. 1994b. Human. respiratory tract. model. for. radiological protection. ICRP. Publication 66. Ann.
4599 ICRP. 24(1–3).
4600 ICRP. 1995a. Age-dependent doses. to. members of. the. public from. intake of. radionuclides: Part. 3,
4601 ingestion dose. coefficients. ICRP. Publication 69
4602 ICRP, 1995b. Age-dependent Doses to Members of the Public from Intake of Radionuclides: Part 4.
4603 Inhalation Dose Coefficients, ICRP Publication 71. Ann. ICRP 25(3/4).
4604 ICRP, 1995c. Age-dependent Doses to the Members of the Public from Intake of Radionuclides - Part
4605 5 Compilation of Ingestion and Inhalation Coefficients. ICRP Publication 72. Ann. ICRP 26(1).
4606 ICRP, 2001. Doses to the Embryo and Fetus from Intakes of Radionuclides by the Mother. ICRP
4607 Publication 88. Ann. ICRP 31(1–3).
4608 ICRP, 2004. Doses to Infants from Ingestion of Radionuclides in Mothers' Milk. ICRP Publication 95.
4609 Ann. ICRP 34(3–4).
4610 ICRP, 2007. The 2007 Recommendations of the International Commission on Radiological Protection.
4611 ICRP Publication 103. Ann. ICRP 37 (2-4).
4612 ICRP, 2008. Nuclear Decay Data for Dosimetric Calculations. ICRP Publication 107. Ann. ICRP 38
4613 (3).
4614 ICRP, 2010. Conversion Coefficients for Radiological Protection Quantities for External Radiation
4615 Exposures. ICRP Publication 116, Ann. ICRP 40(2-5).
4616 ICRP, 2015. Occupational Intakes of Radionuclides: Part 1. ICRP Publication 130. Ann. ICRP 44(2).
4617 ICRP, 2016. Occupational intakes of radionuclides: Part 2. ICRP Publication 134. Ann. ICRP 45(3/4).
4618 ICRP, 2017. Occupational intakes of radionuclides: Part 3. ICRP Publication 137. Ann. ICRP 46(3/4).

ICRP, 2019. Occupational Intakes of Radionuclides: Part 4. ICRP Publication 141. Ann. ICRP 48(2/3).
ICRP, 2020. Paediatric Computational Reference Phantoms. ICRP Publication 143. Ann. ICRP 49(1).
ICRP, 2022. Occupational Intakes of Radionuclides: Part 5. ICRP Publication 151. Ann. ICRP 51(1-2)
ICRP. 2024. Dose coefficients for intakes of radionuclides by members of the public: part 1. ICRP Publication 158. Ann. ICRP 53(4-5).
Iinuma, T., Watari K., Nagai T., et al. Comparative studies of Cs- 132 and. Rb-86 turnover in. man. using. a. double-tracer method. J. Radiat Res. 1967,8:100–115.
Institute, of Medicine (IOM). Dietary Reference Intakes for calcium, phosphorus, magnesium, vitamin D., and fluoride. Washington DC: National Academy Press, 1997. 454 p.
Ishiwata, K., Ido T., Monma M., et al. Potential radiopharmaceuticals labeled with titanium- 45. Int. J. Radiat Appl. Instrum A. 1991,42:707–712.
Izumi, Y., Fujita M., Yabe A., et al. Retention and distribution of inorganic mercury- 197 and. -203 in. the. human. body. after. single inhalation. In: Proceedings of. the. 3rd International Congress of. the. International Radiological Protection Association, 1973, Washington. p. 1384–1389.
Jamre, M., Salek N., Jalilian AR, Moghaddam L., Shamsaee M., Mazidi M., Ghannadi-Maragheh M. Development of an in vivo radionuclide generator by labeling bleomycin with 191Os. J. Radioanal Nucl. Chem. 2011,290:543–549.
Janghorbani, M., Kasper LJ, Young VR. Dynamics of selenite metabolism in young men: studies with the stable isotope tracer method. Am J., Clin Nutr. 1984,40:208–218.
Jarup, L., Rogenfelt A., Elinder CG, et al. Biological half-time of cadmium in the blood of workers after cessation of exposure. Scand J., Work Environ Health. 1983,9(4):327–331.
Jasani, BM, Edmonds CJ. Kinetics of potassium distribution in man using isotope dilution and whole-body counting. Metabolism. 1971,20:1099–1106.
JECFA. Cadmium. WHO Food Additives Series No. 46. Geneva: World. Health Organization, 2001.
Jeffcoat, MK, McNeil BJ, Davis MA. Indium and iron as tracers for erythroid precursors. J., Nucl Med. 1978,19:496–500.
Jeffrey, MR, Freundlich HF, Bailey DM. Distribution and excretion of radiogold in animals. Ann Rheum Dis. 1958,17:52–60.
Jellum, E., Munthe E., Guldal G., et al. Fate of the gold and the thiomalate part after intramuscular administration of aurothiomalate to mice. Ann Rheum Dis. 1980,39:155–158.
Jereb, M., Falk R., Jereb B., et al. Radiation dose to the human body from intravenously administered 75Se-sodium selenite. J. Nucl. Med. 1975,16:846–850.
Johnson, JE, Hartsuck JH, Zollinger RM, Moore FD. Radio-potassium equilibrium in total body potassium: studies using 43K and. 42K. Metabolism. 1969,18:663–668.
Johnson, JR. Whole body retention following an intravenous injection of 75Se as. selenomethionine. Health Phys. 1977,33:250–251.
Jones, K., Morton J., Smith I., et al. Human in vivo and in vitro studies on gastrointestinal absorption of titanium dioxide nanoparticles. Toxicol Lett. 2015,233:95–101.
Jönsson BA. Biokinetics and localization of some In- 111-radiopharmaceuticals in. rats. at. the. macroscopic and. microscopic level: an. approach towards small. scale. dosimetry [doctoral thesis]. Lund. (Sweden): Lund. University, 1991.
Jonsson, F., Sandborgh-Englund G., Johanson G. A., compartmental model for the kinetics of mercury vapor in humans. Toxicol Appl Pharmacol. 1999,155:161–168.
Jugdaohsingh, R. Silicon and bone health. J., Nutr Health Aging. 2007,11:99–110.
Kabe, I., Omae K., Nakashima H., et al. In vitro solubility and in vivo toxicity of indium phosphide. J., Occup Health. 1996,38:6–12.
Kato, M. Distribution and excretion of radiomanganese administered to the mouse. Q. J., Exp Physiol. 1963,48:355–369.
Kaye, SV. Distribution and retention of orally administered radiotungsten in the rat. Health Phys. 1968,15:399–417.
Keen, CL, Bell JG, Lonnerdal B. The effect of age on manganese uptake and retention from milk and infant formulas in rats. J., Nutr. 1986,116:395–402.
Kerger, BD, Finley BL, Corbett GE, Dodge DG, Paustenbach DJ. Ingestion of chromium(VI) in drinking water by human volunteers: absorption, distribution, and excretion of single and repeated doses. J., Toxicol Environ Health. 1997,50(1):67–95.

Kernan, RP. Accumulation of caesium and rubidium in vivo by red and white muscles of the rat. J., Physiol. 1969,204:195–205.

Khayat, A., Dencker L. Whole-body and liver distribution of inhaled mercury vapour in the mouse: influence of ethanol and aminotriazole pretreatment. J., Appl Toxicol. 1983,3:66–74.

Khayat, A., Dencker L., 1984. Organ. and. cellular distribution of. inhaled metallic mercury in. the. rat. and. marmoset monkey (Callitrix jacchus): influence of. ethyl. alcohol pretreatment. Acta. Pharmacol Toxicol 55:145–152.

Kiesswetter, E., Schäper M., Buchta M., et al. 2007. Longitudinal study. on. potential neurotoxic effects of. aluminium: I. Assessment of. exposure and. neurobehavioural performance of. Al. welders in. the. train. and. truck. construction industry over. 4 years. Int. Arch. Occup. Environ Health 81:41–67.

Kiesswetter, E., Schäper M., Buchta M., et al. 2009. Longitudinal study. on. potential neurotoxic effects of. aluminium: II. Assessment of. exposure and. neurobehavioural performance of. Al. welders in. the. automobile industry over. 4 years. Int. Arch. Occup. Environ Health 82:1191–1210.

Kilpatrick, R., Renschler HE, Munro DS, Wilson GM. 1956. A. comparison of. the. distribution of. K-42 and. Rb-86 in. rabbit and. man. J. Physiol 133:194–201.

Kirman, CR, Hays SM, Aylward LL, et al. 2012. Physiologically based. pharmacokinetic model. for. rats. and. mice. orally exposed to. chromium. Chem. Biol. Interact 200(1):45–64. https://doi.org/10.1016/j.cbi.2012.08.016

Kittle, CF, King ER, Bahner CT, Brucer M., 1951. Distribution and. excretion of. radioactive hafnium sodium mandelate in. the. rat. Proc. Soc. Exp. Biol. Med. 76:278–282.

Klaassen, CD. 1979. Biliary excretion of. silver in. the. rat, rabbit, and. dog. Toxicol Appl. Pharmacol 50:49–55.

Kleinsorge, H., 1967. Die. Resorption therapeutisch anwendbarer Goldsalze und. Goldsole. Arzneim-Forsch 17:100–102.

Klosterkötter W., 1960. Effects of. ultramicroscopic gamma-aluminium oxide. on. rats. and. mice. Arch. Indust Health 21:458–472.

Knudsen, E., Sandstrom B., Solgaard P. 1996. Zinc, copper and. magnesium absorption from. a. fibre-rich diet. J. Trace. Elem. Med. Biol. 10:68–76.

Kojima, K., Fujita M., 1973. Summary of. recent studies in. Japan. on. methyl mercury poisoning. Toxicology 1:43–62.

Kolanz, ME. 2001. Introduction to. beryllium: uses, regulatory history, and. disease. Appl. Occup. Environ Hyg. 16:559–567.

Korst, DR. 1968. Blood. volume and. red. blood. cell. survival. In: Wagner HN, Saunders WB, editors. Principles of. nuclear medicine. Philadelphia. p. 429–471.

Kostial, K., Kello D., Jugo S., et al. 1978. Influence of. age. on. metal. metabolism and. toxicity. Environ Health Perspect 25:81–86.

Krahwinkel, W., Herzog H., Feinendegen LE. 1988. Pharmacokinetics of. thallium-201 in. normal individuals after. routine myocardial scintigraphy. J. Nucl. Med. 29:1582–1586.

Kreiss, K., Day GA, Schuler CR. 2007. Beryllium: a. modern industrial hazard. Annu. Rev. Public Health 28:259–277. https://doi.org/10.1146/annurev.publhealth.28.021406.144011

Kreyling, WG, Hirn S., Möller W., et al. 2014. Air-blood barrier translocation of. tracheally instilled gold. nanoparticles inversely depends on. particle size. ACS. Nano. 8(1):222–233. https://doi.org/10.1021/nn403256v

Kreyling, WG, Holzwarth U., Haberl N., 2017. Quantitative biokinetics of. titanium dioxide nanoparticles after. intravenous injection in. rats: Part. 1. Nanotoxicology 11(4):434–442. https://doi.org/10.1080/17435390.2017.1306892

Kreyling, WG, Holzwarth U., Schleh C., et al. 2017. Quantitative biokinetics of. titanium dioxide nanoparticles after. oral. application in. rats: Part. 2. Nanotoxicology 11(4):443–453. https://doi.org/10.1080/17435390.2017.1306893

Kreyling, WG, Holzwarth U., Haberl N., et al. 2017. Quantitative biokinetics of. titanium dioxide nanoparticles after. intratracheal instillation in. rats: Part. 3. Nanotoxicology 11(4):454–464. https://doi.org/10.1080/17435390.2017.1306894

Kreyling, WG, Möller W., Holzwarth U., et al. 2018. Age-dependent rat. lung. deposition patterns of. inhaled 20 nanometer gold. nanoparticles and. their. quantitative biokinetics in. adult. rats. ACS. Nano. 12(8):7771–7790.
Kriegel, H., 1984. Biokinetics and. metabolism of. radiogallium. Nuklearmedizin 23:53–57.
Kristiansen, J., Christensen JM, Iversen BS, Sabbioni E., 1997. Toxic. trace. element reference levels in. blood. and. urine: influence of. gender and. lifestyle factors. Sci. Total. Environ 204:147–160.
Kumana, CR, Au WY, Lee NSL, et al. 2002. Systemic availability of. arsenic from. oral. arsenic-trioxide used. to. treat. patients with. hematological malignancies. Eur. J. Clin. Pharmacol 58:521–526.
Kutzner, J., Brod KH. 1971. Studies on. absorption and. secretion of. tin. following oral. administration of. 113Sn. NuklearMedizin 10(3):286–297.
Lachine, EE, Noujaim AA, Ediss C., Wiebe LI. 1976. Toxicity, tissue distribution and. excretion of. 46ScCl3, and. 46Sc-EDTA in. mice. Int. J. Appl. Radiat Isot. 27:373–377.
Lange, RC, Spencer RP, Harder HC. 1973. The. anti-tumor agent. cis-Pt(NH3)2Cl2: distribution studies and. dose. calculations for. 193mPt and. 195mPt. J. Nucl. Med. 14:191–195.
Langham-New, SA, Lambert H., 2012. Potassium. Adv. Nutr. 3:820–821.
Larsen, RH, Slade S., Zalutsky MR. 1998. Blocking [211At]astatide accumulation in. normal tissues: preliminary evaluation of. seven. potential compounds. Nucl. Med. Biol. 25:351–357.
Lathrop, KA, Harper PV, Gloria IV, Rich M. 1975. Intestinal localization of. Tl-201. J. Nucl. Med. 16:545.
Lathrop, KA, Tsui BMW, Chen CT, Harper PV. 1989. Multiparameter extrapolation of. biodistribution data. between species. Health Phys. 57(Suppl 1):121–126.
Lathrop, KA, Harper PV, Malkinson FD. 1968. Human. total-body retention and. excretory routes of. 75Se for. selenomethionine. Strahlentherapie 67:436–443.
Lathrop, KA, Johnston RE, Blau M., et al. 1972. Radiation dose. to. humans from. 75Se-L-selenomethionine. J. Nucl. Med. 6(Suppl 6):7–30.
Laval, M., Dumesny C., Eutick M., et al. 2018. Oral. trivalent bismuth ions. decrease, and. trivalent indium or. ruthenium ions. increase, intestinal tumor. burden in. ApcΔ14/+ mice. Metallomics 10:194–200.
Lawrence, JS. 1961. Studies with. radioactive gold. Ann. Rheum. Dis. 20:341–352.
Lazzara, R., Hyatt K., Love WD, Cronvich J., Burch GE. 1963. Tissue distribution, kinetics, and. biologic half-life of. 28Mg in. the. dog. Am. J. Physiol 204:1086–1094.
Lebedev, OV, Yakovlev VA. 1993. The. correlation between 137Cs half-time and. age, body. mass. and. height in. individuals contaminated from. the. Chernobyl accident. In: Merwin SE, Balonov MI, editors. The. Chernobyl papers. Vol. 1. Doses. to. the. Soviet population and. early. health effects studies. p. 219–243.
Lefevre, ME, Joel DD. 1986. Distribution of. label. after. intragastric administration of. 7Be-labeled carbon to. weanling and. aged. mice. Proc. Soc. Exp. Biol. Med. 182(1):112–119.
Leggett, R., O'Connell C. 2018. Biokinetic models for. Group. VB. elements. J. Radiol Prot. 38(2):564–586. https://doi.org/10.1088/1361-6498/aab1c1
Leggett, R. 2011. A. biokinetic model. for. manganese. Sci. Total. Environ 409:4179–4186.
Leggett, RW, Williams LR. 1989. A. biokinetic model. for. Rb. in. humans. Health Phys. 55:685–702.
Leggett, RW. 1997. A. model. of. the. distribution and. retention of. tungsten in. the. human. body. Sci. Total. Environ 206:147–165.
Leggett, RW, Williams LR. 1986. A. model. for. the. kinetics of. potassium in. healthy humans. Phys. Med. Biol. 31:23–42.
Leggett, RW, Munro NB, Eckerman KF. 2001. Proposed revision of. the. ICRP. model. for. inhaled mercury vapour. Health Phys. 81:450–455.
Leggett, RW, Williams LR, Melo DR, et al. 2003. A. physiologically based. biokinetic model. for. caesium in. the. human. body. Sci. Total. Environ 317:235–255.
Leverton, RM, Binkley ES. 1944. The. copper metabolism and. requirement of. young. women. J. Nutr. 27:43–52.
Lewis, GP, Coughlin L., Jusko W., et al. 1972. Contribution of. cigarette smoking to. cadmium accumulation in. man. Lancet 1:291–292.

Lie, R., Thomas RG, Scott JK. 1960. The. distribution and. excretion of. thallium-204 in. the. rat, with. suggested MPCs. and. a. bioassay procedure. Health Phys. 2:334–340.
Lim, TH, Sargent T., Kusubov N. 1983. Kinetics of. trace. element chromium(III) in. the. human. body. Am. J. Physiol Regul. Integr Comp. Physiol. 244:R445–454.
Lindberg, JS, Zobitz MM, Poindexter JR, et al. 1990. Magnesium bioavailability from. magnesium citrate and. magnesium oxide. J. Am. Coll. Nutr. 9:48–55.
Linder, MC, Hazegh-Azam M. 1996. Copper biochemistry and. molecular biology. Am. J. Clin. Nutr. 63:797S–811S.
Lindgren, A., Vahter M., Dencker L., 1982. Autoradiographic studies on. the. distribution of. arsenic in. mice. and. hamsters administered 74As-arsenite or. arsenate. Acta. Pharmacol Toxicol. 51:253–265.
Ling, MP, Liao CM. 2009. A. human. PBPK/PD model. to. assess arsenic exposure risk. through farmed tilapia consumption. Bull. Environ Contam Toxicol. 83:108–114.
Lippmann, M., Albert RE. 1969. The. effect of. particle size. on. the. regional deposition of. inhaled aerosols in. the. human. respiratory tract. Am. Ind. Hyg. Assoc. J. 30:257–275.
Litterst, CL, Gram TE, Dedrick RL, Leroy AF, Guarino AM. 1976. Distribution and. disposition of. platinum following intravenous administration of. cis-diamminedichloroplatinum(II) (NSC119875) to. dogs. Cancer Res. 36:2340–2355.
Ljunggren, KG, Lidums V., Sjögren B. 1991. Blood. and. urine. concentrations of. aluminium among. workers exposed to. aluminium flake. powders. Br. J. Ind. Med. 48:106–109.
Lloyd, RD, Mays CW, McFarland SS, Zundel WS, Tyler FH. 1972. Rb-86 and. Cs-137 metabolism in. persons affected by. muscle disease. Univ. Utah. Rep. COO-119-247.
Lloyd, RD, Mays CW, McFarland SS, Zundel WS, Tyler FH. 1973. Metabolism of. Rb-83 and. Cs-137 in. persons with. muscle disease. Radiat Res. 54:463–478.
Love, WD, Burch GE. 1953. A. comparison of. K-42, Rb-86, and. Cs-134 as. tracers of. potassium in. the. study. of. cation metabolism of. human. erythrocytes in. vitro. J. Lab. Clin. Med. 41:351–362.
Love, WD, Romney RB, Burch GE. 1954. A. comparison of. the. distribution of. potassium and. exchangeable rubidium in. the. organs of. the. dog, using. rubidium. Circ. Res. 2:112–122.
Lown, BA, Morganti JB, Stineman CH. 1980. Tissue organ. distribution and. behavioural effects of. platinum following acute. and. repeated exposure of. the. mouse. to. platinum sulfate. Environ Health Perspect. 34:203–212.
Luckey, TD, Venugopal B., Hutcheson D., 1975. Heavy. metal. toxicity, safety and. hormonology. Stuttgart: Georg. Thieme.
Luten, JB, Riekwel-Booy G., Rauchbaar A., 1982. Occurrence of. arsenic in. plaice (Pleuronectes platessa), nature of. organo-arsenic compound present and. its. excretion by. man. Environ Health Perspect. 45:165–170.
Mabille, H., Larcan A., Streiff F., et al. 1961. Etude. de. la. répartition du. rubidium radioactif chez. l'homme (86Rb). In: Comptes rendus des. seances de. la. societe de. biologie et. de. ses. filiales, Paris, France. p.571. Masson éditeur.
MacDonald, E., Bahner CT. 1953. Hafnium complexes for. biological investigations. Proc. Soc. Exp. Biol. Med. 83:801–804.
Magos, L., Clarkson TW, Hudson AR. 1989. The. effects of. dose. of. elemental mercury and. first-pass circulation time. on. exhalation and. organ. distribution of. inorganic mercury in. rats. Biochim Biophys Acta. 991:85–89.
Mahoney, JP, Small WJ. 1968. Studies on. manganese. III. The. biological half-life of. radiomanganese in. man. and. factors which. affect this. half-life. J. Clin. Invest. 47:643–653.
Mann, S., Droz PO, Vahter M. 1996. A. physiologically based. pharmacokinetic model. for. arsenic exposure. II. Validation and. application in. humans. Toxicol Appl. Pharmacol. 140:471–486.
Manzo, L., Rade-Edel J., Sabbioni E., 1983. Environmental toxicology research on. thallium: metabolic and. toxicological studies in. the. rat. as. carried out. by. nuclear and. radioanalytical methods.
Mappes, R., 1977. Experiments on. excretion of. arsenic in. urine. Int. Arch. Occup. Environ Health. 40:267–272.
Marafante, E., Vahter M., 1987. Solubility, retention and. metabolism of. intratracheally and. orally administered inorganic arsenic compounds in. the. hamster. Environ Res. 42:72–82.

4835 Marafante, E., Rade J., Sabbioni E., 1981. Intracellular interaction and. metabolic fate. of. arsenite in.
4836 the. rabbit. Clin. Toxicol. 18:1335–1341.
4837 Mascarenhas, BR, Granda JL, Freyberg RH. 1972. Gold. metabolism in. patients with. rheumatoid
4838 arthritis treated with. gold. compounds—reinvestigated. Arthritis Rheum. 15:391–402.
4839 Mashitsuka, S., Inoue M., 1998. Urinary excretion of. aluminum from. antacid ingestion and. estimation
4840 of. its. apparent biological half-time. Trace. Elem. Electrolytes. 15:132–135.
4841 Mason, J., Mulryan G., Lamand M., et al. 1989. Behaviour of. [185W] thiotungstates injected into.
4842 sheep. and. the. influence of. copper: their. fate. and. the. effect of. the. compounds upon. plasma
4843 copper. J. Inorg. Biochem. 35:115–126.
4844 Massarella, JW, Pearlman RS. 1987. Gold. disposition in. the. rat: studies of. its. plasma half-life and.
4845 its. urinary, biliary and. faecal elimination pathways. J. Pharmacol Exp. Ther. 243:247–257.
4846 Maynard, LS, Fink S. 1956. The. influence of. chelation on. radiomanganese excretion in. man. and.
4847 mouse. J. Clin. Invest. 8:831–836.
4848 McAughey, J., Newton D., Talbot R., et al. 1998. Uptake and. excretion of. inhaled 26Al-aluminium
4849 oxide. AEA. Technology Report (AEA-2221).
4850 McIntyre, PA, Larson SM, Eikman EA, et al. 1974. Comparison of. the. metabolism of. iron-labeled
4851 transferrin (Fe-TF) and. indium-labeled transferrin (In-TF) by. the. erythropoietic marrow. J. Nucl.
4852 Med. 15:856–862.
4853 McLaughlin, AI, Kazantzis G., King E., et al. 1962. Pulmonary fibrosis and. encephalopathy associated
4854 with. the. inhalation of. aluminium dust. Br. J. Ind. Med. 19:253–263.
4855 McNeil, BJ, Holman BL, Button LN, Rosenthal DS. 1974. Use. of. indium chloride scintigraphy in.
4856 patients with. myelofibrosis. J. Nucl. Med. 15:647–651.
4857 McQueen, EG, Dykes PW. 1969. Transport of. gold. in. the. body. Ann. Rheum. Dis. 28:437–442.
4858 Mealey, J., Brownell GL, Sweet WH. 1959. Radioarsenic in. plasma, urine, normal tissues, and.
4859 intracranial neoplasms. Arch. Neurol Psychiatry. 81:310–320.
4860 Meek, SF, Harrold GC, McCord CP. 1943. The. physiologic properties of. palladium and. its.
4861 compounds. Ind. Med. Surg. 12:447–448.
4862 Mehard, CW, Volcani BE. 1975. Similarity in. uptake and. retention of. trace. amounts of. 31Silicon
4863 and. 68Germanium in. rat. tissues and. cell. organelles. Bioinorg Chem. 5:107–124.
4864 Mena, I. 1981. Manganese. In: Brommer F. Coburn JW, editors. Disorders of. Mineral Metabolism, vol.
4865 I. New. York: Academic Press. p.233–236.
4866 Mena, I., Marin O., Fuenzalida S., Cotzias GC. 1967. Chronic manganese poisoning. Clinical picture
4867 and. manganese turnover. Neurology 17:128–136.
4868 Meneely, GR, Auerbach SH, Woodcock CC, et al. 1953. Transbronchial instillation of. radioactive gold.
4869 colloid in. the. lung. of. the. dog. Distribution studies, survival and. pathology. Am. J. Med. Sci.
4870 225:172–177.
4871 Menzel, DB, Ross M., Oddo SV, et al. 1994. A. physiologically based. pharmacokinetic model. for.
4872 ingested arsenic. Environ Geochem Health 16:209–218.
4873 Merritt, K., Brown SA. 1995. Distribution of. titanium and. vanadium following repeated injection of.
4874 high-dose salts. J. Biomed Mater. Res. A. 29:1175–1178.
4875 Merritt, K., Margevicius RW, Brown SA. 1992. Storage and. elimination of. titanium, aluminum, and.
4876 vanadium salts. in. vivo. J. Biomed Mater. Res. 26:1503–1515.
4877 Mertz, W. 1993. Chromium in. human. nutrition: a. review. J. Nutr. 123:626–633.
4878 Mertz, W., Roginski EE, Reba RC. 1965. Biological activity and. fate. of. trace. quantities of.
4879 intravenous chromium(III) in. the. rat. Am. J. Physiol 209:489–494.
4880 Miettinen, JK, Rahola T., Hattula T., Rissanen K., Tillander M., 1971. Elimination of. 203-
4881 methylmercury in. man. Ann. Clin. Res. 3:116–122.
4882 Miller, H., Munro DS, Wilson GM. 1957. The. human. use. of. 22Na. Lancet 272:734.
4883 Miller, JK, Madsen FC, Hansard SL. 1976. Absorption, excretion, and. tissue deposition of. titanium in.
4884 sheep. J. Dairy. Sci. 59:2008–2010.
4885 Miller, JK, Byrne WF. 1970. Comparison of. scandium-46 and. cerium-144 as. nonabsorbed reference
4886 materials in. studies with. cattle. J. Nutr. 100:1287–1292.
4887 Miller, JK, Byrne WF, Lyke WA. 1972. Comparison of. faecal excretions of. scandium-46 tagged sand.
4888 and. soluble cerium-144 by. calves. Health Phys. 22:461–465.

4889 Miller, MR, Raftis JB, Langrish JP, et al. 2017. Inhaled nanoparticles accumulate at. sites. of. vascular
4890 disease. ACS. Nano. 11:4542–4552.
4891 Milne, DB, Sims RL, Ralston NVC. 1990. Manganese content of. the. cellular components of. blood.
4892 Clin. Chem. 36:450–452.
4893 MIRD. 1973. Summary of. current radiation dose. estimates to. humans from. 66Ga, 67Ga, 68Ga, and.
4894 72Ga citrate. J. Nucl. Med. 14:755–756.
4895 Miyao, K., Onishi T., Asai K., et al. 1980. Toxicology and. phase. I. studies on. a. novel.
4896 organogermanium compound, Ge-132. Curr. Chemother Infect Dis. 2:1527–1529.
4897 Mochizuki, H. 2019. Arsenic neurotoxicity in. humans. Int. J. Mol. Sci. 20:3418.
4898 Mole, RH. 1984. Sodium in. man. and. the. assessment of. radiation dose. after. criticality accidents.
4899 Phys. Med. Biol. 29:1307–1327.
4900 Moore, W. Jr, Hysell D., Crocker W., Stara J., 1974. Biological fate. of. 103Pd in. rats. following
4901 different routes of. exposure. Environ Res. 8:234–240.
4902 Moore, W., Hysell D., Hall L., Campbell K., Stara J., 1975. Preliminary studies on. the. toxicity and.
4903 metabolism of. palladium and. platinum. Environ Health Perspect 10:63–71.
4904 Moore, W., Malanchuk M., Crocker W., Hysell D., Cohen A., Stara JF. 1975. Biological fate. of. a.
4905 single administration of. 191Pt in. rats. following different routes of. exposure. Environ Res. 9:152–
4906 158.
4907 Moore, W., Stara JF, Crocker WC. 1973. Comparison of. 115Cd retention in. rats. following different
4908 routes of. administration. Environ Res. 6:473–478.
4909 Morgan, DL, Shines CJ, Jeter SP, et al. 1997. Comparative pulmonary absorption, distribution, and.
4910 toxicity of. copper gallium diselenide, copper indium diselenide, and. cadmium telluride in. Sprague-
4911 Dawley rats. Toxicol Appl. Pharmacol 147:399–410.
4912 Morris, ME, Leroy S., Sutton SC. 1987. Absorption of. magnesium from. orally administered
4913 magnesium sulfate in. man. Clin. Toxicol 25:371–382.
4914 Morrow, PE, Gibb FR, Johnson L., 1964. Clearance of. insoluble dust. from. the. lower. respiratory
4915 tract. Health Phys. 10:543–555.
4916 Morrow, PE, Gibb FR, Davies H., et al. 1968. Dust. removal from. the. lung. parenchyma: an.
4917 investigation of. clearance stimulants. Toxicol Appl. Pharmacol 12:372–396.
4918 Moskalev, YI, Bugryshev PF, Zaikina TI. 1988. Effect of. age. on. the. metabolism of. inhaled beryllium
4919 fluoride in. rats. Ann. Occup. Hyg. 32:963–967.
4920 Mühlbauer B., Schwenk M., Coram WM, et al. 1991. Magnesium-L-aspartate-HCl and. magnesium-
4921 oxide: bioavailability in. healthy volunteers. Eur. J. Clin. Pharmacol 40:437–438.
4922 Mullen, AL, Bretthauer EW, Stanley RE. 1976. Absorption, distribution and. milk. secretion of.
4923 radionuclides by. the. dairy. cow. V. Radiotungsten. Health Phys. 31:417–424.
4924 Mullen, AL, Stanley RE, Lloyd SR, et al. 1972. Radioberyllium metabolism by. the. dairy. cow. Health
4925 Phys. 22:17–22.
4926 Münker C., Pfänder JA, Weyer S., Büchl A., Kleine T., Mezger K., 2003. Evolution of. planetary cores.
4927 and. the. Earth-Moon system from. Nb/Ta systematics. Science 301:84–87.
4928 Mussi, I., Calzaferri G., Buratti M., et al. 1984. Behaviour of. plasma and. urinary aluminum levels in.
4929 occupationally exposed subjects. Int. Arch. Occup. Environ Health 54:155–161.
4930 Nagata, N., Yoneyama T., Yanagida K., et al. 1985. Accumulation of. germanium in. the. tissues of. a.
4931 long-term user. of. germanium preparation died. of. acute. renal. failure. J. Toxicol Sci. 10:333–341.
4932 Nakagawara, S., Goto T., Nara M., et al. 1998. Spectroscopic characterization and. the. pH. dependence
4933 of. bactericidal activity of. the. aqueous chlorine solution. Anal. Sci. 14:691–698.
4934 Nakamura, K., Nishiguchi I., Takagi Y., et al. 1985. Distribution of. 201Tl in. blood. Radioisotopes
4935 34:550–554.
4936 Nelson, B., Hayes RL, Edwards CL, Kniseley RM, Andrews GA. 1972. Distribution of. gallium in.
4937 human. tissues after. intravenous administration. J. Nucl. Med. 13:92–100.
4938 Nelson, N., Byerly TC, Kolbye AC, et al. 1971. Hazards of. mercury. Special report to. the. Secretary's
4939 Pesticide Advisory Committee, Department of. Health, Education, Welfare. Environ Res. 4:1–69.
4940 Neuman, WF, Neuman MW. 1958. The. chemical dynamics of. bone. mineral. Chicago: University of.
4941 Chicago Press.
4942 Newton, D., Fry FA. 1978. The. retention and. distribution of. radioactive mercuric oxide. following
4943 accidental inhalation. Ann. Occup. Hyg. 21:21–32.

4944 Newton, D., Holmes A. 1966. A. case. of. accidental inhalation of. zinc-65 and. silver-110m. Radiat
4945 Res. 29:403–412.
4946 Nicolaou, G., Pietra R., Sabbioni E., Mosconi G., Cassina G., Seghizzi P. 1987. Multielement
4947 determination of. metals in. biological specimens of. hard. metal. workers: a. study. carried out. by.
4948 neutron activation analysis. J. Trace. Elem. Electrolytes Health Dis. 1:73–77.
4949 Nordberg, GF, Sherfving S., 1972. Metabolism. In: Mercury in. the. environment: an. epidemiological
4950 and. toxicological appraisal. Vol. 3. Cleveland, OH: CRC. Press.
4951 Nordberg, GF, Kjellstrom T., Nordberg M. 1985. Kinetics and. metabolism. In: Friberg L. Elinder CG,
4952 Kjellstrom T. eds. Exposure, dose, and. metabolism. Boca. Raton, FL: CRC. Press, 103–178.
4953 Novak, LP. 1973. Total-body potassium during the. first. year. of. life. determined by. whole-body
4954 counting of. 40K. J. Nucl. Med. 14:550–557.
4955 Nygren, O., Lundgren C., 1997. Determination of. platinum in. workroom air. and. in. blood. and. urine.
4956 from. nursing staff. attending patients receiving cisplatin chemotherapy. Int. Arch. Occup. Environ
4957 Health 70:209–214.
4958 O'Flaherty EJ. 1996. A. physiologically based. model. of. chromium kinetics in. the. rat. Toxicol Appl.
4959 Pharmacol 138:54–64.
4960 O'Flaherty EJ, Kreger BD, Hays SM, Paustenbach DJ. 2001. A. physiology based. model. for. the.
4961 ingestion of. chromium(III) and. chromium(VI) by. humans. Toxicol Sci. 60:196–213.
4962 Oberdoerster, G., Baumert HP, Hochrainer D., et al. 1979. The. clearance of. cadmium aerosols after.
4963 inhalation exposure. Am. Ind. Hyg. Assoc. J. 40:443–450.
4964 Oberdörster G. 1988. Lung. clearance of. inhaled insoluble and. soluble particles. J. Aerosol Med.
4965 1:289–330.
4966 Oberdorster, G., Cox C., Baggs R. 1987. Long. term. lung. clearance and. cellular retention of. cadmium
4967 in. rats. and. monkeys. J. Aerosol Sci. 18:745–748.
4968 Oberdörster G., Oldiges H., Zimmermann B. 1980. Lung. deposition and. clearance of. cadmium in.
4969 rats. exposed by. inhalation or. by. intratracheal instillation. Zentralbl Bakteriol B. 170:35–43.
4970 Olsen, I., Jonsen J., 1979. Whole-body autoradiography of. 63Ni in. mice. throughout gestation. Toxicol
4971 12:165–172.
4972 Olsson, KA, Söremark R., Wing KR. 1969. Uptake and. distribution of. rubidium-86 and. potassium-
4973 43 in. mice. and. rats—an autoradiographic study. Acta. Physiol Scand. 77:322–332.
4974 Onkelinx, C. 1977. Compartment analysis of. metabolism of. chromium(III) in. rats. of. various ages.
4975 Am. J. Physiol 232:E478–E484.
4976 Onkelinx, C., Becker J., Sunderman FW Jr. 1973. Compartmental analysis of. the. metabolism of.
4977 63Ni(II) in. rats. and. rabbits. Res. Commun Chem. Pathol Pharmacol 6:663–676.
4978 Osredkar, J., Sustar N. 2011. Copper and. zinc, biological role. and. significance of. copper/zinc
4979 imbalance. J. Clin. Toxicol S3:1–18.
4980 Östlund K., 1969. Studies on. the. metabolism of. methyl mercury in. mice. Acta. Pharmacol Toxicol
4981 Suppl. 1:5–132.
4982 Owen, CA. 1965. Metabolism of. radiocopper (64Cu) in. the. rat. J. Lab. Clin. Med. 65:637–646.
4983 Palmer, BF (2015). Regulation of. potassium homeostasis. Renal. Physiol 10:1050–1060.
4984 Paquet F. Houpert P. Verry. M. et. al. (1998). The. gastrointestinal absorption of. 63Ni and. 95Nb in.
4985 adult. and. neonatal rats: effect of. the. chemical form. administered. Radiat Prot. Dosimetry 79:191–
4986 195.
4987 Parker K. Sunderman FW. Jr. (1974). Distribution of. 63Ni in. rabbit tissues following intravenous
4988 injection of. 63NiCl2. Res. Commun Chem. Pathol Pharmacol 7:755–762.
4989 Partington JR. (1954). In: General and. Inorganic Chemistry. London: Macmillan, pp. 834–835.
4990 Patri A. Umbreit T. Zheng. J. et. al. (2009). Energy dispersive X-ray analysis of. titanium dioxide
4991 nanoparticle distribution after. intravenous and. subcutaneous injection in. mice. J. Appl. Toxicol
4992 29(8):662–672.
4993 Patrick G. Stirling C. (1992). Transport of. particles of. colloidal gold. within and. from. rat. lung. after.
4994 local. deposition by. alveolar microinjection. Environ Health Perspect 97:47–51.
4995 Patrick G. Stirling C. (1994). The. redistribution of. colloidal gold. particles in. rat. lung. following local.
4996 deposition by. alveolar microinjection. In: Dodgson J. McCallum RI. (eds) Inhaled Particles VII.
4997 Proc. Seventh Int. Symp. Inhaled Particles, Edinburgh, UK, 17–21 Sep. 1991, 38(Suppl 1):225–234.

4998 Patrick G. Stirling C. (1997a). Particle dissolution contributes to. long-term alveolar clearance of.
4999 colloidal gold. in. the. rat. In: Cherry N. Ogden. T. (eds) Inhaled Particles VIII. Proc. Eighth Int.
5000 Symp. Inhaled Particles, Cambridge, UK, 26–30 Aug. 1996, 41(Suppl 1):601–606.
5001 Patrick G. Stirling C. (1997b). Slow. clearance of. different-sized particles from. rat. trachea. J. Aerosol
5002 Med. 10(1):55–65.
5003 Patten JR, Whitford GM, Stringer GI, et. al. (1978). Oral. absorption of. radioactive fluoride and. iodide
5004 in. rats. Arch. Oral. Biol. 23:215–217.
5005 Patterson BH, Levander OA, Helzlsouer K. et. al. (1989). Human. selenite metabolism: a. kinetic model.
5006 Am. J. Physiol 257(3):R556–R567.
5007 Pavelka S. (2004). Metabolism of. bromide and. its. interference with. the. metabolism of. iodine.
5008 Physiol Res. 53(Suppl 1):S81–S90.
5009 Pechova A. Pavlata L. (2007). Chromium as. an. essential element: a. review. Veterinarni Medicina
5010 52(1).
5011 Pele LC, Thoree V. Bruggaber SFA, et. al. (2015). Pharmaceutical/food grade. titanium dioxide
5012 particles are. absorbed into. the. bloodstream of. human. volunteers. Part. Fibre. Toxicol 12:26.
5013 Phalen RF, Morrow PE. (1973). Experimental inhalation of. metallic silver. Health Phys. 24:509–518.
5014 Philipson K. Falk. R. Gustafsson J. et. al. (1996). Long-term lung. clearance of. 195Au-labelled teflon
5015 particles in. humans. Environ Lung. Res. 22:65–83.
5016 Pierre F. Baruthio F. Diebold F. et. al. (1995). Effect of. different exposure compounds on. urinary
5017 kinetics of. aluminium and. fluoride in. industrially exposed workers. Occup. Environ Med. 52:396–
5018 403.
5019 Pierre F. Diebold F. Baruthio F. (1998). Biomonitoring of. aluminium in. production workers. In: Priest
5020 ND, O'Donnell TV. (eds) Health in. the. Aluminium Industry. London: Middlesex University Press,
5021 pp. 68–89.
5022 Pleban PA, Pearson KH. (1979). Determination of. manganese in. whole. blood. and. serum. Clin. Chem.
5023 25:1915–1918.
5024 Poirier J. Semple H. Davies J. et. al. (2011). Double-blind, vehicle-controlled randomized twelve month.
5025 neurodevelopmental toxicity study. of. common aluminum salts. in. the. rat. Neuroscience 193:338–
5026 362.
5027 Polachek AA, Cope. CB, Williard RF, et. al. (1960). Metabolism of. radioactive silver in. a. patient
5028 with. carcinoid. J. Lab. Clin. Med. 56:499–505.
5029 Pomroy C. Charbonneau SM, McCullough RS, et. al. (1980). Human. retention studies with. 74As.
5030 Toxicol Appl. Pharmacol 53:550–556.
5031 Popplewell JF, King. SJ, Day. JP, et. al. (1998). Kinetics of. uptake and. elimination of. silicic acid. by.
5032 a. human. subject: a. novel. application of. 32Si and. accelerator mass. spectrometry. J. Inorg.
5033 Biochem 69:177–180.
5034 Potter GD, Vattuone GM, McIntyre DR. (1971). The. fate. and. implications of. ingested 204Tl in. a.
5035 dairy. cow. and. a. calf. Health Phys. 20:657–662.
5036 Poulheim KF. (1984). Zur. retention von. 60Co, 58Co/54Mn und. 110mAg nach. inhalativer Aufnahme
5037 im. Menschen. Isotopenpraxis 20:299–300.
5038 Powles J. Fahimi S. Micha. R. et. al. (2013). Global, regional and. national sodium intakes in. 1990 and.
5039 2010: a. systematic analysis of. 24 h. urinary sodium excretion and. dietary surveys worldwide. BMJ.
5040 Open. 3:e003733.
5041 Priest ND, Newton D. Day. JP, Talbot RJ, Warner AJ. (1995). Human. metabolism of. aluminium-26
5042 and. gallium-67 injected as. citrates. Hum. Exp. Toxicol 14:287–293.
5043 Priest ND. (1997). Biokinetics and. availability of. aluminium in. man. In: Managing Health in. the.
5044 Aluminium Industry (ed. ND. Priest), Montreal, Canada.
5045 Priest ND. (2004). The. biological behaviour and. bioavailability of. aluminium in. man, with. special
5046 reference to. studies employing aluminium-26 as. a. tracer: review and. study. update. J. Environ
5047 Monit. 6:375–403.
5048 Priest ND, Newton D. Day. JP, et. al. (1995). Human. metabolism of. aluminium-26 and. gallium-67
5049 injected as. citrates. Hum. Exp. Toxicol 14:287–293.
5050 Priest ND, Talbot RJ, Austin JG, et. al. (1996). The. bioavailability of. 26Al-labelled aluminum citrate
5051 and. aluminum hydroxide in. volunteers. BioMetals 9(3):221–228.

5052 Priest ND, Talbot RJ, Newton D. et. al. (1998). Uptake by. man. of. aluminum in. a. public water. supply.
5053 Hum. Exp. Toxicol 17(6):296–301.
5054 Proescher F. Seil. HH, Stillians AW. (1917). A. contribution to. the. action of. vanadium with. particular
5055 reference to. syphilis. Am. J. Syphilis 1:347–405.
5056 Rahola T. Hattula T. Korolainen A. et. al. (1973). Elimination of. free. and. protein bound. ionic.
5057 mercury (203Hg2+) in. man. Ann. Clin. Res. 5(4):214–219.
5058 Rahola T. Aaran. RK, Miettinen JK. (1972). Half-life studies of. mercury and. cadmium by. whole-
5059 body counting. In: Assessment of. radioactive contamination in. man. IAEA, Vienna, pp. 553–562.
5060 Ranade VV, Somberg JC. (2001). Bioavailability and. pharmacokinetics of. magnesium after.
5061 administration of. magnesium salts. to. humans. Am. J. Ther. 8:345–357.
5062 Rauws AG. (1983). Pharmacokinetics of. bromide ion. – an. overview. Food. Chem. Toxicol 21(4):379–
5063 382.
5064 Ray CT, Burch. GE, Threefoot SA. (1952). Biologic decay. rates. of. chloride in. normal and. diseased
5065 man, determined with. long-life radiochlorine, 36Cl. J. Lab. Clin. Med. 39:673–696.
5066 Ray CT, Threefoot SA, Burch. GE. (1955). The. excretion of. Rb-86, K-42, and. potassium, sodium,
5067 and. chloride by. man. with. and. without congestive heart. failure. J. Lab. Clin. Med. 45:408–430.
5068 Reeves AL. (1965). The. absorption of. beryllium from. the. gastrointestinal tract. Arch. Environ Health
5069 11:209–214.
5070 Reid AF, Forbes GB, Bondurant J. et. al. (1956). Estimation of. total. body. chlorine in. man. by. radio-
5071 bromide dilution. J. Lab. Clin. Med. 48:63–68.
5072 Reinhold JG, Faradji B. Abadi. P. et. al. (1976). Decreased absorption of. calcium, magnesium, zinc.
5073 and. phosphorus by. humans due. to. increased fiber. and. phosphorus consumption as. wheat. bread.
5074 J. Nutr. 106:493–503.
5075 Relman AS. (1956). The. physiological behaviour of. rubidium and. caesium in. relation to. that. of.
5076 potassium. Yale. J. Biol. Med. 29:248–262.
5077 Rhoads K. Sanders CL. (1985). Lung. clearance, translocation and. acute. toxicity of. arsenic, beryllium,
5078 cadmium, cobalt, lead, selenium, vanadium and. ytterbium oxides following deposition in. rat. lung.
5079 Environ Res. 36:359–378.
5080 Richmond CR. (1980). Retention and. excretion of. radionuclides of. the. alkali metals by. five.
5081 mammalian species. Health Phys. 38:1111–1153.
5082 Richmond CR, Furchner JE, Cummins BM. (1962). Effect of. age, sodium depletion and. sodium
5083 repletion on. the. retention of. sodium-22 by. rats. J. Nutr. 76:210–214.
5084 Richmond CR, Furchner JE, Trafton GA. (1960). Metabolism of. Zr-95 and. ruthenium-106 in.
5085 mammals. In: Biological and. Medical Research Group. (H4) of. the. Health Division, Semiannual
5086 Report July. through December 1959. Los. Alamos Scientific Laboratory, pp. 90–93.
5087 Riihimäki V., Valkonen S., Engström B., et al. 2008 Behaviour of. aluminum in. aluminum welders
5088 and. manufacturers of. aluminum sulfate–impact on. biological monitoring. Scand. J. Work. Environ
5089 Health 34 451–462
5090 Rodushkin, I., Engström E., Sörlin D., et al. 2011 Uptake and. accumulation of. anthropogenic Os. in.
5091 free-living bank. voles. (Myodes glareolus). Water. Air. Soil. Pollut 218 603–610
5092 Roels, H., Meiers G., Delos M., 1997 Influence of. the. route. of. administration and. the. chemical form.
5093 (MnCl2, MnO2) on. the. absorption and. cerebral distribution of. manganese in. rats. Arch. Toxicol
5094 71 223–230
5095 Röllin HB, Theodorou P., Kilroe-Smith TA. 1991 Deposition of. aluminium in. tissues of. rabbits
5096 exposed to. inhalation of. low. concentrations of. Al2O3 dust. Br. J. Ind. Med. 48 389–391
5097 Röllin HB, Theodorou P., Nogueira CMCA, et al. 2001 Aluminium uptake and. excretion in. potroom
5098 workers of. a. new. primary aluminium smelter during the. construction stage. J. Environ Monit. 3
5099 560–564
5100 Rosenfeld, G., 1954 Studies of. the. metabolism of. germanium. Arch. Biochem Biophys 48 84–94
5101 Roshchin, A., Ordzhonikidze E., Shalganova I. 1980 Vanadium–toxicity, metabolism, carrier state. J.
5102 Hyg. Epidemiol Microbiol Immunol 24 377–383
5103 Rosoff, B., Siegel E., Williams GL, Spencer H. 1963 Distribution and. excretion of. radioactive rare-
5104 earth compounds in. mice. Int. J. Appl. Radiat Isot. 14 129–135
5105 Rosoff, B., Spencer H., Cohn SH, Gusmano EA. 1965 Metabolism of. scandium-46 in. man. Int. J. Appl.
5106 Radiat Isot. 16 479–485

5107 Roth, P., Werner E. 1979 Intestinal absorption of. magnesium in. man. Int. J. Appl. Radiat Isot. 30 523–
5108 526
5109 Rothstein, A., Hayes AD. 1960 The. metabolism of. mercury in. the. rat. studied by. isotope techniques.
5110 J. Pharmacol Exp. Ther. 130 166–176
5111 Rubin, M., Sliwinski A., Photias M., Feldman M., Zvaifler N., 1967 Influence of. chelation on. gold.
5112 metabolism in. rats. Proc. Soc. Exp. Biol. Med. 124 290–296
5113 Rubow, S., Klopper J., Scholtz P. 1991 Excretion of. gallium 67 in. human. breast milk. and. its.
5114 inadvertent ingestion by. a. 9-month-old child. Eur. J. Nucl. Med. 18 829–833
5115 Ruoff, W., 1995 Relative bioavailability of. manganese ingested in. food. or. water. In: Proceedings,
5116 Lexington, MA, 1995, pp. 65–75. Eastern Research Group. Inc.
5117 Rusch, GM, O'Grodnick JS, Rinehart WE. 1986 Acute. inhalation study. in. rat. of. comparative uptake,
5118 distribution and. excretion of. different cadmium containing materials. Am. Ind. Hyg. Assoc. J. 47
5119 754–763
5120 Russell, MA, King LE, Boyd AS. 1996 Lichen planus after. consumption of. a. gold. containing liquor.
5121 N. Engl. J. Med. 334 603
5122 Ryan, JW, Harper PV, Stark VS, et al. 1985 Radiation absorbed dose. estimate for. rubidium-82
5123 determined from. in. vivo. measurements in. human. subjects. In: Shalafke-Stelson AT, Watson EE,
5124 editors. Radiopharmaceutical Dosimetry Symposium CONF–85113. Springfield VA: NTIS. 346–
5125 358
5126 Rydzynski, K., Pakulska D. 2012 Vanadium, Niobium, and. Tantalum. In: Bingham E. Cohrssen B.
5127 editors. Patty's Toxicology. Hoboken NJ: Wiley-Blackwell p. 6
5128 Sabatier, M., Arnaud MJ, Turnlund JR. 2003 Magnesium absorption from. mineral water. Eur. J. Clin.
5129 Nutr. 57 801–802
5130 Sabatier, M., Pont F., Arnaud MJ, Turnlund JR. 2003 A. compartmental model. of. magnesium
5131 metabolism in. healthy men. based. on. two. stable isotope tracers. Am. J. Physiol Regul. Integr
5132 Comp. Physiol 285 R656–R663
5133 Sabbioni, E., Marafante E., Amantini L., Ubertalli L., Birattari C., 1978 Similarity in. metabolic patterns
5134 of. different chemical species of. vanadium in. the. rat. Bioinorg Chem. 8 503–515
5135 Sabbioni, E., Marafante E., Rade J., Gregotti C., Di Nucci A., Manzo L., 1981 Biliary excretion of.
5136 vanadium in. rats. Toxicol Eur. Res. 3 93–98
5137 Sabbioni, E., Loetz L., Marafante E., et al. 1980 Metabolic fate. of. different inorganic and. organic
5138 species of. thallium in. the. rat. Sci. Total. Environ 15 123–125
5139 Sallsten, G., Baregard L., Schutz A. 1993 Decrease in. mercury concentration in. blood. after. long.
5140 term. exposure: a. kinetic study. of. chloralkali workers. Br. J. Ind. Med. 50 814–821
5141 Samuels, C., Leggett R. 2021 A. biokinetic model. for. systemic sodium. J. Radiol Prot. 41 1045
5142 Sandborgh-Englund, G., Elinder CG, Johanson G., et al. 1998 The. absorption, blood. levels, and.
5143 excretion of. mercury after. a. single dose. of. mercury vapour in. humans. Toxicol Appl. Pharmacol
5144 150 146–153
5145 Sargent, T., Lim TH, Jenson RL. 1979 Reduced chromium retention in. patients with. hemochromatosis,
5146 a. possible basis. of. hemochromatotic diabetes. Metabolism 28 70–79
5147 Sarmiento-Gonzalez, A., Encinar JR, Marchante-Gayon JM, Sanz-Medel A., 2009 Titanium levels in.
5148 the. organs and. blood. of. rats. with. a. titanium implant, in. the. absence of. wear, as. determined
5149 by. double-focusing ICP-MS. Anal. Bioanal Chem. 393 335–343
5150 Sasser, LB, Jarboe GE. 1977 Intestinal absorption and. retention of. cadmium in. neonatal rat. Toxicol
5151 Appl. Pharmacol 41 423–431
5152 Sasser, LB, Jarboe GE. 1980 Intestinal absorption and. retention of. cadmium in. neonatal pigs.
5153 compared to. rats. and. guinea pigs. J. Nutr. 110 1641–1647
5154 Sasser, LB, Jarboe GE, Walter BK, Kelman BJ. 1978 Absorption of. mercury from. ligated segments
5155 of. the. rat. gastrointestinal tract. Proc. Soc. Exp. Biol. Med. 157 57–60
5156 Sauer, F., Laughland DH, Davidson WM. 1959 The. silica content of. guinea pig. tissues as. determined
5157 by. chemical and. isotopic techniques. Can. J. Biochem Physiol 37 1173–1181
5158 Sayato, Y., Nakamuro K., Matsui S., Ando M. 1980 Metabolic fate. of. chromium compounds. I.
5159 Comparative behaviour of. chromium in. rat. administered with. Na251CrO4 and. 51CrCl3. J.
5160 Pharmacobiodyn 3 17–23

5161 Sayle, BA, Helmer E., Birdsong BA. 1982 Bone. marrow imaging with. indium-111 chloride in. aplastic
5162 anemia and. myelofibrosis: concise communication. J. Nucl. Med. 23 121–125
5163 Scaffidi-Argentina, F., Longhurst GR, Shestakov V., et al. 2000 Beryllium R&D. for. fusion
5164 applications. Fusion Eng. Des. 51–52 23–41
5165 Scansetti, G., 1992 Exposure to. metals that. have. recently come. into. use. Sci. Total. Environ 120 85–
5166 91
5167 Schauss, AG. 1991 Nephrotoxicity in. humans by. the. ultratrace element germanium. Ren. Fail. 29
5168 267–280
5169 Schiepers, C., Nuyts J., Bormans G., et al. 1997 Fluoride kinetics of. the. axial. skeleton measured in.
5170 vivo. with. fluorine-18-fluoride PET. J. Nucl. Med. 38 1970–1976
5171 Schinohara, N., Danno N., Ichinose T., et al. 2014 Tissue distribution and. clearance of. intravenously
5172 administered titanium dioxide (TiO2) nanoparticles. Nanotoxicology 8 132–141
5173 Schleh, C., Holzwarth U., Hirn S., et al. 2013 Biodistribution of. inhaled gold. nanoparticles in. mice.
5174 and. the. influence of. surfactant protein D. J. Aerosol Med. Pulm. Drug. Deliv. 26 24–30
5175 Schleh, C., Semmler-Behnke M., Lipka J., et al. 2012 Size. and. surface charge of. gold. nanoparticles
5176 determine absorption across intestinal barriers and. accumulation in. secondary target organs after.
5177 oral. administration. Nanotoxicology 6 36–46
5178 Schönholzer KW, Sutton RAL, Walker VR, et al. 1997 Intestinal absorption of. trace. amounts of.
5179 aluminum in. rats. studied with. 26aluminum and. accelerator mass. spectrometry. Clin. Sci. 92 379–
5180 383
5181 Schroeder, HA, Balassa JJ. 1967 Abnormal trace. metals in. man: germanium. J. Chronic Dis. 20 211–
5182 224
5183 Schwartz, R., Spencer H., Wentworth RA. 1978. Measurement of. magnesium absorption in. man. using.
5184 stable 26Mg as. a. tracer. Clin. Chim. Acta. 87:265–273.
5185 Scott, JK, Neuman WF, Allen R. 1950. The. effect of. added. carrier on. the. distribution and. excretion
5186 of. soluble 7Be. J. Biol. Chem. 182:291–298.
5187 Scott, KC, Turnland JR. 1994. Compartmental model. of. copper metabolism in. adult. men. J. Nutr.
5188 Biochem 5:342–350.
5189 Scott, KG. 1952. The. metabolic properties of. various metals. USAEC, UCRL. 1694, pp.7–11.
5190 Scott, KG, Hamilton JG. 1950. The. metabolism of. silver in. the. rat. with. radio-silver used. as. an.
5191 indicator. Univ. Calif. Publ. Pharmacol 2:241–262.
5192 Semenov, DI, Balashova GN, Borisova NN. 1966. Behaviour of. niobium in. the. animal organism. Tr.
5193 Inst. Biol. Akad. Nauk. SSSR. Ural. Fil. 46:5–16. (Translated in. AEC-tr-7169: 3–14 1970)
5194 Semmler-Behnke, M., Kreyling WG, Lipka J., et al. 2008. Biodistribution of. 1.4- and. 18-nm gold.
5195 particles in. rats. Small. 4:2108–2111.
5196 Setyawati, IA, Thompson KH, Yuen VG, et al. 1998. Kinetic analysis and. comparison of. uptake,
5197 distribution, and. excretion of. 48V-labeled compounds in. rats. J. Appl. Physiol 84(2):569–575.
5198 Sharma, RP, Flora SJ, Drown DB, Oberg SG. 1987. Persistence of. vanadium compounds in. lungs.
5199 after. intratracheal instillation in. rats. Toxicol Ind. Health 3:321–329.
5200 Shaw, PA. 1933. Toxicity and. deposition of. thallium in. certain game. birds. J. Pharmacol Exp. Ther.
5201 48:478–487.
5202 Sheehan, RM, Renkin EM. 1972. Capillary, interstitial, and. cell. membrane barriers to. blood-tissue
5203 transport of. potassium and. rubidium in. mammalian skeletal muscle. Circ. Res. 30(5 Suppl. 1):588–
5204 607.
5205 Shellabarger, CJ, Godwin JT. 1954. Studies of. the. thyroidal uptake of. astatine in. the. rat. J. Clin.
5206 Endocrinol Metab. 14:1149–1160.
5207 Shelley, WB. 1973. Chondral dysplasia induced by. zirconium and. hafnium. Cancer Res. 33:287–292.
5208 Shi, H., Magaye R., Castranova V., Zhao J. 2013. Titanium dioxide nanoparticles: A. review of. current
5209 toxicological data. Part. Fibre. Toxicol 10(1):15.
5210 Shinogi, M., Masaki T., Mori I. 1989. Determination and. biokinetics of. germanium in. mouse. tissues
5211 by. atomic absorption spectrometry with. electrothermal atomization. J. Trace. Elem. Electrolytes
5212 Health Dis. 3:25–28.
5213 Silva, AJ, Fleshman DG, Shore B., 1973. The. effects of. penicillamine on. the. body. burdens of.
5214 several heavy. metals. Health Phys. 24:535–539.

5215 Simonsen, JA, Braad PE, Veje A., et al. 2009. 111Indium-transferrin for. localization and.
5216 quantification of. gastrointestinal protein loss. Scand. J. Gastroenterol 44:1191–1197.
5217 Sjodin, RA. 1959. Rubidium and. caesium fluxes in. muscle as. related to. the. membrane potential. J.
5218 Gen. Physiol 42:983–1003.
5219 Sjögren B., Elinder CG, Lidums V., et al. 1998. Uptake and. urinary excretion of. aluminium amongst
5220 welders. Int. Arch. Occup. Environ Health 60:77–79.
5221 Sjögren B., Lidums V., Håkansson M., et al. 1985. Exposure and. urinary excretion of. aluminum during
5222 welding. Scand. J. Work. Environ Health 11:39–43.
5223 Skalsky, HL, Carchman RA. 1983. Aluminum homeostasis in. man. Int. J. Toxicol 2(6):405–423.
5224 Smilay, MG, Dahl LK, Spraragen SC, Silver L. 1961. Isotopic sodium turnover studies in. man:
5225 evidence of. minimal sodium (22Na) retention 6 to. 11 months after. administration. J. Lab. Clin.
5226 Med. 58:60–66.
5227 Smith, GA, Thomas RG, Scott JK. 1960. The. metabolism of. indium after. administration of. a. single
5228 dose. to. the. rat. by. intratracheal, subcutaneous, intramuscular and. oral. injection. Health Phys.
5229 4:101–108.
5230 Smith, JC, Allen PV, Turner MD, Most B., Fisher HL, Hall LL. 1994. The. kinetics of. intravenously
5231 administered methyl mercury in. man. Toxicol Appl. Pharmacol 128:251–256.
5232 Smith, JF. 1996. Methyl mercury pharmacokinetics in. man: a. reevaluation. Toxicol Appl. Pharmacol
5233 137:245–252.
5234 Smith, JRH, Bailey MR, Etherington G., et al. 2007. Further study. of. the. effect of. particle size. on.
5235 slow. particle clearance from. the. bronchial tree. Radiat Prot. Dosim. 127:35–39.
5236 Smith, JRH, Bailey MR, Etherington G., et al. 2008. Effect of. particle size. on. slow. particle clearance
5237 from. the. bronchial tree. Exp. Lung. Res. 34:287–312.
5238 Smith, PHS, Taylor DM. 1974. Distribution and. retention of. the. antitumor agent. 195mPt-cis-
5239 dichlorodiammine platinum (II) in. man. J. Nucl. Med. 15:349–351.
5240 Sollenberger, DM. 1981. The. fate. of. intragastrically or. intratracheally administered or. inhaled
5241 vanadium-48 oxydichloride in. juvenile and. mature rats. PhD. thesis, Purdue Univ, West. Lafayette,
5242 IN.
5243 Söremark R., 1960. The. biological half-life of. bromide ions. in. human. blood. Acta. Physiol Scand.
5244 50:119–123.
5245 Söremark R., 1960. Excretion of. bromide ions. by. human. urine. Acta. Physiol Scand. 50:306–310.
5246 Spencer, H., Norris C., Williams D. 1994. Inhibitory effects of. zinc. on. magnesium balance and.
5247 magnesium absorption in. man. J. Am. Coll. Nutr. 13:479–484.
5248 Sripanyakorn, S., Jugdaohsingh R., Dissayabutr W., et al. 2009. The. comparative absorption of. silicon
5249 from. different foods. and. food. supplements. Br. J. Nutr. 102:825–834.
5250 Sripanyakorn, S., Jugdaohsingh R., Elliott H., et al. 2004. The. silicon content of. beer. and. its.
5251 bioavailability in. healthy volunteers. Br. J. Nutr. 91:403–409.
5252 Stahlhofen, W., Gebhart J., Heyder J. 1980. Experimental determination of. the. regional deposition of.
5253 aerosol particles in. the. human. respiratory tract. Am. Ind. Hyg. Assoc. J. 41:385–398.
5254 Stahlhofen, W., Gebhart J., Heyder J., et al. 1981. Intercomparison of. regional deposition of. aerosol
5255 particles in. the. human. respiratory tract. and. their. long. term. elimination. Exp. Lung. Res. 2:131–
5256 139.
5257 Stahlhofen, W., Gebhart J., Rudolf G., et al. 1986a. Clearance from. the. human. airways of. particles
5258 of. different sizes. deposited from. inhaled aerosol boli. Aerosols: Formation and. Reactivity. 2nd
5259 Int. Aerosol Conf, West. Berlin, Germany:192–196.
5260 Stahlhofen, W., Gebhart J., Rudolf G., et al. 1986b. Measurement of. lung. clearance with. pulses of.
5261 radioactively labelled aerosols. J. Aerosol Sci. 17:333–336.
5262 Stahlhofen, W., Gebhart J., Rudolf G., et al. 1987. Human. lung. clearance of. inhaled radioactively
5263 labelled particles in. horizontal and. vertical position of. the. inhaling person. J. Aerosol Sci. 18:741–
5264 744.
5265 Stahlhofen, W., Koebrich R., Rudolf G., et al. 1990. Short. term. and. long. term. clearance of. particles
5266 from. the. upper. respiratory tract. as. a. function of. particle size. J. Aerosol Sci. 21 Suppl. 1:407–
5267 410.
5268 Stanek, EJ, Calabrese EJ, Barnes RM, et al. 2010. Bioavailability of. arsenic in. soil: Pilot. study. results
5269 and. design considerations. Hum. Exp. Toxicol 29(11):945–960.

5270 Steinhagen, WH, Cavender FL, Cockrell BY. 1978. Six. month. inhalation exposures of. rats. and.
5271 guinea pigs. to. aluminum chlorhydrate. J. Environ Pathol Toxicol 1:267–277.
5272 Steinhausen, C., Kislinger G., Winklhofer C., et al. 2004. Investigation of. the. aluminum biokinetics
5273 in. humans: A. 26Al tracer study. Food. Chem. Toxicol 42(3):363–371.
5274 Sterns, RH, Feig PU, Pring M., Guzzo J., Singer I., 1979. Disposition of. intravenous potassium in.
5275 anuric man: a. kinetic analysis. Kidney Int. 15(6):651–660.
5276 Stiefel, T., Schulze K., Zorn H., et al. 1980. Toxicokinetic and. toxicodynamic studies of. beryllium.
5277 Arch. Toxicol 45:81–92.
5278 Stone, CJ, McLaurin DA, Steinhagen WH, et al., 1979. Tissue deposition patterns after. chronic
5279 inhalation exposures of. rats. and. guinea pigs. to. aluminum chlorhydrate. Toxicol Appl. Pharmacol
5280 49: 71–76.
5281 Strain, WH, Berliner WP, Lankau CA, McEvoy RK, Pories WJ, Greenlaw RH, 1964. Retention of.
5282 radioisotopes by. hair, bone. and. vascular tissue. J. Nucl. Med. 5: 664–674.
5283 Strauss, HW, Harrison K., Langan JK, Lebowitz E., Pitt B., 1975. Thallium-201 for. myocardial
5284 imaging. Circulation 51: 641–645.
5285 Sue, YJ, 1994. Mercury. In: Goldfrank LR, Flomenbaum NE, Lewin. NA, editors. Goldfrank's
5286 toxicologic emergencies. 5th ed. Norwalk, CT: Appleton and. Lange.
5287 Sugawa-Katayama, Y., Koishi H., Danbara H., 1975. Accumulation of. gold. in. various organs of. mice.
5288 injected with. gold. thioglucose. J. Nutr. 105: 957–962.
5289 Sullivan, MF, Miller BM, Goebel JC, 1984. Gastrointestinal absorption of. metals (51Cr, 65Zn, 95mTc,
5290 109Cd, 113Sn, 147Pm, and. 238Pu) by. rats. and. swine. Environ Res. 35: 439–453.
5291 Suttie, JW, Phillips PH, 1959. The. effect of. age. on. the. rate. of. fluorine deposition in. the. femur. of.
5292 the. rat. Arch. Biochem Biophys 83: 355–359.
5293 Suzuki, M., Morikawa M., Tomita K., et al., 1978. Thallous chloride-201Tl – fundamental studies on.
5294 its. behaviour and. clinical evaluation. Kaku. Igaku. Japanese J. Nucl. Med. 15: 27–40.
5295 Takahashi, S., Moriguchi K., Kubota Y., et al., 1989. The. deposition pattern of. insoluble particles with.
5296 different sizes. in. the. rat. trachea. Hoken. Butsuri 24: 19–24.
5297 Takenaka, S., Karg E., Kreyling W., et al., 2006. Distribution pattern of. inhaled ultrafine gold. particles
5298 in. the. rat. lung. Inhal. Toxicol 18(10): 733–740.
5299 Takenaka, S., Karg E., Moller W., et al., 2000. A. morphologic study. on. the. fate. of. ultrafine silver
5300 particles: distribution pattern of. phagocytized metallic silver in. vitro. and. in. vivo. Inhal. Toxicol
5301 12(Suppl 3): 291–299.
5302 Takenaka, S., Karg E., Roth C., et al., 2001. Pulmonary and. systemic distribution of. inhaled ultrafine
5303 silver particles in. rats. Environ Health Perspect 109(Suppl 4): 547–551.
5304 Talbot, RJ, Newton D., Priest ND, Austin JG, Day JP, 1995. Inter-subject variability in. the. metabolism
5305 of. aluminium following intravenous injection as. citrate. Hum. Exp. Toxicol 14: 595–599.
5306 Tam, GKH, Charbonneau SM, Bryce F., Pomroy C., Sandi E., 1979. Metabolism of. inorganic arsenic
5307 (74As) in. humans following oral. ingestion. Toxicol Appl. Pharmacol 50: 319–322.
5308 Tam, GKH, Charbonneau SM, Bryce F., et al., 1982. Excretion of. a. single oral. dose. of. fish-arsenic
5309 in. man. Bull. Environ Contam Toxicol 28: 669–673.
5310 Tao, SH, Bolger PM, 1997. Hazard assessment of. germanium supplements. Regul. Toxicol Pharmacol
5311 25: 211–219.
5312 Task, Group on Lung Dynamics (TGLD), 1966. Deposition and. retention models for. internal
5313 dosimetry of. the. human. respiratory tract. Health Phys. 12: 173–207.
5314 Taylor, DM, Lehmann M., Planas-Bohne F., Seidel A., 1983. The. metabolism of. radiohafnium in. rats.
5315 and. hamsters: a. possible analog of. plutonium for. metabolic studies. Radiat Res. 95: 339–358.
5316 Taylor, DM, Seidel A., Doerfel H., 1985. The. metabolism of. radiohafnium in. marmosets and.
5317 hamsters. Int. J. Med. Biol. 12: 387–391.
5318 Taylor, DM, 1966. The. metabolism of. scandium-47 produced by. the. decay. of. calcium 47 in. vivo.
5319 Br. J. Radiol 39: 620–622.
5320 Teisinger, J., Fiserova-Bergerova V., 1965. Pulmonary retention and. excretion of. mercury vapors in.
5321 man. Ind. Med. Surg. 34: 580–584.
5322 Tepperman, K., Finer R., Donovan S., et al., 1984. Intestinal uptake and. metabolism of. auranofin, a.
5323 new. oral. gold-based antiarthritis drug. Science 225(4660): 430–432.

5324 Teraoka, H., 1981. Distribution of. 24 elements in. the. internal organs of. normal males. and. the.
5325 metallic workers in. Japan. Arch. Environ Health 36: 155–165.
5326 Thomas, RG, Archuleta RF, 1980. Titanium retention in. mice. Toxicol Lett. 6: 115–118.
5327 Thomas, SR, Stabin MG, Castronovo FP, 2005. Radiation-absorbed dose. from. 201Tl-thallous chloride.
5328 J. Nucl. Med. 46: 502–508.
5329 Thomassen, PR, Leicester HM, 1964. Uptake of. radioactive beryllium, vanadium, selenium, cerium,
5330 and. yttrium in. the. tissues and. teeth. of. rats. J. Dent. Res. 43: 346–352.
5331 Thomson, CD, Stewart RDH, 1973. Metabolic studies of. [75Se]selenomethionine and. [75Se]selenite
5332 in. the. rat. Br. J. Nutr. 30: 139–147.
5333 Thomson, CD, Stewart RDH, 1974. The. metabolism of. 75Se selenite in. young. women. Br. J. Nutr.
5334 32: 303–323.
5335 Thorne, MC, Jackson D., Smith AD, 1986. Pharmacodynamic models of. selected toxic. chemicals in.
5336 man. Review of. metabolic data. Lancaster: MTP. Press. Limited.
5337 Threefoot, S., Burch G., Reaser P., 1949. The. biologic decay. periods of. sodium in. normal man, in.
5338 patients with. congestive heart. failure and. in. patients with. the. nephrotic syndrome as. determined
5339 by. 22Na as. the. tracer. J. Lab. Clin. Med. 34: 1–13.
5340 Tian, N., Zhang Z., Loustalot G., Yang Q., Cogswell ME, 2013. Sodium and. potassium intakes among.
5341 US. infants and. preschool children, 2003–2010. Am. J. Clin. Nutr. 98: 1113–1122.
5342 Tipton, I., Stewart P., Martin P., 1966. Trace. elements in. diet. and. excreta. Health Phys. 12: 1683–
5343 1689.
5344 Tompsett, SL, 1934. The. excretion of. copper in. urine. and. faeces and. its. relation to. the. copper
5345 content of. the. diet. Biochem J. 28: 2088–2091.
5346 Tompsett, SL, 1935. The. copper and. “inorganic” iron. contents of. human. tissues. Biochem J. 29:
5347 480–486.
5348 Toohey, RE, Essling MA, Huff DR, 1979. Retention and. gross. distribution of. 75Se following
5349 intravenous injection of. 75Se-selenomethionine. Health Phys. 37: 395–397.
5350 Turner, A., Price S., 2008. Bioaccessibility of. platinum group. elements in. automotive catalytic
5351 converter particulates. Environ Sci. Technol 42: 9443–9448.
5352 Turnland, JR, 1998. Human. whole-body copper metabolism. Am. J. Clin. Nutr. (Suppl.) 67: 960S–
5353 964S.
5354 Tyor, MP, Eldridge JS, 1956. A. comparison of. the. metabolism of. rubidium-86 and. potassium-42
5355 following simultaneous injection into. man. Am. J. Med. Sci. 232: 186–193.
5356 U.S., EPA, 2001. Toxicological review of. bromate in. support of. Integrated Risk. Information System
5357 (IRIS). Washington, DC: United States Environmental Protection Agency (EPA).
5358 U.S., EPA, 2009. IRIS. Toxicological review of. thallium and. compounds (Final report). EPA/635/R-
5359 08/001F. Washington, DC: United States Environmental Protection Agency (EPA).
5360 U.S., EPA, 2012. Compilation and. review of. data. on. relative bioavailability of. arsenic in. soil.
5361 Washington, DC: United States Environmental Protection Agency (EPA). Available at:
5362 http://www.epa.gov/superfund/bioavailability/pdfs/Arsenic%20Bioavailability%20SCIENCE%20
5363 Report_.
5364 Uchiyama, M., Akiba S., Ohmomo Y., et al., 1976. 203Hg-labelled methyl mercury chloride retention
5365 in. man. after. inhalation. Health Phys. 31: 335–342.
5366 Udensi, KU, Tchounwou PB, 2017. Potassium homeostasis, oxidative stress, and. human. disease. Int.
5367 J. Clin. Exp. Physiol 4: 111–122.
5368 Underwood, EJ, 1977. Trace. elements in. human. and. animal nutrition. 4th ed. London: Academic
5369 Press.
5370 United, Nations Environment Programme (UNEP), International Labour Organization and World
5371 Health Organization, editors, 1982. Titanium. Environmental Health Criteria 24. Geneva: World.
5372 Health Organization.
5373 United, Nations Environment Programme (UNEP), International Labour Organization and World
5374 Health Organization, editors, 1988. Vanadium. Environmental Health Criteria 81. Geneva: World.
5375 Health Organization. Available at: http://hdl.handle.net/20.500.11822/29388.
5376 Usuda, K., Kono R., Ueno T., et al., 2014. Risk. assessment visualization of. rubidium compounds:
5377 comparison of. renal. and. hepatic toxicities, in. vivo. Biol. Trace. Elem. Res. 159: 263–268.

5378 Vacher, J., Stoner HB, 1968. The. removal of. injected beryllium from. the. blood. of. the. rats. The.
5379 role. of. the. reticulo-endothelial system. Br. J. Exp. Pathol 49: 315–323.
5380 Vahter, M., 2002. Mechanisms of. arsenic biotransformation. Toxicology 181–182: 211–217.
5381 Vahter, M., Norin H., Metabolism of 74As-labeled trivalent and. pentavalent inorganic arsenic in. mice.
5382 Environ Res. 1980,21:446–467.
5383 Vahter, M., Marafante E., Reduction and binding of arsenate in marmoset monkeys. Arch Toxicol.
5384 1985,57:119–124.
5385 Vahter, M., Mechanisms of arsenic biotransformation. Toxicology. 2002,182:211–217.
5386 Valberg, LS, Flanagan PR, Haist J., et al. Gastrointestinal metabolism of gallium and indium: Effect of
5387 iron deficiency. Clin Investig Med. 1981,4:103–108.
5388 Van, Cleave CD, Kaylor CT. Distribution and retention of carrier-free radioberyllium in the rat. AMA
5389 Arch Ind Hyg Occup Med. 1953,7:367–375.
5390 Van, Cleave CD, Kaylor CT. Distribution, retention, and elimination of 7Be in. the. rat. after.
5391 intratracheal injection. AMA. Arch. Ind. Hyg. Occup. Med. 1955,11:375–392.
5392 Valentine, R., Fisher GL. Pulmonary clearance of intratracheally administered 63Ni3S2 in. strain A/J.
5393 mice. Environ Res. 1984,34:328–334.
5394 Van, Hulle M., De Cremer K., Vanholder R., et al. In vivo distribution and fractionation of indium in
5395 rats after subcutaneous and oral administration of [114mIn]InAs. J., Environ Monit. 2005,7:365–
5396 370.
5397 Van, Paemel M., Dierick N., Janssens G., et al. Selected trace and ultratrace elements: Biological role,
5398 content in feed and requirements in animal nutrition – Elements for risk assessment. Technical report
5399 submitted to EFSA (Question No EFSA-Q- 2008-04990). Ghent. University, 2010. DOI:
5400 10.2903/sp.efsa.2010.EN-68.
5401 Veall, N., Fisher AJ, Browe JC, Bradley JE. An improved method for clinical studies of total
5402 exchangeable sodium using 22Na and. a. whole-body counting technique. Lancet. 1955,1:419–422.
5403 Velasquez, DJ, Morrow PE. Estimation of guinea pig tracheobronchial transport rates using a
5404 compartment model. Exp Lung Res. 1984,7:163–176.
5405 Velikyan, I., Antoni G., Sörensen J., Estrada S. Organ biodistribution of germanium- 68 in. rat. in. the.
5406 presence and. absence of. [68Ga]Ga-DOTA-TOC for. the. extrapolation to. the. human. organ. and.
5407 whole-body radiation dosimetry. Am. J. Nucl. Med. Mol. Imaging. 2013,3:154–165.
5408 Vendeland, SC, Deagen JT, Whanger PD. Uptake of selenotrisulfides of glutathione and cysteine by
5409 brush border membranes from rat intestines. J., Inorg Biochem. 1992,47:131–140.
5410 Vendeland, SC, Deagen JT, Butler JA, et al. Uptake of selenite, selenomethionine and selenate by brush
5411 border membrane vesicles isolated from rat small intestine. BioMetals. 1994,7:305–312.
5412 Vennart, J., External counting. In: Diagnosis and Treatment of Radioactive Poisoning. Vienna: IAEA,
5413 1963. p. 3–22.
5414 Verhas, M., Gueronniere V., Grognet JM, et al. Magnesium bioavailability from mineral water: A. study
5415 in adult men. Eur J., Clin Nutr. 2002,56:442–447.
5416 Versieck, J., Cornelis R., Normal levels of trace elements in human blood plasma or serum. Anal Chim
5417 Acta. 1980,116:217–254.
5418 Versieck, J., Vanballenberghe L., De Kesel A., More on determination of manganese in biological
5419 materials. Clin Chem. 1988,34:1659–1660.
5420 Veterans, Administration Hospital and Hines IL. Metabolism of 90Sr and. of. other. elements in. man.
5421 Nucl. Sci. Abstr. 1976,33(8):1791.
5422 Visser, GWM, Diemer EL, Vos CM, et al. The biological behaviour of some organic astatine
5423 compounds in rats. Int J., Appl Radiat Isot. 1981,32:913–917.
5424 Vormann, J., Magnesium: nutrition and metabolism. Mol Aspects Med. 2003,24:27–37.
5425 Wagner, MJ. Absorption of fluoride by the gastric mucosa in the rat. J., Dent Res. 1962,41:667–674.
5426 Walker, AF, Marakis G., Christie S., Byng M., Mg citrate found more bioavailable than other Mg
5427 preparations in a randomized, double-blind study. Magnes Res. 2003,16(3):183–191.
5428 Wallace, TC, Cowan AE, Bailey RL. Current sodium intakes in the United States and the modeled
5429 effects of glutamate incorporation into select savory products. Nutrients. 2019,11:2691.
5430 https://doi.org/10.3390/nu11112691.
5431 Walsh, CT. The influence of age on the gastrointestinal absorption of mercuric chloride and methyl
5432 mercury chloride in the rat. Environ Res. 1982,27:412–420.

Wase, AW. Absorption and distribution of radio-tungstate in bone and soft tissues. Arch Biochem Biophys. 1956,61:272–277.
Watanabe, K., Shima S., Tachikawa S., et al. Biotoxicity and beryllium distribution in organs by oral administration of beryllium compounds for long periods II. Rodo Kagaku. 1985,61:235–246.
Watson, WS, Hilditch TE, Horton PW, Davies DL, Lindsay R., Magnesium metabolism in blood and the whole body in man using 28Mg. Metab. Clin. Exp. 1979,28:90–95.
Weber, H. Long-term study of the distribution of soluble chromate- 51 in. the. rat. after. a. single intratracheal administration. J. Toxicol Environ Health. 1983,11:749–764.
Weberg, R., Berstad A. Gastrointestinal absorption of aluminium from single doses of aluminium-containing antacids in man. Eur J., Clin Invest. 1986,16(5):428–432.
Wehner, AP, Craig DK. Toxicology of inhaled NiO and CoO in Syrian golden hamsters. Am Ind Hyg Assoc J., 1972,33:146–155.
Weininger, J., Issachar D., Lubin E., Zabari M., Trumper J. Influence of pH adjustment agents on the biologic behaviour of osmium- 191 impurity in. iridium-191m generator eluates. J. Nucl. Med. 1990,31:523–525.
Welsh, LW, Welsh JJ. Laryngeal lymphatics, human in vivo studies. Am Acad Ophthalmol Otolaryngol. 1963,67:524–529.
West, B., Wyzan H., Investigations of the possible absorption of titanium dioxide from the gastrointestinal tract. In: FAO/WHO. Toxicological Evaluation of Some Food Colours, Emulsifiers, Stabilizers, Anti-Caking Agents and Certain Other Substances. 1970. p. 55–56.
Wester, PO. Trace elements in serum and urine from hypertensive patients before and during treatment with chlorthalidone. Acta Med Scand. 1973,194:505–512.
Wester, PO. Trace element balances in relation to variations in calcium intake. Atherosclerosis. 1974,20:207–215.
Whanger, PD, Pedersen ND, Hatfield J., et al. Absorption of selenite and selenomethionine from ligated digestive tract segments in rats. Proc Soc Exp Biol Med. 1976,153:295–297.
Whitford, GM. Intake and metabolism of fluoride. Adv Dent Res. 1994,8:5–14.
WHO, (ed). Trace Elements in Human Nutrition and Health. Geneva: World Health Organization, 1996.
WHO. Environmental Health Criteria 106: Beryllium. Geneva: World. Health Organization, 1990.
WHO. Chapter 6.1 Arsenic. In: WHO. Air. Quality Guidelines. 2nd ed. Copenhagen: WHO. Regional Office for. Europe, 2000.
WHO. Cadmium in drinking-water. Background document for development of WHO Guidelines for Drinking-water Quality. WHO/SDE/WSH/ 03.04/80/Rev/1. Geneva: World. Health Organization, 2011a.
WHO. Copper in drinking-water. Background document for development of WHO Guidelines for Drinking-water Quality. WHO/SDE/WSH/ 03.04/88. Geneva: World. Health Organization, 2011b.
WHO. Mercury in drinking-water. Background Document for development of WHO guidelines for drinking-water quality. WHO/SDE/WSH/ 05.08/10. Geneva: World. Health Organization, 2015.
Wiegmann, TB, Day HD, Patak RV. Intestinal absorption and secretion of radioactive vanadium (48VO3–) in. rats. and. effect of. Al(OH)3. J. Toxicol Environ Health. 1982,10:233–245.
Wilhelm, M., Zhang XJ, Hafner D., et al. Single-dose toxicokinetics of aluminum in the rat. Arch Toxicol. 1992,66:700–705.
Willard, DH, Bair WJ. 1961. Behaviour of. ^{131}I. following its. inhalation as. a. vapour and. as. a. particle. Acta. Radiol 55:486–496.
Williams, LR, Leggett RW. 1987. The. distribution of. intracellular alkali metals in. Reference Man. Phys. Med. Biol. 32:173–190.
Williams, RH, Maturen A., Sky-Peck HH. 1987. Pharmacologic role. of. rubidium in. psychiatric research. Compr. Ther. 13:46–54.
Wiseman, G., 1964. Absorption from. the. Intestine. London: Academic Press.
Wootton, R. 1974. The. single passage extraction of. ^{18}F. in. rabbit bone. Clin. Sci. Mol. Med. 47:73–77.
Wright, N., Yeoman WB, Carter GF. 1980. Massive oral. ingestion of. elemental mercury without poisoning [letter]. Lancet 1(8161):206.
Wu, X., Li J., Hu JN, Deng ZY. 2012. The. effects of. glutamate and. citrate on. absorption and. distribution of. aluminum in. rats. Biol. Trace. Elem. Res. 148:83–90.

Xie, GP, Wang C., Sun J., et al. 2011. Tissue distribution and. excretion of. intravenously administered titanium dioxide nanoparticles. Toxicol Lett. 205:55–61.

Yamauchi, H., Takahashi K., Yamamura Y., Fowler BA. 1992. Metabolism of. subcutaneous administered indium arsenide in. the. hamster. Toxicol Appl. Pharmacol 116:66–67.

Yanaga, M., Enomoto S., Hirunuma R., et al. 1996. Multitracer study. on. uptake and. excretion of. trace. elements in. rats. Appl. Radiat Isot. 47(2):235–240. https://doi.org/10.1016/0969-8043(95)00279-0

Yoakum, AM, Steward PL, Sterrett JE. 1975. Method development and. subsequent analysis of. biological tissues for. platinum, lead. and. manganese content. Environ Health Perspect 10:85–93.

Yokel, RA, Florence RL. 2006. Aluminum bioavailability from. the. approved food. additive leavening agent. acidic sodium aluminum phosphate, incorporated into. a. baked. good, is. lower. than. from. water. Toxicol 227:86–93.

Yokel, RA, McNamara PJ. 1988. Influence of. renal. impairment, chemical form, and. serum. protein binding on. intravenous and. oral. aluminum kinetics in. the. rabbit. Toxicol Appl. Pharmacol 95(1):32–43.

Yokel, RA, McNamara PJ. 2001. Aluminium toxicokinetics: an. updated mini-review. Pharmacol Toxicol 88(4):159–167. https://doi.org/10.1111/j.1600-0773.2001.880401.x

Yokel, RA. 2002. Brain. uptake, retention, and. efflux of. aluminum and. manganese. Environ Health Perspect 110(Suppl 5):699–704.

Yu, DH. 1999. A. pharmacokinetic modeling of. inorganic arsenic: a. short-term oral. exposure model. for. humans. Chemosphere 39:2737–2747.

Yu, YQ, Yang JY. 2019. Oral. bioaccessibility and. health risk. assessment of. vanadium(IV) and. vanadium(V) in. a. vanadium titanomagnetite mining region by. a. whole. digestive system in-vitro method (WDSM). Chemosphere 215:294–304.

Zafar, A., Javed S., Akram N., Naqvi SA. 2024. Health Risks. of. Mercury. In: Kumar. N. editor. Mercury Toxicity Mitigation: Sustainable Nexus. Approach. Earth. and. Environmental Sciences Library. Springer, Cham. https://doi.org/10.1007/978-3-031-48817-7_3

Zafar, TA, Weaver CM, Martin BR, Flarend R., Elmore D., 1997. Aluminum (^{26}Al) metabolism in. rats. Proc. Soc. Exp. Biol. Med. 216(1):81–85. https://doi.org/10.3181/00379727-216-44159

Zalikin, GA, Tronova IN, Denisov II. 1969. Distribution of. scandium-46 in. the. body. of. rats. for. different paths. of. administration. In: Radioaktivonye Izotopy i. Organizm. Moscow: Izdatel'stvo Meditsina.

Zalups, RK. 1998. Intestinal handling of. mercury in. the. rat: implication of. intestinal secretion of. inorganic mercury following biliary ligation or. cannulation. J. Toxicol Environ Health 53:615–636.

Zheng, W., Kim H., Zhao Q., 2000. Comparative toxicokinetics of. manganese chloride and. methylcyclopentadienyl manganese tricarbonyl (MMT) in. Sprague-Dawley rats. Toxicol Sci. 54:295–301.

Zheng, W., Winter SM, Kattnig MJ, et al. 1994. Tissue distribution and. elimination of. indium in. male. Fischer 344 rats. following oral. and. intratracheal administration of. indium phosphide. J. Toxicol Environ Health 43:483–494.

Zheng, Y., Wu J., Ng JC, et al. 2002. The. absorption and. excretion of. fluoride and. arsenic in. humans. Toxicol Lett. 133(1):77–82.

Zhu, H., Wang N., Zhang Y., Wu Q., Chen R., Gao J., Chang P., Liu Q., Fan T., Li J., Wang J., 2010. Element contents in. organs and. tissues of. Chinese adult. men. Health Phys. 98:61–71.

Zuckier, LS, Dohan O., Li Y., Chang CJ, Carrasco N., Dadachova E. 2004. Kinetics of. perrhenate uptake and. comparative biodistribution of. perrhenate, pertechnetate, and. iodide by. NaI. symporter-expressing tissues in. vivo. J. Nucl. Med. 45:500–507.

ACKNOWLEDGEMENTS

This report is the third in a series of documents replacing the *Publication 56* series (ICRP, 1989, 1993, 1995b,c, 1996a, 2001, 2004) to provide revised age-dependent dose coefficients for members of the public for environmental intakes of radionuclides by inhalation and ingestion. The revised dose coefficients have been calculated using the Human Alimentary Tract Model (HATM) described in *Publication 100* (ICRP, 2006) and the revised Human Respiratory Tract Model (HRTM) described in *Publication 130* (ICRP, 2015). Revisions have also been made to many of the models that describe the systemic biokinetics of radionuclides absorbed to blood, making them more physiologically realistic representations of uptake and retention in organs and tissues and of excretion.

This third report in the series includes biokinetic and dosimetric models for individual elements and their radioisotopes plus dose coefficients. Additional data accompanying this series are available on the ICRP website and give extensive additional information. This current report provides the above data for the elements already described in OIR Part 5 [*Publication* 151 (ICRP, 2022)] i.e.: beryllium (Be), fluorine (F), sodium (Na), magnesium (Mg), aluminium (Al), silicon (Si), chlorine (Cl), potassium (K), scandium (Sc), titanium (Ti), vanadium (V), chromium (Cr), manganese (Mn), copper (Cu), gallium (Ga), germanium (Ge), arsenic (As), bromine (Br), rubidium (Rb), rhodium (Rh), palladium (Pd), cadmium (Cd), indium (In), tin (Sn), hafnium (Hf), tantalum (Ta), tungsten (W), rhenium (Re), osmium (Os), platinum (Pt), gold (Au), mercury (Hg), thallium (Tl), astatine (At), and francium (Fr).

ICRP thanks all those involved in the development of this publication for their hard work and dedication over many years.

Task Group 95 members

F. Paquet (Chair)	Ä. Degenhardt	R. W. Leggett
M. R. Bailey	A. Giussani	M.A. Lopez
V. Berkovski	D. Gregoratto	G. Ratia
E. Blanchardon	D. Jokisch	C. Samuels
E. Davesne	S. Lamart	T. Smith

Committee 2 critical reviewers

M. Andersson	F. Bochud

Main Commission critical reviewers

M. Kai	S. Romanov

Editorial members

C.H. Clement (Scientific Secretary and *Annals* of *the ICRP* Editor-in-Chief)
Q. Fan (Assistant Scientific Secretary and *Annals* of *the ICRP* Associate Editor)

Committee 2 members during preparation of this publication

(2021-2025)

F. Bochud (Chair)	A. Giussani	J. Li
F. Paquet (Vice-chair)	D. Jokisch	N. Petoussi-Henss
M.A. Lopez (Secretary)	C.H. Kim	T. Sato
M. Andersson	M.S. Kulkarni	T. Smith
V. Berkovskyy	S. Lamart	A. Ulanowski
D. de Souza Santos	C. Lee	Y.S. Yeom

(2025-2029)

F. Bochud (Chair)	D. de Souza Santos	L. Liu
F. Paquet (Vice-chair)	J. Eakins	T. Sato
M.A. Lopez (Secretary)	A. Giussani	T. Smith
S. Anand	D. Jokisch	A. Sokolova
M. Andersson	S. Lamart	F. Vanhavere
V. Berkovskyy	C. Lee	Y.S. Yeom

Committee 2 emeritus members

K. Eckerman

Main Commission members at the time of approval of this publication

Chair: W. Rühm, *Germany*
Vice-Chair: S. Bouffler, *UK*
Scientific Secretary and CEO: C.H. Clement, *Canada*; sci.sec@icrp.org*

N. Ban, *Japan*	D. Sutton, *UK*	**Emeritus members**
F. Bochud, *Switzerland*	A. Wojcik, *Sweden*	R.H. Clarke, *UK*
K.W. Cho, *Korea*		C. Cousins, *UK*
E. Gallego, *Spain*		J. Lochard, *France*
M. Hosono, *Japan*		F.A. Mettler Jr, *USA*
D. Laurier, *France*		R.J. Pentreath, *UK*
S. Liu, *China*		R.J. Preston, *USA*
N. Martinez, *USA*		C. Streffer, *Germany*
T. Schneider, *France*		E. Vañó, *Spain*

*Although formally not a Main Commission member since 1988, the Scientific Secretary is an integral part of the Main Commission.